UNIVERSITY OF CAPE TOWN
IYUNIVESITHI YASEKAPA • UNIVERSITEIT VAN KAAPSTAD

GENERATION AND CHARACTERIZATION OF HIV-1 SUBTYPE C CANDIDATE VACCINES THAT WILL INDUCE HIGH TITRE ANTIBODY RESPONSES TO HIV-1 ENVELOPE GLYCOPROTEIN

Michiel Theodoor van Diepen

A dissertation submitted in fulfilment of the requirements for the degree of Doctor of Philosophy (PhD) in the Faculty of Health Sciences, Division of Medical Virology, Department of Pathology, Faculty of Health Sciences, University of Cape Town

July 2020

Supervisor: Professor Anna-Lise Williamson
Co-supervisors: Dr Ros Chapman and Professor Ed Rybicki

University of Cape Town

The copyright of this thesis vests in the author. No quotation from it or information derived from it is to be published without full acknowledgement of the source. The thesis is to be used for private study or non-commercial research purposes only.

Published by the University of Cape Town (UCT) in terms of the non-exclusive license granted to UCT by the author.

University of Cape Town

GENERAL TABLE OF CONTENTS

ACKNOWLEDGEMENTS

I want to thank my supervisors ***Professor Anna-Lise Williamson, Dr Ros Chapman and Professor Ed Rybicki,*** for all their support throughout this project and their help with drafting this thesis and of course for putting up with me...

Another shout goes out to all the other members of the SHIP team: ***Dr Niki Douglass, Dr Ann Meyers, Dr Mani Margolin, Shireen Galant***, ***Phindile Ximba*** and ***Fatima Abrahams.*** This holds especially true for ***Shireen*** and ***Phindile*** who had to deal with some wild experiments we regularly cooked up, and without whom this thesis would be a whole lot shorter.

Ah, the office, I guess it is a good thing that the walls are very thick, ***Henry Munyanduki, Ruzaiq Omar, Warren de Moor*** and ***Mani Margolin,*** especially ***Mani,*** thanks for hanging out.

Finally a big thanks to family. My ***parents*** in encouraging my curiosity and letting me find my own path. ***Nikki Zigras***, my wife, for putting up with me, being the best companion in life and not afraid of challenges such as moving to Cape Town to see if we can make it stick. I am still glad that we went for it!

All the work presented within this PhD thesis has been generated for The Strategic Health Innovation Partnerships ***(SHIP)*** project '***Novel HIV Vaccine Candidates for South Africa'*** which was funded by the ***SAMRC*** and ***DST*** to ***Anna-Lise Williamson***. As part of the SHIP project, I had line management responsibilities for ***Shireen Galant (SG)*** and ***Fatima Abrahams (FA)*** and supervised ***Phindile Ximba (PTX)*** in the lab. Some of the data generated by ***SG, FA*** and ***PTX*** are included in this thesis, all these experiments were devised by *MvD*. The DNA constructs and cloning strategies were designed by ***Ros Chapman (RC)*** and *MvD*. The MVA transfer vectors, cloning strategy and targeting strategy were devised by ***RC, Niki Douglass*** and *MvD*. The different recombinant MVA constructs were isolated by ***SG, FA*** and *MvD*. All high titre recombinant MVA stocks were generated and verified by ***SG***. Studies using Immunofluorescence (confocal and lice-cell staining experiments) were designed by *MvD,* performed by ***SG*** or ***SG****+MvD* and analysed by *MvD*. The strategy for soluble Env stable cell lines was designed by *MvD*. Stable CHO cell lines were made by *MvD* and stable HEK293 cell lines by ***PTX***. The procedure for the isolation of soluble Env protein was adapted and optimised from literature by ***Mani Margolin, PTX*** and *MvD*. Soluble Env protein used in this PhD thesis was isolated by *MvD* and ***PTX***. Finally, I'd like to acknowledge ***Alana Keyser*** for her help with the FACS assay.

I want to thank ***Brandon Weber*** at the UCT Centre for Imaging & Analysis for assisting with size exclusion chromatography to isolate fractions containing soluble, trimeric Env. My gratitude goes towards ***Inge Botes*** and ***Rodney Lucas*** at the UCT Research Animal Facility performed all rabbit procedures. Our collaborators at ***NICD***: ***Lynn Morris, Penny Moore, Tandile Hermanus, Carol Growther*** and ***Nigel Makoah*** were kind enough to share reagents (α-Env monoclonal antibodies, BG505_664 trimeric Env and scaffolded CAP256 V1V2-loop protein) and perform the pseudo-virion neutralisation assays of rabbit sera. I would like to recognise ***N. Murugan*** and ***P. Christophe*** at Microscopy & Microanalysis Unit of ***UKZN*** for their electron microscopy work on VLPs.

DECLARATION

The work described in this thesis was conducted in the Institute of Infectious Diseases and Molecular Medicine, University of Cape Town. Research was conducted under the supervision of Professor Anna-Lise Williamson, Dr Ros Chapman and Professor Ed Rybicki

I, Michiel Theodoor van Diepen, hereby declare that the work outlined in this thesis is my original work (except where acknowledgements indicate otherwise) and that neither the whole work nor any part of it has been or is being submitted for another degree in this or any other university. All assistance provided by other people has been acknowledged. All citations in this manuscript are reflected using the style of the Journal of Virology as the convention. Furthermore, I authorise the university to reproduce for the purpose of research either the whole or any portion of the contents in any manner whatsoever.

Signed by candidate

Michiel Theodoor van Diepen

ABBREVIATIONS

%	Percentage
(e)GFP	(enhanced) green fluorescent protein
(k)bp	(1000) base pairs
(k)Da	kilo Dalton
(m)RNA	(messenger) Ribonucleic acid
(r)MVA	(recombinant) Modified Vaccinia Ankara
<	smaller than
>	greater than
°C	degrees Celsius
µg	microgram
µl	micorlitre
µM	micromolar
4PL curve	Four Parameter Logistic Regression curve
AA	amino acid
Ad	adenovirus
ADCC	antibody-dependent cellular cytotoxicity
AIDS	acquired immunodeficiency syndrome
AIDSVAX	Protein based HIV vaccine, used in VAX003/4 clinical trials
ALVAC	recombinant canarypox vaccine backbone
AMP	Antibody Mediated Prevention
Amp(R)	ampicillin resistance gene
ANOVA	analysis of variance
AP	Alkaline phosphatase
APC	antigen presenting cells
ART	antiretroviral therapy
ASP	Anti-Sense Protein
BCG	Mycobacterium bovis Bacille Calmette Guerin
BCR	B cell receptor
BHK-21	Baby hamster kidney cells
BN PAGE	Blue native polyacrylamide gel electrophoresis
bnAb	broadly cross-neutralising antibodies
BSA	Bovine serum albumin
C(1-5)	gp120 conserved regions 1-5
CA	capsid domain (P24)
CAPRISA	the Centre for the AIDS Programme of Research in South Africa
CAP	CAPRISA
CCR5	C-C chemokine receptor type 5
CD4 receptor	cluster of differentiation 4 glycoprotein
CEFs	chick embryo fibroblasts
ChAd	chimpanzee adenovirus
CHO-K1	Chinese Hamster epithelial-like cells
CmpR	chloramphenicol resistance gene
ConM	HIV-1 consensus M sequence
ConS	HIV-1 consensus S sequence
CpG ODNs	CpG oligodeoxynucleotides
CPGR	The Centre for Proteomic and Genomic Research
CXCR4	C-X-C chemokine receptor type 4
Cy3	Cyanine dye 3
ddH_2O	Double Distilled Water
DMEM	Dulbecco's Modified Eagle's Medium
DNA	Deoxyribonucleic acid
DSR	disulphide bonded region
E. coli	*Escherichia coli*
EBV	Epstein–Barr virus
EC50	Half maximal effective concentration
ELISA	enzyme-linked immunosorbent assay
ELISPot	enzyme-linked spot assay
EM	electron microscopy
Env	HIV-1 viral envelope glycoprotein
ER	endoplasmic reticulum
ESCRT	endosomal sorting complex required for transport
Fab	antigen-binding fragment
FACS	Fluorescence-activated cell sorting
Fc	tail region of an antibody that interacts with cell surface (Fc) receptors
FCS	Fetal Calf Serum
FDA	Food and Drug Administration
FITC	Fluorescein isothiocyanate
FL	flexible linker
FSC	forward scatter
FSP	fusion peptide
g	gravitational force
g	gram
Gag	group specific antigen
Gag^M	subtype C mosaic Gag
GNL	*Galanthus nivalis* lectin
gp120	HIV-1 Env glycoprotein 120 subunit
gp41	HIV-1 Env glycoprotein 41 subunit
HA_2	influenza viral hemagglutinin subunit 2
HEK293	human embryonic kidney cells
HEK293T	human embryonic kidney cells SV40 large T antigen
HeLa	Human cervical epithelial cells
HESN	HIV-exposed seronegative
HIV	human immunodeficiency virus
HLA	human leukocyte antigen

HMSS	honeybee melittin protein signal peptide
HR	α-helical coiled coil
HRP	Horseradish peroxidase
HVTN	The HIV Vaccine Trials Network
ID50	plasma/serum dilution causing a 50% reduction of relative light units
IgG	Immunoglobulin G
IN	viral enzyme integrase
IP	Modification to HIV-1 Env: I559P mutation
IRES	internal ribosome entry site
l	litre
LB	Luria Bertani
LC-MS	liquid chromatography–mass spectrometry
lncRNA	long non-coding RNA
Log	logarithm with base 10
LTRs	Long terminal repeats
M	molar
MA	matrix (P17)
MFI	mean fluorescent intensity
MHC	major histocompatibility complex
min	minutes
miRNA	microRNA
ml	millilitre
mm	milimeter
mM	millimolar
MOI	multiplicity of infection
Mos	Mosaic sequence
MPER	membrane-proximal external region
MW	molecular weight
nAb	(autologous) neutralising antibody
NC	nucleocapsid (P7)
Neo(RC)	Neomycin resistance cassette
NFL	native flexible linker
ng	nanogram
nm	nanometer
nM	nanomolar
NHP	non-human primate
NICD	The national institute for communicable diseases
NIH	National Institutes of Health
NLR	nucleotide-binding oligomerization domain-like receptors
Nrf	negative regulatory factor
NYVAC	attenuated vaccinia virus strain, Copenhagen isolate
O/N	overnight
PBS(T)	Phosphate-buffered saline (+0.1% Tween20)
pCAP	core sequence of porcine circovirus type I capsid promoter
pCMV	human cytomegalovirus immediate-early enhancer and promoter
PCR	Polymerase chain reaction
PEI	polyethylenimine-branched
Pen/Strep	Penicillin Streptomycin mixtures
pfu	plaque forming units
pMExT	plasmid for Mammalian Expression with tPA leader
PR	viral enzyme protease
PrEP	Pre-Exposure Prophylaxis
pSSPEx	plasmid Shuttle and Selection for Pox Expression
QC	Quality control
Rev	regulator of expression of viral proteins
rhCMV	rhesus cytomegalovirus (attenuated)
RK13	Rabbit kidney cells
rpm	rounds per minute
rVSV	Recombinant vesicular stomatitis virus (attenuated)
SAMRC	South African Medical Research Council
SCID	severe combined immunodeficiency
SDS PAGE	sodium dodecyl sulfate and polyacrylamide gel electrophoresis
SEC	Size Exclusion Chromatography
SEM	standard error of the mean
SHIP	The Strategic Health Innovation Partnerships
SHIV	SIV but Env adapted from HIV-1 Env sequences
SIV	simian immunodeficiency virus
SOS	Modification to HIV-1 Env: a disulfide between residues 501 and 605
SOSIP	Modifications to HIV-1 Env: SOS, a disulfide between residues 501 and 605; IP, I559P mutation
SSC	side scatter
Tat	trans-activator of transcription
TF	trans-frame protein
TfH cells	T follicular helper cells
TM(D)	transmembrane domain
tPA	tissue plasminogen activator
TR	viral enzyme reverse transcriptase
t-test	Student's t-test
UCT	University of Cape Town
UFO	uncleaved pre-fusion Env trimer
UNAIDS	Joint United Nations Programme on HIV/AIDS
V	Volt

V(1-5)	gp120 variable regions 1-5
v/v	volume over volume
VACV	vaccinia virus
Vif	viral infectivity factor
VLPs	virus-like particles
Vpr	viral protein R
Vpu	viral protein U
vs	versus
w/v	weight over volume
WT	Wild type
α	anti

ABSTRACT

Despite huge strides being made towards decreasing the number of individuals getting newly infected with HIV-1, and in reducing AIDS-related deaths, unfortunately current predictions are that the 2020 UNAIDS goals (90-90-90 targets, where 90% of people living which HIV-1 are diagnosed as such, from which 90% will will receive sustained antiretroviral therapy, resulting in viral suppression in 90% of these individuals by 2020) are out of reach. This of course means that the numbers of newly infected indivuals and AIDS-related deaths will be above the target derived from the 2020 UNAIDS goals. The development of an effective HIV vaccine could therefore be an important step towards realising these objectives. In work done for this thesis, a heterologous HIV-1 vaccine platform regimen was developed using antigen sequences from the predominant circulating HIV-1 subtype (subtype C) in South Africa. Specifically, this involved use of the envelope glycoprotein sequence of the CAP256 superinfecting virus (CAP256_SU) from the CAPRISA 002 cohort, and a mosaic Gag sequence which resulted in robust autologous Tier 2 neutralisation of CAP256_SU pseudovirions.

The envelope glycoprotein sequence was modified so as to replace the native leader sequence with the tissue plasminogen activator leader, the furin cleavage site with a glycine rich flexible linker, and to introduce an I559P mutation. DNA and modified vaccinia virus Ankara (MVA) vaccines were generated where Env was truncated to gp150, thereby retaining the transmembrane domain and a partial cytoplasmic tail (Env). The Env sequence for the protein vaccine was further trimmed by removal of the transmembrane domain to give gp140, leading to a soluble, secreted protein (soluble Env). This allowed for the latter vaccine to be affinity purified using lectin (soluble Env (GNL)), and after generating stable cell lines, soluble Env yields were high enough to enable size exclusion chromatography which allowed isolation of the trimeric fraction of Env as determined by molecular weight (soluble trimeric Env). A C-terminal His-tagged version of soluble Env was generated as well. Surprisingly, the folding of Env-His was inferior to soluble Env, with a switch in profile from mainly trimeric Env to mainly monomeric Env. Nevertheless, soluble Env-His (GNL) and soluble trimeric Env-His were assessed for the presence of Env broadly neutralising antibody (bnAb) epitopes in an ELISA assay. The V3-glycan supersite (binding of bnAbs PGT128 and PGT135), the CD4-binding site (VRC01) and the V2-glycan site (PG9) were detected for both Env-His (GNL) and soluble trimeric proteins, whereas low signals for PG16, PGT145 and CAP256-VRC26.08, bnAbs which specifically recognise Env trimers in a native-like conformation, were only detectable for soluble trimeric Env-His.

Soluble Env (GNL) was subsequently used as a protein vaccine in rabbits to test the immunomodulatory effects of the two adjuvants AlhydroGel (similar to alum) or the MF59-like squalene-based oil-in-water nano-emulsion AddaVax. Soluble Env (GNL) adjuvanted in AlhydroGel resulted in improved immune response in rabbits, with significantly higher serum binding antibodies to soluble Env (GNL) and scaffolded CAP256 V1V2-loop in comparison to AddaVax and unadjuvanted protein. Furthermore, significantly higher neutralisation titres to Tier 1A subtype C virus (MW965.26), in combination with an improved breadth to subtype C Tier 1A and 1B viruses, were observed in the AlhydroGel group. However, no neutralisation of Tier 2 viruses was detected. Nonetheless, AlhydroGel was selected as the best protein adjuvant for all further rabbit immunogenicity studies. Furthermore, in all subsequent experiments, soluble trimeric Env was used as a protein vaccine.

DNA and recombinant MVA vaccines were generated using a membrane anchored gp150 (Env) with the aim that co-expression with mosaic Gag (Gag^{M}) would lead to the incorporation of Env into Gag virus-like particles (VLPs). Electron microscopy of cells expressing $Env+Gag^{M}$ from DNA and recombinant MVA vaccines verified VLP formation from these constructs, and the presence of Env was observed in VLPs purified using a two-step OptiPrep gradient centrifugation protocol. The presence of Env bnAb epitopes in cellular membrane-bound Env was verified by qualitative immunofluorescent microscopy of live-cell stainings and a quantitative FACS assay. The same bnAb epitopes as for the Env protein vaccine were detectable, including bnAbs recognising only native-like Env trimers (PG16, PGT145 and CAP256-VRC26_08). However, expression levels of native-like Env trimers were lower, at approximately 20% when normalised to VRC01.

These HIV-1 DNA, rMVA and soluble trimeric Env protein vaccines were tested in different heterologous vaccine platform immunogenicity studies in rabbits. These consisted of either priming with two recombinant MVA vaccines and boosting with three protein vaccines (MMPPP), or priming with DNA vaccines followed by two MVA vaccines, followed by two protein vaccines (DDMMPP). Furthermore, the inclusion of Gag^{M} into the DNA and MVA vaccines was compared to use of Env alone. Both vaccine regimens resulted in binding antibodies to soluble trimeric Env and a scaffolded CAP256 V1V2-loop; however, these were induced by MVA and protein vaccines, but not by DNA vaccines. Despite the lack of Env binding antibodies after DNA vaccination, better neutralisation was observed for the DDMMPP regimen compared to MMPPP, resulting in higher sera neutralisation titres towards vaccine-matched, autologous Tier 2 CAP256_SU virus. Most encouragingly, when compared to Env alone, the inclusion of Gag ($Env+Gag^{M}$) into DNA and MVA vaccines improved the immunogenicity of the DDMMPP regimen even further. For $Env+Gag^{M}$ DDMMPP, more animals developed Tier 2 neutralising antibodies, and improved titres, whereas Tier 2

neutralisation in general started to develop after fewer vaccinations, as for most rabbits this was observed after the second MVA inoculation.

In an attempt to improve the spike density of Env on VLPs and the plasma membrane, two Env chimaeras were made replacing parts of gp41 with the corresponding elements of influenza A H5 haemagglutinin (HA_2) (Env:HA_2 chimaeras). Increased Env spike density was observed in a previous study using this strategy for the gp41 transmembrane domain and cytoplasmic tail (gp140HA_2tr). A similar construct was generated here for CAP256_SU and a second chimaera was included replacing the whole of gp41 with HA_2 (gp120HA_2). Surprisingly, in experiments where VLPs were purified from OptiPrep gradients or the whole-cell bnAb FACS assay conducted with these Env:HA_2 chimaeras, there was no evidence of increased spike density on VLPs or the plasma membrane as compared to Env. Furthermore, the folding of Env was severely impacted, especially regarding gp120HA_2 where no binding of PG16, PGT145 and CAP256 VRC26.08 - bnAbs recognising native-like Env trimers - was observed. Although results for gp140HA_2tr was improved over gp120HA_2, in general the data for gp150 (Env) was superior in both the bnAb live-cell staining and FACS assay. Consequently, when both Env:HA_2 chimaeras in combination with Gag^M were tested in the DDMMPP regimen, no improvement was observed with regard to autologous Tier 2 neutralisation. For rabbits receiving gp120HA_2, no animals developed Tier 2 nAbs, whereas for gp140HA_2tr, Tier 2 neutralisation in general developed later and to lower titres compared to Env+Gag^M.

In conclusion, different HIV-1 DNA, recombinant MVA and protein vaccines were generated and characterised both *in vitro* and *in vivo,* leading to a vaccination regimen that induced both high titre Env binding and vaccine-matched Tier 2 neutralising antibodies in rabbits. Furthermore, a new Env sequence, the first from the South African CAPRISA cohort, has been added to the small list of Env sequences that can induce Tier 2 neutralisation.

CHAPTER 1: LITERATURE REVIEW

Infection with the retrovirus known as human immunodeficiency virus type 1 (HIV-1) causes acquired immunodeficiency syndrome (AIDS) due to the progressive depression of cell-mediated immunity [1-4]. The origin of HIV is most likely zoonotic transmission(s) of a simian retrovirus affecting primates in west and central Africa, possibly by hunting or slaughtering infected animals and/or handling of uncooked diseased meat [5]. Although it is thought that this event happened between 1915 and 1945 [5], and with the oldest sample known sample containing HIV found in Congo dating to 1959 [6-8], a clinical description of AIDS was only published in 1981 after reports of homosexual men presenting with a series of unexplained opportunistic infections and rare cancers [9]. The main modes of HIV transmission (in order of importance) are via 1) unprotected sexual contact with an infected person; 2) bodily fluids (blood and blood products) mainly through use of contaminated hypodermic needles or transfusion of infected blood or donor organs, although the latter is much less likely nowadays with adequate screening; and 3) mother-to-child transmission during pregnancy, delivery and/or breastfeeding [10-12].

1.1 HIV origin

Two types of HIV have been identified: these are HIV-1 and HIV-2, with the latter originating from a simian retrovirus found in the sooty mangabey [13-18] and compromising 8 lineages mainly confined to West Africa [19]. HIV-1, however, is ascribed to four unconnected zoonotic transmissions giving rise to groups M, N, O and P [20-23], with groups M and N originating from the chimpanzee (*Pan troglodytes troglodytes)* and groups O and P from gorillas (*Gorilla gorilla gorilla*) [20, 21, 24, 25]. The global pandemic of HIV-1 can be traced back to group M, which is further classified into nine subtypes (A-D, F-H, J and K) [26]. Furthermore, recombination between subtypes has resulted in numerous circulating recombinant forms (CRFs) [26]. The global prevalence of group M subtypes and CRFs has a very distinct distribution (***Figure 1.1***), with subtype C being the predominant subtype in sub-Saharan Africa and South Africa [26-29].

1.2 HIV-1 epidemiology

Based on the 2018 data provided by Joint United Nations Programme on HIV/AIDS (UNAIDS), almost 75 million [58.3 million – 98.1 million] people have become infected with HIV since the start of the pandemic, and 32 million [23.6 million – 43.8 million] people have died from AIDS-related illnesses [30]. Upon closer inspection of the global distribution of this epidemic, it becomes clear that developing countries, especially those situated in eastern and southern Africa, carry the largest burden in people living with HIV, new HIV infections and deaths from AIDS (***Figure 1.2A-C***) [30-32]. For instance, of the ~5000 new daily infections with HIV-1 in

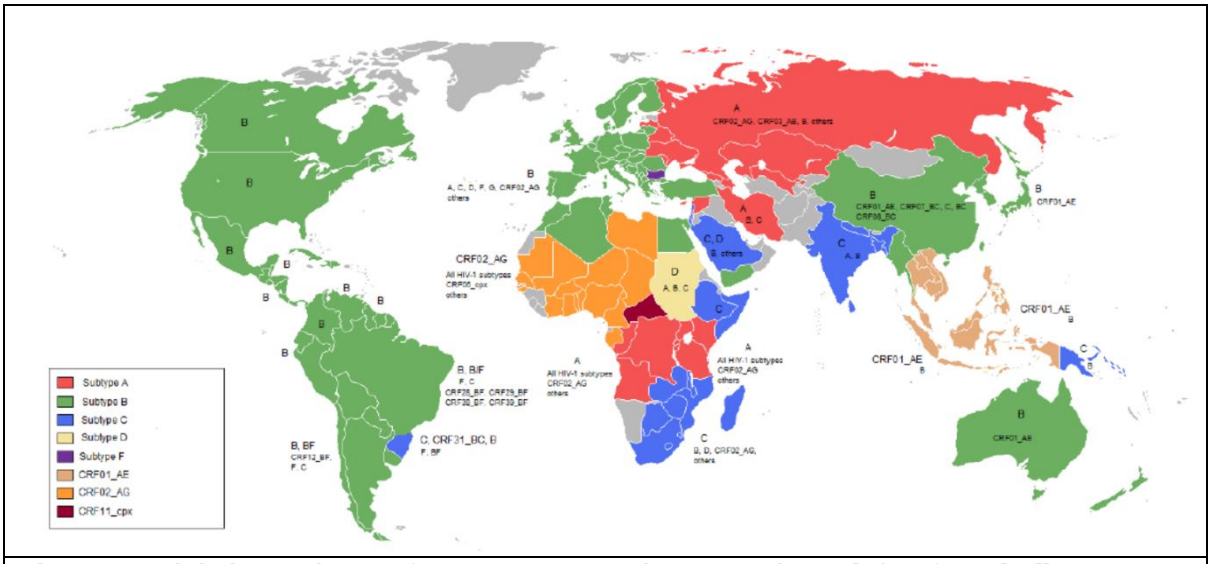

Figure 1.1 Global prevalence of HIV-1 group M subtypes and CRF [taken from: [29]]

2018, 61% occurred in sub-Saharan Africa. Within this region, adolescent girls and young women are most vulnerable to HIV infection with 80% of new infections among adolescents aged 15–19 years in girls, meaning that young women aged 15–24 years are twice as likely to be living with HIV than men [30-32]. Although gains have been made in reducing new infections from a peak in 1997 (2.9 million [2.3 million – 3.8 million]), and of people dying from AIDS-related illnesses (peak 2004, 1.7 million [1.3 million – 2.4 million]), in 2018 these numbers were still staggering at 1.7 million [1.4 million – 2.3 million] new infections and 770 000 [570 000–1.1 million] AIDS-related deaths [31].

1.3 The structure of the HIV-1 virion

HIV-1 virions assembles at the host cell plasma membrane into near-spherical structures to form particles of roughly 120-200nm, encapsulating two copies of the positive-sense RNA genome and viral enzymes required for replication. This is encompassed by a lipid bilayer, taken from the host cell during budding, which has a protein shell on its inside formed by the unprocessed Gag polyprotein, and contains the viral trimeric glycoprotein trimers (Env) that are required for viral entry into target cells (***Figure 1.3A-C***) [33-37]. In a final maturation step after viral budding, the viral Gag polyprotein precursor is proteolytic cleaved, resulting in the iconic conical shape of the capsid and rendering the virion infectious [37].

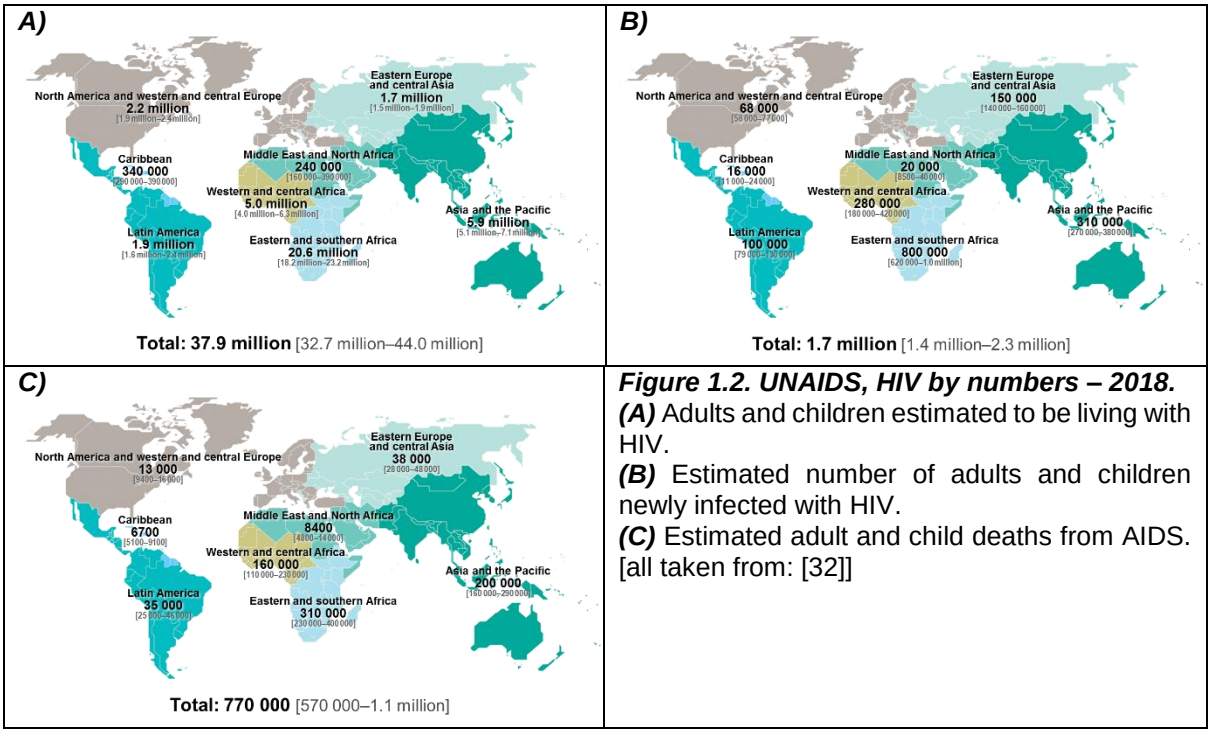

Figure 1.2. UNAIDS, HIV by numbers – 2018.
(A) Adults and children estimated to be living with HIV.
(B) Estimated number of adults and children newly infected with HIV.
(C) Estimated adult and child deaths from AIDS.
[all taken from: [32]]

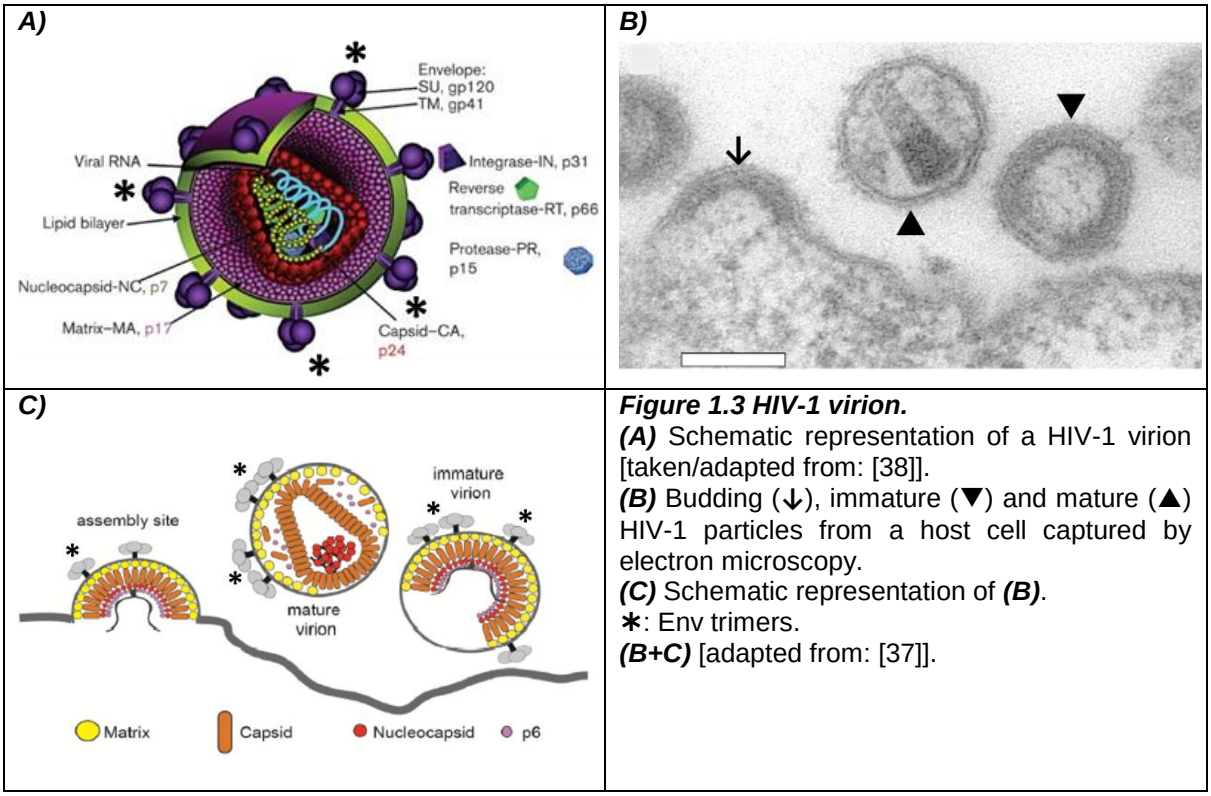

Figure 1.3 HIV-1 virion.
(A) Schematic representation of a HIV-1 virion [taken/adapted from: [38]].
(B) Budding (↓), immature (▼) and mature (▲) HIV-1 particles from a host cell captured by electron microscopy.
(C) Schematic representation of ***(B)***.
✱: Env trimers.
(B+C) [adapted from: [37]].

1.4 The HIV-1 genome

The ssRNA viral genome, present in two copies protected by the viral capsid within the virion, is nearly 10kbp in length and contains nine genes which encode for 15 different proteins in

between 5' and 3' terminal repeats (LTR) (***Figure 1.4***). Transcription of three of these genes results in translation into polyproteins, with *env*, from a spliced mRNA, being translated into a gp160 glycoprotein which is proteolytically cleaved by host cell-derived furin into the extracellular protein gp120 (SU) and the transmembrane protein gp41 (TM). In mature virions, non-covalently linked gp120-gp41 is present as a trimer (native Env trimer) and is responsible for target cell entry through the engagement of the CD4 receptor (cluster of differentiation 4 glycoprotein) and co-receptors CCR5 (C-C chemokine receptor type 5) or CXCR4 (C-X-C chemokine receptor type 4) on the plasma membrane. Secondly, *gag* also provides structural proteins. The 55kDa protein precursor is cleaved into P17, P24, P7, and P6 proteins upon viral maturation, this time by the viral protease within virions (***Figure 1.3***). Each component of Gag plays a crucial role in viral assembly and maturation, with P17 (matrix (MA)) targeting Gag towards the plasma membrane where it assembles as an inner shell against the membrane directing virion assembly, and it is involved in anchoring the gp160 glycoprotein [39-43]. Upon cleavage of Gag during virion maturation, P24 or Capsid domain (CA) multimerises into the conical shaped capsid [44, 45]. Before cleavage, P7 (Nucleocapsid, NC) is essential for the recruitment of the viral genome into the virion, after maturation it associates with the viral genome within the core and is vital in the initiation of reverse transcription of the viral genome during early target cell entry [43, 46-48]. Finally, P6 not only is important in the incorporation of Vpr into the virion but plays a crucial role in recruiting the host cell endosomal sorting complex required for transport (ESCRT) to initiate viral budding [49-53]. Next to the 55kDa Gag precursor, a 160kDa Gag-Pol polyprotein is expressed from an overlapping reading frame at a ratio of 20:1 due to an intentional ribosomal frameshift in Gag translation [54, 55]. Besides coding for MA, CA, NC, trans-frame protein (TF), the Gag-Pol polyprotein precursor produces the viral enzymes protease (PR), reverse transcriptase (RT), and integrase (IN) [34, 56]. Whereas PR cleaves both Gag and Gag-Pol polyprotein precursor during virion maturation, both RT and IN are involved in the early event phase of target cell infection with RT converting the HIV-1 viral genomic RNA into double-stranded DNA and IN facilitating random integration of this into the target cell genome [34, 57-61].

The final six genes encoded by HIV-1 are the regulatory genes *rev* (regulator of expression of viral proteins) and *tat* (trans-activator of transcription), both generated by mRNA splicing and the accessory genes *vif* (viral infectivity factor), *vpr* (viral protein R), *vpu* (viral protein U) and *nef* (negative regulatory factor). Interaction between Tat and the 5' and 3' LTRs regulates viral gene expression, whereas Rev switches mRNA splicing during early and late stages of infection [62-65]. Three accessory genes are involved in modulating the cellular immune response. Firstly, Vpu suppresses the MHC class I response by downregulating HLA 1 [66]. Vif promotes the degradation of the antiviral restriction factor APOBEC3G [67, 68]. Whereas

Nef down-regulates HLA 1 and 2 molecules on the cell surface [69]. Furthermore, Vpu assists with gp160 targeting towards the plasma membrane by downregulating CD4 and thereby preventing trapping of Env by CD4 in the ER [70-72]. An additional role to immune suppression has been ascribed to Nef as well, in which it decreases CD4, CXCR4 and CCR5 to prevent superinfection [69]. The final protein, Vpr, allows for the accumulation of viral mRNA by inducing a G2 cell-cycle arrest in the host cell and assists in macrophage infection [73]. This might however not be the full story, as a predicted product in the negative strand ORF in the HIV-1 Class M genome is expressed in HIV-1 infected patients and induces as specific cellular and humoral response [74-78]. Although the function of this putative transmembrane protein called antisense protein (ASP) is unknown, *in vitro* experiments of chronically infected cell lines, show translocation from the nucleus to the plasma membrane and inclusion into virion upon the right stimulation [74]. Furthermore, reports suggest that the HIV-1 genome can express non-coding RNAs such as microRNA (miRNA) and long non-coding RNA (lncRNA) [79]. However, because of the low expression levels of these products, it is unclear whether these have any functionality *in vivo*.

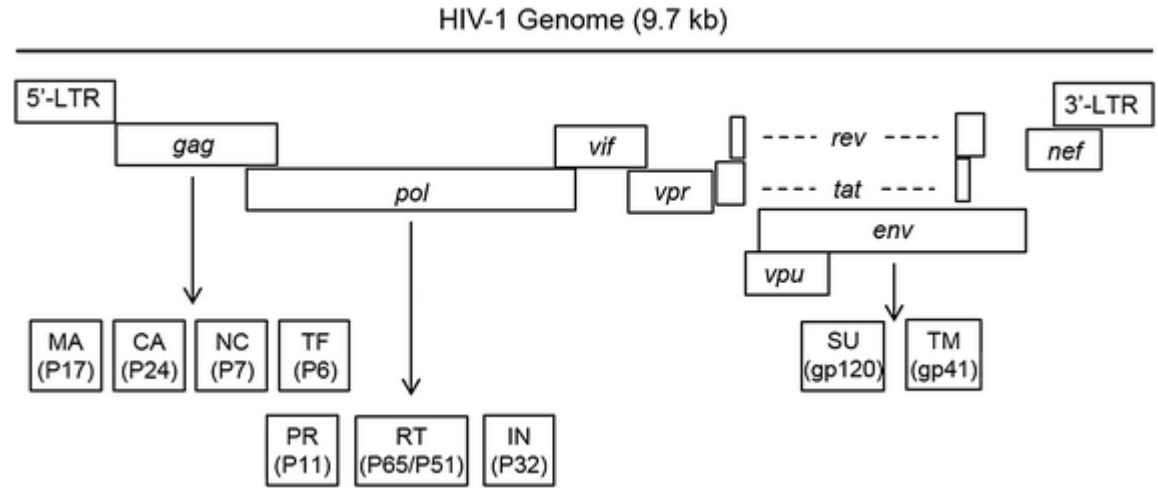

Figure 1.4. Genomic organisation of HIV-1 integrated DNA.
Genes are depicted in *italics* in their representative orientation, and dotted lines indicate RNA splicing event to generate those particular genes. Each arrow specifies proteolytic cleavage events to generate products from polyprotein precursors, with the molecular weight of thus generated proteins in brackets below. *LTR* long-term repeat, Gag (group-specific antigen), MA (matrix protein), CA (capsid domain), NC nucleocapsid, TF (trans-frame protein), Pol (polymerase), PR (protease), RT (reverse transcriptase), IN (integrase), Env (envelope protein), SU (surface membrane protein), TM (transmembrane protein), Vif (viral infectivity factor), Vpr (viral protein R), Vpu (viral protein U), Rev (regulator of expression of viral proteins), Tat (trans-activator of transcription) and Nef (negative regulatory factor) [taken from: [43]].

1.5 Structural characteristics of the Env glycoprotein

A functional HIV-1 Env glycoprotein spike consists of three gp120 molecules, non-covalently linked to three gp41 subunits which anchor the trimeric structure into the virion membrane

[80]. The exterior gp120 protein modular structure consists of five conserved and five variable loops (***Figure 1.6***). Within the conserved regions, several cysteine residues are present which are essential in the formation of a well-folded Env protein by forming intramolecular disulphide bonds [81-83]. Upon interaction with CD4 receptor the gp120 trimer undergoes a conformational change, forming an inner domain, an outer domain and a bridging sheet that leads to surface-exposure of the variable loops [84]. Flanking the aforementioned transmembrane domain, gp41 has an extracellular ectodomain and cytoplasmic tail (***Figure 1.6***) (Checkley et al., 2011). The ectodomain contains a N-terminal fusion peptide and C-terminal membrane-proximal external region (MPER) flanking two α-helical coiled coils (HR1 and HR2) which are split by a disulphide bonded region (DSR) that is important for association between the gp120 and gp41 subunits [85-88].

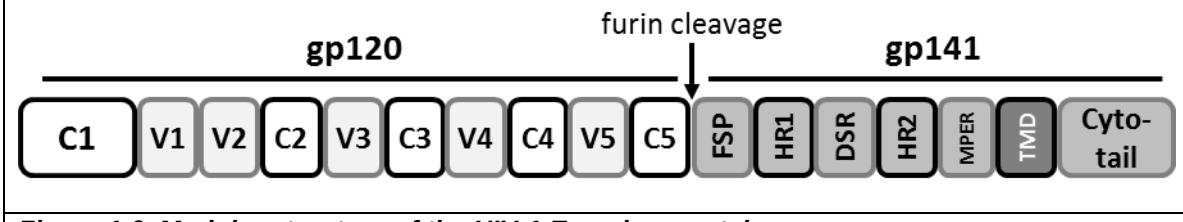

Figure 1.6. Modular structure of the HIV-1 Env glycoprotein.
Linear map of the gp160 precursor protein before furin cleavage. C(1-5): conserved regions, V(1-5): variable regions, FSP: fusion peptide, HR(1-2): α-helical coiled coils, DSR: disulphide bonded region, MPER: membrane-proximal external region, TMD: transmembrane domain and Cyto-tail: intracellular cytoplasmic tail.

Protein crystallography experiments resolving the structure of different versions of Env have further aided in understanding the function of the different domains of the Env protein. The trimer presents gp120 in a characteristic mushroom shape with a distinctive 3-blade propeller on top, with gp41 as a pedestal-like structure at the base of the trimer which anchors it in the viral membrane (***Figure 1.7*** for diagrammatic representation) [89-92]. For gp120 this has elucidated some important characteristics for immune evasion where 1) the positioning of the V1V2 region at the trimer apex restricts access to the CD4 binding site below [92]; 2) access to this region is further hindered by a number of neighbouring glycans [93, 94]; 3) with another set of conserved glycans, this time at the base of the V3 region and 4) the combination of the V1V2 region and the solitary glycan N197 in the V2 region severely obstructs access to the V3 region [90, 92, 95].

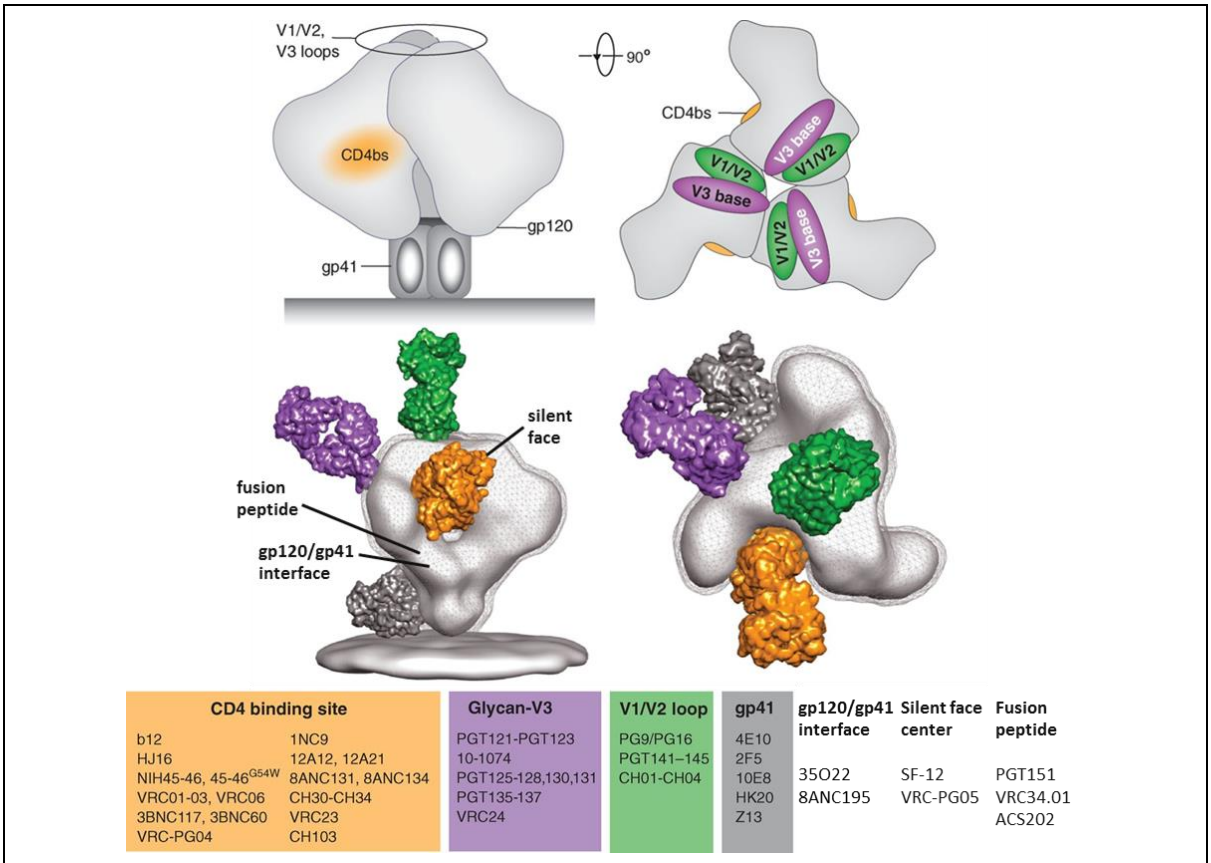

Figure 1.7 Diagram depicting the structure of the Envelope trimer (includes antibody binding sites).
The main regions in Env which are targeted by broadly neutralising antibodies are colour coded (orange: CD4 binding site, purple: V3-glycan supersite, green: V1/V2 region and grey: MPER), with respective, representative broadly neutralising F(ab)s shown approximately to scale (NIH45-46, PGT128, PG16 and 2F5) or lines indicating the approximate region for the gp120/gp41 interface, fusion peptide and silent face centre (under Fab NIH45-46). Table depicts additional examples of bnAbs for the respective regions in Env [adapted from: [96]].

1.6 HIV-1 and immune evasion

Several unique features in HIV-1 are responsible for proficient evasion of the human immune system (***Figure 1.8***), and most of these characteristics are hampering the design of an effective prophylactic vaccine. HIV-1 can only infect cells which express the CD4 receptor and co-receptors CCR5 or CXCR4 on their plasma membrane. Unfortunately, these CD4+ cells are macrophages, dendritic cells and especially helper T cells (specifically CD4+ T cells), which are an integral part of the adaptive immune response and which will be lost upon persistent infection. Not only are CD4+ cells killed as a result of infection and/or viral replication, but it has also been shown that apoptosis can be induced in uninfected CD4+ bystander cells. This can lead to severely impaired lymph nodes, which generally consist of a large quantity of CD4+ target cells or antigen-presenting cells [97-99]. This can be a fairly slow process, as after integration of the HIV-1 viral DNA into the host cell genome, the virus generally replicates extremely slowly or can even lie dormant for a prolonged amount of time,

thus creating a latent HIV-1 reservoir. This trait amplifies the effect of the broad sequence diversity observed in HIV-1. The high error rate of the viral reverse transcriptase, 1–10 mutations/genome/replication cycle, is the underlying mechanism of this sequence variability and can lead to 5–10% sequence divergence in a single infected person [99]. From this, one can imagine that a Darwinian environment evolves in which mutations in HIV-1 allows escape from the surveillance of the (adapting) immune system.

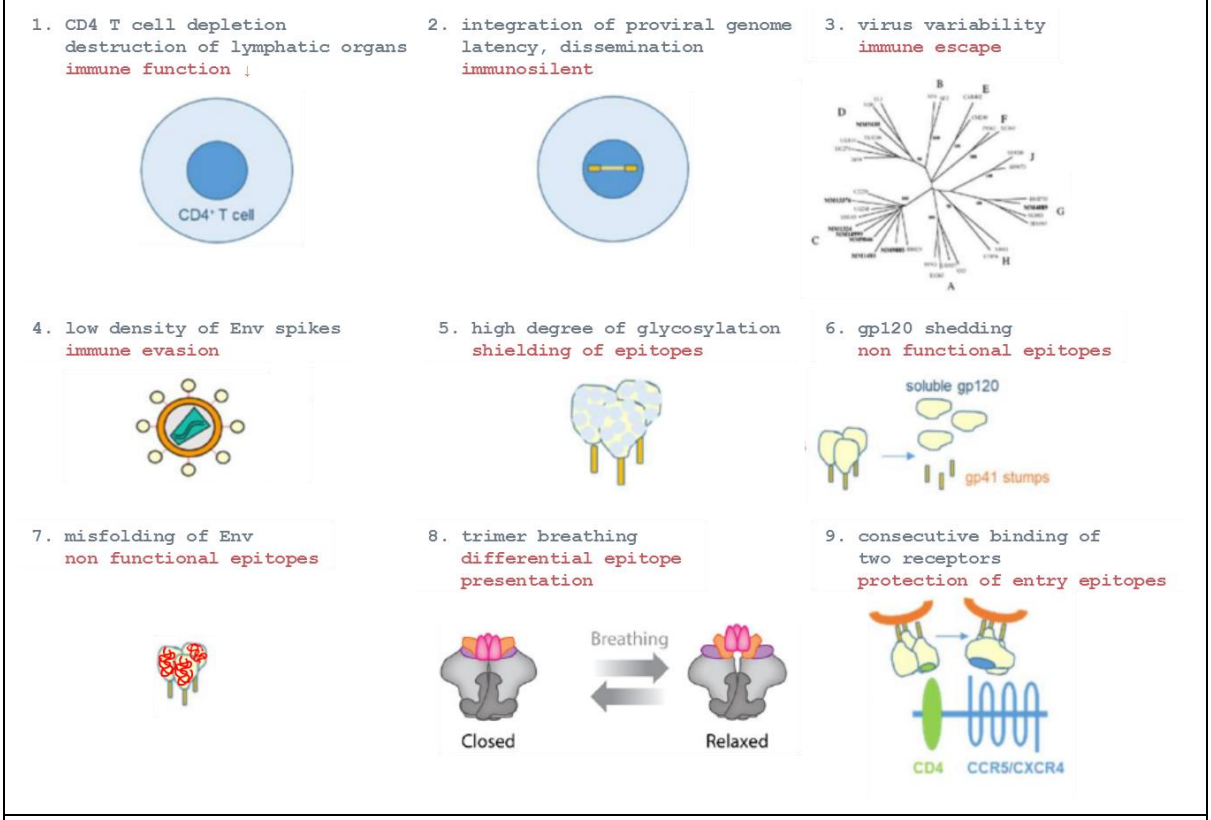

Figure 1.8. Main features in HIV-1 underlying immune evasion. [Adapted from [99, 100]].

Considering that Env is the only viral protein present on the outside of the HIV-1 virion (***Figure 1.3***), and is therefore an ideal target for the immune response to prevent infection, an anthrompomorphic observer might conclude that the virus has gone to great lengths to keep the immunogenicity of the Envelope glycoprotein to a minimum. The HIV-1 virion itself has an extremely low Env surface density (~14 spikes per virion), which could hamper the immune response by preventing cross-linking between surface-bound antibodies and/or induction of an effective B-cell response, due to the large distance between spikes [34, 101-105]. In the host cell, Env is initially produced as the protein precursor gp160 and entered into the secretory pathway, where it multimerises into trimers in the endoplasmic reticulum (ER) with further processing and cleavage into gp120 and gp41 by furin proteases taking place in the Golgi [34, 99, 106, 107]. When in the ER, Env gets heavily glycosylated, acquiring approximately half of its molecular weight in glycans, thereby protecting immunogenic regions

with a glycan shield [99, 108-110]. Because of the non-covalent link between gp120 and gp41, the two subunits can readily dissociate, leading to unbound, monomeric gp120 and gp41 stumps on the plasma membrane and virion in a process called shedding. Both dissociated components will present immunodominant, non-neutralising epitopes, which can divert the antibody-based immune response towards non-neutralising epitopes in a similar way as misfolded and non-functional Env epitopes [99, 111, 112]. In a process called breathing, the native Env trimer can switch between conformations which can lead to exposure of different epitopes, further confounding the immune response [99, 100, 113]. In a final immune-protective measure, although the binding of Env to CD4 leads to a conformational change opening up the native trimer in order to present the binding epitopes to the co-receptor, this happens in close proximity to the plasma membrane, therefore hampering access of antibodies that could potentially prevent cell entry of the virion [99, 114].

1.7 The neutralising antibody response during natural infection

As mentioned previously, the only protein presented on the HIV-1 virion is Env. It is therefore not surprising that although antibodies to other HIV-1 proteins do develop, Env is the main target for the antibody response in an infected person. In general, this response starts with the production of binding Abs, followed by strain-specific neutralising antibodies (nAbs, autologous) and these sometimes develop into cross-neutralising antibodies [115]. The initial response consists of non-neutralising antibodies, with antibodies against free gp41 and gp120 in general developing within the first month of infection [116]. This is followed by the appearance of autologous nAbs which can take between 3 to 12 months to develop [110, 117]. In general these nAbs are targeted towards the V1V2 or V3 region, although interestingly for HIV-1 subtype C, the C3-V4 region is more commonly targeted by these strain-specific neutralising antibodies [118-120]. However, both these non-neutralising and strain-specific neutralising antibodies have negligible effect on viraemia [110, 116, 117]. The latter probably due to their slow development from which the circulating virus can readily escape via the mechanisms outlined in ***Section 1.6*** [110, 117].

Depending on the criteria used to define broadly cross-neutralising antibodies (bnAbs) and/or study cohort, 10-50% of infected individuals develop these bnAbs [121-129]. An extremely small proportion of these individuals, defined as elite neutralisers, go on to develop potent, cross-clade bnAbs which are able to neutralise the bulk of HIV-1 viruses [125]. In most cases the development of this bnAbs response takes over 2.5 years, at which stage the virus has already established a latent reservoir [129, 130]. It is therefore thought that there is minimal clinical advantage of these bnAbs for the infected individual by then, although some viraemic control has been suggested [121, 127, 131, 132]. Interestingly, administration of bnAbs in mice

and non-human primates have shown to be protective in viral challenge models [133-152]. Although the exact mechanisms on how these bnAbs develop in infected individuals is beyond the scope of this thesis, additional background to this can be found in an excellent review from 2018 by Subbaramann *et al.* or the introduction to a paper on HIV-1 vaccine design by Seabright *et al.* in 2019 [151, 153].

Over the last 30 years a large number of these bnAbs from infected individuals have been identified and characterised. It is interesting to note that every single bnAb for HIV-1 identified to date are directed against Env. Initially the identification was an extremely slow and laborious process involving phage display and human hybridomas [154-159]. Advances in technologies such as the use of large cohorts of infected individuals, high throughput screening of culture supernatant from memory B cells and single cell sorting of HIV-1 specific B cells developed in the late 2000s accelerated the identification of bnAbs from HIV-1 infected individuals massively [121, 125, 160-164]. These early identified bnAbs are now usually referred to as First-generation bnAbs, whereas bnAbs identified after 2008/9 are known as Second-generation bnAbs with the latter in general showing increased breadth and potency in their neutralisation profile compared to the First-generation bnAbs. With the identification and characterisation of these bnAbs a picture has emerged of several sites of vulnerability within Env that are specifically targeted (***Figure 1.7***). These regions are nowadays defined as the CD4 binding site, V3 glycan supersite, V1V2 region (trimer apex), MPER region of gp41, the gp120-gp41 interface, silent face centre and fusion peptide [96, 100, 165, 166]. An in depth analysis of the HIV-1 bnAb field lies outside the remit of this thesis. However, a recent review published in 2020 by Wang and Zhang can be recommended for that [166].

The flipside of the identification of the different bnAbs and their site of recognition allows them to be used to interrogate the presence of these epitopes in Env and the structure of Env produced for vaccines. Together with our collaborators at NICD in Johannesburg, South Africa, a panel was selected which allows this for CD4 binding site, V3 glycan supersite, V1V2 region (trimer apex) and MPER region of gp41 (***Table 1.1***). Three of the bnAbs selected (PG16, PGT145 and CAP256 VRC26.08) are of particular interest as they only recognise native-like Env and are the gold standard in assessing correctly folded Env trimers [167]. Whereas F105 and 447-52D, originally identified as bnAbs [168, 169] are nowadays regarded to recognise Env in a particular open state and are as measure of misfolded Env.

Table 1.1 Overview bnAbs and MAbs used for characterisation of Env vaccines in this thesis

bnAb	Neutralisation breadth	Epitope	Native-like trimer	Reference
VRC01	Broad	CD4 binding site	No	[170, 171]
F105	Narrow	CD4 binding site	No	[169]
PGT128	Broad	V3 glycan supersite	No	[172, 173]
PGT135	Broad	V3 glycan supersite	No	[172]
447-52D	Narrow	V3	No	[168]
PG9	Broad	V1V2 region (trimer apex)	No	[161]
PG16	Broad	V1V2 region (trimer apex)	Yes	[161]
PGT145	Broad	V1V2 region (trimer apex)	Yes	[160]
CAP256 VRC26.08	Broad	V1V2 region (trimer apex)	Yes	[174]
10E8	Broad	MPER	No	[175].

1.8 Justification for an HIV-1 vaccine

The decline in both new HIV-1 infections and AIDS-related deaths can for a large part be ascribed to a combined strategy of blood product screening [176, 177], education/counselling of the public and health workers, condom use [178-184], free hypodermic needles for drug users [185], male circumcision [186-189] and antiretroviral therapy (ART) [190-195]. The latter not only prevents disease progression in HIV-1 infected patients but by decreasing viral loads below detectable levels, counteracts transmission to sexual partners and mother-to-child transmission. Furthermore, when given as Pre-Exposure Prophylaxis (PrEP) it can prevent infection [196-198]. However, adherence to life-long antiretroviral medication is challenging [199-204]. The stigmatisation of HIV-1 positive individuals and ART/PrEP usage is another reason for the lack of compliance [205-209]. Whereas costs can form a barrier as well, even after countries start with free ART treatment [210-213]. It is also worth noting that in developing countries and especially in sub-Saharan Africa, there is still a lack of access to treatment for HIV-1 infected individuals [214]. All of this could be compounding factors as to why the current predictions of the 2020 UNAIDS goals (90-90-90 targets, where 90% of people living which HIV-1 are diagnosed as such, from which 90% will will receive sustained antiretroviral therapy, resulting in viral suppression in 90% of these individuals by 2020) will not be reached, leading to higher new HIV-1 infection and AIDS-related death rates then was aimed for under these goals (***Figure 1.9A+B***) [31]. Therefore, the development prophylactic HIV-1 vaccine would

hugely benefit the effort to control the HIV-1 pandemic in a similar way to how vaccines have been able to eradicate or nearly eliminate severe and/or life-threatening infectious diseases such as smallpox [215], measles [216, 217] and polio [218, 219]. Diseases such as malaria, meningitis, diphtheria, hepatitis B, tetanus, mumps and rubella, are now controlled in especially the developed world through vaccines and healthcare management [220]. Although research into a prophylactic HIV-1 vaccine has been hugely frustrating in the last 35 years, the 31% efficacy of a HIV-1 vaccine used in the RV144 clinical trial [221] has reinvigorated the field again, and top experts have suggested that a HIV-1 vaccine with suboptimal efficacy would be sufficient to control the epidemic if combined with other prevention and treatment strategies [222, 223], making the task slightly less daunting.

Figure 1.9. Global numbers in new HIV infections.
(A) The number of new HIV infections, worldwide, 1990–2018 and 2020 target.
(B) The number of AIDS-related deaths, global, 1990–2018 and 2020 goal [both taken from: [31]].

There is reason to be optimistic that an HIV-1 vaccine is achievable. Even though the development of nAbs and bnAbs against Env in HIV-1 infected individuals fails to impact

clininal outcome, when the administration of a select number of bnAbs were tested in non-human primates and humanised mice, this was protective in viral challenge models [133-152]. Furthermore, cell-mediated immune responses to other HIV-1 genes have been implicated in viraemic control. CD4+ and CD8+ T-cell responses especially towards Gag are correlated with decreased viral loads in natural infection of children, long-term non-progressors (HIV-1 positive controlling viral replication, not developing AIDS, viral loads <1000 HIV RNA copies/ml) and elite controllers (as long-term non-progressors but viral loads <50 copies/ml) [224-229]. Interestingly, in so called HIV-exposed seronegative (HESN) individuals, such as observed within commercial sex workers cohorts, persistent T-cell responses towards Gag are low, but detectable [230-232]. Therefore, a cell-mediated immune response could be important in controlling viraemia and potentially disease progression or viral transmission [233]. This suggests that a vaccine regimen combining HIV-1 Env for the induction of an antibody response, together with Gag for generating a cell-mediated response, would have the best chance to succeed.

1.9 Preventative HIV-1 vaccines in clinical trials

It is not by want of effort in the last 35 years that the development of a prophylactic HIV-1 vaccine has eluded scientists. Currently, for instance, there are more than 25 recruiting and/or active phase I HIV vaccine clinical trials ongoing (search on https://clinicaltrials.gov). However, few of these studies make it into Phase IIb/II, with only six completed studies (See ***Section 1.9.1***). Even in these studies, only one (RV144) resulted in modest protection in HIV-1 acquisition [234]. A mechanism in which HIV-1 evades the immune system such as was discussed in section 1.5 might be underlying this lack of success, and specifically the focus in earlier vaccines on immunising with gp120. However, the outcome of these studies have been taken into account, and in recent years two new studies have entered Phase IIb/III testing (discussed in ***Section 1.9.2***). Furthermore, several novel vaccine strategies aimed at inducing broadly neutralising antibodies, dubbed HIV-1 vaccine 2.0 by Professor R. W. Sanders at the 2018 HIV R4P meeting in Madrid [222], are entering vaccine safety testing in healthy volunteers and will be briefly highlighted in ***Section 1.9.3***.

1.9.1 HIV-1 vaccines evaluated in efficacy trials

In the 6 Phase IIb/III studies finished to date, with the vaccine design similar in VAX003 to VAX004 and HVTN 502 to HVTN 503, four different vaccine concepts have been tested in late-phase clinical trials studies (***Table 1.2***).

Table 1.2 Overview of all finalised Phase II/III HIV-1 clinical trials investigating prophylactic vaccines

Study	Phase	Period	Site	Volunteers (risk group)	Vaccine regimen	Immune response		Efficacy	Note	Ref
						Desired	Observed			
VAX004	III	1998 - 2003	USA, Europe	MSM, women at high risk*	AIDSVAX B/B gp120 (Subtype B: MN and GNE8) in Alum adjuvant	Humoral	Non-neutralising antibodies ADCVI	No efficacy		[235]
VAX003	III	1999 - 2003	Thailand	Injecting drug users	AIDSVAX B/E gp120 (Subtype B MN and CRF01_AE CM244), in Alum adjuvant	Humoral	Non-neutralising antibodies	No efficacy		[236]
HVTN 502 - STEP	IIb	2004 - 2007	USA	MSM, heterosexual men and women	Ad5 Subtype B gag/pol/nef	Cellular	HIV-1 specific $CD4^+$ and $CD8^+$ responses	No efficacy, increased risk of infection	Stopped pre-maturely due to increased risk of HIV infection	[237-239]
HVTN 503 - Phambili	IIb	2007	South Africa	Heterosexual men and women	Ad5 Subtype B gag/pol/nef	Cellular	HIV-1 specific $CD4^+$ and $CD8^+$ responses	No efficacy, increased risk of infection	Terminated because of STEP study result	[240, 241]

Table 1.2 Overview of all finalised Phase II/III HIV-1 clinical trials investigating prophylactic vaccines (continued)

Study	Phase	Period	Site	Volunteers (risk group)	Vaccine regimen	Immune response		Efficacy	Note	Ref
RV144	III	2003 - 2009	Thailand	Community risk	ALVAC-HIV, and AIDSVAX B/E gp120 in Alum adjuvant	Humoral + cellular	V1V2 binding antibodies ADCC HIV-1 specific IgG3	31.2 % at 42 months 60.5% at 12 months		[234, 242, 243]
HVTN 505	IIb	2009 - 2013	USA	MSM, seronegative for Ad5	DNA Gag, Pol, Nef (Subtype B) and Env (Subtype A, B and C), Ad5 clade B Env and Gag-Pol fusion	Humoral + cellular	$CD4^+$ and $CD8^+$ T-cell responses to Gag + Env Poor tier 1 neutralising antibody titres	No efficacy	Stopped pre-maturely due to lack in efficacy	[244]

* For HIV infection. HVTN: human vaccine trials network; MSM: men who have sex with men; ADCC: antibody-dependent cellular cytotoxicity; ADCVI: antibody-dependant cell-mediated viral inhibition. Ad5: Adenovirus type 5 Table adapted from: [221, 245-247]

In the late 90s, VAX003 and VAX004 were the first prophylactic HIV-1 vaccines to be tested in efficacy studies. In these trials, recombinant Env subunit vaccines were tested to prevent HIV-1 infection by inducing neutralising antibodies [235, 236, 248]. Both studies consisted of bivalent monomeric gp120 protein vaccines adjuvanted in alum, but differed in vaccine antigen depending on trial site, with Subtype B (viral isolates MN and GNE8) in VAX004 (USA and The Netherlands) and Subtype B/E (viral isolates MN and CRF01_AE CM244) in VAX003 (Thailand). Furthermore, different groups at risk of HIV-1 acquisition were tested with MSM (men who have sex with men) and heterosexual individuals in VAX004 compared to injecting drug users in Thailand. However, both studies failed to show any vaccine efficacy in preventing HIV-1 acquisition or affect post-acquisition HIV-1 viraemia [235, 236]. This disappointing outcome can probably be mainly attributed to vaccine design, as these recombinant Env subunit vaccines only induced neutralising antibodies against laboratory-adapted HIV-1 isolates (Tier 1) but failed to induce neutralising antibodies against primary HIV-1 strains in sera from the matching phase I trial [249]. Similarly, sera collected in VAX003 only caused weak and transient neutralisation against Tier 1 HIV-1 isolates [250].

A second vaccine concept was tested in the HVTN 502 (STEP) and HVTN 503 (Phambili) studies: this used a replication defective-adenovirus serotype 5 (Ad5) vector for the expression of Gag, Pol and Nef antigens in order to induce cell-mediated immune response which might result in protection and/or control viraemia [237, 240, 245, 251]. The rationale for this concept can be explained with the observations that a robust T-cell response has been associated with viral control in both nonhuman primate models and more importantly patients which are long term non-progressors after HIV-1 infection [252-256]. In both HVTN 502 and HVTN 503 the same Clade B vaccine was tested, this was matched to the primary circulating HIV-1 virus for HVTN 502 (North America, the Caribbean, South America and Australia), but not for HVTN 503 (South Africa, Subtype C) [237, 240]. Unfortunately, already during the active phase of the HVTN 502 trial, an increase in HIV-1 acquisition was observed in the vaccine arm compared to the placebo group which was associated with circumcision state and pre-existing immunity towards Ad5 [237, 238]. A similar higher rate in HIV-1 infection was consequently observed in the then recently started HVTN 503 study, although without the association of the same risk factors as reported for HVTN 502 [241]. Because of the lack of vaccine efficacy and more importantly, the increased HIV-1 acquisition rates, both trials were terminated prematurely. In a subsequent study in NHPs it was found that chronic infection with Ad5 prior to a rAd5 vaccine containing SIVmac239 Gag, Pol and Nef increased the number of activated CD4+ T-cells, which correlated with an increased acquisition in a SIV challenge model [257]. This would suggest that pre-existing immunity in humans against Ad5 might have led to vaccine-induced increased CD4+ T-cell activation, thereby increasing the pool of HIV-1 target

cells and thus making vaccinees more susceptible to HIV-1 acquisition. Therefore, these findings do underline the importance of avoiding vaccine platforms with circulating pre-existing immunity in the broader population for an effective HIV-1 vaccine.

With HVTN 502 and 503 trials in mind, volunteers recruited from MSM and transgender risk groups in the USA were only enrolled into the Phase IIb HVTN 505 study if they were seronegative for Ad5 and circumcised [244]. In this trial, the Ad5 clade B Env and Gag-Pol fusion protein vaccine was primed with six different DNA vaccines (Subtype B Gag, Pol and Nef and Subtype A-C Env. Again, no vaccine efficacy was observed during this trial, although no increase in HIV-1 acquisition was reported either. The lack of effectiveness combined with the futility of a vaccine only safe in an Ad5 seronegative population, the study was terminated prematurely [244].

Despite disapproval within part of the vaccine research community upon initiating of the study due to a perceived lack of efficacy at earlier clinical testing of the regimen, the RV144 trial conducted in Thailand has so far been the only late-phase study resulting in partial protection in HIV-1 acquisition [234, 258]. The trial aimed at inducing both a cellular and humoral response in heterosexual volunteers by priming with a recombinant canarypox virus prime encoding Gag, Pol and Env (ALVAC-HIV [vCP1521]) which was boosted with ALVAC-HIV plus a bivalent gp120 protein vaccine (AIDSVAX B/E) formulated in the adjuvant alum with antigen sequences matched to circulating subtype B and CRF01_AE isolates [234]. The vaccine regimen resulted in moderate efficacy of 60.5% after one year. However, this declined over time resulting in the reported lower efficacy against HIV acquisition of 31.2% after 42 months [234, 259]. Analysis of immune correlates identified serum IgA binding to Env to correlate directly with the rate of infection, whereas the protective effect of the vaccine was correlated to serum IgG binding to the V1V2-loop [243]. The importance of the V1V2-loop in vaccine efficacy was further emphasised in genetic sieve analysis where improved vaccine efficacy against viruses with the conserved residue K169 (as present in the vaccine) was observed [260, 261].

Although antibody-dependent cellular cytotoxicity (ADCC) wasn't a primary immune correlate, high levels of ADCC combined with low levels of low plasma IgA Env antibodies associated with a reduced risk of HIV-1 acquisition in a secondary analysis [243, 262]. Furthermore, ADCC towards HIV-1-infected CD4+ T cells was observed by several V2-specific monoclonal antibodies that were isolated from participants of the RV144 trial, again stressing the importance of the V1V2-loop in the vaccine efficacy in this study [263]. Interestingly, a comparison between RV144 and VAX003 trials which both used the same protein vaccine revealed that IgG3 responses correlated with protection in RV144 [264]. Re-evaluation of the

CD4+ T-cell data from RV144 trial showed that the vaccine-induced two subsets of polyfunctional CD4+ T-cell, which correlated with decreased HIV-1 acquisition [265]. Some recent gene transcriptome studies using PBMCs isolated from participants of RV144 identified the IRF7 antiviral pathway as a correlate of protection from HIV-1 infection, whereas activation of mTORC1 was associated with the risk of acquisition [266]. It should be noted that all humoral correlates of protection from the RV144 trial are binding antibodies and not neutralising antibodies, and are primarily targeted towards the V2 region in Env, which should be taken into account in vaccine design and efficacy assays in vaccine studies.

Several follow-up studies have been conducted with vaccinees of the RV144 trial, notably RV305 and RV306. In both studies, uninfected participants of RV144 received late boosts with either ALVAC-HIV, AIDSVAX B/E or a combination of both. So far only data from RV305 has been released. In this study volunteers received the two boosts 24 weeks apart 6-8 years after the conclusion of RV144. Transient increases in IgG binding to gp120 and the VV2-loop were reported when AIDSVAX B/E was part of the boosting, but not for ALVAC-HIV alone [242, 267]. Interestingly, increased CD4+ functionality upon stimulation with HIV-1 Env peptides two weeks after each boost was reported for the same groups which displayed an increased humoral response [242].

1.9.2 Ongoing HIV-1 vaccine efficacy trials

Currently, two efficacy trials are still underway, one in Africa and another study outside this continent which started in the second half of 2019 (***Table 1.3***). A third trial (HVTN 702 or Uhambo) which started in 2016 was recently cancelled. This particular study conducted in South Africa was aimed at building on the foundations of the RV144 trial. It was using the same canarypox virus (ALVAC) and boosting with a gp120 protein, but differed in several key elements: 1) antigens were matched to the main circulating subtype in southern Africa (subtype C) in ZM59 for membrane-anchored gp120 for the canarypox platform (ALVAC-HIV [vCP2438]) and TV1.C gp120 Env + 1086.C gp120 Env for proteins; 2) an additional ALVAC-HIV [vCP2438] + bivalent gp120 Env boost was included and 3) a different adjuvant in MF59 was selected for the current study [268, 269]. Unfortunately, from provisional analysis of the data emerged a picture of similar HIV-1 acquisitions rates for vaccinated and unvaccinated participants, and due to this lack in vaccine efficacy, the sponsors decided terminate the trial prematurely [270].

Table 1.3 Overview active Phase IIb/III HIV-1 prophylactic vaccine clinical trials

Study	Phase	Period	Site	Volunteers (risk group)	Vaccine regimen	Desired immune response	Note
HVTN 702 - Uhambo	IIb/III	2016 - 2021	South Africa	Men + women at high risk*	ALVAC-HIV (vCP2438) and Bivalent Subtype C gp120 in MF59 adjuvant	Humoral + cellular	Adaptation of RV144 - Cancelled due to lack of vaccine efficacy in February 2020
HVTN 705 - Imbokodo	III	2017 - 2022	Sub-Saharan Africa	Women at high risk*	Ad26.Mos4.HIV and Trimeric Clade C gp140 in Alum adjuvant	Humoral + cellular	
HVTN 706 - MOSAICO	III	2019 - 2023	USA, Central + South America, Europe	cis-gender men and transgender individuals	Ad26.Mos4.HIV and Bivalent Trimeric Clade C + Mosaic gp140 in Alum adjuvant	Humoral + cellular	

* For HIV infection. Data from: https://clinicaltrials.gov/

Mos: Mosaic sequences generated *in silico* to maximise potential T-cell epitopes

Ad26.Mos4.HIV: Mos1.Env, Mos2.Env Ad26.Mos1.Gag-Pol, Ad26.Mos2.Gag-Pol (Mos: Mosaic sequences generated *in silico* to maximise potential T-cell epitopes)

It should be noted that when the HVTN 702 protocol was tested in a Phase I study (HVTN 100), it did perform better in inducing IgG binding antibodies to vaccine-matched gp120 proteins, and inciting CD4+ T-cell responses upon ZM96.C env protein stimulation, compared to the data from vaccine matched assays for RV144 [268]. However, IgG binding antibodies towards the V1V2-loop in HVTN100 were observed in fewer individuals compared to RV144, which was disappointing as this was the main correlate of protection in that trial. Although the responder rate towards the V1V2-loop was lower in HVTN100, it was still well above predicted 63% threshold needed for 50% vaccine efficacy using a V1V2 correlate of protection model [268]. Strong neutralising antibody responses were measured for highly sensitive Tier 1A isolates, whereas the response rates dropped for slightly less susceptible Tier 1B isolates; no Tier 2 isolates were neutralised [268]. Interestingly, in a vaccine safety study in South Africa (HVTN 097) where the exact regimen of RV144 was combined with a tetanus toxoid vaccine and hepatitis B vaccine, significantly higher cellular and humoral immune responses were measured compared to those in RV144, despite the use of Subtype B/E antigens [271]. It will be interesting whether it can be established if any of these observations from HVTN 100 and 097 are responsible for the failure of the HVTN 702 study.

A new vaccine concept is being tested in the first currently active efficacy trial with the use of mosaic antigens. Mosaic sequences (Mos) are generated *in silico* to maximise potential T-cell epitopes within the antigen, thereby hopefully increasing immunogenicity [272]. Participants from southern Africa in the HVTN 705 (Imbokodo) study will receive a total of four vaccinations with a mixture of four different adenovirus serotype 26 (Ad26) vectors for the expression of Mos1.Env, Mos2.Env Ad26.Mos1.Gag-Pol, Ad26.Mos2.Gag-Pol, with all mosaic sequences based on Group M HIV-1 viruses. For the last two inoculations, vaccinees will also receive trimeric Clade C gp140 protein (isolate C97ZA.012). Therefore both a cellular and humoral response will be anticipated. Although the Ad5 vaccine platform was discredited in the HVTN 502 and HVTN 503 studies, the Ad26 vector is deemed to be much safer in humans [273]. In the APPROACH phase I/IIa clinical trial similar vaccine regimen was tested with the only difference being that Ad26.Mos2.Env wasn't included. In the APPROACH study, all participants developed binding antibodies against vaccine matched clade C gp140, several cross-clade gp140 isolates and the V1V2-loop in 81% of vaccinees. Furthermore, antibody-dependent cellular phagocytosis was detected in 80% of participants after the final boost. Moderate neutralising antibody responses were measured for a highly sensitive Tier 1A isolate, with neutralisation observed against Tier 2 isolates. Apart from these antibody responses, cellular immune responses against Env, Gag and Pol peptide pools were observed in most participants as well [273]. With these exciting results obtained in HVTN 100, HVTN

097 and APPROACH phase I/IIa clinical trials, the results of the Uhambo and Imbokodo studies are eagerly anticipated.

A second Phase III clinical trial (HVTN 706) has started at the end of 2019: this is in design reasonably similar to the HVTN 705 study, but contains a Clade C and Mosaic gp140 HIV bivalent protein vaccine instead. Furthermore, this study is conducted in a geographical region outside of sub-Saharan Africa (USA, Mexico, Brazil, Argentina and Europe), and will enrol cisgender men and transgender individuals having sex with cisgender men and/or transgender individuals, rather than women at risk of HIV-1 acquisition.

Although not HIV-1 vaccine studies, two other essential efficacy trials for HIV-1 prevention are currently underway. HVTN 703/HPTN 081 and HVTN 704/HPTN 085 are both studies into Antibody Mediated Prevention (AMP). Conducted in either women in sub-Saharan Africa (HVTN703) or men and transgender persons who have sex with men in North America, South America, and Switzerland (HVTN704), participants are receiving the anti-Env broadly neutralising monoclonal antibody VRC01 intravenously every 8 week for two years to test if neutralising antibodies can prevent HIV-1 acquisition in a human setting. Complete protection was observed against SHIV challenge in rhesus macaques after infusion of VRC01 [152]. Results for both efficacy studies are expected in late 2020. I do not support these studies for the reason that HIV-1 viral breakthrough events will almost certainly occur because only a single monoclonal antibody is used, which negates the idea of a prevention study.

1.9.3 HIV-1 vaccine 2.0

Discussing all the different HIV-1 vaccine hypotheses currently being tested in Phase I/IIa clinical trials will go beyond the purpose of this review. However, with the recent pre-clinical HIV-1 vaccine studies heavily focussed on inducing broadly-neutralising antibodies (bnAbs) towards circulating HIV-1 sequences (Tier 2) in animal models, I will discuss a subset of Phase I safety studies testing several vaccine concepts aiming to achieve this in humans (***Table 1.4***). These ideas were dissected into four different hypotheses at the 2018 HIV R4P meeting in Madrid, and coined “HIV-1 vaccine 2.0” [222]. Most of these have been covered in a review in the same year by Kwong and Mascola [274]. The first principle was developed around molecular strategies for producing correctly folded Env trimers as protein vaccines which resemble the native trimer on HIV-1 virions (in-depth discussion in **Section 1.10.3**). One of the earliest successful examples of this is soluble, trimeric cleavage-dependent BG505.664 SOSIP Env, which has now entered phase I clinical trials (IVAI W001) [275-277]. Similar studies are also planned for Env protein vaccines ConM SOSIP.v7 and ConS SOSL.UFO.

Table 1.4 Phase I HIV-1 vaccine clinical trials investigating HIV-1 vaccine 2.0

Study	Phase	Period	Site	Healthy volunteers	Vaccine regimen	Desired immune response
IAVI W001	I	2018 - 2020	USA + Kenya	Men + women	Trimeric BG505 SOSIP.664 gp140 in ASO1B adjuvant	Humoral + cellular
HVTN 115	I	2017 - 2019	USA	Men + women	EnvSeq-1 Envs in GLA-SE adjuvant +/- DNA Mosaic-Tre env	Humoral + cellular
IAVI G001	I	2018 - 2020	USA	Men + women	eOD-GT8 60mer with ASO1B adjuvant	Humoral
HVTN 133	I	2019 - 2021	USA	Men + women	HIV-1 gp41 MPER-656 liposome vaccine/alum	Humoral

IAVI: The International AIDS Vaccine Initiative. Data from: https://clinicaltrials.gov/

The next two strategies are collectively known as antibody lineage-based vaccine design or B cell ontogeny-based vaccine design, which is aimed at guiding the immune system through the different stages or B-cell lineages to arrive at the final B-cell producing the intended broadly neutralising antibody [274]. This can potentially be achieved in vaccinees with a series of lineage Env immunogens from individuals who developed broadly neutralising antibodies against Env over time after HIV-1 infection. An approach which was effective in an animal model, using four different gp120 sequences matched to those which developed during natural infection with virus isolate CH505, will be administered as sequential protein vaccines in the Phase I clinical study HVTN 115 [278]. Similar studies are planned for CH505 SOSIP series and Env SOSIP trimers from acute neutralisers.

In a far more specific concept, engagement of specific bnAb germline precursor B cells by specific germline-targeting Env immunogens will be tested to investigate if this will lead to the induction of this bnAb. For the bnAb VRC01, such a strategy has been developed with the germline-targeting immunogen (eOD-GT8) which has progressed to a Phase I clinical study (IAVI G001) [279].

In the final hypothesis, bnAbs are to be induced by epitope focusing to circumvent potential immune-dominant non-neutralising epitopes within the Env sequence. Two different strategies using fusion-peptide targeting immunogen FP8_v1-rTTHC and MPER liposomes have been used successfully in animal models [280-283]. The latter is currently being tested in the Phase I clinical trial HVTN 133.

1.10 Vaccine platforms

Vaccines which are currently approved for the use in humans can broadly be divided in two groups. The first contains whole pathogens which are either live-attenuated or inactivated preparations to reduce or remove the pathogen virulency. Safety concerns (such as reversion of attenuated vaccine, recombination between vaccine and circulating virus and incomplete inactivation) with regards to an HIV-1 vaccine using these whole pathogen approach makes these strategies non-viable options. Therefore, there is an intense focus on the second group of vaccines, which are defined by the use of only a part of the pathogen. This group includes toxoid vaccines, carbohydrate vaccines, conjugate vaccines and antigen vaccines. Antigen vaccines can be either the purified (recombinant) protein or antigen expression from vectors. For HIV-1 vaccines, a broad array of these expression vectors have been tested as vaccine platforms, including naked DNA plasmids, bacteria (such as *Mycobacterium bovis* Bacille Calmette Guerin (BCG)), and replication competent and attenuated viruses. Especially the viral platforms have received a lot of attention in the HIV-1 vaccine research community, with the current focus on adenovirus (Ad) 5 alternatives such as Ad35 and Ad26; poxviral vectors (including ALVAC, NYVAC and MVA); and replication competent viral vectors (for example rhCMV and rVSV). With such a vast array of different vaccine platforms used for HIV-1 vaccines, it is beyond the scope of this thesis to review all of them and the focus will be on the platforms used in this thesis, which is DNA, recombinant MVA and protein vaccines. An excellent review on HIV-1 viral vaccine vectors was recently published by Alayo *et al*. [284].

1.10.1 DNA vaccines

The use of plasmid DNA as a vaccine regimen is a relatively recent development, first explored in mice for an influenza vaccine in the early 1990s [285]. The interest in DNA vaccines can be explained by its multiple apparent advantages in usage: 1) production is relatively cheap, easy and similar between different vaccines; 2) vaccines are thermostable and can be lyophilised for additional stability, thereby decreasing the cost of the supply chain; 3) plasmid DNA has no risk of virulence and is safe in humans even when they are immunocompromised; 4) no anti-vector immunity is anticipated; and 5) multiple antigens can be targeted by combining different vaccines [286]. The main mechanism of action through which DNA vaccines work is by inducing a cellular response to antigens expressed within transfected cells, where antigen presenting cells (APCs) are either activated directly or indirectly within the inoculation site. In the first instance, APCs themselves have taken up the DNA vaccine, whereas in the latter they are activated by non-immune cells which express the antigen after uptake of the DNA vaccine. Subsequent migration of the activated APCs towards draining lymph nodes results in antigen presentation leading to the induction of immune responses [287-291]. Furthermore, antigen

presentation from DNA vaccines by APCs is through the major histocompatibility complex molecules class I, similar as for viral pathogens upon infection [292]. However, it should be emphasised that in general DNA vaccines only induce a short and transient cell-mediated immune response, and usually fail to induce an antibody response. This lack in immunogenicity of DNA vaccines is reflected in the fact that so far, no DNA vaccine has been licensed for use in humans [286]. Nonetheless, they are being investigated in clinical trials for the use in HIV-1 vaccines and although these have mainly been Phase I studies, DNA vaccines were used in the vaccine efficacy study HVTN 505.

Research has gone into enhancing the weak immunogenicity of DNA vaccines. For instance, measures include improving DNA, mRNA and protein (including codon usage) characteristics, resulting in increased stability, translation and expression [293-298]. These kinds of modifications can of course be used for all recombinant systems, including viral and protein expression platforms. Next, improving expression of DNA vaccine can be achieved by promoter and/or enhancer usage within the plasmid, which can consequentely enhance the immune response [286, 299-302]. As an example, in this thesis an enhanced mammalian expression plasmid pTHpCapR was used, which was shown to enhance *in vitro* expression and *in vivo* immunogenicity compared to the unaltered donor plasmid pTH, which has previously been used in HIV vaccine trials [286, 299]. Furthermore, DNA vaccine delivery methods such as electroporation and the use of needleless devices such as from PharmaJet can also increase immunogenicity [303-310]. Additionally, genetic adjuvanting (co-expression of immunomodulatory genes such as IL-2 or GM-CSF) and use of polymer or lipid adjuvants have also been shown to improve the immune responses to DNA vaccines [311-313].

1.10.2 Modified Vaccinia Ankara (MVA) virus vaccines

The use of vaccinia virus (VACV) as a smallpox vaccine was instrumental in the eradication of variola virus. One of the reasons why VACV was so effective is that it was an infectious live vaccine. Despite the successful campaign, incidental cases of severe complications, including fatalities upon VACV administration, have been reported. Therefore, it was proposed to generate attenuated strains of VACV to assist in the eradication approach. An example of this is the highly attenuated modified vaccinia Ankara (MVA) virus, obtained after passaging a Turkish VACV strain almost 600 times in chick embryo fibroblasts (CEFs) [314]. This caused mutations and large deletions of the genome (~15%), resulting in MVA becoming replication - deficient in mammalian cells (including in humans), bar a handful of select cell lines [315-317]. Many of the genetic changes affected genes with functions in virus–host interaction, which may underlie this replication deficient phenotype [316, 317]. MVA was used on a small scale in Germany as part of the smallpox eradication campaign, in which no severe adverse

reactions associated with VACV were reported, indicating MVA as a safe vaccine platform [318, 319]. Therefore, MVA is now frequently used as a vaccine platform for the expression of recombinant antigens. MVA has several key advantages over other viral vaccine platforms: 1) MVA replicates and is located solely in the cytoplasm, minimising integration into the host genome; 2) MVA can tolerate large insertions of DNA (>15kbp), and when an antigen (or multiple) is inserted into the MVA genome under a pox promoter, strong transgene expression is observed *in vitro* and *in vivo*; 3) MVA is thermostable and can be lyophilised for additional stability, thereby decreasing the cost of the supply chain; 4) MVA can induce both a humoral and cellular response; and 5) high titres stocks of recombinant MVA can be generated in CEFs and BHK-21 cells, both can be used in cGMP production of vaccines. The induction of a strong humoral and cellular immune response could be due to self-adjuvanting effects of MVA: these are due to the deletion of viral immunomodulators within the MVA genome, which could lead to immune response skewing towards genes (antigens) inserted into recombinant vector [317, 320, 321]. Finally, as vaccinations after the eradication of smallpox have ceased since 1979, a large proportion of the worldwide population, especially those <40 years of age, will have very little chance of developing vector immunity towards MVA. Incidentally, this same age group is mostly at risk for becoming HIV-1 infected, especially in southern Africa. All of this underlines the attractiveness of recombinant MVA as a vaccine platform. A particularly thorough review on all aspects of MVA was published by Volz and Sutter in 2018 if more background is required [317].

1.10.3 Protein vaccines

A popular component of experimental HIV-1 vaccines is the use of Env protein to induce a mainly humoral immune response. Protein vaccines are highly successful in activating B-cells to produce antigen-specific binding antibodies. However, the aim of an Env protein vaccine is to induce antibody pathway maturation in B-cells towards generating antibodies which can neutralise HIV-1 viral entry into cells - preferably to a broad spectrum of HIV-1 isolates - and/or antibodies that have antibody-dependent cell-mediated effector cell functions [99, 100]. The advantage of using Env protein vaccines is that the antigen can be specifically designed and purified to contain the specific characteristics for inducing this kind of B-cell maturation, which might not easily be feasible for DNA and viral vector based vaccines platforms. The safety risks for protein vaccines are extremely low as they contain no live viral components. However, the immune response is much less broad compared to whole cell vaccines or viral vector vaccine platforms, and could be even different. For instance, the subunit vaccine for pertussis (whooping cough) used in children by some countries induces a Th2 response compared to Th1 + Th17 for the inactivated, whole cell preparation vaccine. These differences might be one of the underlying factors in the increase in pertussis disease rates observed in children

that received the subunit vaccine, even though one of the main correlates of protection are pertussis toxin antibodies [322-325]. Furthermore, production costs of complex proteins are often extremely high, and vaccine thermostability is poor especially upon lyophilising, thus requiring increased supply chain costs.

1.10.4 Heterologous use of vaccine platforms (prime-boost)

As HIV-1 is particularly efficient in evading the immune system, an effective vaccine will almost certainly require the activation of both the cellular and humoral arms of the immune response. Although most vaccines exert their effectiveness through an antibody response*, cell-mediated immunity plays a crucial role in inducing this response, mainly through activation of T follicular helper (Tfh) cells and CD4+ T cells [246, 326, 327]. Tfh cells play a pivotal role in this process within the germinal centre by stimulating B-cell proliferation, antibody affinity maturation and B-cell differentiation, which, as mentioned above, are thought to be extremely important for the induction of neutralising antibodies [246, 328]. This effect can be enhanced by vaccine boosting [246, 329]. Considering the different qualities of the vaccine platforms (DNA: cellular immunity; MVA or other viral platforms: cellular+humoral immunity; and protein: humoral immunity), heterologous vaccine platform prime-boosting could potentially broaden the immune response by activating both arms of the adaptive immune response, preventing the potential development of vector-based immunity when multiple vaccines are required. Further improvements on these kind of heterologous vaccine platform regimens can be realised by the addition of different Env sequences. This is of course not a novel concept and has been extensively used in the development of an HIV-1 vaccine: for instance, past (RV144, HVTN 505) and current (HVTN 702, 705 and 706) phase II-III clinical trials have made use of this strategy. With regard to the vaccine platforms used in the experiments discussed in this thesis, combinations involving MVA have been extensively studied by different groups [273, 330-358], either as a prime for protein vaccines and/or boost for DNA or other viral vaccine platforms. These experiments have given rise to the notion that although DNA vaccines in general lead to a fairly weak immune response, they are very effective in priming cell-mediated immune responses towards MVA, whereas MVA itself acts as an excellent prime for protein vaccines. These studies using MVA in different heterologous vaccine platform regimens have not only been done in animal models [343-358], but also in clinical trials [273, 330-342]. A final advantage worth considering for the use of heterologous vaccines platforms over especially a protein vaccine alone, is the much lower production and supply chain costs of DNA and MVA compared to protein vaccines. Developing a vaccine regimen which requires substantially less protein vaccines would be a more cost-effective solution.

Authors note: most clinical tests are antibody based, whereas testing of cellular responses is much less common. Therefore the importance of cell-mediated responses as correlates of protection could be grossly underestimated [359].

1.11 Vaccine adjuvants

With the advantage of an improved safety profile of subunit vaccines comes the disadvantage of decreased immunogenicity with the lack of the whole pathogen [360]. Therefore, adjuvants have been widely used to improve the vaccine-induced immune response, where the adjuvant acts as an immunomodulator or immune potentiator of the immune response targeted by the vaccine. Surprisingly, there is only limited research into vaccine adjuvants, resulting in only a very small number of reagents being approved by the FDA (Food and Drug Administration , USA) for the use in human vaccines [361]. HIV-1 vaccines have mainly been adjuvanted using aluminium salts, but recently scientists have started to utilise AS01B (liposomes with MPL + QS-21) and oil-in-water emulsions such as MF59 and AS03 (based on [362]). In my research, the adjuvants AlhydroGel and AddaVax were selected to test if they could improve the immunogenicity of the soluble Env protein vaccine: both will be discussed briefly below. An informative review on all FDA approved adjuvants was recently published by Shi *et al*. [361].

1.11.1 Aluminium salt-based adjuvants (AlhydroGel)

Aluminium salt-based vaccine adjuvants have been used for at least 80 years, and were for a long period of time the only adjuvant approved in human vaccines. Currently, different formulations such as aluminium hydroxide, aluminium phosphate and amorphous aluminium hydroxyphosphate sulphate are approved by the FDA [361]. Of these formulations, a 2% aluminium hydroxide wet gel suspension, often referred to as alum, is the most widely used for HIV-1 vaccines. In the research for this thesis, alum was acquired from InvivoGen under the brand name AlhydroGel®.

Aluminium adjuvants mainly enhance antibody based immune responses without significantly promoting Th1 cellular responses [361]. Originally it was assumed that this was mainly accomplished by the adjuvant acting as a depot for the adsorbed antigen, resulting in a slow release at the inoculation site [361]. However, later studies have falsified this concept. In mice, aluminium phosphate-adsorbed antigen is rapidly cleared from the injection site, and removal of the inoculation site containing alum several hours after administration of ovalbumin-adsorbed alum had no effect on the antibody responses [363, 364]. The immune enhancing properties of aluminium adjuvants can however be explained through several other mechanisms. Firstly, they enhance infiltration of immune cells into the injection site, with these cells subsequently migrating to the draining lymph node [365]. Secondly, they increase antigen uptake and presentation by antigen presenting cells [361], and inflamosome activation via the

nucleotide-binding oligomerization domain-like receptors (NLR) pathway, specifically through the pattern recognition receptor NLRP4 [361]. Furthermore, interaction of aluminium adjuvants with the membrane of dendritic cells enhances soluble antigen uptake and induces lipid reordering in the membranes of dendritic cells and CD4+ T-cells, increasing antigen uptake for the first while activating the latter [361]. Furthermore, evidence is emerging that aluminium adjuvants can both stimulate and induce differentiation of CD4+ T-cells. Finally, activation of the complement system by aluminium hydroxide has been reported as well [361]. Interestingly, several of the mechanisms of the immunostimulatory effects of aluminium adjuvants described above are through a cellular response, despite its reputation as acting mainly though the Th2 antibody response.

1.11.2 Oil-in-water emulsion adjuvant AddaVax

The oil-in-water nano-emulsion AddaVax from InvivoGen is similar in formulation to the Novartis adjuvant MF59, in containing squalene (a natural oil originally derived from shark liver), Tween 80 and sorbitan trioleate buffered in trisodium citrate dehydrate (https://www.invivogen.com/addavax and [366]). Although MF59 is licensed and mainly used for influenza vaccines, it has replaced alum (used in the RV144 trial) as adjuvant for the HVTN 702 study. As MF59 not only improves antigen specific antibody production, it also enhances both Th1 and Th2 immune responses, therefore making MF59 in theory an attractive adjuvant compared to aluminium adjuvants [361]. The main mechanism by which MF59 enhances immunogenicity is by creating an immune competent environment in the injection site. Attracted immune cells show improved antigen uptake and are stimulated to produce and secrete different chemokines and cytokines, leading to additional influx of immune cells into the injection site [361]. Upon antigen uptake and activation, these different classes of antigen presenting cells accumulate in the draining lymph nodes where it is proposed they can prime naïve CD4+ T-cells [361].

1.12 Modifications to improve the antigenic profile of Env

The majority of vaccines which are licensed for the use in humans exert their protective properties through the induction of an effective broadly neutralising antibody response towards the pathogen [325]. Therefore, this remains the main target for an HIV-1 vaccine as well. This of course limits the target selection to the envelope glycoprotein, despite the fact that Env-specific bnAbs development in infected individuals fails to improve clinical outcomes (discussed in ***Section 1.7***). In favour of the notion that the induction of bnAbs against Env could be protective in HIV-1 acquisition are experiments in non-human primates and humanised mice, in which administration of bnAbs are protective in viral challenge models [133-152]. Encouragingly, bnAbs concentrations showing efficacy in some of these

experiments are within the range which could be achieved with vaccines [142, 147, 151]. However, this raises a new issue as to how to induce this bnAb response using HIV-1 Env vaccines. Almost all bnAb epitopes are conformational, formed by the quaternary structure of the Env trimer, so that mAbs interact with the different, correctly folded subunits [112, 165, 367, 368]. Therefore the characteristics of native-like Env trimers need to be reflected in the vaccine design, as a large proportion of misfolded Env would skew the antibody response towards immunodominant non-neutralising epitopes. Design concepts and modifications of Env relevant to this thesis are discussed below. Additional approaches can be found in ***Section 1.9.3***.

1.12.1 Stabilising the Env trimer

Two vital issues need to be addressed in this project in order to get to the stage where a high proportion of Env produced as a vaccine is in this favoured native-like conformation. Critical for this was the use of soluble Env constructs lacking the transmembrane and cytoplasmic tail by truncation at residue 664 [369]. First was the observation that proteolytic cleavage of the polyprotein into gp120 and gp41 is essential for the formation of native-like trimers [370, 371]. Co-expression of furin and optimisation of the native furin cleavage site in Env (from REKR to 6x Arg residues, RRRRRR) significantly improves processing of Env by furin [372]. This elegant solution now amplified the second problem, in which the non-covalent link between gp120 and gp41 is readily disrupted in a process called shedding, leading to disassembly of the trimer which again would result in the display of immunodominant non-neutralising epitopes. The most well studied solution to this was the introduction of a *de novo* disulphide bond (SOS) between gp120 and gp41, thereby stabilising the two subunits after cleavage [373]. In seminal work, this SOS mutation was combined with the single amino acid mutation I559P that stabilize the pre-fusion conformation of gp41 and promote trimer formation in the subtype A transmitted/founder virus BG505 [374]. Expression of this BG505 SOSIP.664 resulted in high levels of native-like Env trimers presenting mainly bnAbs epitopes, which was poorly recognised by non-neutralising antibodies [275, 375, 376]. As a protein vaccine tested in rabbits, BG505 SOSIP.664 trimers were the first to induce robust, vaccine matched (autologous) Tier 2 neutralising antibodies (nAbs) [277]. These immunogenicity results and high-resolution X-ray and cryo-electron microscopic structures of BG505 SOSIP.664 have assisted towards improvements in (BG505 SOSIP.664) trimer design and has been fundamental in developing SOSIP trimers for different Env sequences which are now eliciting Abs that cross-react with different subtypes [377, 378]. For instance, BG505 SOSIP.664 mutants are now being generated with improved presentation of bnAb epitopes in the V2 region, whilst displaying increased trimer stability [379]. Another has the V3 region, considered neutralisation irrelevant, being sequestered away within the trimer, resulting in decreased

induction of V3 binding antibodies without affecting the autologous Tier 2 neutralisation response [380]. Encouragingly, rhesus macaques vaccinated with native-like SOSIP Env trimers displayed protection in a vaccine matched SHIV challenge model, but only when serum contained high nAb titres [381]. An informative review was written in 2018 by Torrents de la Peña and Sanders about the evolution of SOSIP Envs over the years [377].

To emphasise that the generation of native-like Env trimers is extremely complicated, and that there is no guarantee of success, can be seen in an example where this was applied to an Env consensus M sequence (ConM) [382]. ConM SOSIP.v6 failed to produce enough protein required for characterisation full stop. Protein yields were improved when based on a SOSIP.v4.2 design (four additional mutation to SOSIP) or on SOSIP.v5.2 (v4.2 plus additional intermolecular disulphide bond). However, high-quality trimer yields were much lower compared to SOSIP.v7, which contained eight additional amino acid mutations within the trimer interface based on BG505. Disappointingly, despite the excellent *in vitro* properties of ConM SOSIP.v7, when it was subsequently tested as a protein vaccine in rabbits, sera was all but devoid of autologous Tier 2 neutralisation.

Alternative strategies circumventing the need for processing of Env by furin to produce native-like Env trimers have also been developed. In one approach, the furin site was replaced with a flexible linker: these were initially of varying size, but work by Sharma *et al*. let to identification of an optimal motif (GGGGS GGGGS) that is being used often nowadays [383, 384]. From that same paper, the name native flexible linker (NFL) was dubbed, which is now the defining name of this concept as long as native-like Env trimers are produced. Interestingly, SOSIP-stabilising mutations improve native-like trimer yields from these NFL Env constructs [371, 384, 385]. As with SOSIP Envs, additional mutations improving trimer stability are identified regularly [371, 384-387]. Although not as intensively studied in animal models as SOSIP Envs, it has been shown that NFL Envs are able to induce nAbs as well [386, 388-395].

A completely novel approach was taken by Kong *et al.,* where *in silico* modelling was utilised to re-design the HR1 region in gp41, which led to the stabilisation of uncleaved trimers in a pre-fusion conformation (UFO). This led to increased trimer stability compared to equivalent SOSIP constructs [396]. Subsequent testing of these UFO Env trimers in animal models showed the induction of Tier 2 nAbs [397].

In the context of work reported in this thesis, heterologous platforms in DNA, recombinant MVA and protein vaccines were to be tested. Given that the first two strategies rely on host-cell expression of the Env antigen where adequate furin processing might not take place, it was decided to opt for introduction of the same flexible linker as optimised by Sharma et al. [384]. A case in point for this decision was that poor furin cleavage was observed for BG505

SOSIP.664 expressed *in vitro* from chimpanzee adenovirus (ChAd) and MVA vaccines [343]. For the protein vaccine used in this thesis, Env was truncated at a similar position as BG505 SOSIP.664, whereas for DNA and MVA vaccines the transmembrane domain was retained (see ***Section 1.12.2*** for further information). However, gp160 was truncated to AA 730, which was shown to result in higher expression levels and increased stability of gp150, the latter holding especially true for the rMVA platform [398-400]. Furthermore, the I559P mutation was included in the constructs used within this project; however, the original intramolecular cysteine bridge between gp41 and gp120 (SOS) was not included.

1.12.2 Presentation of Env on virus-like particles

Recently, there has been an increased interest in particulate vaccine designs for displaying Env. These can take form of self-assembling protein nanoparticles such as virus-like particles (VLPs), those which use protein scaffolds (for example, the popular bacterial protein ferritin), or synthetic nanoparticles including lipid nanoparticles/liposomes, silica nanoparticles and particles based on polymers [401, 402]. Interestingly, the recombinant protein subunit vaccines currently licensed for hepatitis B and human papillomavirus are VLP-based vaccines [403, 404]. A particulate vaccine approach could be an especially powerful tool for presenting Env antigens: for example, after isolation and purification of native-like trimers, these could be assembled into nanoparticles, which would circumvent the presentation of unwanted, non-native Env epitopes on the underside of the Env trimer [401, 402, 405]. One of the main objectives of Env particulate vaccines is better engagement of B-cell activation, where the repetitive display of high density Env trimers might improve B cell receptor (BCR) cross-linking and could potentially compensate for low affinity antigen-BCR interactions between Env and naïve B-cells [402, 405]. One such approach is to display Env on the surface of HIV-1 Gag VLPs. Work from the early 1990s showed that Env readily incorporates into Pr55Gag VLPs when the proteins are co-expressed *in vitro* [406-412]. It has also been suggested that by anchoring Env into the native environment of a lipid bilayer, the trimeric conformation is further stabilised [405]. As discussed previously (***Section 1.8***), cell-mediated immune responses to especially HIV-1 Gag (CD4+ and CD8+ T-cell responses) have been implicated in viraemic control. Therefore, inclusion of Gag in a vaccine regimen has the potential to increase the efficacy of such a strategy; consequently, this concept has been widely used within the HIV-1 vaccine community, including in vaccine efficacy studies such as RV144, HVTN 702, 705 and 706.

For the research presented in this thesis, the aim was to have VLP- based vaccines for the DNA and recombinant MVA vaccine platforms by either combining two DNA vaccines (one for Gag, the other for Env), or by co-expression of Gag and Env from the same recombinant MVA

genome. For this purpose, a HIV-1 mosaic Gag sequence was selected. This sequence, designed *in silico* to maximise potential T-cell epitopes derived from HIV-1 subtype C sequences, was known to improve immunogenicity in mice as a BCG, DNA and recombinant MVA vaccine [272, 413, 414]. For Env to incorporate into VLPs, it would require the Env to contain the transmembrane domain and at least a partial cytoplasmic tail. However, while a shorter tail is known to increase spike density, this could still potentially result in low Env spike density on the VLP, thereby thwarting the intended increased B-cell activation. Therefore, some modifications to the Env were included that could potentially lead to higher expression levels and therefore increase spike density on VLPs. As mentioned previously, the gp160 encoding sequence was truncated in the C-terminal tail region so as to produce gp150, for improved stability and expression. Sequences were humancodon-optimised by GenScript, as these optimisations usually lead to significantly increased expression [294, 302, 415]. Additionally, replacing the native Env signal peptide with the commonly used human tissue plasminogen activator (tPA) leader could potentially increase cellular trafficking towards the plasma membrane and subsequent budding and/or secretion [302, 399, 416, 417].

Alternatively, a number of labs have used chimaeric constructs between HIV-1 Env and glycoproteins from high spike-density viruses to improve HIV-1 Env display on virus-like particles. In general, this was done by replacing the transmembrane domain (TM) and cytoplasmic tail (CT) of gp41 with those of other viral glycoproteins, in combination with changing the Env native signal peptide. In one early paper, the whole of HIV-1 Env gp41 was replaced with the TM of Epstein–Barr virus gp220/350 (EBV) without changes to signal peptide [418]. The display of this resulting gp120-EBV-TM fusion protein onto Gag VLPs was 10 times higher compared to the equivalent HIV-1 gp160 [418]. Significantly increased incorporation of Env chimaeras into Gag VLPs produced in insect cells was also observed when the TM and CT of HIV-1 Env was replaced with those of the mouse mammary tumour virus, influenza haemagglutinin or baculovirus gp64 envelope glycoproteins, in combination with honeybee melittin protein signal peptide (HMSS) instead of the HIV-1 Env native signal peptide [399, 419]. Similar results were obtained for a SOSIP modified gp140 containing the HMSS and fused to the TM and CT of baculovirus gp64 envelope glycoprotein [420]. It should however be emphasised that although spike density on HIV-1 Gag VLPs was increased for all the Env chimaeras, folding of these constructs was never assessed with bnAbs recognising only native-like Env trimers. Furthermore, when some of these VLP preparations were tested as vaccines in animal models, they failed to induce vaccine-matched Tier 2 neutralisation. For this thesis, Env chimaeric constructs were designed using the influenza haemagglutinin protein HA_2 from the influenza A H5N1 strain. Either the whole HIV-1 gp41 was replaced with influenza haemagglutinin HA_2, or only the TM and CT of gp41 would be substituted for the

corresponding domain of HA_2. These chimaeric Env (Env:HA_2 chimaeras) constructs would then be characterised in depth *in vitro*, including spike density on Gag VLPs, bnAb epitope mapping on cell-surface expressed protein and immunogenicity in rabbits, and compared to the corresponding HIV-1 gp150 construct. One of the driving reasons for the selection of influenza haemagglutinin HA_2 to generate these Env:HA_2 chimaeras has been that depending on the expression platform, these proteins can assemble into particles without the need of Gag or other structural viral proteins [421]. An overview of all the different Env and Env:HA_2 chimaeras that were generated for the work in this thesis can be found in ***Figure 1.10***.

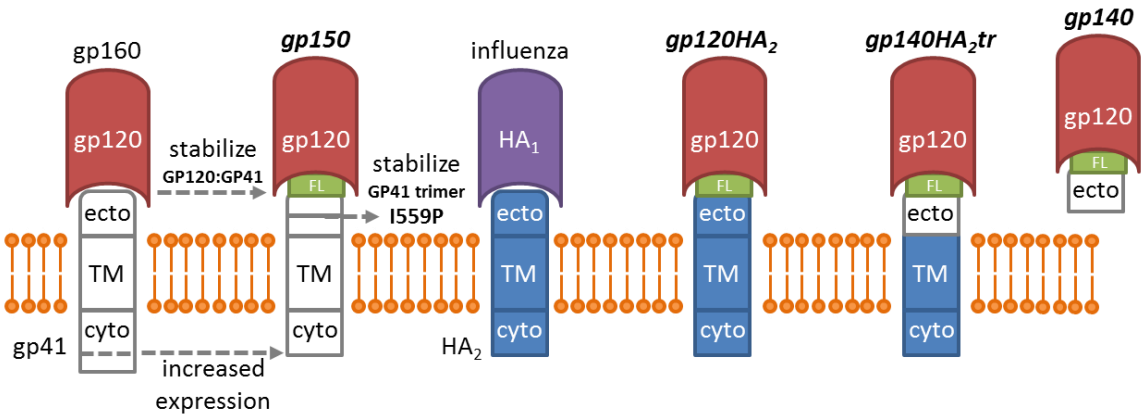

Figure 1.10. Schematic representation of Env immunogens.
Env constructs in ***bold*** and ***italics*** were generated. HIV-1 Env gp120 in red, corresponding influenza HA_1 in purple. In white ectodomain (ecto), transmembrane domain (TM) and cytoplasmic tail (cyto) modules of HIV-1 Env gp41 and matching influenza HA_2 domains in blue. A flexible linker (FL) consisting of two glycine rich motifs (GGGGS) replaced the Env furin cleavage site. The I559P mutation was introduced to stabilise the gp41 trimer and is present in all Env immunogens apart from gp120HA_2. Env immunogens containing a transmembrane domain were used for DNA and rMVA vaccines whereas the transmembrane domain was removed to generate a soluble Env (gp140) for the protein vaccine. For all constructs the Env native signal peptide was replaced with the tissue plasminogen activator (tPA) leader.

1.13 Concluding remarks

Despite over 35 years of research into prophylactic HIV-1 vaccines, progress has been underwhelming. In general, the main lessons learned is what doesn't work, rather than what does. Even after stretching the analysis of the only partially successful clinical trial (RV144) as far as possible in order to gain insight into correlates of protection, this has failed to aid vaccine design, as can be seen from the early termination of the follow-up Phase IIb/III clinical trial HVTN 702 in Africa due to lack of vaccine efficacy. Part of the problem is the lack of effective pre-clinical models. Small animal models such as guinea pigs and rabbits are being used to investigate vaccine-induced bnAbs. However, the immune systems in these models are poorly understood, and although guinea pigs and rabbits can develop bnAbs to a certain degree, the underlying mechanisms are unknown. Furthermore, research is hampered by the

fact that no assays are available to assess cellular responses (T-cell assays) in guinea pigs and rabbits. To top this off, translatability between small animal models and non-human primates (NHPs) is weak, with vaccine-induced development of bnAbs in one model not being predictive to garner the same response in the other. Challenge models in NHPs present their own set of problems, as in general these either consist of simian immunodeficiency virus (SIV) or SHIV (SIV but Env adapted from HIV-1 Env sequences), and therefore fail to completely mimic HIV-1 infection and progression to AIDS. The humanised mouse model is even more precarious. In this model, the bone marrow of severe combined immunodeficiency (SCID) mice is destroyed with radiotherapy and replaced with material from human embryonic tissue whereupon these mice are subjected to vaccine regimens. The question is how informative data from immune responses in these extremely sick and severely immune-compromised animals really is.

The current obsession in the HIV-1 vaccine community with Env-based protein vaccines, B cell ontogeny-based vaccines and the induction of bnAbs appears misguided, or at the least flawed. The flimsy evidence of bnAbs being protective in NHP challenge models can be counteracted with evidence where 1) no clinical benefits are reported in HIV-1 infected individuals which develop bnAbs; 2) viraemic control is correlated CD4+ and CD8+ T-cell responses towards Gag, not the development of bnAbs; and furthermore 3) development of bnAbs was also not a correlate of protection in the RV144 trial. Even if bnAbs against HIV-1 Env are protective against acquisition, as is the case for almost all other vaccines licensed for human use, the scientific community has so far failed to develop a vaccine regimen that induces this in animal models. Infusion of bnAbs as in the AMP trials (HVTN 702 and 704) is aspirational at most, as the production volumes needed and the cost of application will be extremely prohibitive, to say nothing of the impracticalities of rolling out mass intravenous infusions. Additionally, adherence to monthly or even annual treatments will slowly diminish over time, putting people back at risk.Furthermore, the logistics and infrastructure for mass rollout in developing countries for this kind treatment is essentially nonexistent.

There is, however, some reason for optimism as well. Even though currently no vaccine regimens are able to induce bnAbs, HVTN 702 and 704 will inform the scientific community if the induction of bnAbs in humans could potentially be protective against HIV-1 acquisition. Furthermore, the vaccine efficacy trials HVTN 705 and 706 where mosaic antigens theoretically could result in improved immunogenicity compared to all other regimens tested, as a superior cell-mediated response is anticipated because of the mosaic antigens which could prime the antibody/humoral response more effectively. However, it is clear that there is still a long way to go and additional pre-clinical work is required. The work presented in this thesis fits nicely into this category. HIV-1 subtype C Env and Gag antigens were selected to

target the prevalent subtype circulating in South Africa. Furthermore, the Env sequence was modified to improve stability and trimer formation. For Gag, a subtype C mosaic Gag was selected which already had been shown to result in improved immunogenicity compared to a naturally occurring subtype C Gag. As a final remark though, the best advice is still as it was 40 years ago: that is, protect yourself, have safe sex, please use a condom.

1.14 Project aims

The HIV/AIDS pandemic is putting a large burden on the social economics of developing countries. Developing an effective vaccine against HIV, therefore, would be both a large step towards eradication of AIDS, and towards improved economies. As HIV-1 subtype C is the most prominent strain in sub-Saharan Africa, in this project the aim was to generate and characterise HIV-1 subtype C (1C) candidate immunogens that will induce high titre antibody responses to HIV-1 envelope glycoproteins (Env), as well as generating neutralising antibodies in rabbits.

To achieve the aforementioned aims the following objectives are addressed:

1. Generation and *in vitro* characterisation of a soluble Env protein vaccine candidate.
2. Immunogenicity studies in rabbits testing the immune enhancing properties of different adjuvants for the soluble Env protein vaccine.
3. Generation and *in vitro* characterisation of DNA and recombinant MVA vaccine platforms which express Env alone, or Env combined with Gag (including VLP formation)
4. Immunogenicity studies in rabbits testing different heterologous vaccine platforms in prime-boost regimens: these are comparing recombinant MVA vaccines with or without DNA priming, boosted by a soluble Env protein vaccine with the preferred adjuvant from Objective 2. This will include characterising the effect of the inclusion of Gag in the DNA and recombinant MVA vaccines
5. Generation and *in vitro* characterisation of DNA and recombinant MVA vaccine platforms which express Env or Env:HA_2 chimaeras, all combined with Gag to allow VLP formation
6. Immunogenicity studies in rabbits with an optimised vaccine regimen (objective 4), comparing Env to Env:HA_2 chimaeras in the relevant DNA and/or recombinant MVA vaccine background (Objective 4).

CHAPTER 2: PRODUCTION AND CHARACTERISATION OF ENGINEERED HIV-1 SUBTYPE C GP140

2.1 Introduction

The remit of this project was to develop a HIV-1 subtype C vaccine for sub-Saharan Africa eliciting high-titre antibody responses to HIV-1 envelope glycoproteins (Env). Therefore, a subtype C Env sequence was chosen from the Centre for the AIDS Programme of Research in South Africa (CAPRISA) 002 acute infection cohort [167, 174]. This particular virus was the superinfecting virus (SU) from participant CAP256 who developed broadly cross-neutralising antibodies targeting the V1V2 loop 15 weeks after the second viral infection event. Furthermore, the CAP256_SU virus was shown to be sensitive to a range of broadly neutralising antibodies (bnAbs) targeting different epitopes within the Env sequence [167]. Therefore this Env sequence has the potential not only to induce high-titre antibodies towards Env, but also to elicit a neutralising antibody response in animal models. The sequence of CAP256_SU Env will be referred to as CAP256 Env throughout this thesis.

The emphasis in current HIV-1 vaccine research on developing neutralising responses is mainly with the use of protein vaccines, focused on soluble, native-like Env trimers [367, 368]. Mammalian cell lines are the main vehicle for the production of HIV-1 Env protein vaccines [275, 383-385, 422], with HEK293, HEK293T and CHO-K1 cells, using transient and stable expression platforms, being explored for production of a soluble CAP256 Env mimetic. To this end, and keeping in mind the ever-increasing knowledge base as to how to manipulate soluble Env proteins to direct the immune response towards desired attributes within Env [377], I investigated several modifications of CAP256 Env aimed at making a stable, immunogenic trimeric molecule. I focussed on making a soluble CAP256 Env mimetic generated by removing the cytoplasmic tail and transmembrane domain, with the truncation in a similar position as for BG505 SOSIP [275]. Similarly, I investigated stabilising the gp41 trimer by introducing the I559P present in BG505 SOSIP [275, 374]. In order to prevent furin processing, which is necessary for the Env trimer to take on a native-like conformation, I tested use of a glycine-rich flexible linker which successfully mimics this folding event [384]. Lastly, I investigated replacing the native single peptide of Env with the human tissue plasminogen activator (tPA) leader, as a means of improving secretion [416, 417].

Following successful scale up of production in the laboratory, the aim was to purify and characterise the CAP256 soluble Env produced in mammalian cells, and test the immunogenicity of the protein vaccine in rabbit immunogenicity studies. Considering protein vaccines have a tendency to be poorly immunogenic, different vaccine adjuvants were to be tested in order to improve the immune response in the animals [360]. Adjuvants act as immunomodulators or potentiators of the immune response targeted by the vaccine. HIV-1 protein vaccines have mainly been adjuvanted using aluminium salts, but recently researchers

have started to utilise AS01B (liposomes with MPL + QS-21) and oil-in-water emulsions such as MF59 and AS03 (based on [362]). In this project, the adjuvants AlhydroGel and AddaVax were selected to test their ability to improve the immunogenicity of the soluble CAP256 Env protein vaccine. AlhydroGel (InvivoGen) is a 2% aluminium hydroxide wet gel suspension and this formulation is often referred to as alum. The oil-in-water nano-emulsion AddaVax (InvivoGen) is similar in formulation to the Novartis adjuvant MF59 (https://www.invivogen.com/addavax and [366]). Although MF59 is licensed and mainly used for influenza vaccines, it has replaced alum (used in the RV144 trial) as adjuvant for the HVTN 702 study. As MF59 not only improves antigen specific antibody production, it also enhances both Th1 and Th2 immune responses, therefore making MF59 in theory an attractive adjuvant compared to aluminium adjuvants [361]. Importantly, both AlhydroGel and AddaVax have no detrimental effect on the native-like Env trimeric structure after adjuvanting [423].

2.2 Materials and methods

2.2.1 Antibodies, plasmids, cell lines, media and reagents

Goat anti-HIV-1 gp160 (MRC ADP 72 408/5104) (MRC, Potters Bar) and mouse monoclonal anti-goat/sheep IgG–AP GT34 (Sigma, St Louis) were used for western blotting. See Appendix A for western blot protocol.

Chinese Hamster ovary cells subclone K1 (CHO-K1) (ATCC® CCL-61™), human embryonic kidney 293 cells (HEK293) (ATCC® CRL-1573™) and HEK293 cells expressing the simian virus 40 (SV40) large T antigen (HEK293T) cells (ATCC® CRL-3216™) (ATTC, Manassas) were grown in Dulbecco's Modified Eagle's medium (DMEM) High Glucose + L-Glutamine (Lonza, Basel) + 10% fetal calf serum (FCS) + 1x penicillin (Pen)/streptomycin (Strep) (both Thermo Fisher Scientific, Waltham). Serum-free medium: DMEM High Glucose + L-Glutamine + 1x Pen/Strep. Small scale transfections (tissue culture plates) were performed using X-TremeGENE (Roche, Basel), whereas large scale transfections (tissue culture flasks) were done with polyethyleneimine (PEI) (Sigma, St Louis). See Appendix B for tissue culture protocols.

The enhanced mammalian expression plasmid pTHpCapR [299] was used as a backbone for all DNA expression plasmids.

CAP256 SU V1V2 scaffolded protein was produced as described by McLellan et al. (2011) [424] and supplied by Professor Lynn Morris and Dr Penny Moore (NICD, Johannesburg). Anti-HIV-1 Env human monoclonal antibodies PG9, PG16, PGT128, PGT135, PGT145, CAP256-VRC26.08, VRC01, F105 and 447-52D were expressed in FreeStyle 293F cells (Thermo Fisher Scientific, Waltham) using the PEIMAX transfection reagent (Polysciences,

Warrington). Monoclonal antibodies were purified from cell-free supernatants after 6 days using Protein-A affinity chromatography [425]. All these monoclonal antibodies were supplied by Professor Lynn Morris and Dr Penny Moore.

CLC Main Workbench (Qiagen, Hilden) was used for *in-silico* cloning, generation of plasmid maps and DNA sequencing analysis.

2.2.2 Design of soluble CAP256 Env

The sequence of CAP256_SU gp160 (clone CAP256.206sp.032.C9) has been previously described (GenBank: KF241776.1) [167]. The Env sequence was altered as follows: the native leader (signal peptide) was removed; the furin cleavage site was replaced with two glycine-serine based repeats (GGGGS) to form a flexible linker (FL) [383, 384], and an I548P mutation equivalent to the I559P in the SOSIP trimers was introduced to stabilise trimerisation of gp41 [374]. Finally, the sequence was truncated to gp140 (AA 653), thus generating gp140-FL-IP. The Env sequences were human codon optimised and synthesised by GenScript (Nanjing).

2.2.3 Soluble CAP256 Env expression plasmids

The human tissue plasminogen activator (tPA) leader sequence (GenBank: CAX11668.1) was human codon optimised and synthesised by GenScript and cloned into pTHpCapR to increase secretion of the target antigen. This plasmid was renamed pMExT for Mammalian Expression with tPA leader (***Figure 2.1A***). CAP256 gp140-FL-IP was cloned into pMExT in-frame, behind the tPA leader using the NgoMIV and EcoRI sites to generate pMExT CAP256 gp140-FL-IP (***Figure 2.1B***). In this process, the NgoMIV site was lost. In order to create a stable cell line, an internal ribosome entry site + Neomycin resistance cassette (IRES Neo(RC)) was cloned directly downstream of CAP256 gp140-FL-IP in pMExT using EcoRI + XbaI restriction sites, thus generating pMExT CAP256 gp140-FL-IP IRES Neo(RC) (***Figure 2.1C***). The IRES Neo(RC) was synthesised by GenScript (Nanjing) with the Neo(RC) gene human codon optimised. An additional constructs were generated where a 6x His-tag with an alanine linker (AAA HHHHHH) was introduced in front of the STOP codon at the C-terminus of gp140-FL-IP to allow NiNTA trapping of soluble Env (pMExT gp140-FL-IP-His and pMExT gp140-FL-IP-His-IRES-Neo(RC)). See Appendix A for general cloning and plasmid isolation protocols.

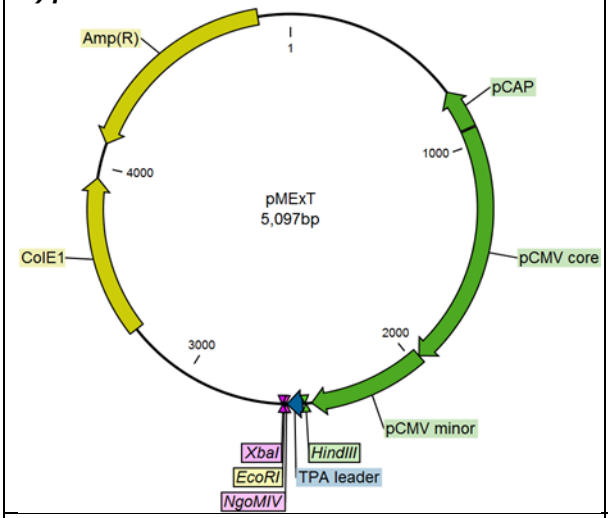

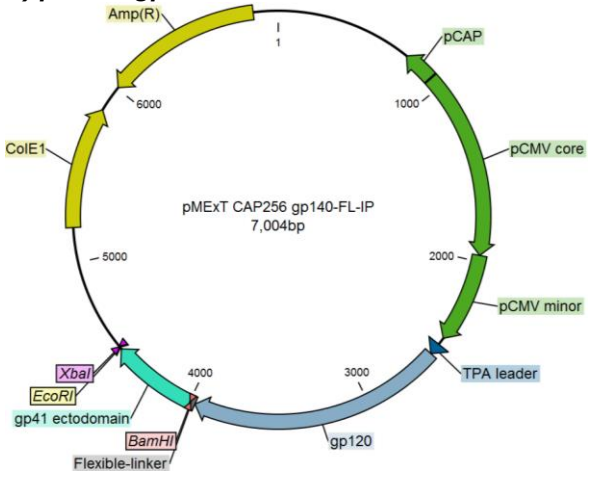

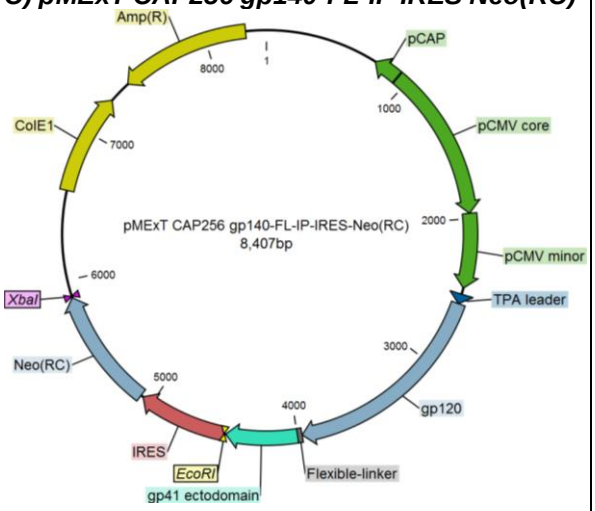

Figure 2.1. Plasmid map of DNA vectors expressing CAP256 Env.
(A-C) Amp(R): ampicillin resistance gene for bacterial selection. ColE1: bacterial origin of replication. Mammalian expression is driven by a promoter containing a porcine circovirus enhancer (pCAP) in the reverse orientation, the essential component of the CMV promoter (pCMV core) and the non-essential part of the CMV promoter (pCMV minor) for maximal expression. TPA leader: human tissue plasminogen activator leader sequence. IRES: internal ribosome entry site. Neo(RC): Neomycin resistance cassette. Arrows indicate the direction of all promoters and transcripts.

2.2.4 Generation of soluble Env stable cell lines

The construct pMExT CAP256 gp140-FL-IP IRES Neo(RC) was transfected into HEK293 cells or CHO-K1 cells (T75 flask, 30µg plasmid DNA and 90µl PEI (Sigma, St Louis)) and passaged at least 10 times in medium containing 600µg/ml Geneticin (Thermo Fisher Scientific, Waltham) to generate the HEK293 or CHO CAP256 soluble Env stable cell line. Soluble Env expression was confirmed in media from these cells at passage 5 and 10 by western blotting. A stable cell line using CAP256 gp140-FL-IP-His IRES Neo(RC) in HEK293 cells was generated in a similar fashion.

2.2.5 Soluble Env protein affinity purification

2.2.5.1 Transient transfection of HEK293T cells

For transient transfections, 20-30 confluent T150 flasks with HEK293T cells were switched to serum-free medium and transfected individually with 60µg of pMExT CAP256 gp140-FL-IP

plasmid DNA and 180µl PEI. Agarose conjugated *Galanthus nivalis* lectin (Sigma, St Louis) affinity purification columns were used to purify CAP256 gp140-FL-IP (soluble Env) protein from media four days after transfection (***Figure 2.2***). Columns were first washed with PBS+0.5M NaCl, followed by PBS only. Protein was eluted in PBS + 1M methyl α-D-manno-pyranoside (Sigma, St Louis) and subsequently concentrated and buffer exchanged into PBS using Vivaspin 20 MWCO 30 000 columns (GE Healthcare, Chicago). Thus purified CAP256 soluble Env will be referred to throughout this dissertation as CAP256 soluble Env (GNL). 100µl of concentrated protein was plated onto Luria Bertani (LB) agar plates without antibody selection, plates were incubated for 3 days at 37 °C to test for bacterial, fungal and yeast contamination. Protein was aliquoted and stored at -80°C for downstream usage. Protein concentration was determined using the DC Protein Assay (Bio-Rad, Hercules) against a BSA standard (Bio-Rad, Hercules) (see Appendix A for protocol).

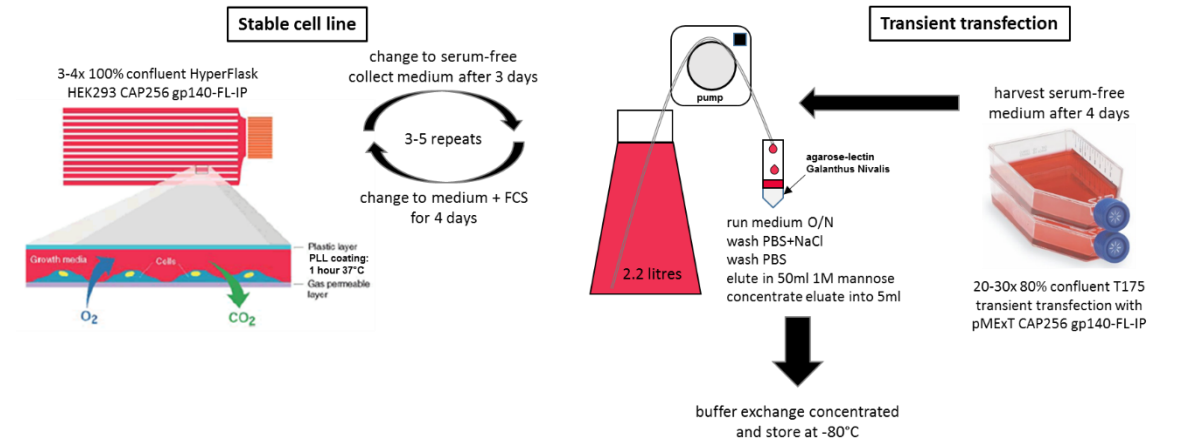

Figure 2.2. Schematic representation of CAP256 soluble Env protein isolation.
Cleared media from HEK293 CAP256 soluble Env stable cell line or HEK293T cells transiently transfected with pMExT CAP256 gp140-FL-IP is dripped over an agarose lectin (*Galanthus nivalis*) affinity chromatography column using a peristaltic pump. After two wash steps, soluble Env is eluted off the column with ~50ml 1M methyl α-D-manno-pyranoside and concentrated to 5ml.

2.2.5.2 HEK293 soluble Env stable cell lines

Three to four Hyperflasks (Corning, New York) were coated with 0.006% *w/v* poly-l-lysine (Sigma, St Louis) in PBS (1 hour at 37°C) and seeded with HEK293 CAP256 soluble Env or HEK293 CAP256 soluble Env-His stable cell lines (passage >10) from two-three T175 flasks. An additional 50ml of FCS was added one day after seeding. When flasks had grown to 100% cell confluency, media was switched to serum-free and harvested after three days. CAP256 soluble Env (GNL) isolation was performed as described above, including contaminant testing. The coating with Poly-L-Lysine allowed repeat harvesting where cells were switched from media + FCS (on Mondays) to serum-free media (on Fridays) for a total of 3-5 cycles. Protein concentration was determined using the DC Protein Assay against a BSA standard.

2.5.5.3 Verification and characterisation

To confirm isolation of soluble CAP256 Env protein and trimers, precast Native PAGE™ Novex® 3-12% Bis-Tris Protein Gels (Thermo Fisher Scientific, Waltham) were run. Gels were either stained with Bio-Safe Coomassie or blotted onto PVDF membrane (both Bio-Rad, Hercules) for western blotting. NativeMark™ Unstained Protein Standard (Thermo Fisher Scientific, Waltham) for native gel electrophoresis was used for estimating molecular weight. Furthermore, liquid chromatography–mass spectrometry, analysis and raking was performed by the Centre for Proteomic and Genomic Research (CPGR) in Cape Town to identify proteins present in CAP256 soluble Env (GNL) and CAP256 soluble, trimeric Env protein preparations.

In order to characterise the antigenic structure of the CAP256 soluble Env protein isolated using the above strategies Ni-NTA HisSorb Plates (Qiagen, Hilden) were coated with 200 ng/well CAP256 SU GP140-FL-IP-His protein for two hours at room temperature. Subsequently, plates were washed with PBS (3x) and blocked with 5% non-fat milk (Sigma, St Louis) in PBS (block buffer) for 1 hour at room temperature. After 3x PBS washes, plates were incubated with 100µl of serial dilutions (steps of 1:3) of anti-Env human monoclonal antibodies PG9, PG16, PGT128, PGT135, PGT145, CAP256 VRC26_08, VRC01, F105 and 447-52D in block buffer. After 2 hours of incubation at room temperature, plates were washed with PBS (5x) and incubated with anti-human IgG HRP (1:10,000) (Dako, Santa Clara) in block buffer for one hour at room temperature. After washing with PBS (5x), 100µl TMB ELISA Substrate (Abcam, Cambridge) was added for detection and the reaction was stopped after 10 minutes with 100µl 1N H_2SO_4. ELISA signal was analysed using a VersaMax ELISA Microplate Reader (Molecular Devices, Sunnyvale), which subtracted absorbance at 540 nm from 450 nm. Experiments were repeated for three different isolations (n=3) and these data points were averaged and fitted to a Four Parameter Logistic Regression curve (4PL curve) in GraphPad Prism 5.0 (GraphPad Software, San Diego).

2.2.6 Rabbit immunisation for adjuvant testing using soluble Env protein

Female New Zealand white rabbits were housed in the Research Animal Facility in the Faculty of Health Sciences at the University of Cape Town. All the animal procedures were approved by the UCT Animal Research Ethics Committee (UCT AEC 14-030 & UCT AEC 015/051) and performed by trained animal technologists Rodney Lucas and Inge Botes. The rabbits were monitored daily for any signs of pain, discomfort or stress and were weighed weekly.

Three groups of 5 rabbits were selected to compare formulations of CAP256 soluble Env (GNL) protein with squalene oil-in-water emulsion AddaVax™ and with alum-based AlhydroGel® (both InvivoGen, San Diego) (see ***Table 2.1*** for groups). Rabbits were immunised intramuscularly in the hind leg with 42-45µg of CAP256 soluble Env (GNL) in PBS,

at weeks 0, 4, 12 and 20. The protein suspension was mixed 1:1 (*v*/*v*) with the adjuvants. All animals were bled 2 months before the first immunisation to obtain pre-bleed sera and were bled every four weeks once protein inoculations had started. Animals were sacrificed on week 24. For the final collection of blood at the end of the experiment the rabbits received an intravenous injection of ACP, followed by a mixture of ketamine + xylazine and animals were monitored during treatment for respiratory rate, body temperature, heart rate and absence of pedal reflex. The rabbits were then exsanguinated.

Table 2.1. Groups in adjuvant testing rabbit experiment

		week protein vaccine				week serum collection							†
animal	adjuvant	0	4	12	20	-10	4	8	12	16	20	22	24 †
1986	x (PBS)	✓	✓	✓	✓	✓	✓	✓	✓	✓	✓	✓	✓
1987	x (PBS)	✓	✓	✓	✓	✓	✓	✓	✓	✓	✓	✓	✓
1988	x (PBS)	✓	✓	✓	✓	✓	✓	✓	✓	✓	✓	✓	✓
1995	x (PBS)	✓	✓	✓	✓	✓	✓	✓	✓	✓	✓	✓	✓
1996	x (PBS)	✓	✓	✓	✓	✓	✓	✓	✓	✓	✓	✓	✓
1989	AddaVax (1:1)	✓	✓	✓	✓	✓	✓	✓	✓	✓	✓	✓	✓
1990	AddaVax (1:1)	✓	✓	✓	✓	✓	✓	✓	✓	✓	✓	✓	✓
1991	AddaVax (1:1)	✓	✓	✓	✓	✓	✓	✓	✓	✓	✓	✓	✓
1997	AddaVax (1:1)	✓	✓	✓	✓	✓	✓	✓	✓	✓	✓	✓	✓
1998	AddaVax (1:1)	✓	✓	✓	✓	✓	✓	✓	✓	✓	✓	✓	✓
1971*/1992**	AlhydroGel (1:1)	✓	✓	✓	✓	✓	✓	✓	✓	✓	✓	✓	✓
1993	AlhydroGel (1:1)	✓	✓	✓	✓	✓	✓	✓	✓	✓	✓	✓	✓
1994	AlhydroGel (1:1)	✓	✓	✓	✓	✓	✓	✓	✓	✓	✓	✓	✓
1999	AlhydroGel (1:1)	✓	✓	✓	✓	✓	✓	✓	✓	✓	✓	✓	✓
2000	AlhydroGel (1:1)	✓	✓	✓	✓	✓	✓	✓	✓	✓	✓	✓	✓
*Lost tag													
**New tag													
† sacrificed													

2.2.7 Rabbit serum characterisation

2.2.7.1 Soluble Env binding ELISA

To assess Env binding antibody titres in rabbit sera, a matching soluble CAP256 Env binding ELISA was performed. Nunc MaxiSorp® flat-bottom 96 well plates (Sigma, St Louis) were coated with 10ng/well CAP256 soluble Env (GNL) overnight at 4°C. After protein coating, plates were washed 3x with PBS, blocked in PBS + 5% non-fat milk (block buffer) at room temperature for one hour. After washing (3x PBS), rabbit sera was used in the primary incubation in a serial dilution range in block buffer, starting at 1:10, for 2 hours at room temperature. Plates were washed 3x with PBS + 0.1% Tween20 (Sigma, St Louis) (PBST) and anti-rabbit IgG HRP (1:10,000 in block buffer) (Roche, Basel) was used for detection (1 hour at room temperature). After washing (3x PBST) ELISA signal was visualised with TMB

ELISA Substrate (Abcam, Cambridge). The reaction was stopped after 10 minutes with 1N H_2SO_4. The ELISA signal was analysed using a VersaMax ELISA Microplate Reader, which subtracted absorbance at 540nm from 450nm. ELISAs for the whole time course and each group were performed at the same time on duplicate plates. Duplicate data points were averaged and fitted to a 4PL curve in GraphPad Prism 5.0. Antibody end-point titres were calculated from 4PL curves with the threshold set as twice the geometric mean of the ELISA signal over the whole, matching pre-bleed serial dilution range:

$$End\ point\ titre = EC50 * \left(\frac{Standard\ Error\ Curve\ Min}{Curve\ Max - (geometric\ mean\ pre \cdot bleed)}\right)^{1/Hill\ Slope}$$

Data plotted as mean +/- SEM for whole group.

2.2.7.2 V1V2-loop binding ELISA

To test for antibodies to the CAP256_SU V1V2-loop, serum from the week 22 bleed was tested in a binding ELISA to CAP256 SU V1V2 scaffolded protein (provided by Penny Moore and Lynn Morris, NICD). A similar protocol was used as for soluble Env binding ELISA as described above with two permutations. 1) 500ng/well of CAP256 SU V1V2 scaffolded protein was coated onto MaxiSorp® flat-bottom 96 well plates and 2) PBST was replaced with PBS in all steps.

2.2.7.3 Env-pseudotyped virus neutralisation

Rabbit sera from different time points were tested for the ability to inhibit Env-pseudotyped virions to enter a reporter cell line. Neutralisation was measured as a reduction in luciferase gene expression after a single round of infection of JC53bl-13 cells, also known as TZM-bl cells (NIH AIDS Research and Reference Reagent Program), with Env-pseudotyped viruses (MW965.26, 6644, CA146, 1107356, CAP37, CT349, Du156, 188146, CAP256_SU, CAP256_SU K169E or BG0505N332+/CAP256_SU V1V2-loop and CAP84/CAP256_SU V1V2-loop). Titre was calculated as the reciprocal plasma/serum dilution causing a 50% reduction of relative light units (ID_{50}). Dilutions were started at 1:20. For graphs, data was plotted as 19 when ID_{50} was <20. MuLV was used as negative control.

All neutralisation assays were performed by Professor Lynn Morris's group at Center for HIV and STIs, National Institute for Communicable Diseases of the National Health Laboratory Service, Johannesburg, South Africa.

2.2.8 Statistical analysis

All statistical analysis was performed in GraphPad Prism 5.0 and tests are indicated in results and/or corresponding figure legend

2.3 Results

2.3.1 Schematic overview of CAP256 Env

The subtype C Env sequence chosen for this work was derived from the Centre for the AIDS Programme of Research in South Africa (CAPRISA) 002 acute infection cohort [167, 174]. This particular virus was the superinfecting virus (SU) from participant CAP256 who developed broadly cross-neutralising antibodies targeting the V1V2 loop 15 weeks after the second viral infection event and was labelled CAP256_SU. A range of modifications were introduced into CAP256_SU Env with the aim of increasing its yield, stability and immunogenicity (***Figure 2.3***). Firstly, the native signal peptide was replaced with the commonly used human tissue plasminogen activator (tPA) leader to increase cellular trafficking towards the plasma membrane and subsequent budding and/or secretion [416, 417]. Next, the furin cleavage site was replaced with a flexible linker (FL) consisting of two repeats of glycine rich motif (GGGGS) based on the work of Sharma *et al.*, 2015 [384] who showed that trimeric Env retained a native-like state with this particular modification. This would alleviate the furin cleavage of gp120 from gp41 which can be inefficient in mammalian expression systems, and could result in incomplete processing and misfolded Env protein [107, 372]. Thirdly, the equivalent of the I559P mutation was introduced in CAP256 Env to stabilise the gp41 trimer [374]. Finally, the sequence was human codon optimised by GenScript (Nanjing) to increase expression levels. For protein vaccines, the transmembrane domain and cytoplasmic tail of gp160 were deleted by gene truncation to AA 653, equivalent to AA 664 for BG505 SOSIP.664, resulting in a presumably soluble Env protein which should be secreted from cells (***Figure 2.3***).

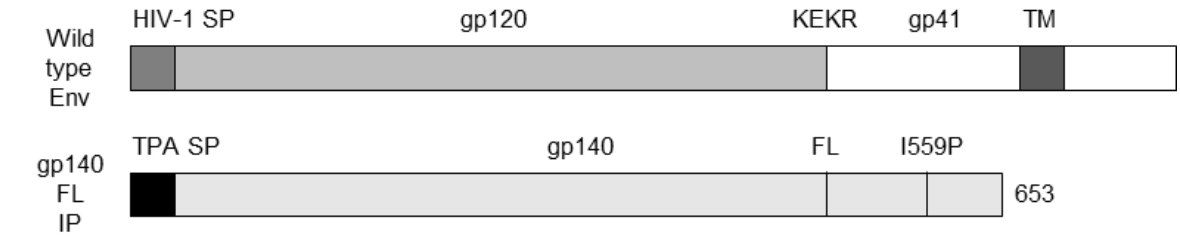

Figure 2.3 CAP256 gp140-FL-IP protein vaccine design.
Schematic representations comparing of wild type Env to soluble CAP256 Env (CAP256 gp140-FL-IP) used for the experiments presented here. Truncation to amino acid 653 rendered CAP256 Env soluble, while containing further modifcations where the wild type signal peptide (HIV-1 SP) was replaced with the human tissue plasminogen activator (TPA) sequence, the furin cleavage site with a flexible linker (FL) sequence and an I559P mutation was introduced.

2.3.2 Characterisation of affinity purified soluble Env

In initial experiments, soluble Env was isolated from media of 20 T150 flasks transiently transfected with pMExT CAP256 gp140-FL-IP. This was done four days after transfection by lectin (*Galanthus nivalis*) affinity chromatography, with cells switched to media without FCS

before transfection to prevent the Env being contaminated with large quantities of alpha-2-macroglobulin. A clear enrichment in soluble Env levels, from (cleared) media to lectin column eluate and concentrated eluate, could be detected by western blotting of SDS PAGE gels (***Figure 2.4A***). However, some soluble Env failed to bind the column (lectin column flow-through) and was washed off with the first wash step (PBS + 0.5M NaCl) or was lost during concentrating (conc. column flow through). A band of the same molecular weight as Env was detected in the concentrated eluate of a Coomassie stained gel (***Figure 2.4B***). This Coomassie stained gel also showed that this lectin eluate did not contain large amounts of impurities of other proteins, which was confirmed by liquid chromatography–mass spectrometry (LC-MS) with soluble Env being the dominant protein present ***(Table 2.2)***.

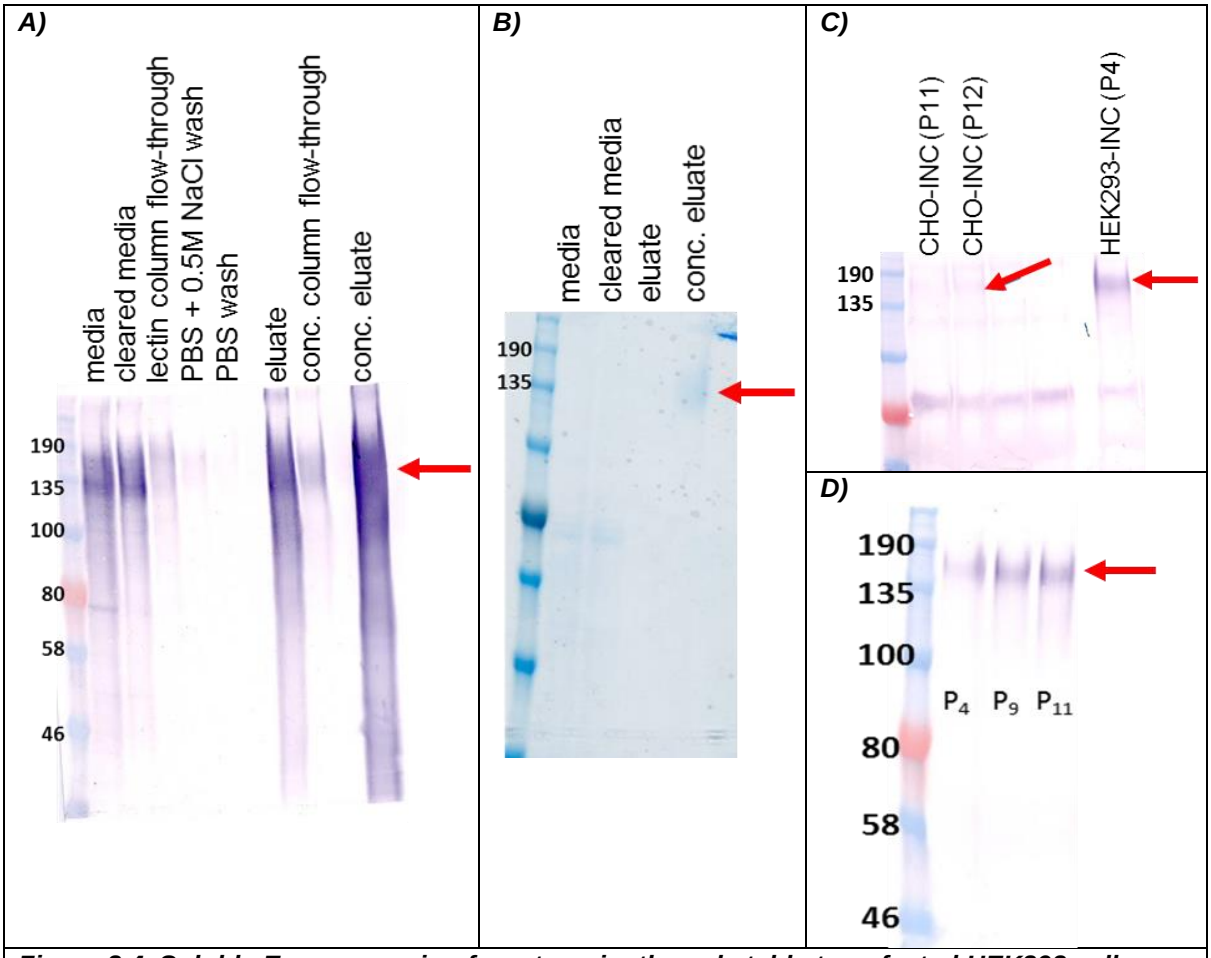

Figure 2.4. Soluble Env expression from transiently and stably transfected HEK293 cells.
(A) Soluble Env was affinity purified from cleared media of HEK293T cells transfected with CAP256 gp140-FL-IP and was clearly enriched in concentrated (conc.) eluate compared to input (cleared media) as detected by α-Env western-blotting.
(B) Coomassie staining revealed a protein band in the concentrated eluate of the same size as Env detected by western blotting indicating adequate yields.
(C) Although a faint band for Env was detected by western blotting in media from the CHO CAP256 gp140-FL-IP stable cell line (CHO-INC) at passage (P)11 and P12, levels were clearly much lower compared to the HEK293 CAP256 gp140-FL-IP stable cell line (HEK293-INC) at P4. ***(D)*** Soluble Env levels in the media of HE293K-INC were similar at P4, P9 and P11.

Table 2.2. Top ten proteins identified in lectin affinity purified soluble Env by LC-MS.
Ranking was based on |Log Probability| (third column).

Rank	Description	|Log Prob|	Total Intensity	# of spectra	# of unique peptides	# of mod peptides	Coverage %
1	***CAP256 soluble Env***	253.22	20766168743	1472	81	12	42.16
2	sp|P24821|TENA_HUMAN Tenascin	93.98	45076102.6	67	29	2	13.86
3	sp|P68371|TBB4B_HUMAN Tubulin beta-4B chain	74.64	136046989	95	21	6	32.58
4	sp|P07602|SAP_HUMAN Prosaposin	52.05	153907594.6	77	12	2	18.13
4	tr|C9JIZ6|C9JIZ6_HUMAN Prosaposin						
5	sp|P14625|ENPL_HUMAN Endoplasmin	48.91	46242792	50	14	1	17.56
6	sp|P0DMV9|HS71B_HUMAN Heat shock 70 kDa protein 1B	48.01	69582202.8	58	16	2	22.78
6	sp|P0DMV8|HS71A_HUMAN Heat shock 70 kDa protein 1A						
7	sp|P14543|NID1_HUMAN Nidogen-1	43.45	18829446.8	29	12	1	11.07
8	sp|Q92820|GGH_HUMAN Gamma-glutamyl hydrolase	41.64	24648663.1	37	14	2	32.39
9	sp|P07942|LAMB1_HUMAN Laminin subunit beta-1	41.44	20222558.8	26	11	0	7.89
9	tr|G3XAI2|G3XAI2_HUMAN Laminin subunit beta-1						
10	sp|P11047|LAMC1_HUMAN Laminin subunit gamma-1	41.29	55247410.1	50	16	2	9.7

Although reasonable Env yields ***(Table 2.3)*** were obtained for small scale animal experiments as assessed by by Protein DC Assay with BSA standard, the transient platform was highly labour intensive for both tissue culture purposes and plasmid DNA generation, making it unsuitable for further upscaling. Therefore, stable cell lines were generated in both HEK293 and CHO cells. For this an IRES-Neo(RC) was cloned directly behind the STOP codon of CAP256 gp140-FL-IP in pMExT (***Figure 2.3***). In this plasmid, Env and the neomycin resistance gene (Neo(RC) are expressed from the same promoter, with the IRES site allowing an additional binding site for the translational machinery to produce neomycin resistance (Geneticin in mammalian cells). This couples neomycin resistance to soluble Env expression, which favours good expression levels of soluble Env following selection. After initial transfection of pMExT CAP256 gp140-FL-IP, cells were passaged for 10 rounds (P10) under Geneticin selection after which the cell line was considered stable. Although both stable CHO and HEK293 CAP256 gp140-FL-IP (P>10) were resistant to Geneticin, only the latter showed high enough expression levels in media to be considered ***(Figure 2.4C)***. All lectin affinity purified CAP256 soluble Env isolated from stable cell lines discussed below is from HEK293 CAP256 gp140-FL-IP (P>10). When yields were compared, isolations from the stable cell lines were similar to transient expression (n=2, ***Table 2.3***). However, ease of use and repeat harvesting of the same flasks favours the stable cell line. Interestingly, soluble Env protein yields appeared to increase after the first harvest (***Table 2.3***). Note that transient expression was in HEK293T cells whereas the stable cell line was generated in HEK293 cells.

Table 2.3. Soluble Env protein yields after lectin affinity chromatography.
Protein concentrations were measured using the DC Protein Assay against a BSA standard (three independent measurements per experimental sample and BSA standard concentration)

platform	flasks	harvest	concentrated eluate (mg/ml)	total mg	mg/flask
transient	20x T150	1	0.17	0.93	0.05
transient	20x T150	2	0.18	1.00	0.05
stable	4x hyperflask	1A*	0.39	2.36	0.06
stable		1B*	0.61	3.67	0.09
stable		1C*	0.42	2.54	0.06
stable		1D*	0.49	2.95	0.07
stable	4x hyperflask	2A*	0.43	2.35	0.06
stable		2B*	0.70	3.85	0.10
stable		2C*	0.64	3.54	0.09
stable		2D*	1.01	5.56	0.14
stable		2E*	0.78	4.30	0.11
		*repeat harvest from same hyperflasks			

To get an indication of the structural integrity of soluble Env isolated from the two platforms, lectin affinity purified protein was separated on Blue-Native PAGE gels and subsequently Coomassie stained or blotted using an α-Env antibody (***Figure 2.5A+B***). The profile appeared largely similar, consisting of mainly trimeric Env protein as determined by molecular weight. However, some monomeric Env, aggregates and dimers were present as well (in order of abundance). Surprisingly, when soluble Env-His was analysed in a similar fashion, the Env trimer appeared much less stable, with mainly Env monomers detected, with lower levels of Env dimers and almost no trimeric Env (***Figure 2.5C***).

In an attempt to further characterise the Env quaternary structure and the presence of bnAb epitopes, several different ELISA protocols were assessed using Env bnAbs (***Table 1.1***). Trapping soluble Env straight on ELISA plates or using ELISA plates pre-coated with lectin (*Galanthus nivalis*) were unsuccessful (data not shown). Therefore, this was repeated with the His-tagged soluble Env, despite the unfavourable profile on Blue-Native PAGE gels. The bnAb 10E8 was excluded from the analysis as soluble Env was truncated within the MPER binding region of this antibody. The bnAb epitopes detected for CAP256 soluble Env-His were for the V3-glycan supersite (PGT128 and PGT135), the CD4-binding site (VRC01) and the V1V2-glycan bnAb PG9 (***Figure 2.6A***). However, no signal was observed for bnAbs that specifically detect native-like Env trimers (PGT145, PG16 and CAP256 VRC26.08) (***Figure 2.6B***). This result is corroborated by the detection ELISA signal for F105 and 446-52D, indicative of the

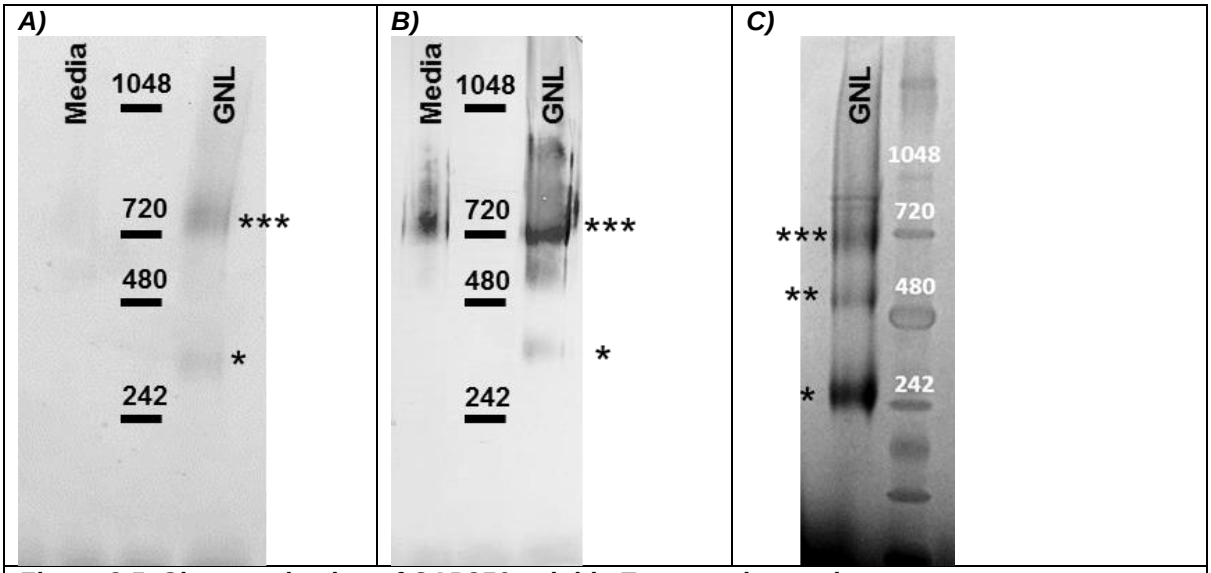

Figure 2.5. Characterisation of CAP256 soluble Env protein vaccines.
Lectin affinity purified soluble Env (GNL) mainly consists in a trimeric conformation (***) as judged by molecular weight on BN PAGE gels stained by Coomassie ***(A)*** or as detected by Env western blotting ***(B)***, although some monomeric Env was detected as well (*). However, similarly purified soluble Env-His is mainly in a monomeric (*) or dimeric (**) configuration with low levels of Env trimers (***) *(C).* Media: input on affinity chromatography column (*Galanthus nivalis* lectin conjugated agarose).

presence of misfolded Env. The assay was verified by using a control His-tagged Env trimer (BG505 SOSIP.664, supplied by NICD) in parallel, where binding of all bnAbs tested was observed, with the lowest signal for F105 and 446-52D (***Figure 2.6C***), whereas the no protein control was negative (***Figure 2.6D***).

2.3.3 Adjuvanting soluble Env with AlhydroGel® or AddaVax™

2.3.3.1 Rabbit immunisation and serum anti-Env antibody characterisation

This HIV-1 Env vaccine project was aimed at assessing different priming platforms (DNA alone, rMVA alone and DNA followed by rMVA) which were then boosted by a protein vaccine to induce higher α-Env binding antibody titres and viral neutralising antibody titres. However, the protein boosting effect can be highly influenced by adjuvanting as well. Therefore, in the first animal experiment the effect of different protein vaccine adjuvants was investigated. For this the adjuvant AddaVax™, a squalene-based oil-in-water nano-emulsion (MF59®-like) was compared to AlhydroGel® (aluminium hydroxide gel) in rabbits. The first can induce both cellular and humoral immune responses [426, 427], whereas the latter mainly enhances a Th2 response [428]. A total of 40µg soluble Env (GNL) from transiently transfected HEK293T cells was injected intramuscularly in the rabbit hind leg in two different adjuvants (1:1 ratio) and compared to no adjuvant PBS control (***Table 2.1, Figure 2.7A***). The same soluble Env (GNL) was used to develop an in-house Env binding ELISA to test rabbit serum α-Env binding antibodies at different time points. Although AddaVax™ failed to improve binding antibody

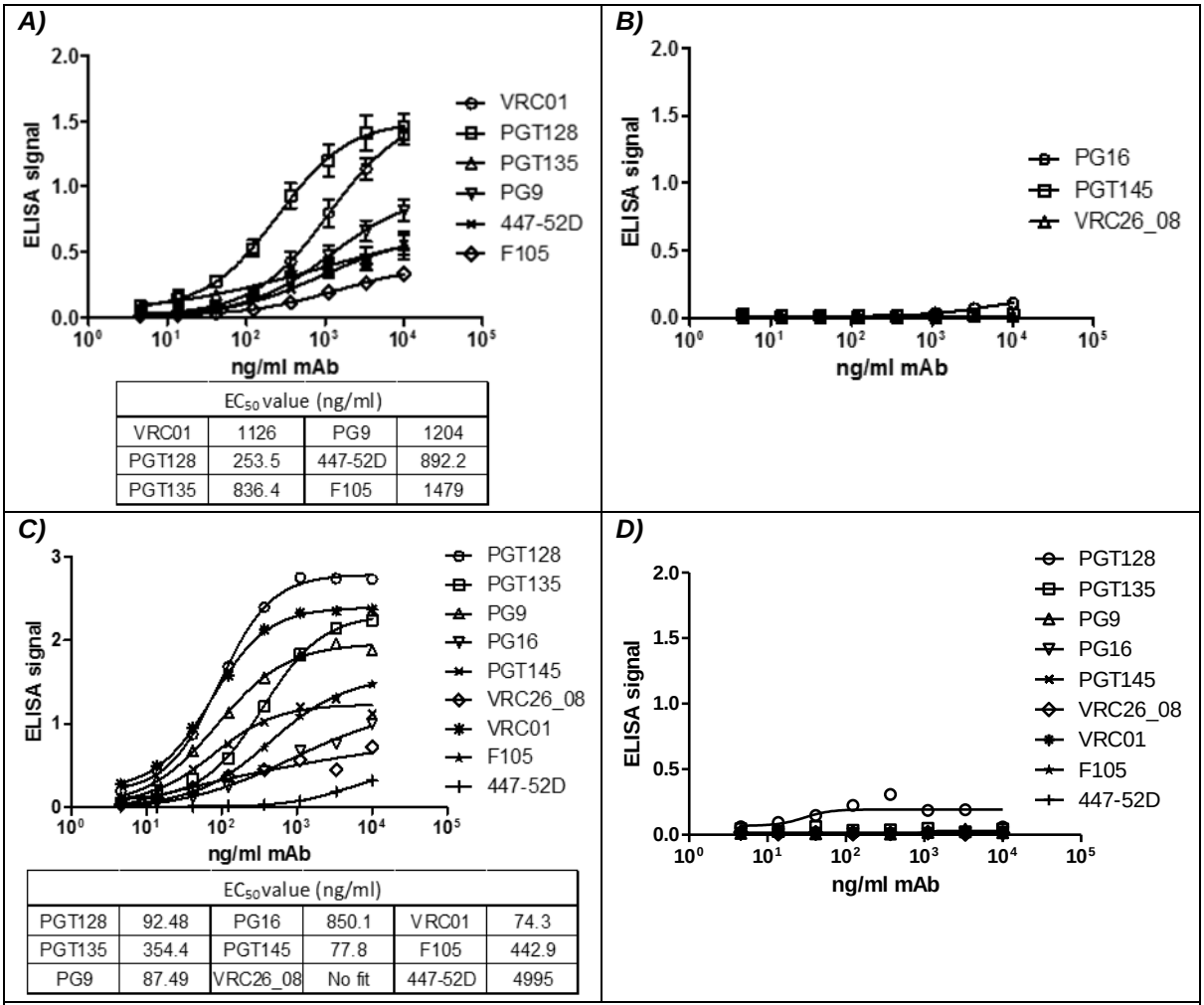

EC_{50} value (ng/ml)			
VRC01	1126	PG9	1204
PGT128	253.5	447-52D	892.2
PGT135	836.4	F105	1479

EC_{50} value (ng/ml)					
PGT128	92.48	PG16	850.1	VRC01	74.3
PGT135	354.4	PGT145	77.8	F105	442.9
PG9	87.49	VRC26_08	No fit	447-52D	4995

Figure 2.6. Soluble Env-His protein α-Env bnAb ELISA.
Binding ELISAs using anti-Env human bnAbs to CAP256 gp140-FL-IP-His.***(A)*** Several bnAb epitopes were verified to be present in CAP256 gp140-FL-IP-His: the Env V3-glycan supersite (PGT128 and PGT135), the CD4 binding site (VRC01) and the V2-glycan epitope (PG9). EC_{50} values, calculated from the curve fit, are given to indicate the affinity of each bnAb to Env. However, no native-like trimers are detected with bnAbs PGT145, PG16 and CAP256 VRC26.08 ***(B)***. Indicative of this are the positive ELISA signals for F105 and 446-52D, which recognise mainly misfolded trimers.
(C) The assay was verified with a control protein: soluble, trimeric BG505_664-His Env. EC_{50} values, calculated from the curve fit, are given to indicate the affinity of each bnAb to Env.
(D) No signal was observed in the no protein control (=PBS).

titres compared to the PBS control group at all time points, animals in the AlhydroGel® group had significantly higher sera α-Env binding antibody levels over the whole time course compared to both the AddaVax™ and control groups (Two-way ANOVA; $p<0.0001$) (***Figure 2.7B***). For all groups, α-Env binding antibody titres peaked at week 22, at a dilution of 1 in 443,199 ±192,842 for the AlhydroGel group, 1 in 66,196 ±27,191 for AddaVax™ and 1 in 71,398 ±34,647 for the PBS group.

Binding antibodies against the V1V2 loop of Env are of particular interest as this was one of the main correlates of protection in the RV144 trial. Therefore, sera of the vaccinated animals at peak α-Env binding antibody titres (week 22) were tested in a binding ELISA against the

autologous CAP256 SU V1V2 loop: this was presented on a scaffold to retain the natively folded state [424], and was kindly provided Dr Penny Moore from the NICD. CAP256 soluble Env (GNL) was able to induce α-Env V1V2 loop-binding antibodies, and again end-point titres for the AlhydroGel® group were significantly higher compared to the other 2 groups (One-way ANOVA; p<0.05) (***Figure 2.7C***).

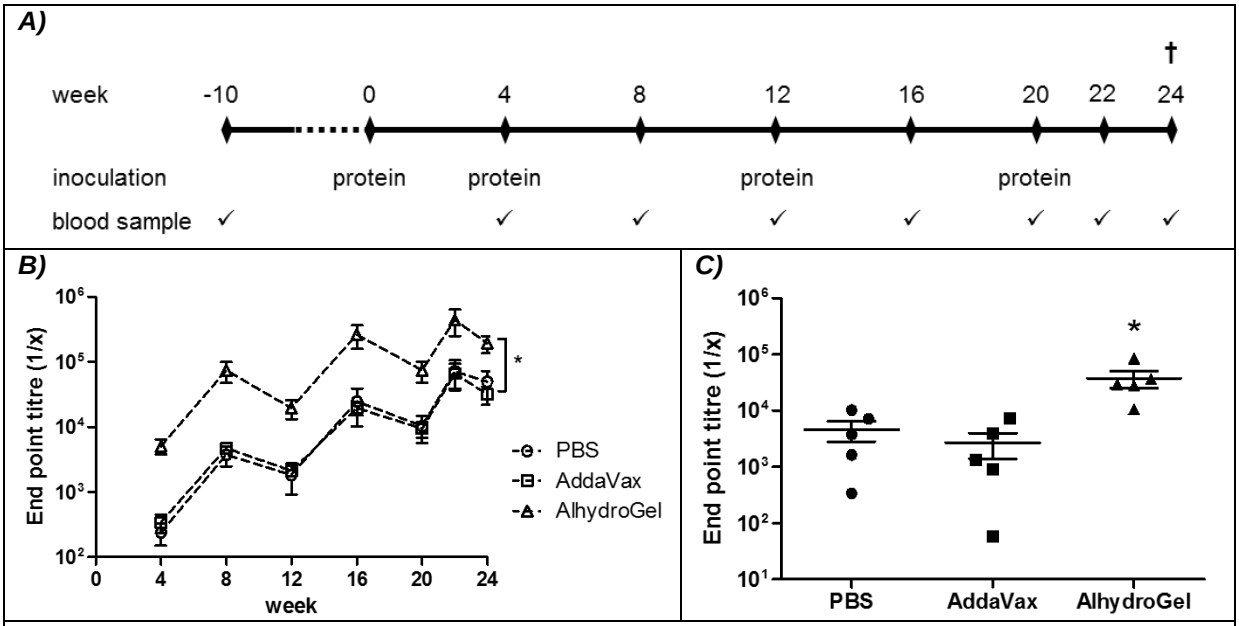

Figure 2.7. Rabbit immunisation protocol and serum characterisation.
(A) Immunisation regimen.
(B) Rabbit sera soluble Env (GNL) binding ELISA. Soluble Env (GNL) adjuvanted in AlhydroGel® induces significantly higher serum anti-Env antibodies titres over the whole time course as compared to PBS control and AddaVax™ (Two-way ANOVA; * p<0.0001). Plates were coated with 10ng/well of soluble Env (GNL).
(C) CAP256 SU V1V2 loop scaffold binding ELISA for week 22 sera. Animals inoculated with adjuvant AlhydroGel® had significantly higher binding to CAP256 V1V2 loop scaffold as compared to control group and AddaVax™ as adjuvant (One-way ANOVA; * p<0.05). Signal from week 0 was subtracted from week 22. Plates were coated with 500ng/well of scaffolded CAP256 V1V2-loop protein.
All end point titres are plotted as group average ±SEM.

2.3.3.2 Neutralisation responses after immunisation

As expected from the two different binding ELISAs, soluble Env (GNL) adjuvanted in AlhydroGel® was superior at inducing antibodies that inhibited cell entry of Env-pseudotyped virions (***Table 2.2, Figure 2.8A+B***). This was most apparent for Tier 1A Clade C virions (MW965.26), where at all time points tested, the serum dilution resulting in a 50% decrease in cell entry (ID_{50}), was significantly higher with all animals responding for the AlhydroGel® group, than for the control or AddaVax™ groups (Two-way ANOVA; p<0.05) (***Figure 2.8B***). Titres at week 16 and 22 were significantly higher (p<0.001 and p<0.05 respectively). Although a similar trend was observed for Tier 1A Clade B (MN.3), this was not significant. Tier 1B Clade C neutralisation titres were only assessed for week 22 sera (peak Env binding titres) and more animals in the AlhydroGel® group showed neutralisation of 6644, CA146, 1107356,

Table 2.2. Serum neutralisation from rabbits vaccinated with different adjuvants as measured by TZM-bl assay.

Sera from immunised animals were assessed for neutralising activity (serum dilution required for a 50% reduction in entry of the infecting virus into a reporter cell line (ID50) against a panel of Env-pseudotyped virions at different time points. The 50% neutralisation titres are color-coded to reflect their potency range as indicated.

Titres below 20 are considered negative. pre= pre-bleed; w = week.

		Clade C - Tier 1A MW965.26 ID_{50} at					Clade B - Tier 1A MN.3 ID_{50} at					Clade C - Tier 1B ID_{50} at							Clade C - Tier 2 CAP256.SU ID_{50} at					Control MuLV ID50 at
												6644	CA146	1107356	CAP37	CT349	Du156	188146					
rabbit	adjuvant	pre	w08	w16	w22	w24	pre	w08	w16	w22	w24	w22	w22	w22	w22	w22	w22	w22	pre	w08	w16	w22	w24	w24
1986	PBS	<20	52	496	386	404	<20	<20	<20	<20	<20	40	<20	<20	<20	<20	<20	<20	<20	<20	<20	<20	<20	<20
1987		<20	<20	<20	<20	<20	<20	<20	<20	<20	<20	<20	<20	<20	<20	<20	<20	<20	<20	<20	<20	<20	<20	<20
1988		<20	24	70	64	74	<20	<20	<20	<20	<20	<20	<20	<20	<20	<20	<20	<20	<20	<20	<20	<20	<20	<20
1995		<20	55	729	391	346	<20	<20	<20	<20	<20	62	<20	<20	<20	<20	<20	<20	<20	<20	<20	<20	<20	<20
1996		<20	<20	<20	20	<20	<20	<20	<20	<20	<20	<20	<20	<20	<20	<20	<20	<20	<20	<20	<20	<20	<20	<20
1989	AddaVax	<20	<20	20	<20	<20	<20	<20	<20	<20	<20	<20	<20	<20	<20	<20	<20	<20	<20	<20	<20	<20	<20	<20
1990		<20	<20	125	298	207	<20	<20	26	22	72	49	<20	<20	<20	<20	43	<20	<20	<20	<20	<20	<20	<20
1991		<20	37	92	58	35	<20	<20	<20	22	<20	25	<20	<20	<20	<20	<20	<20	<20	<20	<20	<20	<20	<20
1997		<20	25	113	228	126	<20	<20	<20	<20	<20	117	20	24	<20	<20	<20	<20	<20	<20	<20	<20	<20	<20
1998		<20	46	121	100	74	<20	<20	<20	<20	<20	<20	<20	<20	<20	<20	<20	<20	<20	<20	<20	<20	<20	<20
1992	AlhydroGel	<20	476	659	2077	1603	<20	<20	<20	34	<20	484	35	22	52	44	<20	<20	<20	<20	<20	<20	<20	<20
1993		<20	448	1824	2057	1026	<20	<20	218	200	220	533	34	<20	<20	<20	<20	<20	<20	<20	<20	<20	<20	<20
1994		<20	1262	1768	1195	933	<20	40	93	<20	<20	253	24	<20	<20	<20	<20	<20	<20	<20	<20	<20	<20	<20
1999		<20	3942	9151	5896	6017	<20	99	42	42	23	1178	43	67	<20	<20	<20	<20	<20	<20	<20	<20	<20	<20
2000		<20	1489	3535	863	639	<20	<20	29	<20	<20	165	29	99	28	22	<20	<20	<20	<20	<20	<20	<20	<20

50% Neutralization titre
1 000 - 10 000
100 - 1 000
20 - 100
<20

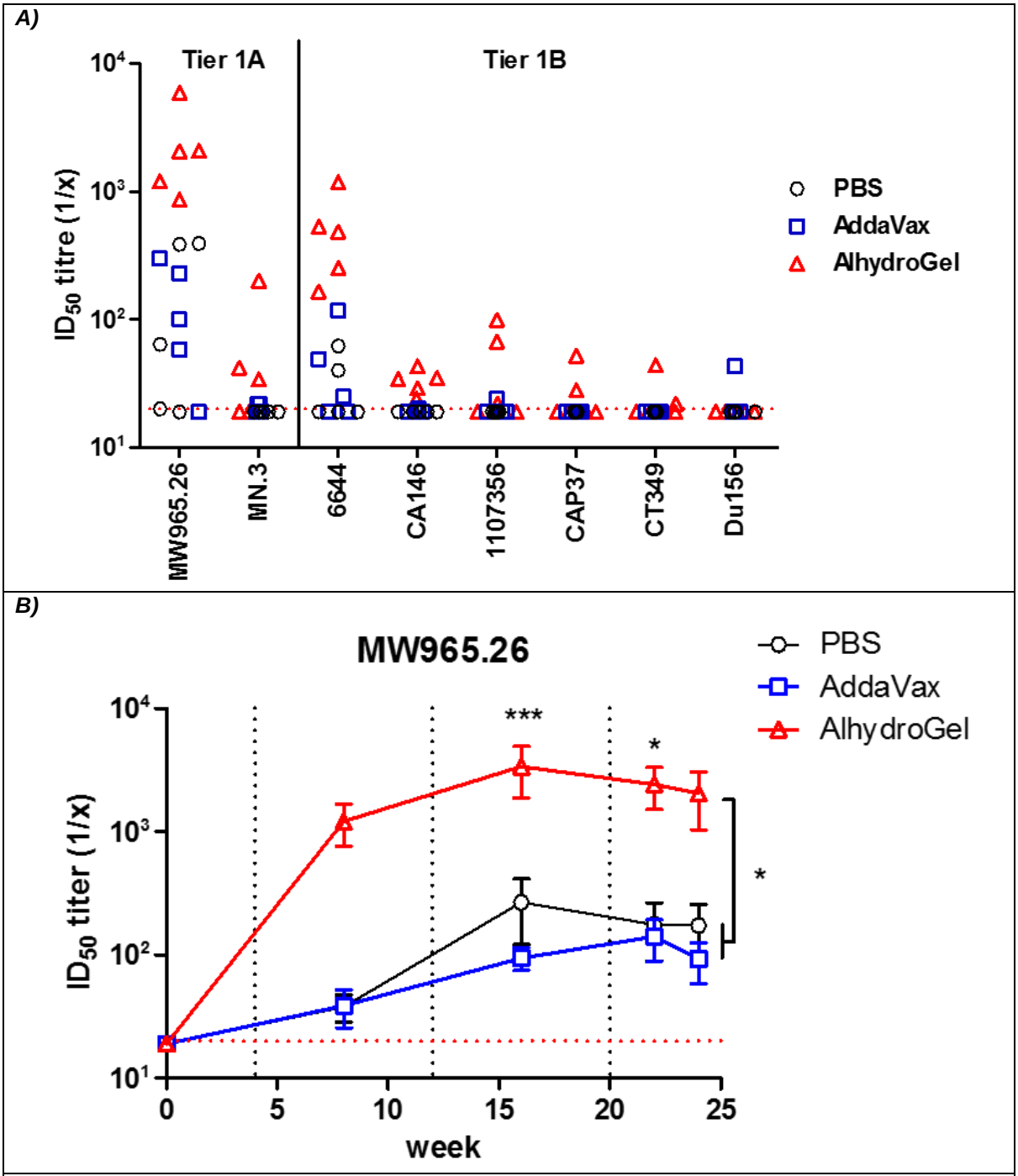

Figure 2.8. Serum neutralisation at week 22 and full time course for MW965.26 as measured by TZM-bl assay.

Dotted red line represents assay detection limit (1/20 dilution). All data points below detection limit are plotted as 19.

(A) ID_{50} titres at week 22 reflecting enhanced neutralisation in the AlhydroGel® group.

(B) Time course of ID_{50} titres for MW965.26 are significantly higher in the AlhydroGel® group (Two-way ANOVA; ***p<0.001; *p<0.05).

Vertical, dotted black lines represent time points of protein boosts. MW965.26 neutralisation titres for the whole time course are plotted as group average ±SEM.

CAP37 and CT349 psuedovirions (***Table 2.2, Figure 2.8A***). Furthermore, neutralisation titres for 6644 and CA146 were significantly higher compared to control or AddaVax™ groups (One-way ANOVA; $p<0.05$ and $p<0.001$). Unfortunately, none of the sera neutralised the vaccine-matched Tier 2 Clade C virus (CAP256 SU WT) at any time point for any of the groups.

2.4 Discussion

2.4.1 Characterisation of CAP256 soluble Env

During the course of this project, a protocol was developed to affinity purify CAP256 soluble Env using *Galanthus nivalis* lectin from the cell media of both transiently transfected HEK293T cells and HEK293 stable cell lines, with a high degree of purity as assessed by LC-MS. Harvesting CAP256 soluble Env from stably transfected cell lines turned out to be easily scalable, with repeat harvesting from the same flasks. As correct Env folding is critical for vaccine studies [112], the Env species present in affinity purify CAP256 soluble Env (GNL) was initially assessed by Blue-Native PAGE electrophoresis, where very similar profiles of

soluble Env (GNL) purified from both transiently transfected and stable cell lines were observed, with Env present in a mainly trimeric conformation as based on molecular weight. Surprisingly, addition of a C-terminal His-tag to CAP256 soluble Env dramatically altered this profile, with monomeric Env representing the bulk of Env species present after affinity purification, whereas the fraction of Env trimers were lower to those observed for both Env dimers and monomers. Although in general the addition of His-tag to a protein has no detrimental effects, it has been reported to in some cases it can affect enzyme activity, protein folding and change disulphide-bonding patterns [429, 430], with the latter two of course being extremely important for HIV-1 Env [431].

Unfortunately, an ELISA-based assay to characterise the quaternary structure of the soluble Env proteins could only be developed for the His-tagged version of soluble Env, by capturing this protein on nickel coated ELISA plates (Ni-NTA plates) in a similar strategy as reported by other groups [277, 371, 432, 433]. The impaired folding of CAP256 soluble Env-His was confirmed by a lack of signal to bnAbs which recognise native-like Env trimers (PG16, PGT145 and CAP256 VRC26.08), and the presence of misfolded Env was confirmed with the binding of F105 and 446-52D. However, bnAb epitopes for the V3-glycan supersite (PGT128 and PG135), the CD4 binding site (VRC01) and the V2-glycan in bnAb PG9 were present in CAP256 soluble Env-His. Although Env folding appeared far from ideal when a His-tag was included, with the far better BN-PAGE profile for CAP256 soluble Env (GNL) which mainly contained trimeric Env (based on molecular weight), an improvement in the presence of bnAb

epitopes for this protein is anticipated, and therefore CAP256 soluble Env (GNL) was taken forward for testing in rabbits.

2.4.2 Soluble Env is more immunogenic when adjuvanted with AlhydroGel® compared to AddaVax™

In order to achieve the full potential of the different DNA, rMVA and protein vaccines generated in this project in different prime/boost protocols, the first round of animal experiments was designed to test the effect of the protein vaccine formulated in different adjuvants for their immunogenic properties as these can be significantly enhanced with the appropriate adjuvant, which is particularly important for subunit vaccines [360]. Different adjuvants can shift the immune system towards a more humoral and/or cellular response upon vaccination. In AddaVax™ (similar to MF59®), a squalene-based oil-in-water nano-emulsion adjuvant was tested. In general these types of adjuvants enhance both a cellular and humoral immune responses [426, 427]. This was compared to AlhydroGel®, an aluminium hydroxide gel akin to Alum, a class of adjuvants which results in stimulating mainly a Th2 helper T cell response [428]. Unadjuvanted protein was included as a control (PBS group) and lectin affinity purified soluble Env (GNL) was used for all three groups. Formulation in AlhydroGel®, AddaVax™ or PBS resulted in Env binding antibodies in rabbit sera, which peaked after every inoculation but then decreased before the next boost. This is a typical pattern for in α-Env binding antibodies titres when soluble Env protein is used and has been reported before [434]. Even to the extent that in the RV144 clinical study this decrease in antibody titres correlated with a loss in protection from HIV infection [221, 242]. Although the pattern in α-Env binding antibody titres was similar for all groups, they were significantly higher for the AlhydroGel® group. This probably underlies the significantly higher antibody titres against the CAP256 V1V2-loop at week 22 in this group as well. In line with this, soluble Env formulated in AlhydroGel® is also more immunogenic based on an improved Tier 1A and 1B neutralisation response compared to AddaVax™ or PBS. Although it should be emphasised that no vaccine matched CAP256_SU Tier 2 neutralisation was observed. This could be due to the Env protein used in this experiment which was only affinity purified using lectin. The neutralisation response might improve when further purification such as size exclusion chromatography for isolation of trimeric Env (as used in later experiments) [277, 371, 433], possibly followed by negative selection of misfolded trimers using MAbs such as F105 or 447-52D [385, 422] or positive selection of native-like trimers with MAbs PG16 or CAP256 VRC26.08 [371, 435].

Of note as well is that using AddaVax™ failed to show an improvement in binding or neutralising antibody responses over PBS in these experiments. This lower immunogenicity of protein vaccines adjuvanted in AddaVax™ compared to AlhydroGel® (in Alum or aluminium

hydroxide) is contrary to what has been reported before [366, 436]. Similarly, in a nonhuman primate studies where in one gp140 TV1ΔV2 protein formulated in MF59® induces higher anti-Env binding and Tier 1A neutralisation titres compared to alum formulation (aluminium hydroxide gel) [437]. Another study showed that ALVAC-SIV plus MF59® adjuvanted gp120 had stronger systemic and mucosal responses to Env than the group receiving alum [438], although this was not tested here. In the latter study though, the alum group gave better protection in a challenge model suggesting qualitative differences in antibody responses [438]. Directly comparing these different adjuvants for soluble Env protein vaccines is difficult however as this has either not been done or animal models (rabbit, mice, nonhuman primates), exact adjuvants (MF59® or AddaVax™; alum, aluminium hydroxide or AlhydroGel®), Env sequences (isolates and/or gp120, gp140) or virus (HIV-1, influenza) differ in these studies. But as AlhydroGel® out performed AddaVax™ to such an extent in this study, it was decided for usage in formulating the protein vaccines in prime-boost experiments even though concerns have been raised that aluminium based adjuvants might impair Env structure. However, this has recently been disproved for two soluble Env antigens (Clade A BG505 SOSIP.664 and clade B B41 SOSIP.v4.1 trimers) formulated in AlhydroGel® [423]. Interestingly, in that same paper aluminium sulphate does disrupt Env structure, suggesting that one should be careful as to how the aluminium in the adjuvant is formulated.

CHAPTER 3: PRODUCTION, CHARACTERISATION AND IMMUNOGENICITY OF CAP256 GP150 AND HIV-1C GAG CANDIDATE VACCINES

3.1 Introduction

Vaccines which are currently approved for the use in humans can be broadly divided in two groups. The first contains whole pathogens which are either live-attenuated or inactivated preparations, made so as to reduce or remove the pathogen virulency. Safety concerns with HIV-1 using these whole pathogen approach, such as reversion of attenuated vaccine, recombination between vaccine and circulating virus and incomplete inactivation, makes these strategies nonviable options. Therefore, there is an intense focus on the second group of vaccines, which is defined by the use of only a part of the pathogen. This group includes toxoid vaccines, carbohydrate vaccines, conjugate vaccines and antigen vaccines. Antigen vaccines can be either a purified recombinant protein, or antigen expressed from vectors *in vivo*. For HIV-1 vaccines, a broad array of expression vectors have been tested as vaccine platforms: these include naked DNA plasmids, bacteria (such as *Mycobacterium bovis* Bacille Calmette Guerin (BCG)), and replication competent or incompetent attenuated viruses. The viral platforms especially have received a lot of attention in the HIV-1 vaccine research community, with the current focus on adenovirus (Ad) 5 alternatives such as Ad35 and Ad26; poxviral vectors including ALVAC, NYVAC and MVA; and replication competent viral vectors such as example rhesus cytomegalovirus (rhCMV) and recombinant vesicular stomatitis virus (rVSV).

The focus in this thesis is on three of these platforms. These are an Env protein vaccine, already discussed in ***Chapter 2***, as protein vaccines are highly successful in activating B-cells to produce antigen specific antibodies. Second, DNA vaccines, which usually induce subtle and transient immune responses that are skewed towards a CD8+ rather than a CD4+ T-cell response [286, 439]. Finally, the attenuated modified vaccinia Ankara (MVA) virus, which can induce strong humoral and cellular immune responses towards antigen genes inserted into a recombinant vaccine [317, 320, 321].

As HIV-1 is particular efficient in evading the immune system, an effective vaccine will almost certainly require the activation of both cellular and humoral immunity. I note that most clinical tests are antibody based, whereas testing of cellular responses is much less common. Therefore the importance of cell-mediated responses as correlates of protection could be grossly underestimated [359]. Although most vaccines are thought to exert their effectiveness predominantly through an antibody response, cell-mediated immunity plays a crucial role in inducing this response, mainly through activation of T follicular helper (Tfh) cells and CD4+ T cells [246, 326, 327]. Tfh cells play a pivotal role in this process within the germinal centres by stimulating B-cell proliferation, antibody affinity maturation and B-cell differentiation, which are thought to be extremely important for the induction of neutralising antibodies [246, 328]. This effect can be enhanced by vaccine boosting [246, 329]. Given that different vaccine platforms

elicit different responses - DNA elicits mainly cellular immunity; MVA or other viral platforms elicit cellular and humoral immunity; and protein generally elicits humoral immunity - heterologous prime-boosting with different platforms could potentially broaden the immune response by activating both arms of the adaptive immune response, and preventing potential development of vector-based immunity when multiple vaccines are required.

With DNA and recombinant MVA vaccines expressing Env relying on host cell expression of the Env antigen where adequate furin processing might not take place, it was decided to opt for introduction of the same flexible linker as optimised by Sharma et al. [384]. An important basis for this decision was observations of poor furin cleavage of BG505 SOSIP.664 expressed *in vitro* from chimpanzee adenovirus (ChAd) and MVA vaccines [343]. For the protein vaccine used in this thesis, Env was truncated at a similar position as BG505 SOSIP.664, whereas for DNA and MVA vaccines, the transmembrane domain was retained. However, the gp160 was truncated to AA 730, which was shown to result in higher expression levels and increased stability of the resulting gp150, the increased stability holding especially true for the rMVA platform [398-400]. Furthermore, the I559P mutation was included in the constructs used for this work; however the BG505 SOSIP intramolecular cysteine bridge between gp41 and gp120 (SOS) was not included.

Furthermore, the DNA and recombinant MVA vaccines were tested for their ability to display Env on the surface of budded HIV-1 Gag VLPs. Work from the early 1990s showed that Env readily incorporates into Pr55Gag VLPs when co-expressed *in vitro* [406-412]. It has also been suggested that by anchoring Env into the native environment of a lipid bilayer, its trimeric conformation is further stabilised [405]. Furthermore, cell-mediated immune responses to especially HIV-1 Gag (CD4+ and CD8+ T-cell responses) have been implicated in viraemic control [226]. Therefore, inclusion of Gag into a vaccine regimen has the potential to increase the efficacy of such a strategy and consequently has been widely used within the HIV-1 vaccine community, including in vaccine efficacy studies such as RV144, HVTN 702, 705 and 706. Here, an HIV-1 mosaic Gag (Gag^{M}) sequence was selected for co-expression with Env. This Gag^{M} sequence, designed *in silico* to maximise potential T-cell epitopes derived from HIV-1 subtype C sequences, improved immunogenicity in mice as a BCG, DNA and recombinant MVA vaccine in previous studies [272, 413, 414].

In this chapter, I report *in vitro* characterisation of DNA and recombinant MVA HIV-1 vaccines before *in vivo* immunogenicity studies. The use of heterologous vaccine platforms was tested in rabbits in two different regimens: 1) two rMVA HIV-1 vaccines followed by three soluble Env protein boosts (MMPPP) and 2) two DNA, followed by two rMVA HIV-1 vaccine, boosted by two protein vaccines (DDMMPP). These rabbit immunogenicity experiments were utilised to

compare the inclusion of Gag^M in the DNA and rMVA vaccines to Env alone. As discussed in ***Chapter 2***, the Env protein vaccine adjuvanted in AlhydroGel resulted in a superior antibody response in rabbits compared to AddaVax or PBS, therefore AlhydroGel was selected for these animal experiments as well.

3.2 Materials and methods

Refer to ***Section 2.2*** for materials and methods common to both investigations.

3.2.1 Antibodies, plasmids, cell lines, media and reagents

Goat anti-HIV-1 gp160 (MRC ADP 72 408/5104 (MRC/CFAR, Potters Bar)), rabbit α-gp120 polyclonal antibody (Sigma, St Louis), rabbit anti-HIV-1 p24 (Gag) (ARP 432, (MRC/CFAR, Potters Bar), donkey anti-goat IgG Cy3, donkey anti-rabbit IgG Alexa 647, donkey anti-rabbit IgG FITC (Thermo Fisher Scientific, Waltham) and goat anti Human IgG (Fc specific)-Cy3 (Sigma, St Louis) were used for immunofluorescence.

Human cervical epithelial cells from adenocarcinoma (HeLa) (ATCC® CCL-2™), rabbit epithelial kidney cells 13 (RK13) (ATCC® CCL-37™), Syrian golden hamster kidney fibroblast cells 21 (BHK) (ATCC® CCL-10™) were grown in Dulbecco's Modified Eagle's medium (DMEM) High Glucose + L-Glutamine (Lonza, Basel) + 10% fetal calf serum (FCS) + 1x penicillin (Pen)/streptomycin (Strep) (both Thermo Fisher Scientific, Waltham). A final concentration of 600µg/ml Geneticin was added to this medium for culturing the HEK293 CAP256 gp140-FL-IP (with or without C-terminal His-tag) stable cell line. Serum-free medium: DMEM High Glucose + L-Glutamine + 1x Pen/Strep.

The mammalian expression plasmid pTJDNA4 containing the subtype C mosaic Gag gene (Gag^M) was described earlier and was cloned into pTHpCapR [299, 413].

Anti-HIV-1 Env human monoclonal antibody 10E8 was expressed in FreeStyle 293F cells (Thermo Fisher Scientific, Waltham) using the PEIMAX transfection reagent (Polysciences, Warrington). Monoclonal antibodies were purified from cell-free supernatants after 6 days using Protein-A affinity chromatography [425]. This monoclonal antibody was supplied by Professor Lynn Morris and Dr Penny Moore (NICD, Johannesburg).

3.2.2 Design of CAP256 Env

The sequence of CAP256_SU gp160 (clone CAP256.206sp.032.C9) has been previously described (GenBank: KF241776.1) [167]. The Env sequence was altered as follows: the native leader (signal peptide) was removed, the furin cleavage site was replaced with two glycine-serine based repeats (GGGGS) to form a flexible linker (FL) [383, 384] and an I548P mutation equivalent to the I559P in the SOSIP trimers was introduced to stabilise trimerisation of gp41

[374]. Finally, the sequence was truncated to gp150 (AA 730) for MVA and DNA vaccines to increase expression and stability [440], thus generating gp150-FL-IP.

3.2.3 CAP256 Env DNA vaccine

The mammalian expression plasmid pTHpCapR was used as a backbone for all DNA vaccines [299]. The human tissue plasminogen activator (tPA) leader sequence (GenBank: CAX11668.1) was human codon optimised and synthesised by GenScript (Nanjing) and cloned into pTHpCapR to increase secretion of the target antigen. This plasmid was renamed pMExT for Mammalian Expression with tPA leader (***See section 2***, ***Figure 2.1A***). CAP256 gp150-FL-IP was cloned into pMExT in-frame, behind the tPA leader using the NgoMIV and EcoRI sites to generate pMExT CAP256 gp140-FL-IP (***Figure 3.1A***). An unique BamHI restriction site was introduced into gp150 within the flexible linker. See appendix A for general cloning and plasmid isolation protocols.

3.2.4 CAP256 Env transfer vector for generating recombinant MVA

A transfer vector was created where in between overlapping flanks of the MVA G1L–I8R locus, a selection cassette containing the eGFP gene under the control of the vaccinia virus (VACV) p7.5 promoter and K1L gene under the VACV pSS promoter was inserted to form the plasmid Shuttle and Selection for Pox Expression (pSSPEx) (***Figure 3.1B***). An Env ORF including the tPA leader was cloned using HindIII and EcoRI sites from the pMExT DNA vector downstream of the VACV mH5 promoter to generate pSSPEx CAP256 gp150-FL-IP (***Figure 3.1C***).

3.2.5 Generation of rMVA CAP256 Env

Wildtype modified vaccinia Ankara (MVA) (provided by Bernard Moss, NIH, Bethesda) [314] and recombinant MVA (rMVA) Gag^{M} [413, 414] were used for targeted integration of CAP256 Env. Inclusion of the overlapping flanks of the MVA G1L–I8R locus in pSSPEx gp150-FL-IP allowed for targeted recombination into this MVA locus containing the G1L and I8R genes which are in convergent open-reading frames within the pox genome. Integration of pSSPEx into MVA can be positive selected for via both K1L host range selection and/or eGFP expression in RK13 cells. For this, BHK cells in 12-well plates were transfected with pSSPEx CAP256 gp150-FL-IP (2µg plasmid DNA and 1.5µl X-tremeGENE (Roche, Basel) two hours after infection with rMVA Gag^{M} with a multiplicity of infection (MOI) of 0.1. As a control, pSSPEx CAP256 gp150-FL-IP was transfected into cells infected with wildtype MVA. After recombination was confirmed by eGFP fluorescence, cells were freeze-thawed to release MVA virus. This virus was passaged for three rounds in RK13 cells, a cell line where MVA is solely permissive in the presence of K1L expression [316, 441], adding a second level of

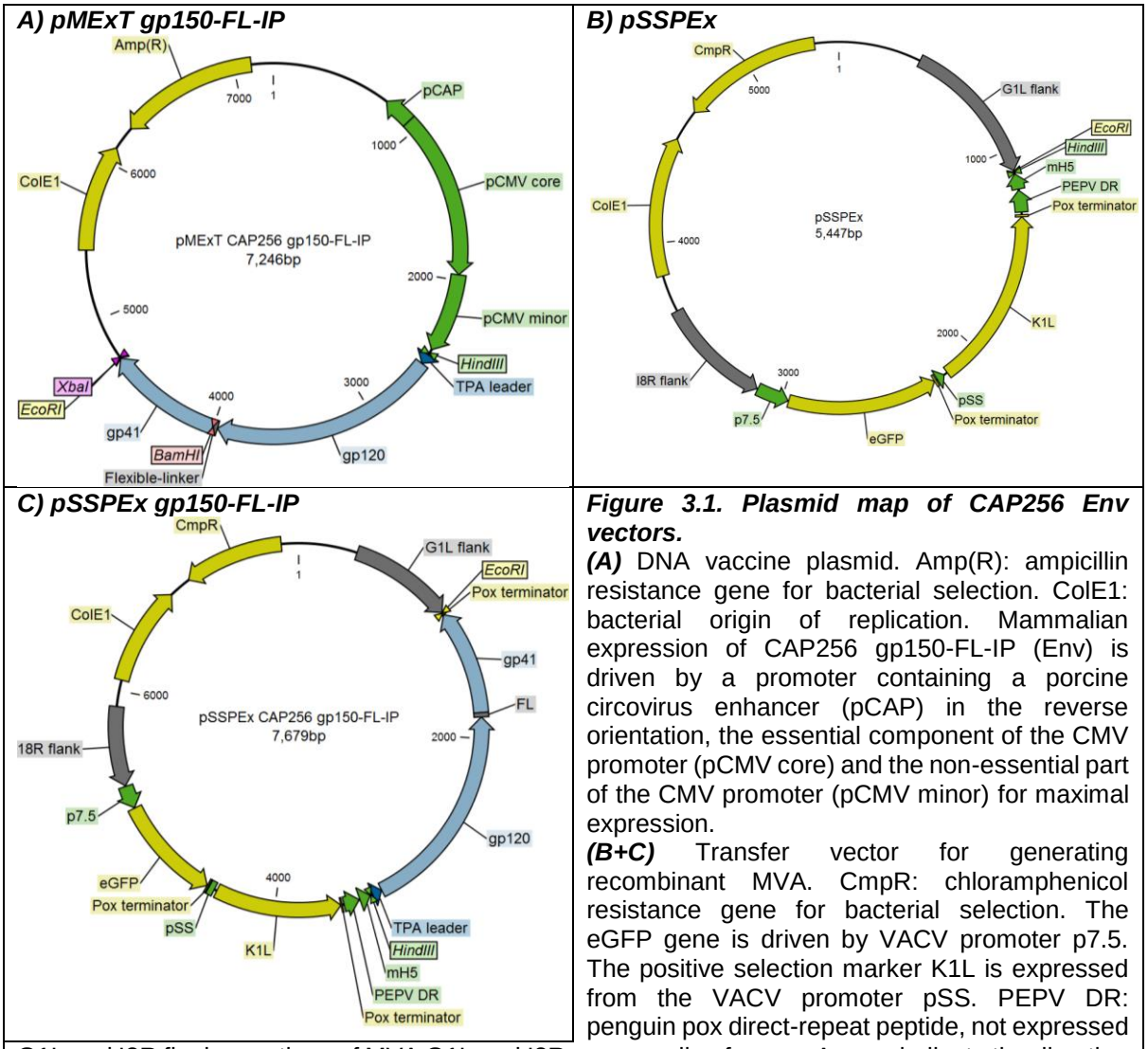

Figure 3.1. Plasmid map of CAP256 Env vectors.

(A) DNA vaccine plasmid. Amp(R): ampicillin resistance gene for bacterial selection. ColE1: bacterial origin of replication. Mammalian expression of CAP256 gp150-FL-IP (Env) is driven by a promoter containing a porcine circovirus enhancer (pCAP) in the reverse orientation, the essential component of the CMV promoter (pCMV core) and the non-essential part of the CMV promoter (pCMV minor) for maximal expression.

(B+C) Transfer vector for generating recombinant MVA. CmpR: chloramphenicol resistance gene for bacterial selection. The eGFP gene is driven by VACV promoter p7.5. The positive selection marker K1L is expressed from the VACV promoter pSS. PEPV DR: penguin pox direct-repeat peptide, not expressed G1L and I8R flanks: portions of MVA G1L and I8R open reading frames. Arrows indicate the direction of all promoters and transcripts.

(C) Transcription of Env is from the modified VACV H5 promoter (mH5). All transcripts include a 3` pox transcriptional termination signal (Pox terminator).

TPA leader: human tissue plasminogen activator leader sequence.

selection stringency. Single fluorescent foci in RK13 cells were selected and screened for correct integration of the targeting construct by PCR and expression of Gag^{M} and/or Env was verified by western blotting and immunofluorescence. Positive single foci were expanded in 3x Hyperflasks for high titre stocks, see Appendix A for full protocol. Thus generated rMVA Gag^{M} CAP256 gp150-FL-IP or rMVA CAP256 gp150-FL-IP stocks were aliquoted and stored at -80°C for downstream usage. Titres were determined in BHK cells where GFP positive plaques were counted 48 hours after infection of a serial dilution range (in steps of 1 in 10) and calculated as plaque forming units (pfu)/ml. High titre stocks were screened for correct integration of the targeting construct by PCR and PCR sequencing. Expression of mosaic Gag and/or Env was verified by western blotting and immunofluorescence. See Appendix A for

detailed protocols for rMVA DNA isolation, PCR screening, primers and large scale MVA production.

3.2.6 Purification of CAP256 soluble Env trimers

All CAP256 soluble Env used in this chapter was isolated from the HEK293 CAP256 soluble Env or CAP256 soluble Env-His stable cell lines (passage >10) as described in ***Section 2.2.5***. The yields of soluble Env from HEK293 CAP256 soluble Env stable cell lines and repeat harvesting from Hyperflasks allowed for downstream Size Exclusion Chromatography (SEC) on a Superdex 200 HiLoad 16/600 column (GE Healthcare, Chicago) where the Env trimers, dimers and monomers could be separated based on molecular weight (***Figure 3.2***). Fractions containing putatively trimeric soluble Env protein were combined. Thus purified protein will be referred to throughout this dissertation as CAP256 soluble trimeric Env protein. Protein was aliquoted and stored at -80°C for downstream usage. CAP256 soluble trimeric Env protein was assessed for the presence of bnAb epitopes as described in ***Section 2.2.5***. Protein concentration was determined using the DC Protein Assay (Bio-Rad, Hercules) against a BSA standard (Bio-Rad, Hercules (see Appendix A for protocol).

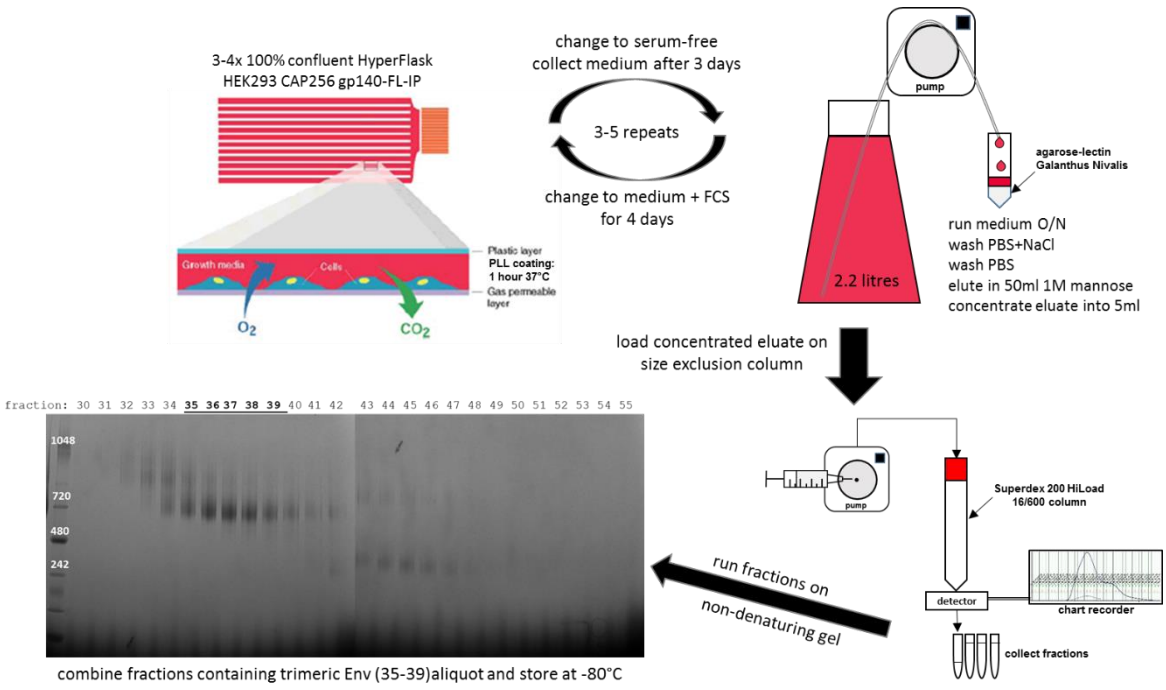

Figure 3.2. Schematic representation of the purification of CAP256 soluble Env trimers. Cleared media from HEK293 CAP256 soluble Env stable cell line or HEK293T cells transiently transfected with pMExT CAP256 gp140-FL-IP is dripped over an agarose lectin (*Galanthus nivalis*) affinity chromatography column using a peristaltic pump. After two wash steps, soluble Env is eluted of the column with ~50ml 1M methyl α-D-manno-pyranoside and concentrated to 5ml before Size Exclusion Chromatography on a Superdex 200 HiLoad 16/600 column. Fractions containing trimeric Env protein as based on molecular weight were isolated.

3.2.7 Verification and characterisation of DNA vaccines

To characterise Gag and Env expression and co-localisation from DNA vaccines, HEK293T cells were co-transfected with pTJDNA4 (contains gag^{M} gene) + pMExT CAP256 gp150-FL-IP or each plasmid by their own. Transfections were performed in 24 well plates (Corning, New York) for western blotting or 4 Well Permanox® Slides (Sigma, St Louis) for immunofluorescent staining, using 1µg of plasmid DNA and 3µl X-tremeGENE. After 72 hours media was harvested from 24-well plates and cleared by low speed spin (5 minutes, 275*g*) for western blot analysis. For immunofluorescent staining, cells were fixed with 4% paraformaldehyde for 10 minutes, permeabilised with methanol (1 minute) and washed with PBS. Cells were blocked and primary goat anti-gp160 and rabbit anti-p24 (both 1:500) was added in block overnight. After washing with PBS (3x), secondary antibody (donkey anti-goat IgG Cy3 and donkey anti-rabbit IgG Alexa 647, both 1:500) in block was added for 1 hour and after PBS washing (3x), coverslips were mounted with mowiol. Cells were imaged on a LSM 880 Fast Airyscan (Zeiss, Oberkochen) at the UCT Confocal & Light Microscope Imaging Facility. Pseudo-colouring for Cy3 is in red and Alexa 647 in green. Single images comprising of 13 merged z-stacks were generated using Zeiss Zen software. Only cells transfected with pTJDNA4 + pMExT CAP256 gp150-FL-IP were analysed by confocal and untransfected cells were used as control. See appendix A for detailed protocols for transfection and western blotting.

The presence of Env bnAb epitopes after expression of the Env DNA vaccine was assessed in HeLa cells using live-cell staining with anti-Env human bnAbs PG9, PG16, PGT128, PGT135, PGT145, CAP256 VRC26.08, VRC01, 10E8 F105 and 447-52D. For this 4 Well Permanox® Slides were transfected as described above and after three days, medium was replaced with medium containing 10µg/ml mAb and for 1 hour. Following 3x PBS washes, cells were incubated with medium containing rabbit anti-Env (1:500) for 30 minutes. Upon a further three washes, cells were treated with media containing goat α-human IgG Cy3 (1:500) + donkey α-rabbit IgG FITC (1:500) for 0.5 hour and after a final 3x PBS washes, cells were imaged in PBS on a Zeiss Axiocam ICm 1 Microscope using Zeiss Zen software.

To investigate the formation of Gag virus-like particles (VLPs) from DNA vaccines, RK13 cells were transfected with pTJDNA4 (contains gag^{M} gene) + pMExT CAP256 gp150-FL-IP or each plasmid by their own. Transfections were performed in 6-well plates using 4µg of plasmid DNA and 12µl X-tremeGENE. After 72 hours cells were collected by scraping, spun briefly and after washing the pellets with PBS fixed overnight in 2.5% glutaraldehyde in PBS (4ºC). The fix was replaced with PBS and pellets were sent to the Microscopy & Microanalysis Unit at the University of Kwazulu-Natal for electron microscopy (EM) post processing as described earlier

[413], and EM imaging. Images were acquired on a JEOL 1010 platform and VLP size was measured with the imaging software.

To characterise Env inclusion into Gag virus-like particles (VLPs), HEK293T cells were transfected with pTJDNA4 (contains *gag*^{M} gene) + pMExT CAP256 gp150-FL-IP or each plasmid by their own. Transfections were performed in T150 flasks, using 60µg of plasmid DNA and 180µl polyethylenimine-branched (PEI) (Sigma, St Louis). After 72 hours VLPs were isolated from the media of transfected cells on OptiPrep (Sigma, St Louis) gradients. In short, media was cleared with a low speed spin (5 minutes, 275*g*), underlayed with 12, 24, and 60% OptiPrep (in 1x PBS, 3ml each) in Thinwall Ultra-Clear™ Tubes (38.5 ml, 25x89 mm, Beckman Coulter, Pasadena) and centrifuged at ~110,000g, 4°C for 90 minutes. A visible band (or equivalent) around the 12-24% interface was isolated, carefully overlayed on an OptiPrep gradient (18, 21, 24, 30, 36, 42% in 1x PBS, 5ml each) and subsequently centrifuged overnight at ~110,000g, 4°C. The only visible band (or equivalent) around 45mm from the bottom was isolated. This band was analysed for the presence of Gag and/or Env by western blotting.

After cloning, verification and characterisation, DNA vaccines were synthesised by Aldevron (Fargo) for immunisation experiments.

3.2.8 Verification and characterisation of recombinant MVA vaccines

The recombinant MVA vaccines rMVA Gag^{M} CAP256 gp150-FL-IP, rMVA CAP256 gp150-FL-IP or rMVA Gag^{M} were characterised in a similar fashion as for DNA vaccines above, with the following permutations. All characterisation was performed 48 hours after infection. For western blotting and confocal microscopy, HE293T cells were infected with a multiplicity of infection (MOI) of 0.5. For assessing the presence of Env bnAb epitopes in a live-cell staining assay, HeLa cells were infected with an MOI=0.5, cells were not stained with the rabbit α-Env antibody as rMVA infected cells could be identified by eGFP expression. RK13 cells were infected with an MOI=1 for EM. Whereas VLP characterisation by western blotting was done in HEK293T cells with an MOI=0.5.

3.2.9 Rabbit immunisation comparing heterologous vaccine platforms

Female New Zealand white rabbits were housed in the Research Animal Facility in the Faculty of Health Sciences at the University of Cape Town. All the animal procedures were approved by the UCT Animal Research Ethics Committee (UCT AEC 14-030 & UCT AEC 015/051) and performed by trained animal technologists Rodney Lucas and Inge Botes. The rabbits were monitored daily for any signs of pain, discomfort or stress and were weighed weekly.

Four groups of 5 rabbits were selected to compare rMVA vaccines Gag^{M} CAP256 gp150-FL-IP and CAP256 gp150-FL-IP with or without matching DNA vaccine priming (see ***Table 3.1*** for groups).

Table 3.1. Groups of rabbits comparing heterologous vaccine platforms

animal	group	Vaccine			Prime		rMVA boost		Protein boost		
		DNA	rMVA	gp140-FL-IP	wk 0	wk 4	wk 8	wk 12	First	Second	Third
6826	1	*N/A*	gp150 + Gag^{M}	AlhydroGel (1:1)	**rMVA**	**rMVA**	*N/A*	*N/A*	wk 12	wk 20	wk 28
6827	1	*N/A*	gp150 + Gag^{M}	AlhydroGel (1:1)	**rMVA**	**rMVA**	*N/A*	*N/A*	wk 12	wk 20	wk 28
6828	1	*N/A*	gp150 + Gag^{M}	AlhydroGel (1:1)	**rMVA**	**rMVA**	*N/A*	*N/A*	wk 12	wk 20	wk 28
6830	1	*N/A*	gp150 + Gag^{M}	AlhydroGel (1:1)	**rMVA**	**rMVA**	*N/A*	*N/A*	wk 12	wk 20	wk 28
6850	1	*N/A*	gp150 + Gag^{M}	AlhydroGel (1:1)	**rMVA**	**rMVA**	*N/A*	*N/A*	wk 12	wk 20	wk 28
6832	2	*N/A*	gp150	AlhydroGel (1:1)	**rMVA**	**rMVA**	*N/A*	*N/A*	wk 12	wk 20	wk 28
6833	2	*N/A*	gp150	AlhydroGel (1:1)	**rMVA**	**rMVA**	*N/A*	*N/A*	wk 12	wk 20	wk 28
6834	2	*N/A*	gp150	AlhydroGel (1:1)	**rMVA**	**rMVA**	*N/A*	*N/A*	wk 12	wk 20	wk 28
6835	2	*N/A*	gp150	AlhydroGel (1:1)	**rMVA**	**rMVA**	*N/A*	*N/A*	wk 12	wk 20	wk 28
6836	2	*N/A*	gp150	AlhydroGel (1:1)	**rMVA**	**rMVA**	*N/A*	*N/A*	wk 12	wk 20	wk 28
6526	3	gp150 + Gag^{M}	gp150 + Gag^{M}	AlhydroGel (1:1)	DNA	DNA	**rMVA**	**rMVA**	wk 20	wk 28	*N/A*
6528	3	gp150 + Gag^{M}	gp150 + Gag^{M}	AlhydroGel (1:1)	DNA	DNA	**rMVA**	**rMVA**	wk 20	wk 28	*N/A*
6529	3	gp150 + Gag^{M}	gp150 + Gag^{M}	AlhydroGel (1:1)	DNA	DNA	**rMVA**	**rMVA**	wk 20	wk 28	*N/A*
6530	3	gp150 + Gag^{M}	gp150 + Gag^{M}	AlhydroGel (1:1)	DNA	DNA	**rMVA**	**rMVA**	wk 20	wk 28	*N/A*
6049#	3	gp150 + Gag^{M}	gp150 + Gag^{M}	AlhydroGel (1:1)	DNA	DNA	**rMVA**	**rMVA**	wk 20	wk 28	*N/A*
6542†	4	gp150	gp150	AlhydroGel (1:1)	DNA	DNA	**rMVA**	**rMVA**	wk 20	wk 28	*N/A*
6543†	4	gp150	gp150	AlhydroGel (1:1)	DNA	DNA	**rMVA**	**rMVA**	wk 20	wk 28	*N/A*
6544	4	gp150	gp150	AlhydroGel (1:1)	DNA	DNA	**rMVA**	**rMVA**	wk 20	wk 28	*N/A*
6546	4	gp150	gp150	AlhydroGel (1:1)	DNA	DNA	**rMVA**	**rMVA**	wk 20	wk 28	*N/A*
6047#	4	gp150	gp150	AlhydroGel (1:1)	DNA	DNA	**rMVA**	**rMVA**	wk 20	wk 28	*N/A*
6048#	4	gp150	gp150	AlhydroGel (1:1)	DNA	DNA	**rMVA**	**rMVA**	wk 20	wk 28	*N/A*
# started 4 week behind											
† Died of unrelated causes											

Groups 1 and 2 received 10^{8} pfu in 500µl PBS + 10% glycerol rMVA Gag^{M} CAP256 gp150-FL-IP or rMVA CAP256 gp150-FL-IP. Recombinant MVA vaccines were administered intramuscularly in the hind leg at week 0 and 4. All rabbits received 40µg of CAP256 soluble trimeric Env protein in 500µl 1:1 (*v*/*v*) AlhydroGel® (InvivoGen, San Diego) at week 12, 20 and 28 to boost the immune response. This experiment is abbreviated as MMPPP. Animals were sacrificed at week 32.

Groups 3 and 4 received 100µg pTJDNA4 (Gag^{M}) combined with 100µg pMExT CAP256 gp150-FL-IP or 100µg pMExT CAP256 gp150-FL-IP only. Concentration of all DNA vaccines was 1mg/ml in PBS. Primes were administered intramuscularly in the hind leg at week 0 and 4. At week 8 and 12, all groups received vaccine matched rMVA boosts. Groups 3 received 10^{8} pfu in 500µl PBS + 10% glycerol rMVA Gag^{M} CAP256 gp150-FL-IP, whereas group 4 received 10^{8} pfu in 500µl PBS + 10% glycerol rMVA CAP256 gp150-FL-IP. These rMVA

boosts were administered intramuscularly in the hind leg. Finally, all rabbits received 40µg of CAP256 soluble trimeric Env protein in 500µl 1:1 (*v*/*v*) AlhydroGel® at week 20 and 28 to boost the immune response. This experiment is abbreviated as DDMMPP. Animals were not sacrificed at week 32 as they were entered into a longitudinal study (not discussed in this dissertation). For each group, the regimen for one animal started 4 weeks later. In group 4, two rabbits died after the first MVA inoculation due to unrelated causes, for this group an additional animal was included in the delayed regimen resulting in 4 rabbits in group 2.

3.2.10 Rabbit sera characterisation

To assess Env or CAP256_SU V1V2-loop binding antibodies titres in rabbit sera, ELISA were performed as described in ***Section 2.2.7***. However, binding ELISAs were run against CAP256 soluble trimeric Env (SEC purified) and antibody end-point titres were calculated from 4PL curves with the threshold set as 4PL curve minimum + standard error of minimum for each time point:

$$End\ point\ titre = EC50 * \left(\frac{Standard\ Error\ Curve\ Min}{Curve\ Max - (Curve\ Min + Standar\ Error\ Curve\ Min)}\right)^{1/Hill\ Slope}$$

Data plotted as mean +/- SEM for whole group.

Rabbit sera from different time points were tested for the ability to inhibit Env-pseudotyped virions from entering a reporter cell line as described in ***Section 2.2.7***. The Env-pseudotypedviruses MW965.26, 6644, 1107356, CAP256_SU, CAP256_SU K169E or BG0505N332+/CAP256_SU V1V2-loop and CAP84/CAP256_SU V1V2-loop were assayed.

All neutralisation assays were performed by Professor Lynn Morris's group at Center for HIV and STIs, National Institute for Communicable Diseases of the National Health Laboratory Service, Johannesburg, South Africa.

3.2.11 Statistical analysis

All statistical analysis was performed in GraphPad Prism 5.0 (GraphPad Software, San Diego) and tests are indicated in results and/or corresponding figure legend

3.3 Results

3.3.1 Transient expression of CAP256 Env and mosaic Gag from DNA vaccines

The CAP256 Env sequence was modified as described in the material and methods and cloned into the the mammalian expression plasmid to generate pMExT CAP256 gp150-FL-IP (***Figure 3.1A and 3.3A***), whereas pTJDNA4 expressing subtype C mosaic Gag (pTJDNA4) was previously described [413]. In this thesis pMExT CAP256 gp150-FL-IP will be referred to as DNA Env, pTJDNA4 as DNA Gag^{M} and when both plasmids are combined DNA Env+Gag^{M}. To test the Env and Gag DNA vaccines for *in vitro* expression and cellular secretion of the transgenes, HEK293T cells were transiently transfected with these vaccines, Env and Gag were detected by western blotting in the cell media 72 hours after transfection (***Figure 3.3B***), indicating secretion of both proteins. Furthermore, immunofluorescence staining and confocal imaging of transfected cells with DNA Env+Gag^{M} showed expression and co-localisation of the two transgenes (***Figure 3.3C***).

The Env DNA vaccine was further characterised for the presence of a select list of Env bnAbs epitopes upon expression (***Table 1.1***) using a live cell staining protocol in HeLa cells. Using this method, only Env present on the plasma membrane would be detected and therefore be a suitable indication of the antigenic properties of the natively expressed (non-denatured) Env trimer. Binding was observed for all epitopes tested (***Figure 3.4***), including the V3-glycan supersite (identified with bnAbs PGT128 and PGT135), the CD4-binding site (bnAb VRC01), the MPER (10E8) and the V2-glycan by PG9. Although some signal was detected as well with the bnAbs F105 and 447-52D, suggesting that some of the Env expressed from the DNA vaccine was misfolded. However, immunofluorescent signals for bnAbs that specifically identify Env in a native-like trimer conformation (PGT145, PG16 and CAP256 VRC26.08) were observed, which is most encouraging. Only immunofluorescence for bnAbs was observed in cells that were positive for the rabbit α-Env polyclonal antibody (as assessed by FITC signal), indicating the specificity of the bnAb live-cell staining. However, especially for PGT145, PG16 and CAP256 VRC26.08, bnAb signals was not detected in all cells positive for Env expression.

3.3.2 Construction and characterisation of rMVA vaccines expressing Env

3.3.2.1 Verification of the integrity of rMVA vaccines

Env was subcloned from pMExT CAP256 gp150-FL-IP into the transfer vector pSSPEx to generate MVA recombinants (***Figure 3.1C and 3.3A***). Using the transfer vector, Env under the vaccinia (VACV) promoter mH5 was targeted into the transcriptionally convergent open reading frames of the essential I8R-G1L genes of rMVA Gag^{M} (***Figure 3.5A***) to generate rMVA Gag^{M} CAP256 gp150-FL-IP (referred to as rMVA Env+Gag^{M}) or when using wildtype MVA:

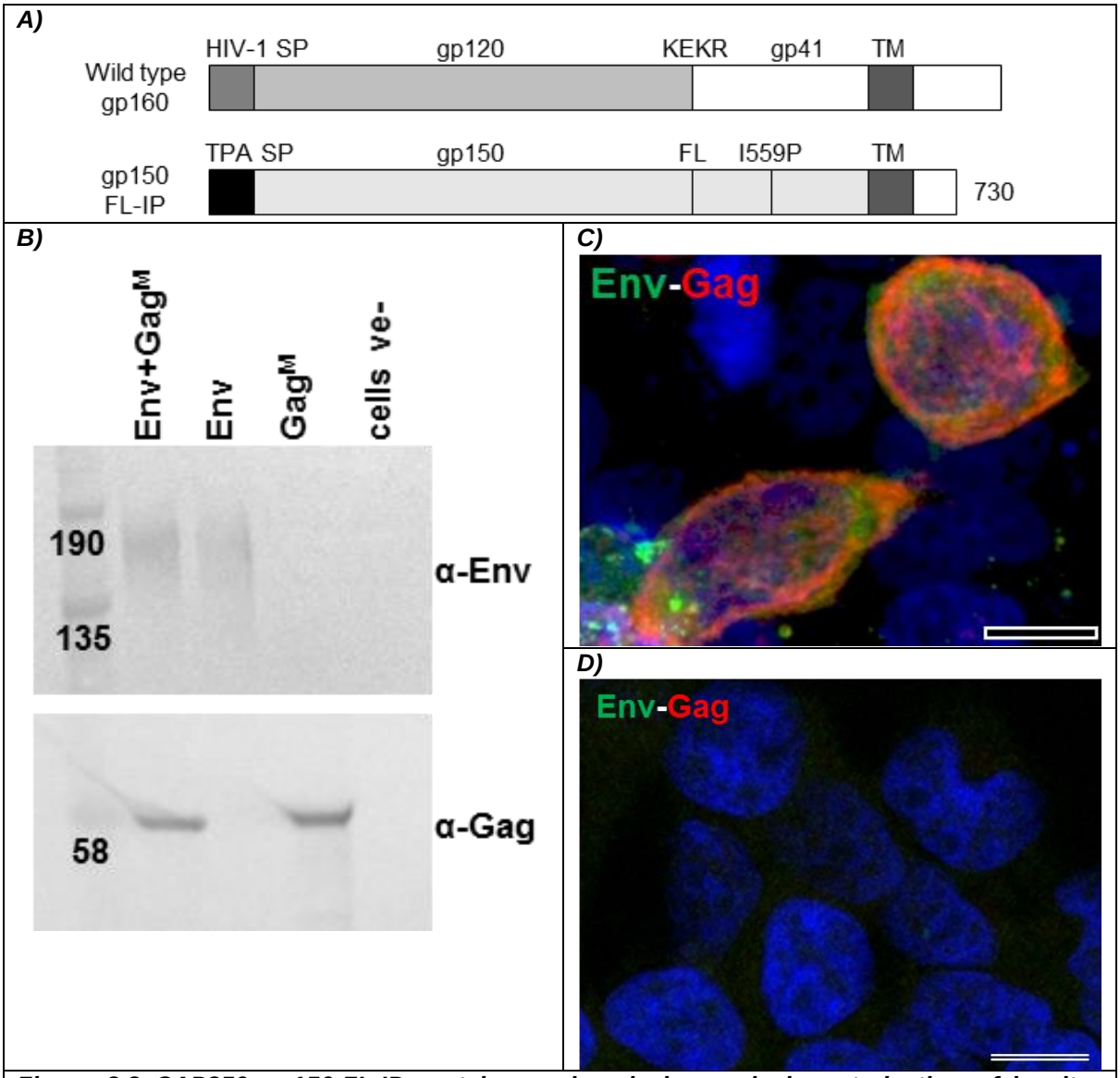

Figure 3.3 CAP256 gp150-FL-IP protein vaccine design and characterisation of* in vitro *expression .
(A) Schematic representations comparing wild type Env to CAP256 Env used in DNA and rMVA vaccines (CAP256 gp150-FL-IP). The Env sequence was truncated to amino acid 730 to improve transgene stability, while containing further modifcations where the wild type signal peptide (HIV-1 SP) was replaced with the human tissue plasminogen activator (TPA) sequence, the furin cleavage site with a flexible linker (FL) sequence and an I559P mutation was introduced.
(B+C) In co-expression studies of HEK293T cells after transfection pMExT CAP256 gp150-FL-IP (DNA Env) and pTJDNA4 (DNA Gag^M) or both (DNA $Env+Gag^M$) western blotting revealed Gag (bottom) and Env (top) secretion in media from HEK293T cells 72 hours after ***(B)***. ***(C)*** Confocal imaging (maximum intensity projections) showing co-localisation of Gag and Env within HEK293T cells after transfection with DNA $Env+Gag^M$.
D) No Env or Gag immunofluorescent signal in untransfected controls.
Pseudo-colouring for Cy3 is in red (Gag) and Alexa 647 in green (Env). Scale bar = 10μm.

rMVA CAP256 gp150-FL-IP (referred to as rMVA Env). The presence of a fluorescent signal from the reporter gene eGFP under the control of the VACV promoter p7.5, was used to select for positive integration. Furthermore, expression of the host range K1L gene under the control

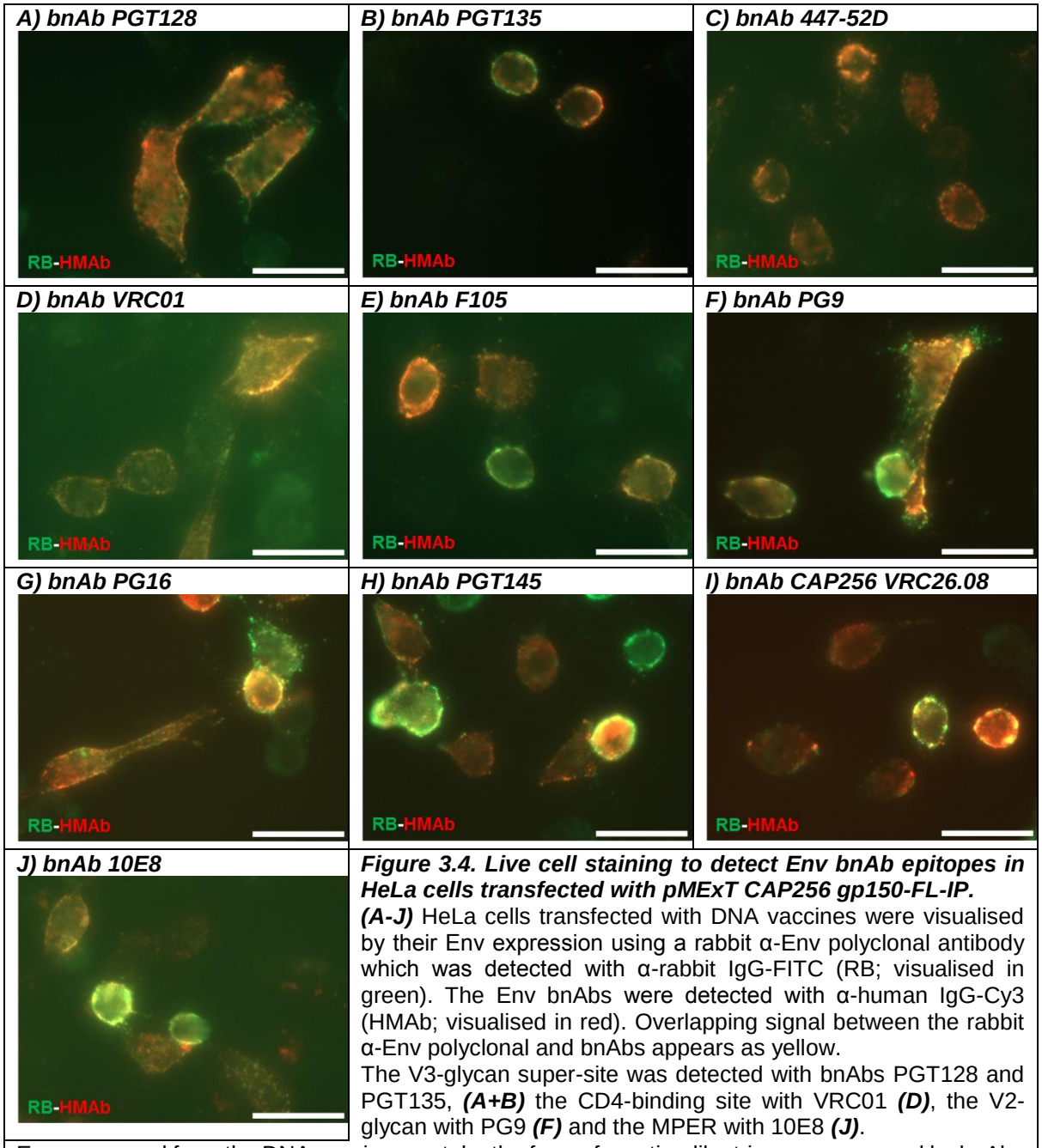

Figure 3.4. Live cell staining to detect Env bnAb epitopes in HeLa cells transfected with pMExT CAP256 gp150-FL-IP.
(A-J) HeLa cells transfected with DNA vaccines were visualised by their Env expression using a rabbit α-Env polyclonal antibody which was detected with α-rabbit IgG-FITC (RB; visualised in green). The Env bnAbs were detected with α-human IgG-Cy3 (HMAb; visualised in red). Overlapping signal between the rabbit α-Env polyclonal and bnAbs appears as yellow.
The V3-glycan super-site was detected with bnAbs PGT128 and PGT135, ***(A+B)*** the CD4-binding site with VRC01 ***(D)***, the V2-glycan with PG9 ***(F)*** and the MPER with 10E8 ***(J)***.
Env expressed from the DNA vaccine can take the form of a native-like trimer as assessed by bnAbs PG16, PGT145 and CAP256 VRC26.08 ***(G-I)***. However, some Env is expressed as a misfolded protein with the binding of bnAbs 446-52D and F105 ***(C+E)***.
Bar = 20µm.

of the VACV pSS promoter allowed for positive selection in RK13 cells which are only permissive to MVA with the expression of K1L. Single clones for all the different MVA vaccines were selected from RK13 cells and expanded to high titres stocks (rMVA Env+Gag^{M} = 1.3*10^{9}; rMVA Env = 0.5*10^{9}) in RK13 cells. To test for correct integration and stability of Env in the I8R-G1L locus, PCRs were carried out on DNA isolated from RK13 cells infected with the high titre stocks rMVA using a primer upstream of the VACV mH5 promoter and a reverse primer

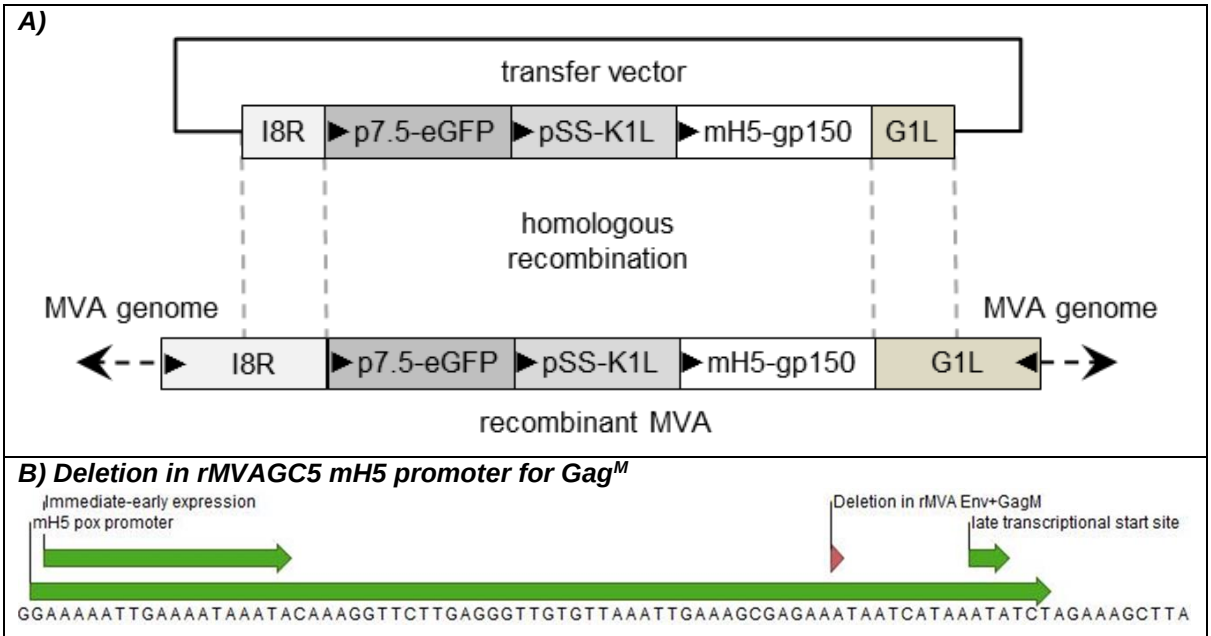

Figure 3.5. Targeting strategy for the generation of recombinant MVA expressing Env.
(A) Schematic representation of targeting for CAP256 gp150-FL-IP into the I8R-G1L locus of wild type MVA or MVA Gag^{M} pox genome. Triangles indicate direction of open-reading frames. Env expression is driven by the VACV mH5 promoter
(B) Deletion in the sequence contig of Gag^{M} insertion site for rMVA Env+Gag^{M}. This deletion is outside the core binding regions for immediate-early or late expression initiation. The arrow heads indicate the promoter element directions.

within the G1L locus but outside the G1L recombination flank in pSSPEx. These PCR products were subsequently sequenced to check for possible mutations. The sequence was exactly as predicted for both recombinant MVA vaccines indicating correct integration of Env into the rMVA vaccines (data not shown). In a similar fashion, the 5' and 3' arms of Gag^{M} were verified for rMVA Env+Gag^{M} and surprisingly, there was one deletion within the mH5 promoter (***Figure 3.5B)***, but as this occurred outside the core binding sites for immediate-early or late expression initiation, it was deemed to have no effect on Gag expression.

3.3.3.2 Expression of Env by rMVA vaccines

To assess rMVA vaccines for *in vitro* expression of the recombinant antigens, HEK293T cells were infected rMVA Env+Gag^{M} or rMVA Env. Env and Gag could be detected by western blotting in the cell media 48 hours after infection (***Figure 3.6A***), indicating that both Env and Gag were secreted. Furthermore, immunofluorescent staining and confocal imaging of infected cells showed expression and co-localisation of Gag and Env (***Figure 3.6B***).

Both rMVA vaccines were characterised for the presence of Env bnAb epitopes upon infection into HeLa cells in similar experiments as for the DNA vaccine, resulting in a very comparable outcome. The same bnAb epitopes as for pMExT CAP256 gp150-FL-IP were detected for rMVA Env+Gag^{M} (***Figure 3.7***) and rMVA Env. (***Figure 3.8***), with the V3-glycan supersite (using bnAbs PGT128 and PGT135), the CD4-binding site (bnAb VRC01), the MPER (10E8) and the

V2-glycan by PG9. Again, some signal was detected as well with the bnAbs F015 and 447-52D, suggesting that some of the Env expressed from the DNA vaccine was misfolded. However, immunofluorescent signals for bnAbs that specifically identify Env in a native-like trimer conformation (PGT145, PG16 and CAP256 VRC26.08) were observed, which was most encouraging. Infected HeLa cells were identified by the presence of an eGFP signal, transcribed from the recombinant MVA.

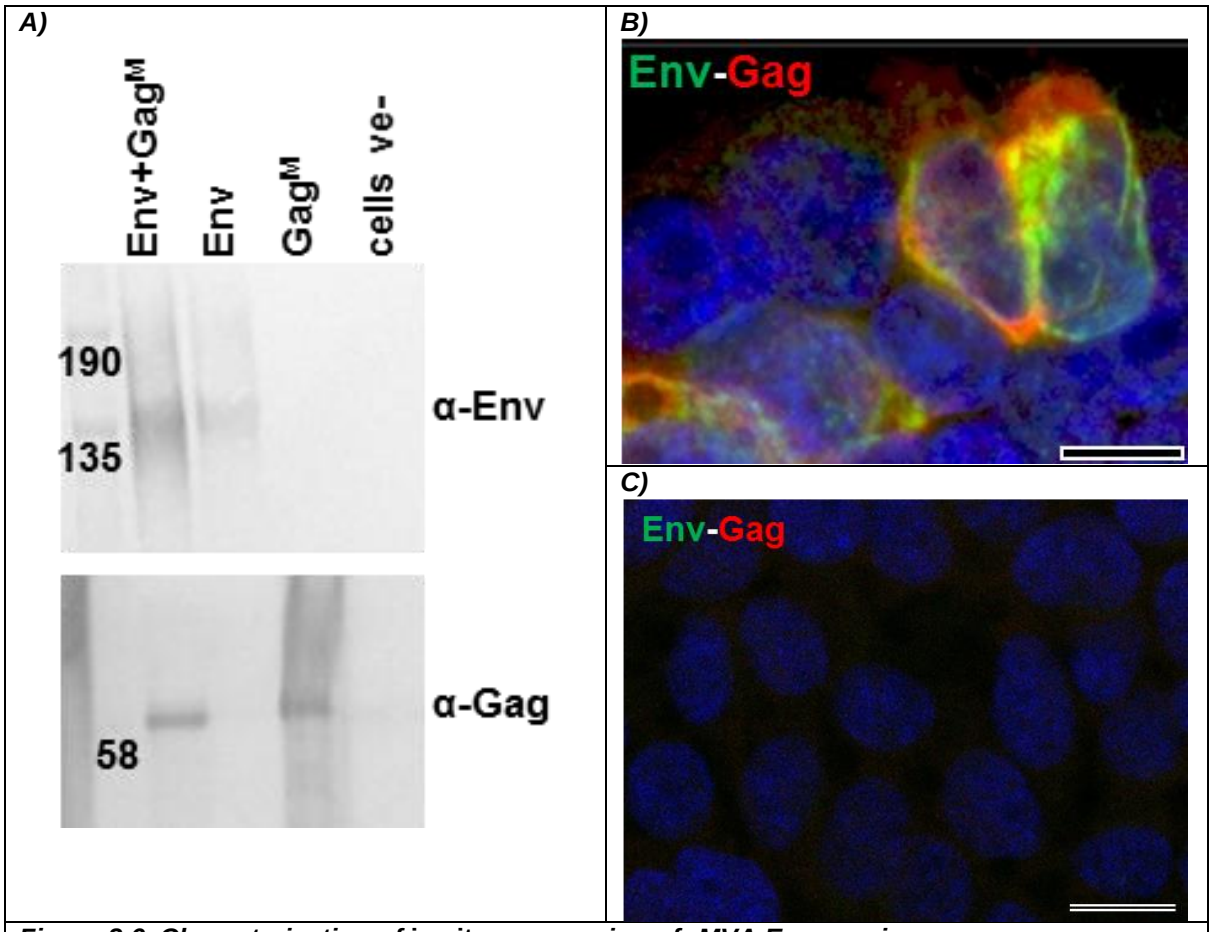

Figure 3.6. Characterisation of* in vitro *expression of rMVA Env vaccines.
(A) Both Env and Gag could be detected in media from HEK293T cells infected with rMVA Env+Gag^{M}, whereas only Env or Gag was detected for rMVA Env or with rMVA Gag^{M} (Gag^{M}) respectively.
(B) Confocal imaging (maximum intensity projections) showing co-localisation of Gag and Env within HEK293T cells after infection with rMVA Env+Gag^{M}.
(C) No Env or Gag immunofluorescent signal in uninfected controls.
Pseudo-colouring for Cy3 is in red (Gag) and Alexa 647 in green (Env). Scale bar=10μm.

3.3.3 Virus-like particle formation from Env DNA and rMVA vaccines

It has previously been shown by electron microscopy that expression of Gag^{M} from DNA or rMVA vaccines in HEK293 cells leads to the formation of VLPs [413], and this was confirmed here in a similar fashion for the DNA vaccine in RK13 cells as well (***Figure 3.9A***). Furthermore, VLPs were also observed when Env was co-expressed for both DNA and rMVA vaccines (***Figure 3.9B+C***). However, no VLPs were observed for the rMVA vaccines expressing Env

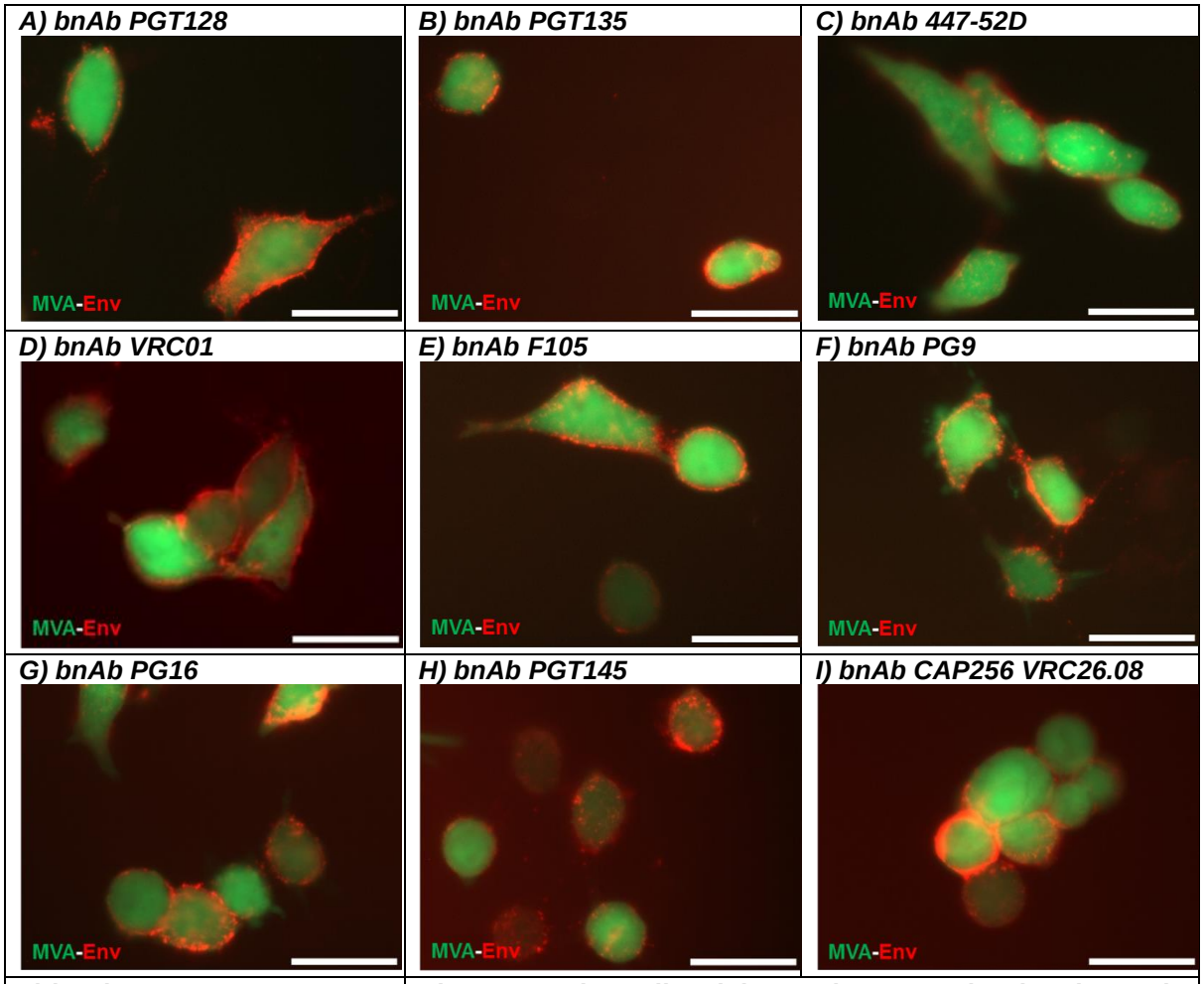

Figure 3.7. Live cell staining to detect Env bnAb epitopes in HeLa cells infected with rMVA Env+Gag^{M}.
(A-J) The Env bnAbs were detected with α-human IgG-Cy3 (HMAb; visualised in red). Cells infected with rMVA are expressing eGFP present in rMVA.
The V3-glycan super-site was detected with bnAbs PGT128 and PGT135, ***(A+B)*** the CD4-binding site with VRC01 ***(D)***, the V2-glycan with PG9 ***(F)*** and the MPER with 10E8 ***(J)***.
Env expressed from this rMVA vaccine can take the form of a native-like trimer as assessed by bnAbs PG16, PGT145 and CAP256 VRC26.08 ***(G-I)***. However, some Env is expressed as a misfolded protein with the binding of bnAbs 447-52D and F105 ***(C+E)***.
Bar = 20µm.

alone (***Figure 3.9D***). Interestingly, viral factories within RK13 cells producing immature and mature MVA particles were observed as well ***(3.9E+F)***. When VLPs from DNA and rMVA vaccines expressing both Env and Gag^{M} were isolated from the media of HEK293T cells by a two-step OptiPrep gradient centrifugation protocol, both Gag and Env were present as confirmed with western blotting of samples from the only visible band (~45mm from the bottom) isolated from the second OptiPrep gradient, suggesting Env inclusion into Gag VLPs (***Figure 3.10***). Encouragingly, no Env band was observed in the equivalent band isolated from DNA or rMVA vaccines containing only Env.

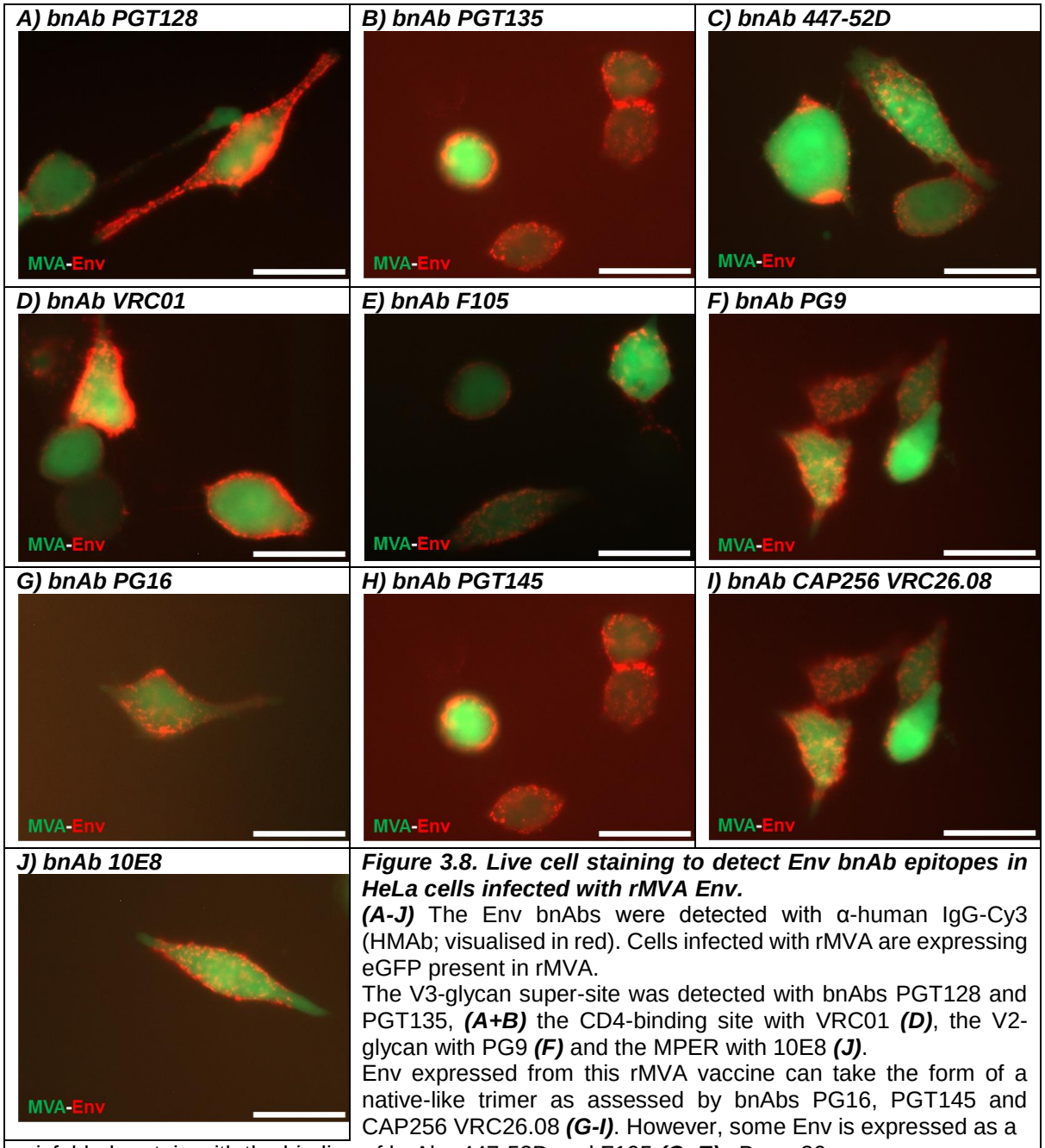

Figure 3.8. Live cell staining to detect Env bnAb epitopes in HeLa cells infected with rMVA Env.
(A-J) The Env bnAbs were detected with α-human IgG-Cy3 (HMAb; visualised in red). Cells infected with rMVA are expressing eGFP present in rMVA.
The V3-glycan super-site was detected with bnAbs PGT128 and PGT135, ***(A+B)*** the CD4-binding site with VRC01 ***(D)***, the V2-glycan with PG9 ***(F)*** and the MPER with 10E8 ***(J)***.
Env expressed from this rMVA vaccine can take the form of a native-like trimer as assessed by bnAbs PG16, PGT145 and CAP256 VRC26.08 ***(G-I)***. However, some Env is expressed as a misfolded protein with the binding of bnAbs 447-52D and F105 ***(C+E)***. Bar = 20µm.

3.3.4 Characterisation of affinity purified soluble Env trimers

As already discussed in ***Chapter 2***, the CAP256 soluble Env affinity purified with lectin from a HEK293 stable cell line was mainly in a trimeric conformation as judged by molecular weight. This trimeric Env fraction was further purified by size exclusion chromatography (SEC). The first and largest peak observed in the SEC profile, fractions 35-39, corresponds to trimeric Env as judged Blue-Native (BN) PAGE electrophoresis (by molecular weight) (***Figure 3.11A+B***). These pooled fractions will be referred to in this thesis as soluble trimeric Env. It was confirmed by LC-MS that the dominant protein present in these pooled fractions was Env (***Table 3.2***). As

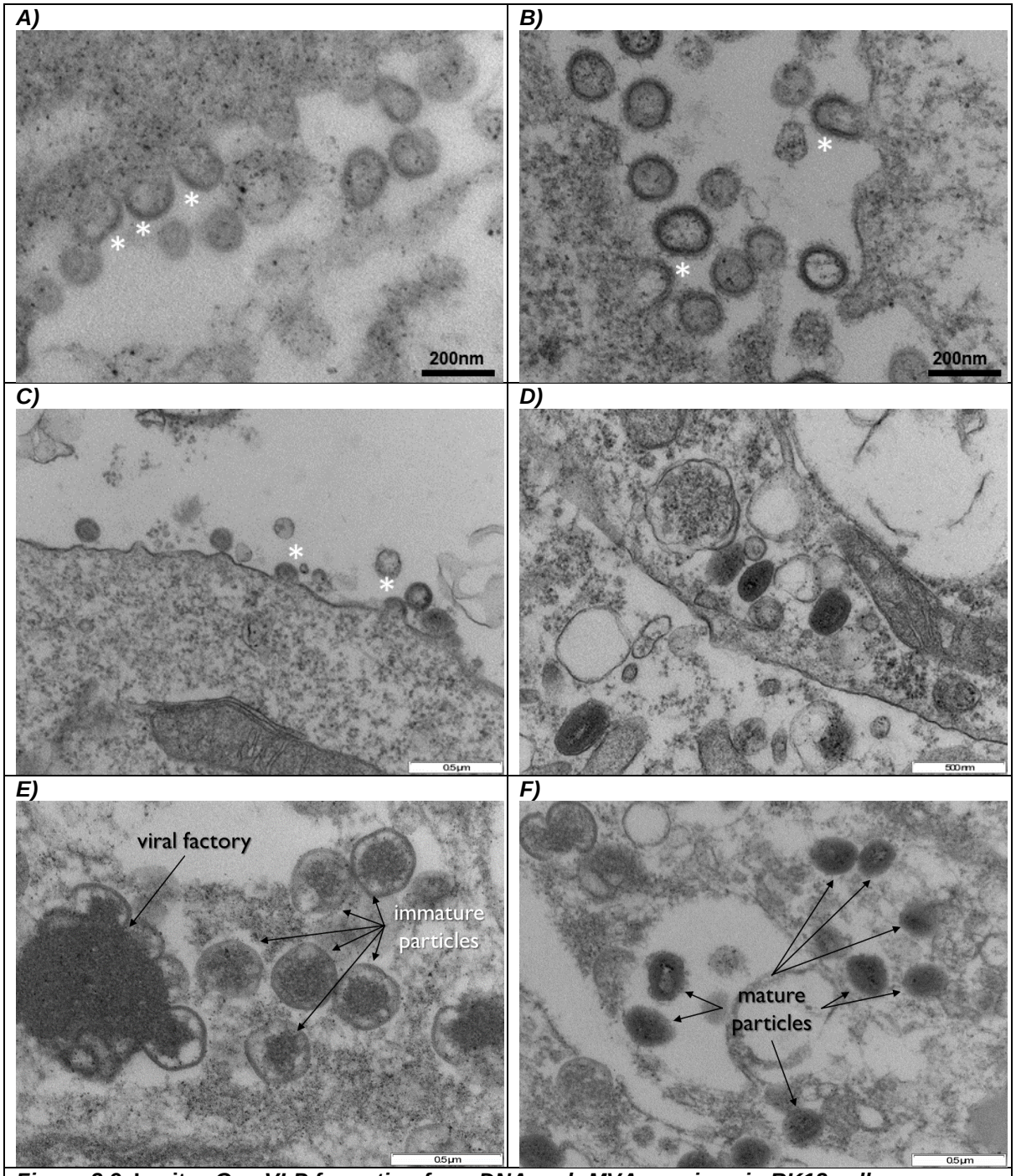

Figure 3.9.* In vitro *Gag VLP formation from DNA and rMVA vaccines in RK13 cells.
(A-C) Electron microscopy images showing *in vitro* formation of VLPs from ***(A)*** DNA Gag^{M}, ***(B)*** DNA $Env+Gag^{M}$ ***(C)*** rMVA $Env+Gag^{M}$ vaccine. VLP budding events are indicated with *.
No VLP-like structures could be detected in wildtype MVA control ***(D)***.
(E-F) Pox viral factories producing immature ***(E)*** and mature ***(F)*** MVA particles in rMVA infected cells.

with lectin purified Env yields, total soluble trimeric Env levels appear to increase with repeat harvesting, as does the percentage of soluble Env trimer divided by total Env protein (***Table 3.3***). When soluble trimeric Env was subsequently run on BN PAGE gels, it had an improved trimeric profile compared to soluble Env just purified by lectin affinity chromatography (GNL) (***Figure 3.12A+B***). Unfortunately, when this purification method of Env trimers was performed

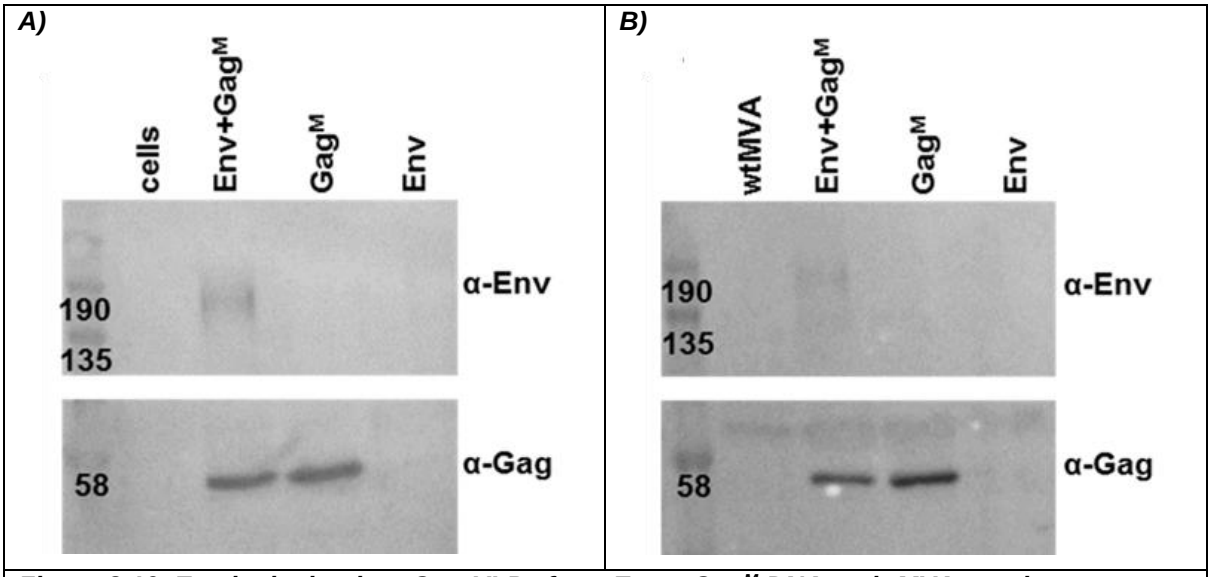

Figure 3.10. Env inclusion into Gag-VLPs from Env + Gag^{M} DNA and rMVA vaccines. ***(A-B)*** Env (top) and Gag (bottom) could be detected by western blotting in VLPs isolated from the second OptiPrep gradient when both Gag^{M} and Env were co-expressed from DNA ***(A)*** and rMVA ***(B)*** vaccines. Likewise, VLPs containing Gag only are detected from DNA or rMVA Gag^{M}, whereas no Gag or Env signal was detected for cells alone, DNA or rMVA Env vaccines or wildtype MVA.

on CAP256 soluble Env-His, some Env dimers were still present (***Figure 3.12C***). However, it was much improved compared to the corresponding CAP256 soluble Env-His GNL, and therefore these SEC purified Env-His fractions (nominally called soluble Env-His trimers) were tested in the bnAb binding ELISA as described in ***Chapter 2***. As to be expected, soluble Env-His trimers performed better compared to soluble Env-His GNL for all bnAb epitopes tested: the V3 glycan supersite (PGT128 and PGT135), the CD4-binding site (VRC01) and the V2 glycan (PG9), but also for bnAbs 447-52D and F105, which would indicate more misfolded Env. In contradiction to this and more encouragingly, low signals for bnAbs recognising native-like Env trimers (PG16 and CAP256 VRC26.08) were detectable (***Figure 3.12D-F***).

3.3.5 Immunogenicity studies in rabbits comparing heterologous vaccine platforms

With the *in vitro* confirmation of the expression of Gag^{M} and Env showing that the Env trimer is able to display in a native-like conformation from DNA and recombinant MVA vaccines, and with confirmation of the inclusion of Env into Gag VLPs, these vaccines were now ready for testing in rabbit immunogenicity studies. Furthermore, additional SEC purification to isolate soluble trimeric Env improved its antigenic properties. Therefore protein boosts adjuvanted in AlhydroGel (as described in ***Chapter 2***) were included as well. For this, four groups of rabbits were selected to either test a regimen of rMVA priming, followed by protein boosting (MMPPP) or a regimen in which the rMVA vaccine was first primed with the matching DNA vaccine and again finishing with protein vaccines (DDMMPP) (***Figure 3.13A***). To investigate if the inclusion

A) SEC profile of soluble Env

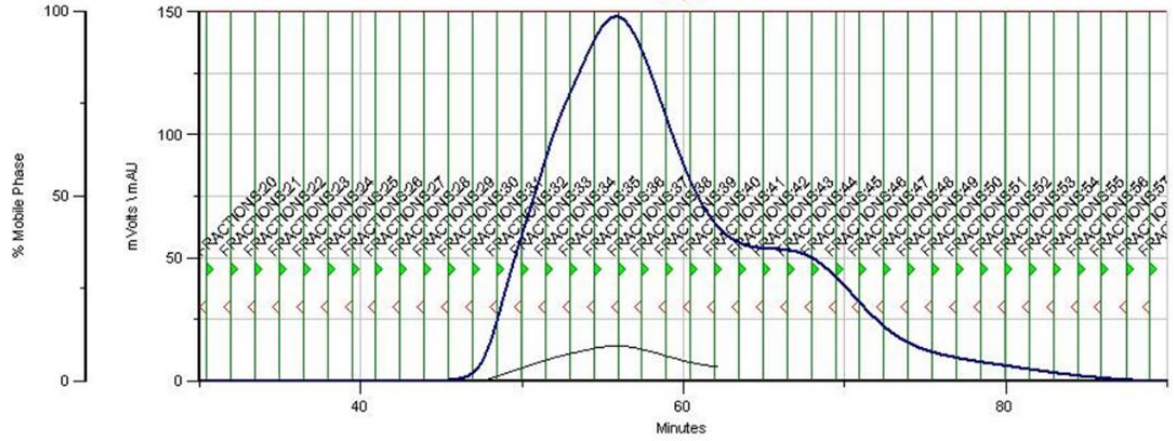

B) BN-PAGE of soluble Env fractions

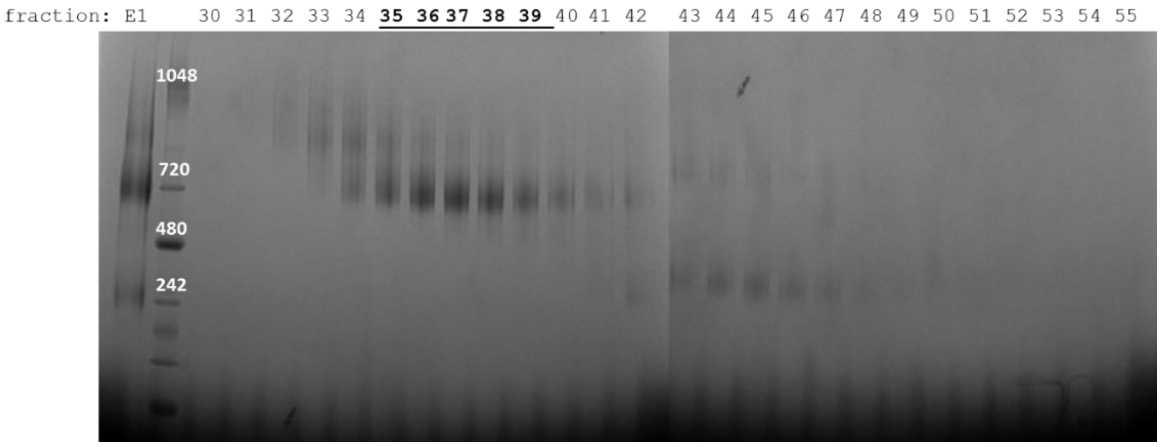

Figure 3.11. Structural characterisation of soluble Env by SEC and BN-PAGE.
(A) SEC profile of soluble Env affinity purified with lectin from the stable cell (soluble Env GNL).
(B) SEC fractions 30-55 were run on a BN-PAGE and stained with Coomassie. Combined SEC fractions 35-39 was enriched for soluble, trimeric Env. Fraction E1: SEC input material: soluble Env GNL.

Table 3.2. Top ten proteins identified in lectin affinity purified soluble trimeric Env by LC-MS. Ranking was based on |Log Probability| (third column).

Rank	Description	|Log Prob|	Total Intensity	# of spectra	# of unique peptides	# of mod peptides	Coverage %
1	***CAP256 soluble Env***	358.94	69351075571	2257	115	19	48.25
2	sp|P07437|TBB5_HUMAN Tubulin beta chain	91.28	290889049.2	110	24	5	36.49
2	tr|Q5JP53|Q5JP53_HUMAN Tubulin beta chain						
3	sp|P11047|LAMC1_HUMAN Laminin subunit gamma-1	67.24	96520216.5	69	19	1	12.55
4	sp|P24821|TENA_HUMAN Tenascin	66.23	76323972.8	60	27	1	12.9
5	sp|P14618|KPYM_HUMAN Pyruvate kinase PKM	58.37	122970676.5	48	15	0	32.96
6	sp|P13639|EF2_HUMAN Elongation factor 2	56.26	83358940.6	55	15	0	20.63
7	sp|P14543|NID1_HUMAN Nidogen-1	51.58	46683246.9	33	14	0	12.67
8	sp|Q14697|GANAB_HUMAN Neutral alpha-glucosidase AB	51.39	79875406.1	54	18	0	20.02
9	sp|P0DMV9|HS71B_HUMAN Heat shock 70 kDa protein 1B	50.45	267819742.4	58	15	1	20.59
9	sp|P0DMV8|HS71A_HUMAN Heat shock 70 kDa protein 1A						
10	sp|P68363|TBA1B_HUMAN Tubulin alpha-1B chain	47.53	86299006.1	62	11	1	27.94
10	sp|Q9BQE3|TBA1C_HUMAN Tubulin alpha-1C chain						
10	tr|F5H5D3|F5H5D3_HUMAN Tubulin alpha chain						

Table 3.3. Soluble trimeric Env protein yields after lectin affinity chromatography
Protein concentrations were measured using the DC Protein Assay against a BSA standard (three indenpent measurements per experimental sample and BSA standard concentration)

platform	flasks	harvest	concentrated eluate (mg/ml)	total mg	mg/flask	trimer (mg/ml)	total mg	% trimer
stable	4x hyperflask	1A*	0.39	2.36	0.06	0.04	0.28	12
stable		1B*	0.61	3.67	0.09	0.20	1.48	40
stable		1C*	0.42	2.54	0.06	0.13	0.94	37
stable		1D*	0.49	2.95	0.07	0.14	1.07	36
stable	4x hyperflask	2A*	0.43	2.35	0.06	0.02	0.13	6
stable		2B*	0.70	3.85	0.10	0.20	1.70	44
stable		2C*	0.64	3.54	0.09	0.17	1.17	33
stable		2D*	1.01	5.56	0.14	0.34	2.74	49
stable		2E*	0.78	4.30	0.11	0.24	1.71	40
		*repeat harvest from same hyperflasks						

of Gag in the DNA and rMVA vaccines improves the immunogenicity of the two different regimens, parallel groups received DNA or rMVA vaccines with Env alone.

Serum was taken at regular intervals and tested in an Env binding ELISA using the same soluble trimeric Env as used as protein vaccine. Interestingly, in the DDMMPP regimen no Env binding antibodies could be detected after the DNA inoculation: these only developed after rMVA boosting (***Figure 3.13B***). Env binding antibodies did develop immediately after the first rMVA vaccine for both regimens (week 4 for MMPPP and week 12 for DDMMPP), and no significant differences were observed between groups inoculated with Env alone or Env+Gag^{M}. It appears that the soluble trimeric Env protein vaccine enhances the α-Env binding antibody response in all four groups. However, there were no significant differences in α-Env antibody titres after the second rMVA vaccine and any of the protein vaccines boost observed as tested in a Two-way ANOVA. The α-Env antibody response seems to plateau at titre of approximately $1*10^5$, which could be the assay maximum. Longitudinal testing using a Two-way ANOVA showed no significant differences between groups receiving rMVA Env+Gag^{M} or Env alone in the MMPPP regimen and a similar result was obtained comparing DNA and rMVA Env+Gag^{M} or Env alone for DNA and rMVA in the DDMMPPP regimen.

Binding antibodies against the V1V2 loop of Env are of particular interest, as this was one of the main correlates of protection in the RV144 trial. Therefore, sera of the vaccinated animals at select time points were tested in a binding ELISA against the autologous CAP256 SU V1V2 loop: this was presented on a scaffold to retain the natively folded state [424] (kindly provided Dr Penny Moore from the NICD). Serum was either tested after the second rMVA vaccine (post MVA) (week 8 for MMPPP and week 14 for DMMPP) or after the final protein (post final protein) (week 30 for both MMPPP and DDMMPP) (***Figure 3.13C***). No significant differences

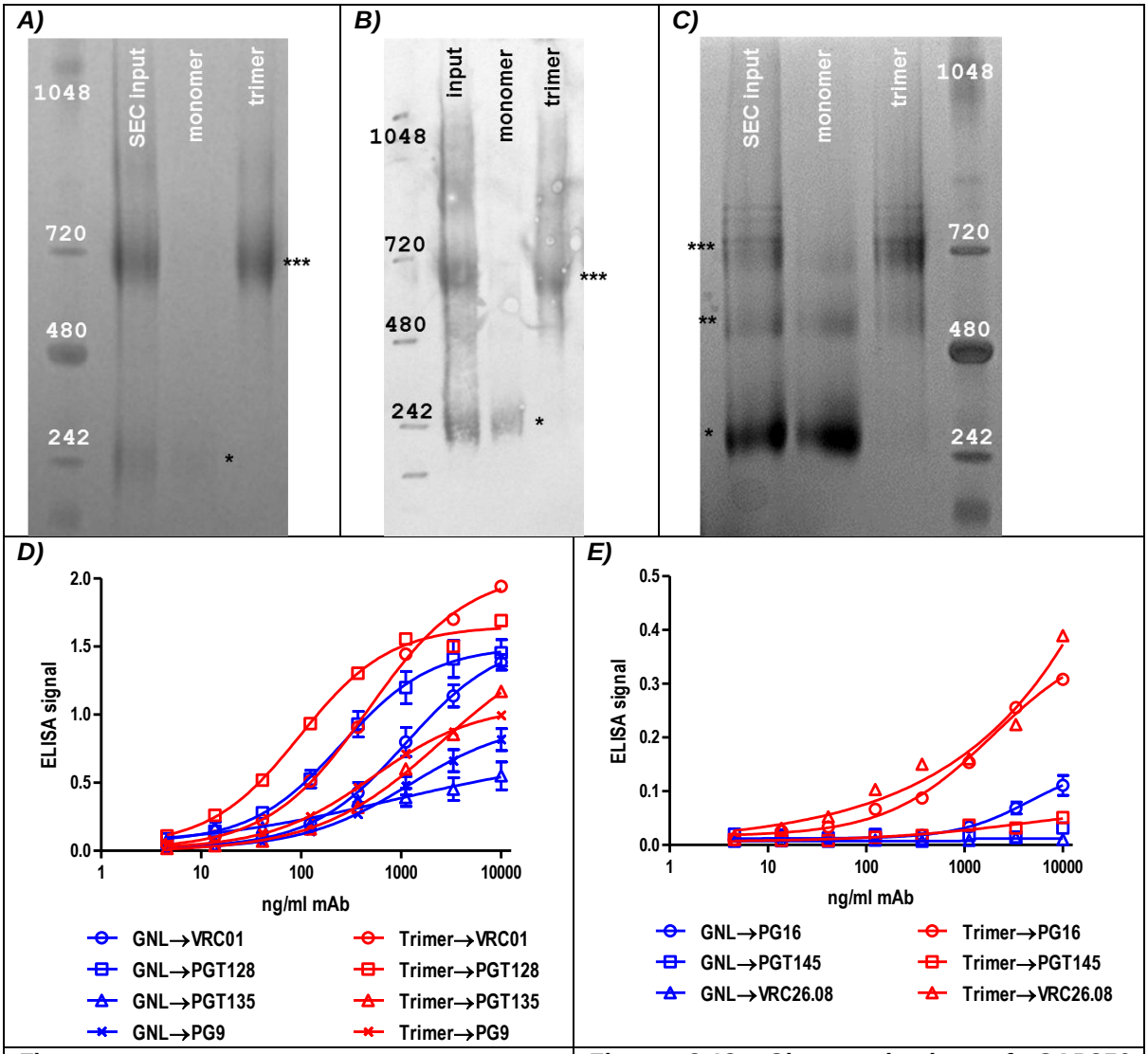

Figure 3.12. Characterisation of CAP256 soluble Env protein vaccine.

(A-C) SEC fractions combined as soluble Env trimers are mainly trimeric (***) as judged by molecular weight on BN PAGE gels stained by Coomassie ***(A)*** or as detected by Env western blotting ***(B).*** Env monomers were detected in SEC fractions combined for this configuration (*). Whereas the SEC trimer fraction for Env-His still contains dimers as detected by Coomassie staining ***(C)***.

(D-F) Better signals are observed for the bnAb ELISA for soluble, trimeric Env-His (**red**) compared to soluble Env-His GNL (**blue**) for all bnAbs tested, including PG16 and CAP256 VRC26.08 which recognise native-like Env trimers.

Note different Y-axis for ***(E)***.
For soluble Env-His trimer: representative traces.
For soluble Env-His average of *n*=3.

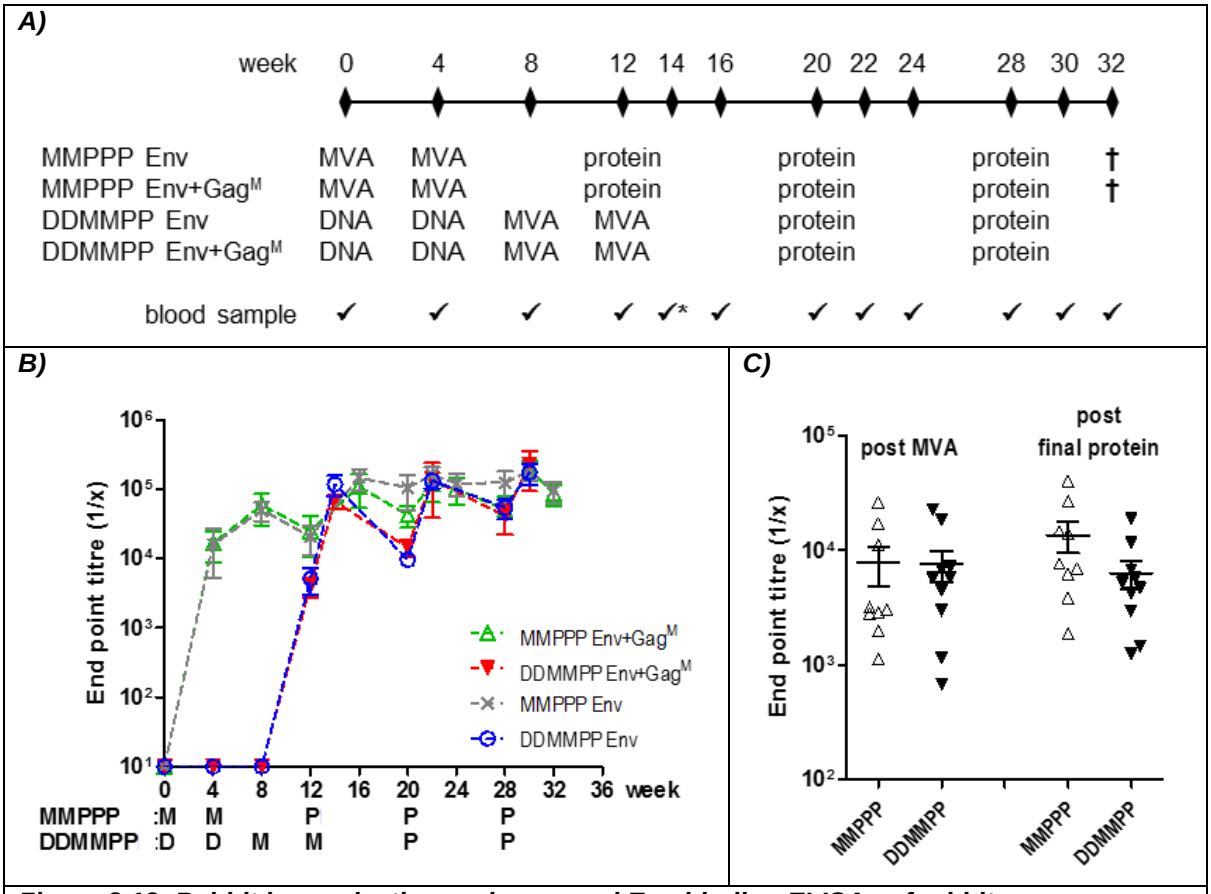

Figure 3.13. Rabbit immunisation regimens and Env binding ELISAs of rabbit sera.
(A) Immunisation protocol for the four different groups. D: DNA and M: rMVA vaccines, expressing Env+Gag^{M} or Env alone. *Week 14 was only taken for the DDMMPP regimen.
(B) Time course depicting binding of rabbit sera to soluble, trimeric CAP256 Env as measured by ELISA. Endpoint titre was plotted as 10 when no ELISA signal was observed.
(C) CAP256 V1V2 loop scaffold binding ELISA of rabbit sera post MVA (second MVA inoculation) or post final protein (second protein boost for DDMMPP, third protein boost MMPPP). This binding ELISA was negative for week 0.
All data are presented as group averages +/- SEMs.

were observed in antibody titres against the V1V2-loop when different permutations were tested in a Two-way ANOVA: no differences between regimens (MMPPP *vs* DDMMPP post MVA or post final protein) or within regimens (MMPPP post MVA *vs* post final protein or DDMMPP post MVA *vs* post final protein. Furthermore, when data was analysed in a similar fashion comparing rMVA or DNA/rMVA Env+Gag^{M} to Env alone, no significant differences were observed as well, therefore the graph in ***Figure 3.13C*** was presented per regimen, combining the data of Env + Gag^{M} and Env alone.

When these rabbit sera were tested for neutralising activity (ID_{50}) against a panel of Env-pseudotyped virions, some interesting patterns appeared ***(Table 3.4, Figure 3.14)***. As DNA priming failed to induce α-Env binding antibodies, these samples weren't included. However, the development of α-Env binding antibodies upon rMVA vaccines corresponded with neutralisation titres for tier 1A virus MW965.26 and tier 1B virus 6644 in serum of rabbits

Table 3.4. Serum neutralisation from rabbits vaccinated with different adjuvants as measured by TZM-bl assay.

Sera from immunised animals were assessed for neutralising activity (serum dilution required for a 50% reduction in entry of the infecting virus into a reporter cell line (ID50) against a panel of Env-pseudotyped virions at different time points. The 50% neutralisation titres are color-coded to reflect their potency range as indicated. Bleeds were taken 4 weeks after the second MVA prime for MMPPPP (primes) or 2 weeks after the second MVA boost for DDMMPP (MVA B2) and 2 weeks after each protein inoculation (P1-3).

As the Env binding ELISA was negative for bleeds after two DNA vaccines for the DDMMPP regimen, they were not tested here.

The pre-bleeds and MuLV control for all rabbits and time points were negative in this assay.

Titres below 20 are considered negative.

The 50% neutralisation titres are color-coded to reflect their potency range as indicated.

Titres below 20 are considered negative.

50% Neutralization titre
10 000 - 100 000
1 000 - 10 000
100 - 1 000
20 - 100
<20
N/A not applicable
NT not tested

		Clade C - Tier 1A MW965.26 ID50 after:					Clade C - Tier 1B 6644 ID50 after:					Clade C - Tier 1B 1107356 ID50 after:					Clade C - Tier 2 CAP256.SU ID50 after:				
Rabbit	Regimen	primes	MVA B2	P1	P2	P3	primes	MVA B2	P1	P2	P3	primes	MVA B2	P1	P2	P3	primes	MVA B2	P1	P2	P3
6526	MMPPP Env + Gag^{M}	91	N/A	251	3147	12403	<20	N/A	29	57	107	<20	N/A	<20	<20	29	<20	N/A	28	59	23
6528		256	N/A	973	9193	8521	47	N/A	160	269	140	<20	N/A	<20	45	34	<20	N/A	<20	<20	<20
6529		119	N/A	872	9968	5703	22	N/A	58	191	82	<20	N/A	<20	45	30	<20	N/A	<20	<20	<20
6530		208	N/A	1021	3239	4433	44	N/A	83	73	57	<20	N/A	<20	31	21	<20	N/A	38	54	48
6049		236	N/A	3290	3971	3537	130	N/A	234	96	75	<20	N/A	30	20	24	<20	N/A	<20	<20	39
6826	DDMMPP Env + Gag^{M}	NT	3426	5286	7840	N/A	NT	85	45	170	N/A	NT	32	<20	29	N/A	NT	70	486	1294	N/A
6827		NT	3892	14601	2748	N/A	NT	120	196	104	N/A	NT	35	<20	<20	N/A	NT	53	519	174	N/A
6828		NT	7239	664	4348	N/A	NT	172	20	136	N/A	NT	62	<20	21	N/A	NT	<20	<20	<20	N/A
6830		NT	12641	20778	3920	N/A	NT	299	172	143	N/A	NT	40	<20	<20	N/A	NT	60	332	296	N/A
6850		NT	1999	1987	787	N/A	NT	78	40	41	N/A	NT	<20	<20	<20	N/A	NT	<20	32	54	N/A
6544	MMPPP Env	387	N/A	1699	18049	11998	89	N/A	476	362	642	22	N/A	<20	49	32	<20	N/A	<20	<20	<20
6546		98	N/A	867	5669	3647	128	N/A	50	87	129	<20	N/A	<20	42	<20	<20	N/A	<20	<20	<20
6047		136	N/A	1399	1533	4759	26	N/A	158	32	56	<20	N/A	21	<20	56	<20	N/A	<20	<20	28
6048		482	N/A	2029	2119	3830	32	N/A	132	37	49	<20	N/A	<20	<20	23	<20	N/A	<20	333	333
6843	DDMMPP Env	NT	1600	2045	828	N/A	NT	131	59	124	N/A	NT	<20	<20	<20	N/A	NT	<20	126	74	N/A
6844		NT	798	5289	5808	N/A	NT	59	64	102	N/A	NT	<20	<20	29	N/A	NT	<20	<20	<20	N/A
6846		NT	1353	4359	2918	N/A	NT	41	25	37	N/A	NT	20	<20	37	N/A	NT	<20	<20	<20	N/A
6847		NT	1716	5312	5618	N/A	NT	34	25	43	N/A	NT	21	<20	35	N/A	NT	<20	<20	<20	N/A
6848		NT	3197	9378	14844	N/A	NT	178	207	125	N/A	NT	23	45	105	N/A	NT	<20	1063	204	N/A

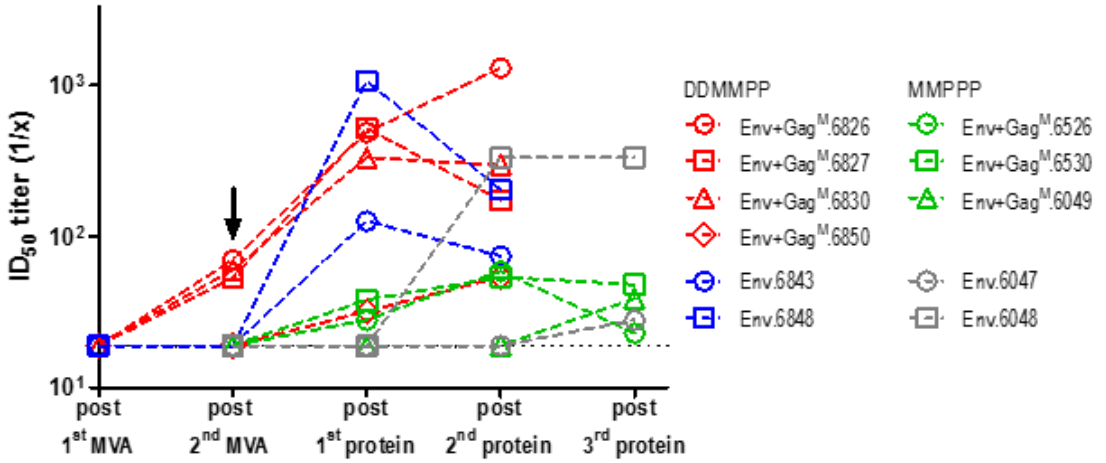

Figure 3.14. Inclusion of Gag^{M} in prime affects serum neutralisation as measured by TZM-bl assay.
Dotted black line represent assay detection limit (1/20 dilution). All data points below detection limit are plotted as 19. ID_{50} titres over time of individual animals with Tier 2, vaccine matched neutralisation titres against CAP256_SU pseudo-virions. The black arrow indicates low titre Tier 2 neutralisation titres after the second MVA boost in 3 out of 4 animals in the DDMMPP Env+Gag^{M} group, before any protein boosting.
For the MMPPP regimen, the neutralisation assay was only performed after the second rMVA vaccine.

after the second rMVA vaccine in all four groups (***Table 3.4***, MMPPP: post primes and DDMMPP: post MVA B2). When data of the groups within a regimen was combined (Env+Gag^{M} and Env alone), neutralisation titres after the second rMVA inoculation towards MW965.26 was significantly higher in the DDMMPP regimen compared to MMPPP (Student *t* test, $p<0.01$). The neutralising titres towards MW965.26 further increased in all four groups after protein boosting, where again after the first protein boost, these were significantly higher DDMMPP regimen compared to MMPPP (Student *t* test, $p<0.05$). DNA priming of the rMVA vaccine also improved the development of neutralising antibodies for tier 1B 1107356 pseudovirions, which developed after the second MVA vaccine for the DDMMPP regimen and only after protein boosting for MMPPP. Most promising, neutralisation titres for vaccine matched Tier 2 neutralisation (autologous) towards CAP256_SU was observed in all four groups of rabbits as well. For the MMPPP regimen these neutralisation titres developed only after protein boosting and in 5 out of 9 animals after the final protein boost. CAP256_SU neutralisation titres were in general low (<1:105), although one animal showed consistently higher neutralisation response of above 1 in 300 after the second and third protein boost. DNA priming clearly increased the autologous Tier 2 neutralisation response in an animal. Although almost a similar number of rabbits developed neutralising antibodies for CAP256_SU (6 out of 10), titres were clearly higher, with four animals having titres above the threshold required

for 50% protection (1 in 105) in a NHP model [147]. Furthermore, in three rabbits this neutralisation response already developed after the second rMVA vaccine.

In depth analysis of the autologous Tier 2 neutralisation response comparing the groups receiving Env+Gag^{M} to those administered with Env alone revealed several exciting observations. First, more animals developed autologous Tier 2 neutralisation when Gag was included in the vaccines, with 3 out of 5 for MMPPP Env+Gag^{M} (60%) compared to 2 out of 4 for Env alone (50%). This was even more pronounced for the DDMMPP regimen with 4 out of 5 (80%) for Env+Gag^{M} compared to 2 out of 5 for Env alone (40%) ***(Figure 3.14)***. Furthermore, with Gag inclusion into the MMPPP or DDMMPP regimen, 5 out of 7 animals (rabbits 6526, 6530, 6826, 6827 and 6830) with autologous Tier 2 neutralising antibodies developed these at an earlier time point compared to animals which received Env alone (rabbits 6047, 6048, 6843 and 6848). For MMPPP Env+Gag^{M} this neutralisation appeared after the first protein for both animals whereas for DDMMPPP Env+Gag^{M} in 3 out of 4 rabbits Tier 2 neutralisation of CAP256_SU developed without a protein boost, after the second rMVA inoculation ***(Figure 3.14, indicated with arrow)***.

As mainly animals from the DDMMPP regimen showed autologous Tier 2 neutralisation titres above 1:105, the week 30 sera from these six rabbits were tested against a global panel of ten Tier 2 HIV-1 Env pseudoviruses. Three out of 6 animals developed a low titre neutralisation response against Clade A 398F1, ranging between 1:20-29 (***Table 3.5***).

Table 3.5. Week 30 serum neutralisation against global panel for DDMMPP rabbit experiment as measured by TZM-bl assay.
Week 30 sera from immunised animals were assessed for neutralising activity (ID50) against a global panel of Tier 2 Env pseudotyped virions.
The 50% neutralisation titres are color-coded to reflect their potency range as indicated.
Titres below 20 are considered negative.

		ID50											
		X1632	398F1	25710	BJX2000	CE0217	CE1176	CH119	CNE8	CNE55	TRO.11	X2278	246F3
Rabbit	Regimen	G	A	C	CRF07	C	C	CRF07	CRF01	CRF01	B	B	AC
6826	DDMMPP Env + Gag^{M}	<20	<20	<20	<20	<20	<20	<20	<20	<20	<20	<20	<20
6827		<20	21	<20	<20	<20	<20	<20	<20	<20	<20	<20	<20
6830		<20	24	<20	<20	<20	<20	<20	<20	<20	<20	<20	<20
6850		<20	<20	<20	<20	<20	<20	<20	<20	<20	<20	<20	<20
6843	DDMMPP Env	<20	<20	<20	<20	<20	<20	<20	<20	<20	<20	<20	<20
6848		<20	29	<20	<20	<20	<20	<20	<20	<20	<20	<20	<20

50% Neutralization titre
1 000 - 10 000
100 - 1 000
20 - 100
<20

The same sera that were tested against the global Tier 2 panel were used to investigate the possible neutralisation site within the Env sequence. A K169E mutation within CAP256_SU

Env leads to the loss of binding of the native-like Env trimer specific MAbs PG16 and CAP256 VRC26.08 [167, 174, 252]. When sera were tested against these CAP256_SU K169E pseudovirions, no differences were observed compared to the CAP256_SU pseudovirion ***(Table 3.6)***, suggesting that the neutralisation response was directed towards a region outside the trimer apex of Env. In line with this, chimaeras formed by replacing the V1V2 region of two heterologous viruses, BG0505N332+ or CAP84, with that of CAP256_SU, were not neutralised, indicating that the Tier 2 NAbs elicited in this study are probably not targeting the V1V2 region.

Table 3.6. Week 30 serum neutralisation against CAP256 Env K169E mutant for DDMMPP rabbit experiment as measured by TZM-bl assay.
Week 30 sera from immunised animals positive for Tier 2 CAP256_SU neutralisation were assessed for neutralising activity (ID50) against CAP256_SU K169E or BG0505N332+ and CAP84 pseudovirions with their V1V2 loop was replaced with that of CAP256_SU.
The 50% neutralisation titres are color-coded to reflect their potency range as indicated.
Titres below 20 are considered negative.

		ID50				ID50	
		Clade C Tier 2				CAP256 V1V2 loop	
		CAP256.SU		CAP256.SU K169E		BG505N332	CAP84
Rabbit	Regimen	2nd prot	3rd prot	2nd prot	3rd prot	2nd prot	2nd prot
6526	MMPPP Env + Gag^{M}	59	23	37	43	NT	NT
6530		54	48	33	56	NT	NT
6049		<20	39	NT	<20	NT	NT
6826	DDMMPP Env + Gag^{M}	1295	N/A	1495	N/A	<20	<20
6827		338	N/A	215	N/A	<20	<20
6830		359	N/A	306	N/A	<20	<20
6850		37	N/A	45	N/A	<20	<20
6047	MMPPP Env	<20	28	NT	22	NT	NT
6048		333	333	394	350	NT	NT
6843	DDMMPP Env	102	N/A	141	N/A	<20	<20
6848		204	N/A	306	N/A	<20	<20

50% Neutralization titre
1 000 - 10 000
100 - 1 000
20 - 100
<20
N/A not applicable
NT not tested

3.4. Discussion

Building on observations discussed in ***Chapter 2*** where the adjuvant AlhydroGel induced a superior immune response with lectin affinity purified soluble CAP256 gp140-FL-IP (soluble Env (GNL)), here several experiments were performed where the protein vaccine was preceded by the DNA and/or recombinant MVA (rMVA) HIV-1 vaccines to test whether this

would improve the immunogenicity and the longevity of this soluble Env protein vaccine. Both DNA and rMVA vaccines were characterised *in vitro* before subsequent animal testing. For DNA vaccines a backbone was used which was shown to elicit improved immunogenicity in mice and to allow significant dose sparing due to a novel enhancer element from porcine circovirus type 1 [299, 413]. The rMVA vaccines used in this study are able to actively infect certain lines of mammalian cells *in vitro*, whilst being replication incompetent *in vivo:* in either

case, this will result in expression of exogenous genes present in MVA. Therefore, rMVA can induce both a humoral and cellular response and activate both CD4+ and CD8+ T-cells [315]. For both DNA and recombinant MVA vaccines, the CAP256 gp160 gene was truncated to gp150 (AA 730), thereby truncating most of the gp41 cytoplasmic tail while retaining the transmembrane domain, and improving expression and genetic stability [440]. The other modifications present in the soluble Env protein vaccine were retained, with the furin cleavage site replaced with two glycine-serine based repeats (GGGGS) to form a flexible linker (FL) [383, 384] and an I548P mutation equivalent to the I559P in the SOSIP trimers introduced to stabilise trimerisation of gp41 [374]. The vaccines generated with this insert were named pMExT gp150-FL-IP (DNA Env) and recombinant MVA gp150-FL-IP (rMVA Env). For both DNA and rMVA vaccines, subtype C mosaic Gag (Gag^{M}) was either co-expressed (DNA vaccine pTJDNA4, also in pTHpCapR backbone) or Env was targeted into rMVA Gag^{M} (abbreviated to DNA or rMVA Env+Gag^{M}). It was anticipated that inclusion Gag^{M} could potentially induce virus-like particle (VLP) formation *in vivo* as was shown in this project *in vitro*. This could lead to presentation of Env to the immune system in its natural membrane-bound state in particles, which has been shown to lead to increased immunogenicity [442-445]. Furthermore, the Gag^{M}, which was designed *in silico* to maximise potential T-cell epitopes, elicited an improved cell mediated immune response as compared to a natural Gag in mice and was therefore predicted to do the same in rabbits [272, 413, 414].

3.4.1 Env expressed from DNA and rMVA HIV-1 vaccines can take on a native-like conformation

For DNA and rMVA vaccines, live-cell staining experiments were performed to identify the presence of epitopes recognised by broadly neutralising epitopes in Env. Although some epitopes characteristic of misfolded Env trimers were detected when Env was expressed from rMVA Env+Gag^{M} or DNA Env in HeLa cells as judged by positive signals for bnAbs F105 and 447-52D, the broadly neutralising epitopes for the V2-superglycan (MAbs PGT128 and PGT135), the CD4-binding site (MAb VRC01) and V1V2 glycan (MAb PG9) were present as well. More importantly, clear fluorescent signals were detected for PG16, PGT145 and CAP256 VRC26.08, all bnAbs which specifically bind to Env in a native-like conformation. These observations are in line with data from Cappuci et al [343], where BG505 SOISP.664 expressed from MVA or simian adenovirus resulted in expression of both native-like and misfolded trimers [343]. It should be emphasised that the live-cell staining used here is a qualitative assay, therefore developing a quantitative assay would greatly assist further characterisation of the DNA and rMVA HIV-1 vaccines. A fluorescence-activated cell sorting (FACS) based on this live-cell staining protocol could be considered.

Compared to the Env protein vaccine used in ***Chapter 2***, an additional round of purification was included where CAP256 soluble Env trimers were isolated from the lectin affinity-purified Env protein (soluble Env (GNL)) by size exclusion chromatography (SEC). These soluble Env trimers were mainly in a trimeric conformation as judged by molecular weight on Blue Native protein PAGE gels. However, when His-tagged soluble Env trimers were isolated by SEC, a full separation between trimers and dimers was not achieved. Despite this, soluble Env-His was tested for the presence of epitopes recognised by broadly neutralising epitopes in Env in an ELISA assay. Similar results were obtained as for the DNA and rMVA HIV-1 vaccines, where bnAb epitopes for V2-superglycan, the CD4-binding site (MAb and V1V2 glycan were present and ELISA signals were higher compared to soluble Env-His (GNL). Most encouragingly, ELISA signals for PG16 and CAP256 VRC26.08 were detectable, indicating that some of the soluble Env trimers were in a native-like conformation. However, clear ELISA signals were present as well for F105 and 447-52D, an indication of misfolded Env trimers. This was hardly surprising as Env-His dimers would have been present in the soluble Env-His trimer preparation. Therefore it is anticipated that the soluble Env trimers used as protein vaccine have an improved antigenic profile compared to the Env-His version considering the better BN-PAGE profile. However, additional purification by positive selection of native-like Env trimers using bnAbs PG16 or CAP256 VRC26.08 [371, 435] or removing misfolded trimers with F105 or 447-52D (negative selection) [385, 422] could be considered to improve the antigenic properties even further. Additional characterisation of the protein vaccine, based on for instance the bio-layer interferometry technology used in the Octet, could be considered as well.

3.4.2 DNA priming improves the immunogenicity of a rMVA prime – protein boost HIV-1 vaccine regimen, including autologous Tier 2 neutralisation

The DNA, rMVA and protein vaccines discussed above where subsequently tested in different heterologous vaccine platform regimens in rabbit immunogenicity studies. In two groups of animals, two rMVA vaccines (rMVA Env+Gag^{M}) were boosted with three trimeric, soluble Env protein vaccines, where group 1 received rMVA Env+Gag^{M} and group 2 rMVA Env (MMPPP). This was compared to two more groups where the same rMVA vaccines were primed with matching DNA vaccines (regimen DDMMPP). As DNA vaccines by themselves in general only lead to subtle and transient immune responses which are skewed towards a CD8+ rather than a CD4+ T-cell response [439], they are effective in priming a cellular immune response of viral vaccines and these heterologous vaccine regimens can lead to more balanced CD4+ and CD8+ T cell responses [446]. It has therefore been investigated in combination with rMVA in

a number of studies [333, 335, 337, 339, 447], including from our group [334, 336, 354, 355, 413].

Both MMPPP and DDMMPP regimens resulted in serum binding antibodies to CAP256 soluble trimeric Env which could be detected after the first rMVA inoculation but not after DNA vaccines alone, and were boosted by the second rMVA. Although there was a trend with antibody titres increasing after each protein vaccine, this was not tested to be significant.

Comparing both vaccine regimens, neutralisation titres for Tier 1A MW965.26 and Tier 1B 6644 after the second rMVA inoculation were significantly higher for this DDMMPP regimen compared to MMPPP. In both regimens, Tier1B neutralisation of 6644 was observed after the second rMVA vaccine, but only in the DDMMPP regimen pseudovirions of 1107365 were neutralised at this time point. The most noteworthy difference between the two different regimes was in neutralisation titres for vaccine-matched Tier 2 CAP256_SU pseudovirions, which were clearly higher for DDMMPP (although failed to test significantly different), ranging between 1:54 and 1:1294 after the final protein boost. Tier 2 autologous neutralisation response rates were roughly similar between groups (DDMMPP 6/10 versus MMPPP 5/9). However, for the DDMMPP regimen, four animals had titres above the threshold required for 50% protection (1 in 105) in a NHP model [147], compared to just one from the MMPPP regimen. Encouragingly as well for the DDMMPP regimen, Tier 2 neutralisation had developed after the first protein vaccine for all animals, whereas for the MMPPP some animals only developed low neutralisation titres after the third protein boost.

The improvement in Tier 2 neutralisation when the rMVA vaccines are primed with matching DNA vaccines correlates with other studies which have shown that DNA primes a good humoral response [380, 448]. The addition of a DNA prime to MVA vaccination regimens also increases the magnitude and quality of T cell responses [347, 448, 449]. Addition of DNA-C priming in the EV01 Phase I Trial increased IgG antibody responses against Env from 27% in the group vaccinated with NYVAC alone to 75% in the DNA + NYVAC group [449]. The DNA prime also significantly boosted the T cell responses. The effectiveness of heterologous vaccines regimens is further emphasised by a study from Capucci *et al*. [343], where three out of four rabbits immunised with the simian adenovirus vaccine, followed by MVA and then ISCOMATRIX^{TM}-adjuvanted BG505s trimer, developed autologous Tier 2 Nabs.

The antibody lineage which developed into broadly neutralising antibodies in donor CAP256, where this Env sequence was taken from, was directed against the trimer apex (V1V2-loop) [425]. The CAP256_SU Tier 2 neutralisation observed in this DDMMPP experiment is most likely targeted outside of this region, as no differences were observed towards the neutralisation of CAP256_SU K169E mutant (where bnAb binding of PG16 and CAP256-

VRC26.08 is lost [94, 167, 174]). Similarly, no neutralisation of pseudorivrions BG505N332+ or CAP84, which both contain the CAP256_SU VIV2 loop, was seen. Further characterisation of the site of neutralisation would be informative, and showing that the site of neutralisation is similar between animals would build confidence that CAP256_SU Env is a suitable sequence for HIV-1 vaccines. Although it appears that Tier 2 neutralisation is outside the V1V2-loop, some low level Tier 2 cross-neutralisation was observed against 398F1. The V3-loop appears to be best conserved between CAP256_SU and 398F1 after aligning both Env sequences (data not shown), which possibly gives a clue towards the neutralisation epitope. It would be interesting to investigate for the 398F1 Env sequence if neutralisation is targeted to the same region as for CAP256_SU. However, the low neutralisation titres for 398F1 might be prohibitive for this analysis.

3.4.3 Inclusion of mosaic Gag in DNA and rMVA prime vaccines improves autologous Tier 2 neutralisation dynamics

For two different rabbit vaccine regimens, DNA and rMVA vaccines for Env were combined with HIV-1 subtype C mosaic Gag (Gag^{M}) with the aim of inducing VLP formation *in vivo,* as was shown in this project *in vitro*. In this way, Env would be presented to the immune system in its natural membrane-bound state in particles, which has shown to lead to increased immunogenicity [442, 443, 445, 450]. Although binding antibodies to soluble Env or scaffolded CAP256 V1V2-loop protein were similar for groups receiving Env and Env+Gag^{M}, Tier 2 neutralisation was positively affected by the inclusion of Gag into the HIV-1 vaccine of MMPPP and DDMMPP regimens. While it is difficult to conclude that Gag increases Tier 2 neutralisation titres, the dynamics of Tier 2 neutralisation development were changed, with a clear increase in the number of animals where neutralisation is induced. For the majority of animals this neutralisation developed at an earlier time point compared to those vaccinated with Env alone. Possibilities are that Env stabilisation and presentation in a more native-like membrane-bound state on Gag VLPs, and/or the adjuvanting properties of the Gag VLPs, might underlie this phenomenon. Tong et al. [405] showed that the surface of HIV-1 derived VLPs often contain uncleaved gp160 and gp41 stumps, that promote the development of non-neutralising responses. The removal of these non-functional Envs with protease treatment resulted in VLPs that were better able to induce Tier 2 NAbs [405, 451]. As the Env used in this paper contains a flexible linker between the gp120 and gp41 there is no necessity for cleavage, and thus it is highly unlikely that there will be any exposed gp41 stumps on the surface of our VLPs. Ingale et al. [389] showed that SOSIP or NFL trimers presented on the surface of nanoparticles were better at activating germinal centre B cells and inducing B cell receptor signalling and activation than soluble Env, further supporting the use of a particle-

based HIV vaccine. The Env presented on the surface of these nanoparticles also showed a trend towards eliciting better neutralising antibody responses compared to the soluble Env [389]. This is a possible mechanism underlying the improved response in with the DNA and rMVA Env+Gag^{M} priming, where this B-cell response is triggered by Env incorporated in Gag VLPs.

Several studies in which Gag was included in the vaccine regimen point towards the value of heterologous vaccine strategies. In a non-human primate (NHP) model, DNA and rMVA vaccines expressing Env-Gag VLPs were moderately successful in generating a low autologous Tier 2 neutralisation response when used in a DNA prime, rMVA boost and rMVA+gp120 protein boost regimen [346]. Work at the Emory Vaccine Center by Amara *et al*., has shown the strength of VLP production from DNA prime – MVA boost (DDMM) regimens by inducing robust systemic cellular and humoral immune-responses in NHPs against HIV/SIV [445, 452-456]. Encouragingly, these DNA prime – MVA boost regimens resulted in delayed acquisition in macaques after SIV challenge [457, 458]. Inclusion of a gp140 protein vaccine in the second MVA inoculation improved antibody response towards Env [459]. Similar results were obtained when gp140 protein or Gag VLPs containing Env vaccines were used to boost DDMM regimens [345, 460, 461], although this might not necessarily improve protection against HIV-1 acquisition [461]. Furhtermore, subtle Tier 2 neutralisation was reported as well in NHPs when a DNA prime- rMVA boosting regimen, containing gp160 and Gag in the DNA vaccine and gp140 and Gag for the rMVA vaccine, was used [462]. A group receiving gp120 protein at the same time as the rMVA vaccine performed best in this particular study. The case for heterologous prime-boost regimens is further strengthened by work in macaques by the Barouch group, who showed that adeno virus priming followed by rMVA boosting of bivalent M mosaic Env/Gag/Pol antigens vaccines is effective in generating low Tier 2 neutralisation response and protection in SHIV challenge models [463]. These studies, together with the data presented in this thesis, emphasises that heterologous prime-boost regimens could potentially lead to more immunogenic HIV-1 vaccines.

It should be emphasised that it is complicated to directly compare the different studies as different antigens are used (such as BG505, ConM, ConS, CAP256 for these studies), Env length (gp160, gp150, gp140), Env mutations (such as SOSIP, stabilising mutations, deleted or optimised furin cleavage site and flexible linker), vaccine platforms (DNA, rMVA, adeno virus, protein and different heterologous combinations of these) and animal models (rabbit, guinea pig, macaques).

Finally, compared to the protein vaccine used in ***Chapter 2***, additional purification of soluble Env by isolating the trimeric fraction using SEC might have been another important factor

driving the induction of autologous Tier 2 neutralisation. However, it should be emphasised that under the right conditions where Env and Gag^{M} were included in the DNA and rMVA vaccine, Tier 2 neutralisation was already observed after the second rMVA vaccine and was further boosted by the protein vaccines, suggesting that the combined effect of all three different vaccine platforms is required to induce the best immune response.

CHAPTER 4: ENV:HA_2 CHIMAERAS FAIL TO IMPROVE THE *IN VITRO* AND *IN VIVO* IMMUNOGENIC PROPERTIES OF ENV

4.1 Introduction

Recently there is an increased interest in particulate vaccine designs for displaying Env in dense arrays. These can take the form of self-assembling protein nanoparticles such as virus-like particles (VLPs), those which use proteins scaffolds such as the popular protein ferritin, or synthetic nanoparticles including lipid nanoparticles/liposomes, silica nanoparticles and particles based on polymers [401, 402]. Interestingly, the protein vaccines currently licensed for hepatitis B and human papillomavirus are VLP-based vaccines [403, 404]. One of the main objectives of particulate Env vaccines is better direct B-cell activation, where the repetitive display of high density Env trimers would probably improve B cell receptor (BCR) cross-linking and could potentially compensate for low affinity antigen-BCR interactions between Env and naïve B-cells [402, 405].

In ***Chapter 3***, an approach was presented in which CAP256 gp150-FL-IP (Env) was displayed on Subtype C mosaic Gag (Gag^M) VLPs from HIV-1 DNA and MVA vaccines. When these Env+Gag^M HIV-1 vaccines were tested in immunogenicity studies in rabbits using different heterologous HIV-1 vaccine platforms, superior autologous Tier 2 neutralisation of CAP256_SU pseudovirions was observed in a regimen of 2x DNA, 2x MVA and 2x protein vaccines (DDMMPP) compared to Env without Gag^M vaccines or a regimen without HIV-1 DNA vaccines (MMPPP). However, as the Env spike density on the native HIV-1 virion is relatively low when compared to other viruses [464], this could very well also be the case for these VLPs. Other groups have tried to improve spike density by replacing the transmembrane domain (TM) and cytoplasmic tail (CT) of gp41 with the corresponding elements from glycoproteins from other viruses. An increase in spike density of Env chimaeras resulted when the TM plus CT of glycoproteins from Epstein Barr virus, mouse mammary tumour virus (MMTV), baculovirus gp64 and HA from influenza A virus were used [399, 418-420, 465]. Therefore, in work reported in this chapter, an effort was made to improve the spike density on VLPs and the plasma membrane by generating chimaeric constructs between HIV-1 Env and the haemagglutinin stalk domain from influenza A, and to investigate if this would improve the spike density of this chimaeric construct on both the plasma membrane and VLPs compared to CAP256 gp150-FL-IP. Two constructs were designed, where either the whole HIV-1 gp41 was replaced with influenza haemagglutinin HA_2 (CAP256 gp120HA_2-FL-IP) or only the TM and CT of gp41 were substituted with the corresponding domain of HA_2 (CAP256 gp120HA_2tr-FL-IP) (collectively named Env:HA_2 chimaeras). One of the driving reasons for the selection of HA_2 to generate these Env:HA_2 chimaeras over the other glycoproteins mentioned above has been that, depending on the expression platform, these chimaeric proteins can assemble into particles without the need of Gag or other structural viral proteins [421]. After *in vitro* characterisation, the intent was that both Env:HA_2 chimaeras would be

used in DNA and MVA vaccines in combination with Gag^{M} for immunogenicity testing in rabbits using the DDMMPP regimen.

4.2 Material and methods

Refer to ***Sections 2.2 and 3.2*** for methods common to all investigations.

4.2.1 Design of CAP256 Env and Env:HA_2 chimaeric constructs

The sequence of the CAP256_SU gp160 (clone CAP256.206sp.032.C9) has been previously described (GenBank: KF241776.1) [167]. The Env sequence was altered as follows: the native leader (signal peptide) was removed, the furin cleavage site was replaced with two glycine-serine based repeats (GGGGS) to form a flexible linker (FL) [383, 384] and an I548P mutation equivalent to the I559P in the SOSIP trimers was introduced to stabilize trimerisation of gp41 [374]. Finally, the sequence was truncated to gp150 (AA 730) for MVA and DNA vaccines to increase expression and stability [440], thus generating gp150-FL-IP. Two different chimeras were generated in which either the whole of HIV-1 gp41 was replaced with the corresponding influenza HA_2 stalk (gp120HA_2-FL), or the ectodomain of gp41 including the I559P mutation was retained, and only the transmembrane domain and cytoplasmic tail of HA_2 was used (gp140HA_2tr-FL-IP). The HA_2 stalk sequence was based on the influenza A H5N1 strain (REFSEQ: accession NC_007362.1). For all three constructs, any potential poxvirus termination signals (TTTTTNT) were removed from the coding sequence and a poxvirus termination signal (TTTTTCT) was added directly after the STOP codon (TGA) of the Env gene. The Env sequences were human codon optimised and synthesised by GenScript (Nanjing). For the Env:HA_2 chimaeric constructs, only the C-terminal portion after the flexible linker (FL) was ordered for subsequent subcloning behind gp120-FL.

4.2.2 Generation of DNA Env and Env:HA_2 chimaeric vaccines

The mammalian expression plasmid pMExT CAP256 gp150-FL-IP described in ***Chapter 3*** was used as a backbone for generating the Env:HA_2 chimaeras. A unique, in-frame BamHI restriction site was introduced into gp150 at the C-terminal end of the flexible linker (FL), which allowed the exchange of gp41 with the influenza HA_2 stalk or ectodomain of gp41 fused to the HA_2 transmembrane domain and cytoplasmic tail using the BamHI and EcoRI sites thereby generating pMExT CAP256 gp120HA_2-FL and pMExT CAP256 gp140HA_2tr-FL-IP respectively (***Figure 4.1A-C***). After verification and characterisation (see ***Section 3.2.7***), the DNA Env:HA_2 chimaeric vaccines were synthesised by Aldevron (Fargo) for immunisation experiments. These DNA vaccines will be abbreviated in this chapter as outlined in ***Table 4.1***.

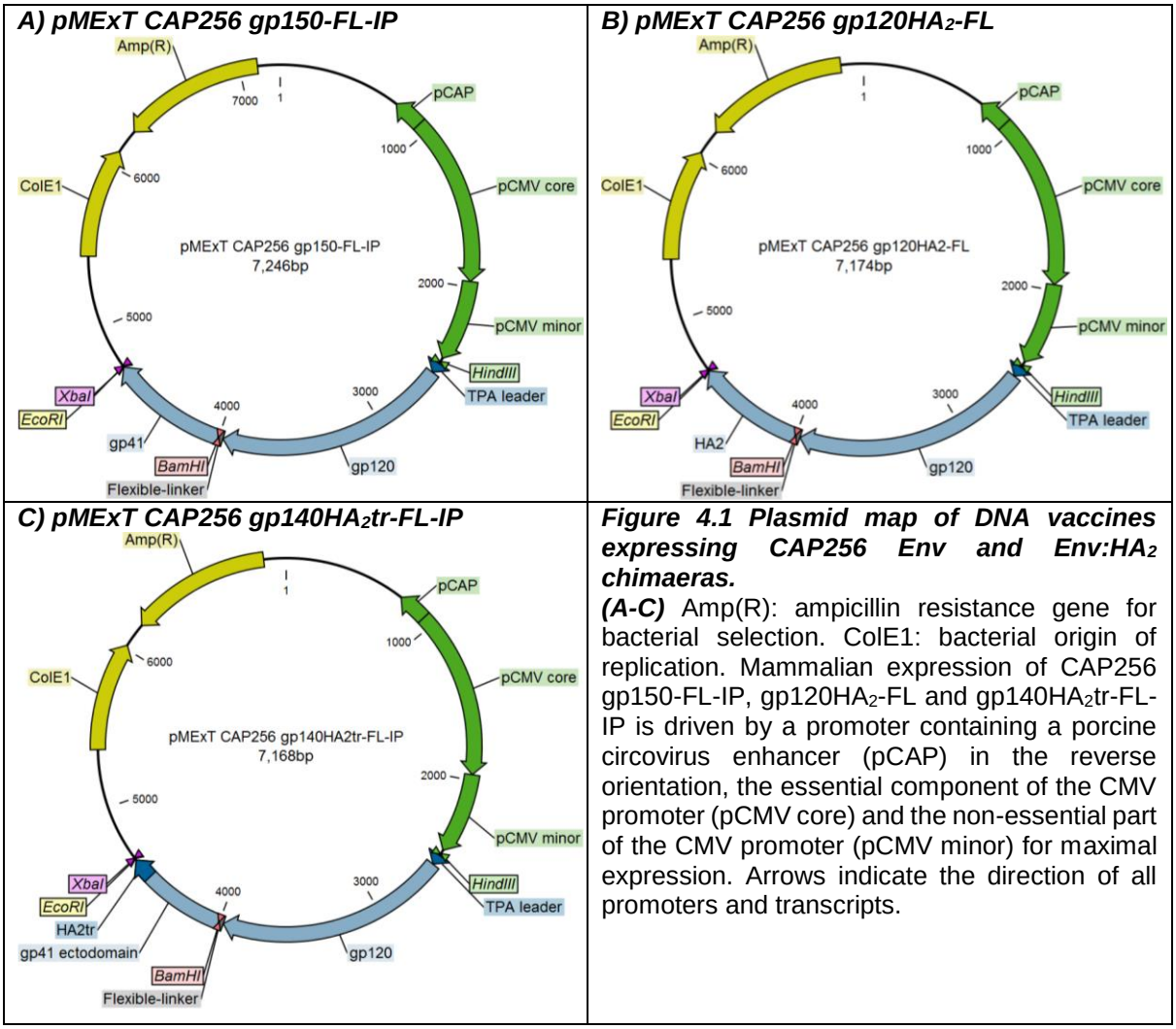

Figure 4.1 Plasmid map of DNA vaccines expressing CAP256 Env and Env:HA$_2$ chimaeras.

(A-C) Amp(R): ampicillin resistance gene for bacterial selection. ColE1: bacterial origin of replication. Mammalian expression of CAP256 gp150-FL-IP, gp120HA$_2$-FL and gp140HA$_2$tr-FL-IP is driven by a promoter containing a porcine circovirus enhancer (pCAP) in the reverse orientation, the essential component of the CMV promoter (pCMV core) and the non-essential part of the CMV promoter (pCMV minor) for maximal expression. Arrows indicate the direction of all promoters and transcripts.

Table 4.1 Abbreviations for Env and Env:HA2 chimaeric DNA vaccines

Abbreviation	Env insert	Mosaic Gag co-expression
DNAC5	CAP256 gp150-FL-IP	x
DNAGC5	CAP256 gp150-FL-IP	Yes
DNAC2	CAP256 gp120HA$_2$-FL	x
DNAGC2	CAP256 gp120HA$_2$-FL	Yes
DNAC4	CAP256 gp140HA$_2$tr-FL-IP	x
DNAGC4	CAP256 gp140HA$_2$tr-FL-IP	Yes
DNA Gag^M	x	Yes

4.2.3 CAP256 Env transfer vector for generating recombinant MVA

A transfer vector was created where in between overlapping flanks of the MVA G1L–I8R locus a selection cassette containing the eGFP gene under the control of the vaccinia virus (VACV) p7.5 promoter and K1L gene under the VACV pSS promoter were inserted to form the plasmid

Shuttle and Selection for Pox Expression (pSSPEx) (***Figure 4.2A***). Similar as to CAP256 gp150-FL-IP (***Chapter 3***), CAP256 gp120HA_2-FL and CAP256 gp140HA_2tr-FL-IP, including the tPA leader, were subcloned using HindIII and EcoRI sites from the pMExT DNA vectors downstream of the VACV mH5 promoter to generate pSSPEx CAP256 gp120HA_2-FL and pSSPEx CAP256 gp140HA_2tr-FL-IP (***Figure 4.2B+C***).

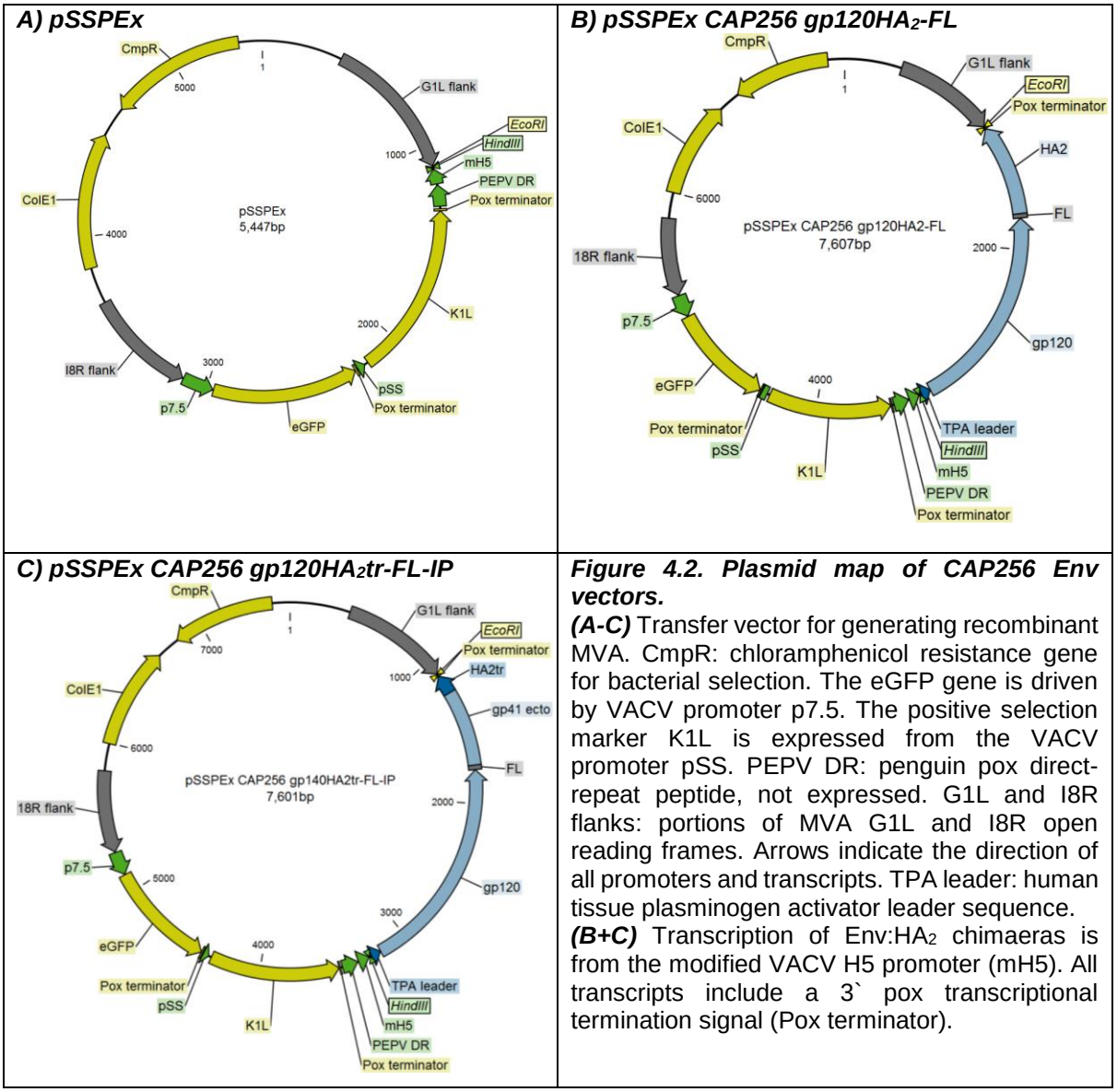

Figure 4.2. Plasmid map of CAP256 Env vectors.
(A-C) Transfer vector for generating recombinant MVA. CmpR: chloramphenicol resistance gene for bacterial selection. The eGFP gene is driven by VACV promoter p7.5. The positive selection marker K1L is expressed from the VACV promoter pSS. PEPV DR: penguin pox direct-repeat peptide, not expressed. G1L and I8R flanks: portions of MVA G1L and I8R open reading frames. Arrows indicate the direction of all promoters and transcripts. TPA leader: human tissue plasminogen activator leader sequence.
(B+C) Transcription of Env:HA_2 chimaeras is from the modified VACV H5 promoter (mH5). All transcripts include a 3` pox transcriptional termination signal (Pox terminator).

4.2.4 Generation of rMVA Gag^M CAP256 Env:HA_2 chimaeras

For Env:HA_2 chimaeras, recombinant MVA (rMVA) vaccines were only constructed in the rMVA Gag^M background [413, 414]. The rMVA vaccines rMVA Gag^M CAP256 gp120HA_2-FL and rMVA Gag^M CAP256 gp140HA_2tr-FL-IP were generated and grown to high titre stocks as described in ***Section 3.2.5***. Both Env:HA_2 chimaeric vaccines were verified and characterised

as described in ***Section 3.2.8***. These rMVA vaccines will be abbreviated in this chapter as outlined in ***Table 4.2***.

Table 4.2 Abbreviations for Env and Env:HA2 chimaeric DNA vaccines

Abbreviation	Env insert	Mosaic Gag present
MVAC5	CAP256 gp150-FL-IP	x
MVAGC5	CAP256 gp150-FL-IP	Yes
MVAGC2	CAP256 gp120HA_2-FL	Yes
MVAGC4	CAP256 gp140HA_2tr-FL-IP	Yes
MVA Gag^M	x	Yes
wtMVA	x	x

4.2.5 Verification and characterisation of DNA and rMVA vaccines

In addition to the assays outlined in ***Section 3.2.7 and 3.2.8*** for the verification and characterisation of the Env and Env:HA_2 chimaeric DNA and rMVA vaccines, a FACS assay was adapted from Samal *et al*. 2019, to quantify the presence of Env bnAb epitopes after expression of the Env and DNA Env:HA_2 chimaeric vaccines in HEK293T cells [466]. For this, T75 flasks, ~80% confluent with HEK293T cells, were transfected with 30µg of Env or Env:HA_2 chimaeric DNA vaccines using 90µl polyethyleneimine-branched (PEI). Three days post infection, completely confluent cell layers were harvested in PBS using a cell-scraper. All subsequent steps were performed at room temperature. First, harvested cells were washed three times with Buffer-1 (DMEM+5% FCS) by spinning cells down for four minutes at 475*g*. After reconstitution of the cells in the pellet after the final spin using Buffer-1, cells were divided between 12 wells in a 96-well round bottom plate and incubated with bnAbs at a final concentration of 10µg/ml) for 60 minutes. Cells were washed with Buffer-1 three times by spinning the 96-well plate for four minutes at 475*g* each time and were subsequently incubated with a 1:500 dilution of anti-Human IgG-Cy3 (Fc specific) antibody in Buffer-1 for one hour. Cells were then washed three times (as above) but with Buffer-2 (5% FCS in PBS) before fixing in Buffer-2 + 0.5% formaldehyde and subsequent analysis on a FACS Canto II Analyzer (BD Biosciences, Sunnyvale) which was programmed to measure FSC (forward scatter), SSC (side scatter), and Cy3 intensity. For each well, 100 000 cells were acquired in BD FACS Flow buffer as the sheath fluid. Data were analysed in the FlowJo software where cell gating cell was used to avoid cellular debris and calculate the mean fluorescent intensity (MFI) of Cy3. For each bnAb, untransfected cells were used as a control to determine the Cy3 negative and positive cell populations after forward and side scatter correction. To compare the gp150 and chimeric envelope constructs, an Env score for each bnAb was calculated based on the mean Cy3 fluorescent intensity (MFI) post FSC and SSC correction:

$$Env\ score = \frac{(MFI\ bnAb\ \times Cy3\ positive\ cells)}{(Cy3\ positive + negative\ cells)}$$

The same anti-Env human bnAbs (PG9, PG16, PGT128, PGT135, PGT145, CAP256 VRC26.08, VRC01, 10E8 F105 and 447-52D) as tested in the live-cell staining were used for these experiments. The following controls were included in the FACS assay: 1) untransfected cells + bnAbs + anti-Human IgG-Cy3 (used for correction as described above), 2) transfected and untransfected cells, incubated with only anti-Human IgG-Cy3, and 3) transfected and untransfected cells alone. This FACS assay was only performed for DNA vaccines (without Gag^M co-expression) as rMVA vaccines all expressed eGFP and the FACS Canto II Analyzer could not distinguish eGFP from Cy3 signals.

Virus-like particles from the different Env and Env:HA_2 chimaeric DNA or MVA vaccines were isolated from HEK293T cells using OptiPrep gradient centrifugation as outlined in Sections ***3.2.7*** and ***3.2.8***. VLPs from the different HIV-1 vaccines were run on SDS-PAGE and blotted onto PVDF membranes. Detection of Env was performed using goat α-HIV 1 gp120 antibody (5000-0557, Bio-Rad, Hercules) allowing for direct comparison of Env and Env:HA_2 chimaeras incorporation into Gag-VLPs. Mosaic Gag was detected using goat α-HIV 1 p24 (Gag) (4999-9007, Bio-Rad, Hercules). After detection with a mouse monoclonal α-goat/sheep IgG-alkaline phosphatase (AP) GT34 (Sigma, St Louis), blots were imaged on a Gel Doc XR+ (Bio-Rad, Hercules) and densitometry was performed with Image Lab 5.2.1 (Bio-Rad, Hercules), which was used to calculate Env:Gag ratios. The data was normalised to the average Env:Gag ratio for CAP256 gp150-FL-IP + Gag^M (=1). The data was a combination of 3 independent experiments from MVA HIV-1 vaccines and 1 experiment from DNA HIV-1 vaccines (*n*=4).

4.2.6 Rabbit immunisation comparing heterologous vaccine platforms

Female New Zealand white rabbits were housed in the Research Animal Facility in the Faculty of Health Sciences at the University of Cape Town. All the animal procedures were approved by the UCT Animal Research Ethics Committee (UCT AEC 14-030 & UCT AEC 015/051) and performed by trained animal technologists Rodney Lucas and Inge Botes. The rabbits were monitored daily for any signs of pain, discomfort or stress and were weighed weekly.

Three groups of 5 rabbits were selected to compare rMVA vaccines Env + Gag^M or Env:HA_2 chimaeras + Gag^M with matching DNA vaccine priming followed by soluble, trimeric Env boosting (see ***Table 4.3*** for groups). All groups received 100µg pTJDNA4 (Gag^M) combined with either 100µg pMExT CAP256 gp150-FL-IP (group 1), pMExT CAP256 gp120HA_2-FL (group 2) or pMExT CAP256 gp140HA_2tr-FL-IP (group 3). Concentration of all DNA vaccines was 1mg/ml in PBS. Primes were administered intramuscularly in the hind leg at week 0 and 4. At week 8 and 12, all groups received vaccine matched rMVA boosts. Groups 1 received

10^8 pfu in 500µl PBS + 10% glycerol rMVA Gag^M CAP256 gp150-FL-IP, group 2 received 10^8 pfu in 500µl PBS + 10% glycerol rMVA Gag^M CAP256 gp120HA_2-FL and group 3 received 10^8 pfu in 500µl PBS + 10% glycerol rMVA Gag^M CAP256 gp140HA_2tr-FL-IP. These rMVA boosts were administered intramuscularly in the hind leg. Finally, all rabbits received 40µg of CAP256 soluble, trimeric Env protein in 500µl 1:1 (*v/v*) AlhydroGel® at week 20 and 28 to boost the immune response. This experiment is abbreviated as DDMMPP. Animals were not sacrificed at week 39 as they were entered into a longitudinal study (not discussed in this dissertation). In group 3, one rabbit died after the first DNA inoculation due to unrelated causes. The data from group 1 is the same as used for ***Chapter 3***.

Table 4.3. Groups of rabbits comparing Env to Env:HA2 chimaeras

animal	group	Vaccine			Prime		rMVA boost		Protein boost	
		DNA	rMVA	gp140-FL-IP	wk 0	wk 4	wk 8	wk 12	wk 20	wk 28
RB6826	1	gp150 + Gag^M	gp150 + Gag^M	AlhydroGel (1:1)	✓	✓	✓	✓	✓	✓
RB6827	1	gp150 + Gag^M	gp150 + Gag^M	AlhydroGel (1:1)	✓	✓	✓	✓	✓	✓
RB6828	1	gp150 + Gag^M	gp150 + Gag^M	AlhydroGel (1:1)	✓	✓	✓	✓	✓	✓
RB6830	1	gp150 + Gag^M	gp150 + Gag^M	AlhydroGel (1:1)	✓	✓	✓	✓	✓	✓
RB6850	1	gp150 + Gag^M	gp150 + Gag^M	AlhydroGel (1:1)	✓	✓	✓	✓	✓	✓
RB6832	2	gp120HA_2 + Gag^M	gp120HA_2 + Gag^M	AlhydroGel (1:1)	✓	✓	✓	✓	✓	✓
RB6833	2	gp120HA_2 + Gag^M	gp120HA_2 + Gag^M	AlhydroGel (1:1)	✓	✓	✓	✓	✓	✓
RB6834	2	gp120HA_2 + Gag^M	gp120HA_2 + Gag^M	AlhydroGel (1:1)	✓	✓	✓	✓	✓	✓
RB6835	2	gp120HA_2 + Gag^M	gp120HA_2 + Gag^M	AlhydroGel (1:1)	✓	✓	✓	✓	✓	✓
RB6836	2	gp120HA_2 + Gag^M	gp120HA_2 + Gag^M	AlhydroGel (1:1)	✓	✓	✓	✓	✓	✓
RB6838	3	gp140HA_2tr + Gag^M	gp140HA_2tr + Gag^M	AlhydroGel (1:1)	✓	✓	✓	✓	✓	✓
RB6839	3	gp140HA_2tr + Gag^M	gp140HA_2tr + Gag^M	AlhydroGel (1:1)	✓	✓	✓	✓	✓	✓
RB6840	3	gp140HA_2tr + Gag^M	gp140HA_2tr + Gag^M	AlhydroGel (1:1)	✓	✓	✓	✓	✓	✓
RB6842	3	gp140HA_2tr + Gag^M	gp140HA_2tr + Gag^M	AlhydroGel (1:1)	✓	✓	✓	✓	✓	✓
RB6849†	3	gp140HA_2tr + Gag^M	gp140HA_2tr + Gag^M	AlhydroGel (1:1)	✓	✓	✓	✓	✓	✓
† Died of unrelated causes										

4.2.7 Rabbit sera characterisation

To assess Env or CAP256_SU V1V2-loop binding antibodies titres in rabbit sera, ELISA were performed as described in ***Section 3.2.10***. However, ELISA data was fitted to a non-linear regression curve (log(agonist) vs. response – variable slope) in GraphPad Prism 5.0 . Antibody end-point titres (X) were calculated from the model used in the software for fitting:

$$Treshold\ (Y) = Curve\ min\left(\frac{Curve\ \max - Curve\ min}{1 + 10^{((LogEC50 - X) \times Hill\ Slope}}\right)$$

Where the threshold (Y) for each time point was set as:

$$Treshold\ (Y) = week\ 0\ Curve\ \min + (2 \times standard\ error\ week\ 0\ Curve\ \min)$$

Data were plotted as the mean +/- SEM for the whole group

Rabbit sera from different time points were tested for the ability to inhibit Env-pseudotype virions to enter a reporter cell line as described in ***Section 3.2.10***. The following Env-pseudotyped viruses (MW965.26, 6644, 1107356, CAP256_SU, CAP256_SU K169E or BG0505N332+/CAP256_SU V1V2-loop and CAP84/CAP256_SU V1V2-loop) were assayed.

All neutralisation assays were performed by Professor Lynn Morris's group at the Centre for HIV and STIs, National Institute for Communicable Diseases of the National Health Laboratory Service, Johannesburg, South Africa.

4.2.8 Statistical analysis

All statistical analysis was performed in GraphPad Prism 5.0 (GraphPad Software, San Diego) and tests are indicated in results and/or corresponding figure legend.

4.3 Results

4.3.1 CAP256 Env immunogens

It is well established that the Env spike density on the HIV-1 virion is relatively low when compared to other viruses [464]. It has previously been shown that substituting the transmembrane domain and cytoplasmic tail of gp41 with the corresponding elements of the hemagglutinin stalk from influenza A improves the spike density of this chimaeric construct on both the plasma membrane and virus-like particles (VLPs) [399]. Therefore, two chimaeric constructs were designed based on the modified CAP256 gp150-FL-IP characterised in ***Chapter 3***, in which either the whole of HIV-1 Env gp41 was replaced with that of the influenza viral hemagglutinin stalk (HA_2) or the ectodomain of gp41 was retained while introducing the HA_2 transmembrane and cytoplasmic tail section, thus generating gp120HA_2 and gp140HA_2tr respectively (***Figure 4.3A***). DNA and rMVA vaccines were made for both chimaeric constructs. The Env protein vaccine used in this chapter is same as described in ***Chapter 3***: that is, CAP256 soluble trimeric Env (***Figure 4.3A***).

4.3.2 Transient expression of CAP256 Env:HA_2 chimaeras from DNA vaccines

As described in ***Chapter 3***, HIV-1 subtype C mosaic Gag (pTJDNA4) was co-expressed with the aim of inducing the formation of VLPs. To test the Env and Env:HA_2 chimaeric vaccines for *in vitro* expression and cellular secretion of transgenes, HEK293T cells were transiently transfected with pTJDNA4 + pMExT CAP256 gp150-FL-IP (DNAGC5, see ***Table 4.1***), pMExT CAP256 gp120HA_2-FL (DNAGC2) or pMExT CAP256 gp140HA_2tr-FL-IP (DNAGC4). Env and Gag could be detected by western blotting in the cell media 72 hours after transfection (***Figure 4.3B***), indicating that both Env and Gag were secreted. A non-specific band just below that of Gag was observed in all samples, including the empty vector control (indicated with *).

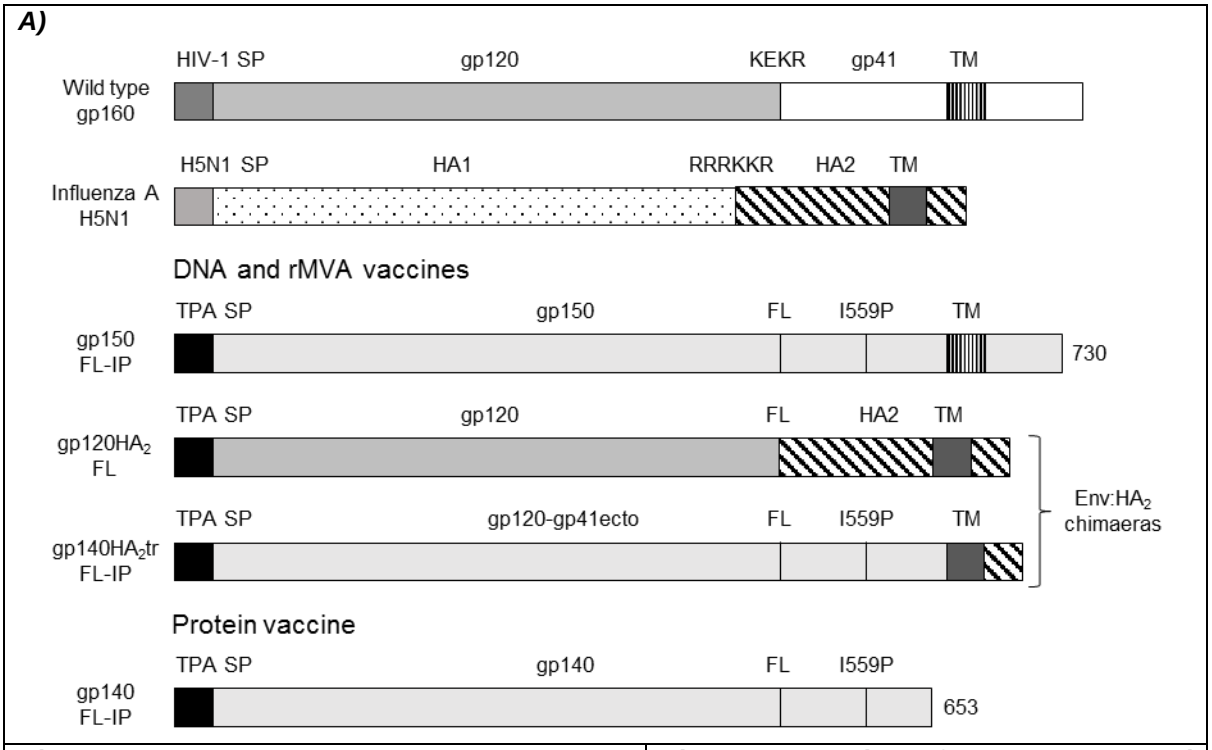

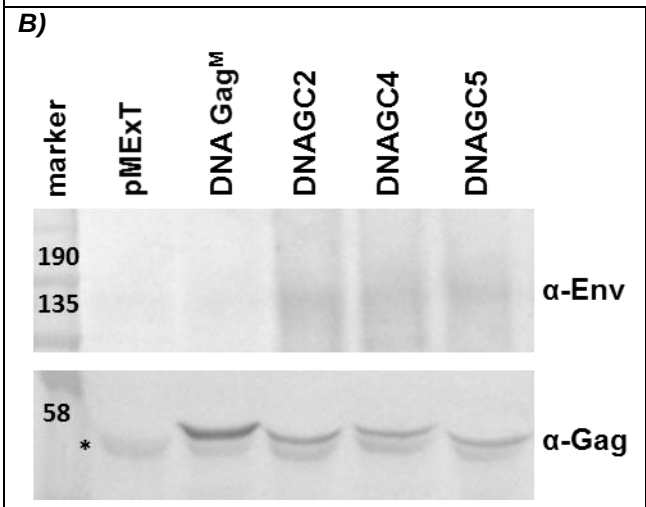

Figure 4.3 Design of CAP256 Env and Env:HA$_2$ chimaeric vaccine inserts and characterisation of* in vitro *expression from DNA vaccines.

(A) Schematic representations comparing wild type Env and Env:HA$_2$ chimaeras used in DNA and rMVA vaccines. The Env sequence was truncated to amino acid 730 to improve transgene stability, while containing further modifcations where the wild type signal peptide (HIV-1 SP) was replaced with the human tissue plasminogen activator (TPA), the furin cleavage site with a flexible linker (FL) sequence and an I559P mutation was introduced (gp150-FL-IP). The whole of Env gp41 was replaced with that of influenza HA$_2$, losing the I559P mutation, thus generating gp120HA$_2$-FL-IP. Or only the transmembrane domain (TM) and cytoplasmic tail of HIV-1 gp41 was substituted for the corresponding elements from influenza HA$_2$, retaining the I559P mutation, thus generating gp140HA$_2$tr-FL-IP.

(B) Co-expression of mosaic Gag (DNA Gag^M, pTJDNA4), and pMExT CAP256 gp150-FL-IP (DNAGC5), gp120HA$_2$-FL-IP (DNAGC2) or gp140HA$_2$tr-FL-IP (DNAGC4) DNA vaccines led to secretion of both Env (top) and Gag (bottom) into the media of HEK293T cells as detected by western blotting. An a-specific band just below that of Gag was detected in all samples, including in the empty vector control (pMExT) (indicated with *), whereas the specific band was present in all other samples, including pTJDNA4 alone.

The Env and Env:HA$_2$ chimaeric DNA vaccines by themselves were further characterised for the presence of a select list of Env bnAbs epitopes upon expression (***Table 1.1***) using a live cell staining protocol in HeLa cells. Using this method, only Env present on the plasma membrane would be detected and therefore be a suitable indication of the antigenic properties

of the natively expressed (non-denatured) Env trimer. Cells expressing Env were positively identified with a rabbit α-Env polyclonal antibody after staining with the different bnAbs. Binding was observed for all epitopes tested for CAP256 gp150-FL-IP (DNAC5) and CAP256 gp140HA_2tr-FL-IP (DNAC4), but not gp120HA_2-FL (DNAC2) (***Table 4.4***, ***Figure 4.4 and Appendix D***).

Table 4.4. Live cell staining using bnAbs in HeLa cells transfected with HIV-1 DNA vaccines

			Native-like	Live cell mapping DNA		
Antibody	Neutralisation	Epitope	trimer	DNAC5	DNAC2	DNAC4
PGT128	Broad	V3-glycan supersite	x	✓	✓	✓
PGT135	Broad	V3-glycan supersite	x	✓	✓	✓
447-52D	Narrow	V3	x	✓	✓	✓
VRC01	Broad	CD4 binding-site	x	✓	✓	✓
F105	Narrow	CD4 binding-site	x	✓	✓	✓
PG9	Broad	V2-glycan	x	✓	✓	✓
PG16	Broad	V2-glycan	Yes	✓	✗	✓
PGT145	Broad	V2-glycan	Yes	✓	✗	✓
CAP256 VRC26_08	Broad	V2-glycan	Yes	✓	✗	✓
10e8	Broad	MPER	x	✓	✗	✓

As expected, no binding of bnAb 10E8 was observed for DNAC2, as the MPER domain of HIV-1 Env was replaced with that of influenza HA_2, whereas the MPER epitope was detected for DNAC5 and DNAC4. All other, non native-like trimer epitopes were present for all three DNA constructs: the V3-glycan supersite (bnAbs PGT128 and PGT135), the CD4-binding site (VRC01) and the V2-glycan (PG9). Although some signal was also detected with the bnAbs F105 and 447-52D, suggesting that some of the Env expressed from the DNA vaccine was misfolded. Interestingly, as with bnAb10E8, bnAbs recognising native-like Env trimers (PG16, PGT145 and CAP256 VRC26.08) also failed to bind to DNAC2 but had very clear signal for DNAC5 and DNAC4 ***(Table 4.4 and Figure 4.4)***. This result implies that only gp150-FL-IP and the Env:HA_2 chimaera where only a short portion of Env is replaced with that of influenza HA_2 (gp140HA_2tr-FL-IP) can induce native-like Env trimers, whereas when gp41 is completely replaced with HA_2 (gp120HA_2-FL) mainly misfolded Env trimers are formed. Only immunofluorescence for bnAbs was observed in cells that were positive for the rabbit α-Env polyclonal antibody (as assessed by FITC signal), indicating the specificity of the bnAb live-cell staining. However, especially for PGT145, PG16 and CAP256 VRC26.08, bnAb signals were not detected in all cells positive for Env expression.

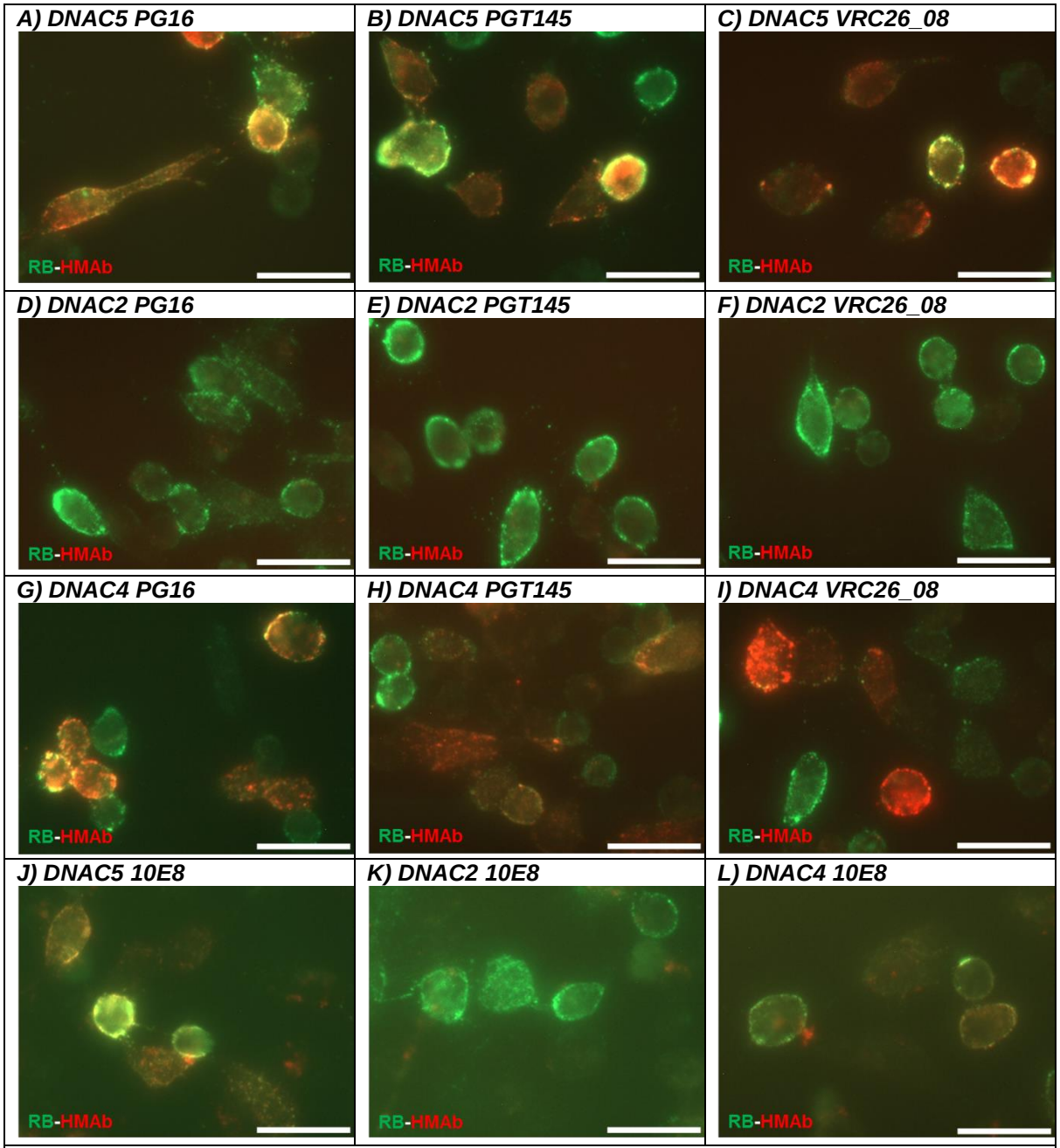

Figure 4.4. Live cell staining using bnAbs recognising native-like Env trimers or MPER domain in HeLa cells transfected with HIV-1 DNA vaccines.
(A-L) HeLa cells transfected with pMExT CAP256 gp150-FL-IP (DNAC5) and gp140HA$_2$tr-FL-IP (DNAC4) and gp120HA$_2$-FL (DNAC2) were visualised by their Env expression using a rabbit α-Env polyclonal and α-rabbit IgG-FITC (**RB**). The bnAbs PG16, PGT145, CAP256 VRC26.08 and 10E8 were detected with anti-human IgG-Cy3 (**HMAb**). The bnAb epitopes for native-like trimers (PG16, PGT145, and CAP256 VRC26.08) or the MPER (10E8) are present for DNAC5 and DNAC4 but not DNAC2. Overlapping signal between the rabbit α-Env polyclonal and bnAbs appears as yellow. Bar represents 20µm.

With the bnAb live-cell staining being a qualitative assay, a fluorescence-activated cell sorting (FACS) experiment in HEK293T cells was performed for a quantitative measure of the bnAb epitopes present in Env or Env:HA2 chimaeras (***Figure 4.5***). The results presented for the FACS assay are expressed as the Env score which better represents the data, as it takes into

account the number of cells with a positive and negative signal for bnAb binding (see ***Section 4.2.5***). Similar to the live-cell staining, for DNAC2 almost no signal is detectable for the MPER bnAb 10E8 or the bnAbs selective for native-like Env trimers (PG16, PGT145 and CAP256 VRC26.08). For DNAC5 and DNAC4, the Env score for all three native-like V2 trimer apex bnAbs (PG16, PGT145 and CAP256 VRC26.08) is lower compared to none native-like trimer epitopes of the V3-glycan supersite (bnAbs PGT128 and PGT135), the CD4-binding site (VRC01) and the V2-glycan (PG9). However, almost 20% of Env is in a native-like state for DNAC5 and DNAC4 when the Env score for PG16, PGT145 or CAP256 VRC26.08 is normalised to VRC01. There are no obvious differences between DNAC5 and DNAC4, however there is a trend towards higher Env scores for DNAC5 for all bnAb epitopes apart from F105 and 447-52D, which are indicative of misfolded Env trimers. Interestingly, for the latter two bnAbs, the highest Env scores are observed for DNAC2. Combined with the extremely low Env scores for PG16, PGT145 and CAP256 VRC26.08 this suggests that expression of DNAC2 leads to a high percentage of misfolded Env trimers. Furthermore, this data would also suggest the Env:HA_2 chimaeras fail to improve the spike density on the plasma membrane as this would have been reflected in higher Env scores. In general, Env scores are highest for DNAC5: the highest Env score for all bnAbs (10E8) is for DNAC5 and the sum of all Env scores is highest for DNAC5.

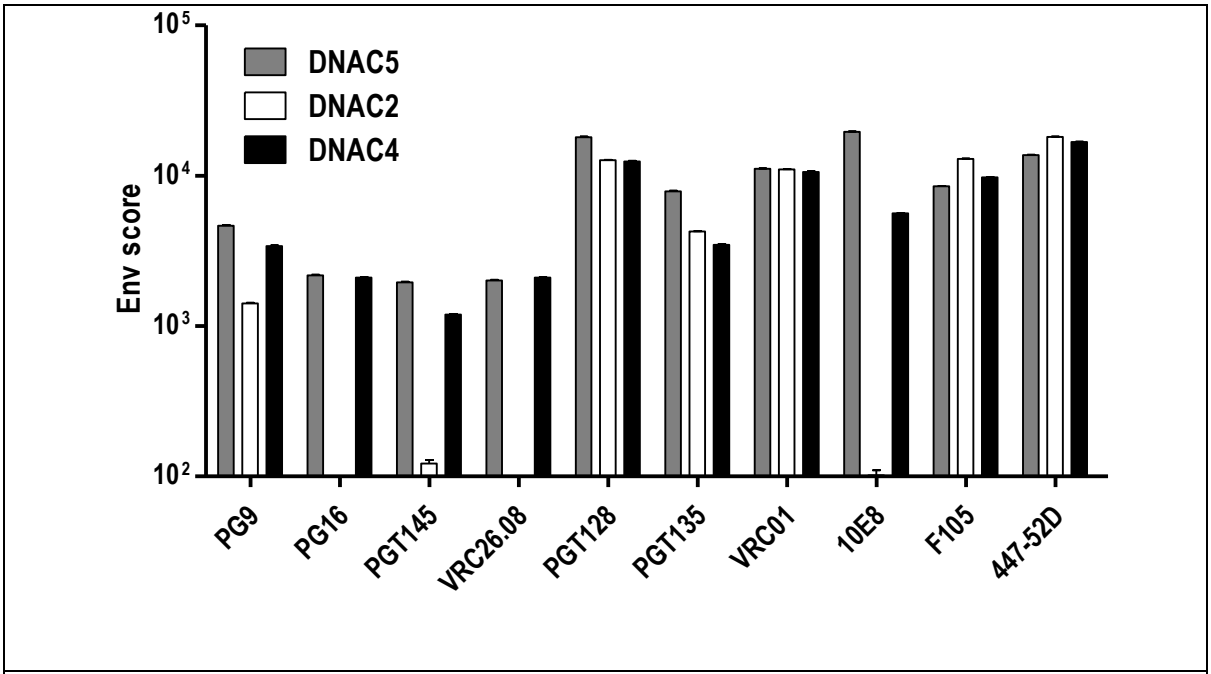

Figure 4.5 FACS based assay to quantify the presence of Env bnAb epitopes from Env and Env:HA2 chimaeric DNA vaccines.
Env expression on the cell membrane of HEK293T cells transfected with CAP256 gp150-FL-IP (DNAC5) and CAP256 gp140HA_2tr-FL-IP (DNAC4) and gp120HA_2-FL (DNAC2) was quantified by bnAbs for V3-glycan supersite (bnAbs PGT128 and PGT135), the CD4-binding site (VRC01), the V2-glycan (PG9) and trimers (PG16, PGT145 and (CAP256) VRC26.08) or non-NAbs F105 and 447-52D in a FACS assay. Env scores +/- SEMs (based on cells positive for Cy3, *n*=1 experiment)

4.3.3 Construction and characterisation of rMVA vaccines expressing Env

4.3.3.1 Verification of the integrity of rMVA vaccines

Recombinant MVA expressing Gag^M and the two different Env:HA_2 chimaeras were generated similarly as was described for rMVA Gag^M + CAP256 gp150-FL-IP in ***Section 3.3.2*** (***Figure 4.6*** for targeting strategy), resulting in MVAGC2 (expressing Gag^M + CAP256 gp120HA_2-FL) and MVAGC4 (expressing Gag^M + CAP256 gp140HA_2tr-FL-IP) (***Table 4.2***). Single clones for both MVA vaccines were selected from RK13 cells and expanded to high titres stocks (MVAGC2 = $2.0*10^9$; MVAGC4 = $1.9*10^9$) in RK13 cells. To test for correct integration and stability of Env in the I8R-G1L locus, PCRs were carried out on DNA isolated from RK13 cells infected with the high titre stocks rMVA using a primer upstream of the VACV mH5 promoter and a reverse primer within the G1L locus but outside the G1L recombination flank in pSSPEx. These PCR products were subsequently sequenced to check for possible mutations. The sequence was exactly as predicted for both recombinant MVA vaccines indicating correct integration of Env:HA_2 chimaeras into the MVAGC2 or MVAGC4 vaccines (data not shown). In a similar fashion, the 5' and 3' arms of Gag^M were verified as well (data not shown).

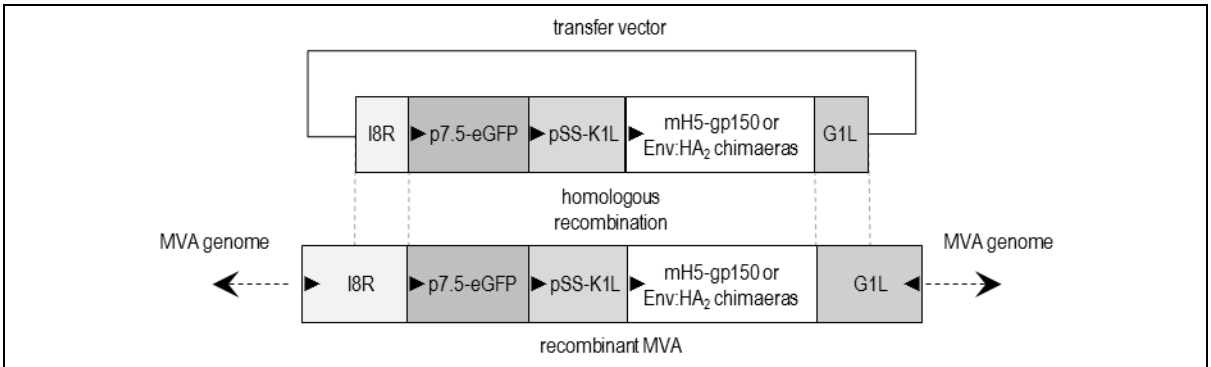

Figure 4.6. Targeting strategy for the generation of recombinant MVA expressing Env and Env:HA_2 chimaeras.
Schematic representation of targeting CAP256 gp150-FL-IP, gp120HA_2-FL or CAP256 gp140HA_2tr-FL-IP into the I8R-G1L locus of the MVA Gag^M pox genome. Triangles indicate direction of open-reading frames. Expression of Env or Env:HA_2 chimaeras is driven by the VACV mH5 promoter

.3.3.2 Expression of Env by rMVA vaccines

To assess for *in vitro* expression of the recombinant antigens, HEK293T cells were infected with Env and Env:HA_2 chimaeric MVA vaccines; namely MVAGC5, MVAGC2 and MVAGC4. Similar to the DNA vaccines, Env and Gag could be detected by western blotting in the cell media 48 hours after infection (***Figure 4.7A***), indicating that both Env and Gag were secreted. Again, a non-specific band just below that of Gag was observed in all samples, including the empty vector control (indicated with *). Furthermore, immunofluorescent staining and confocal imaging of infected cells showed expression and co-localisation of Gag and Env for all three recombinant MVA vaccines (***Figure 4.7B***).

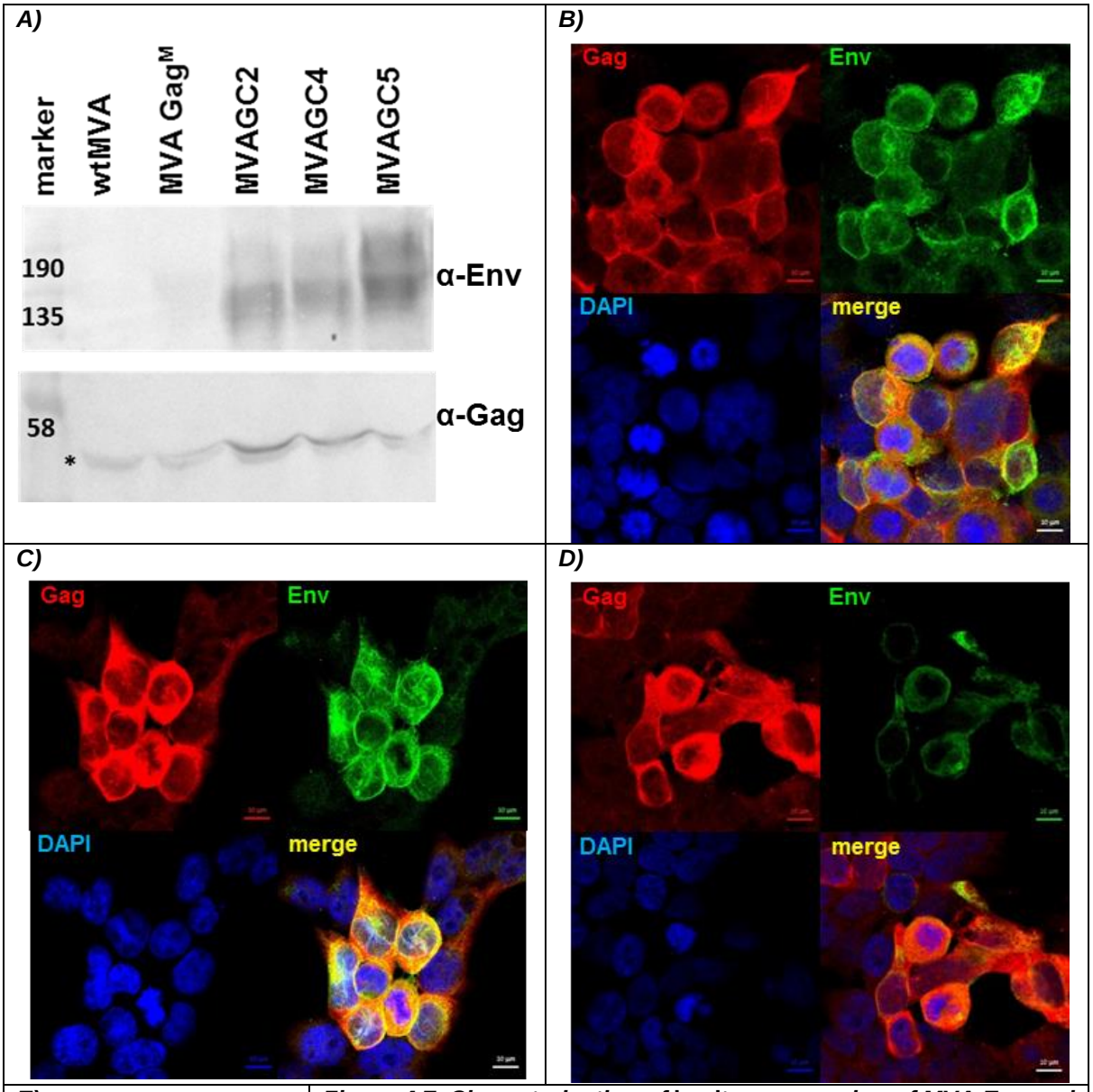

Figure 4.7. Characterisation of* in vitro *expression of MVA Env and Env:HA$_2$ chimaeric vaccines.
(A) Both Env and Gag could be detected in media from HEK293T cells infected with MVA Gag^M + CAP256 gp150-FL-IP (MVAGC5), + gp120HA$_2$-FL-IP (MVAGC2) or + gp140HA$_2$tr-FL-IP (MVAGC4) whereas only Gag was detected for MVA Gag^M (Gag^M). An a-specific band just below that of Gag was detected in all samples, including wild type MVA (wtMVA) (indicated with *).
(B-E) Confocal imaging (maximum intensity projections) showing co-localisation of Gag and Env within HEK293T cells after infection with with MVAGC5 ***(B)***, MVAGC2 ***(C)*** and MVAGC4 ***(D)***. ***(E)*** No Env or Gag immunofluorescent signal in uninfected control cells.
Pseudo-colouring for Cy3 is in red (Gag) and Alexa 647 in green (Env).
Scale bar=10μm.

Env and Env:HA$_2$ chimaeric MVA vaccines, (MVAGC5, MVAGC2 and MVAGC4) were characterised for the presence of bnAb epitopes upon infection of HeLa cells in similar experiments as for the DNA vaccines, resulting in a very comparable outcome. The same

bnAb epitopes, recognising native-like Env trimers (PG16, PGT145 and CAP256 VRC26.08) or the MPER domain (10E8) were undetectable for MVAGC2 (***Table 4.5***, ***Figure 4.8*** and ***supplement E***). All other, non native-like trimer epitopes were present for all three MVA vaccines, the V3-glycan supersite (bnAbs PGT128 and PGT135), the CD4-binding site (VRC01), and the V2-glycan (PG9). Although some signal was detected as well with the bnAbs F105 and 447-52D, suggesting that some of the Env expressed from the Env and Env:HA_2 chimaeric vaccines was misfolded. However, for MVAGC5 and (although fainter) MVAGC4, bnAbs recognising native-like Env trimers (PG16, PGT145 and CAP256 VRC26.08) were detected, suggesting that only these two HIV-1 MVA vaccines can induce native-like Env trimers. Infected HeLa cells were identified by the presence of an eGFP signal, expressed from the recombinant MVA.

Table 4.5. Live cell staining using bnAbs in HeLa cells infected with HIV-1 MVA vaccines

			Native-like	Live cell mapping rMVA		
Antibody	Neutralisation	Epitope	trimer	MVAGC5	MVAGC2	MVAGC4
PGT128	Broad	V3-glycan supersite	x	✓	✓	✓
PGT135	Broad	V3-glycan supersite	x	✓	✓	✓
447-52D	Narrow	V3	x	✓	✓	✓
VRC01	Broad	CD4 binding-site	x	✓	✓	✓
F105	Narrow	CD4 binding-site	x	✓	✓	✓
PG9	Broad	V2-glycan	x	✓	✓	✓
PG16	Broad	V2-glycan	Yes	✓	✗	✓
PGT145	Broad	V2-glycan	Yes	✓	✗	✓
CAP256 VRC26_08	Broad	V2-glycan	Yes	✓	✗	✓
10E8	Broad	MPER	x	✓	✗	✓

4.3.4 Virus-like particle formation from Env:HA_2 chimaeric DNA and rMVA vaccines

As shown for DNAGC5 and MVAGC5 (***Chapter 3 and Figure 4.9+10***), expression of the Env:HA_2 chimaeras from DNAGC2, DNAGC4 (***both Figure 4.9***), MVAGC2 or MVAGC4 (***both Figure 4.10***) resulted in the formation of VLPs as observed by electron microscopy (EM). A small number of VLPs were measured using the EM imaging software and with data combined from both DNA and MVA, no significant differences in VLP diameter was observed between the different Env and Env:HA2 chimaeric constructs or to Gag alone (One-way ANOVA) ***(Figure 4.11D***).

When VLPs resulting from expression of Env and Env:HA_2 from chimaeric DNA or MVA vaccines were isolated from the media of HEK293T cells by a two-step OptiPrep gradient centrifugation protocol, both Gag and Env were present as confirmed with western blotting of

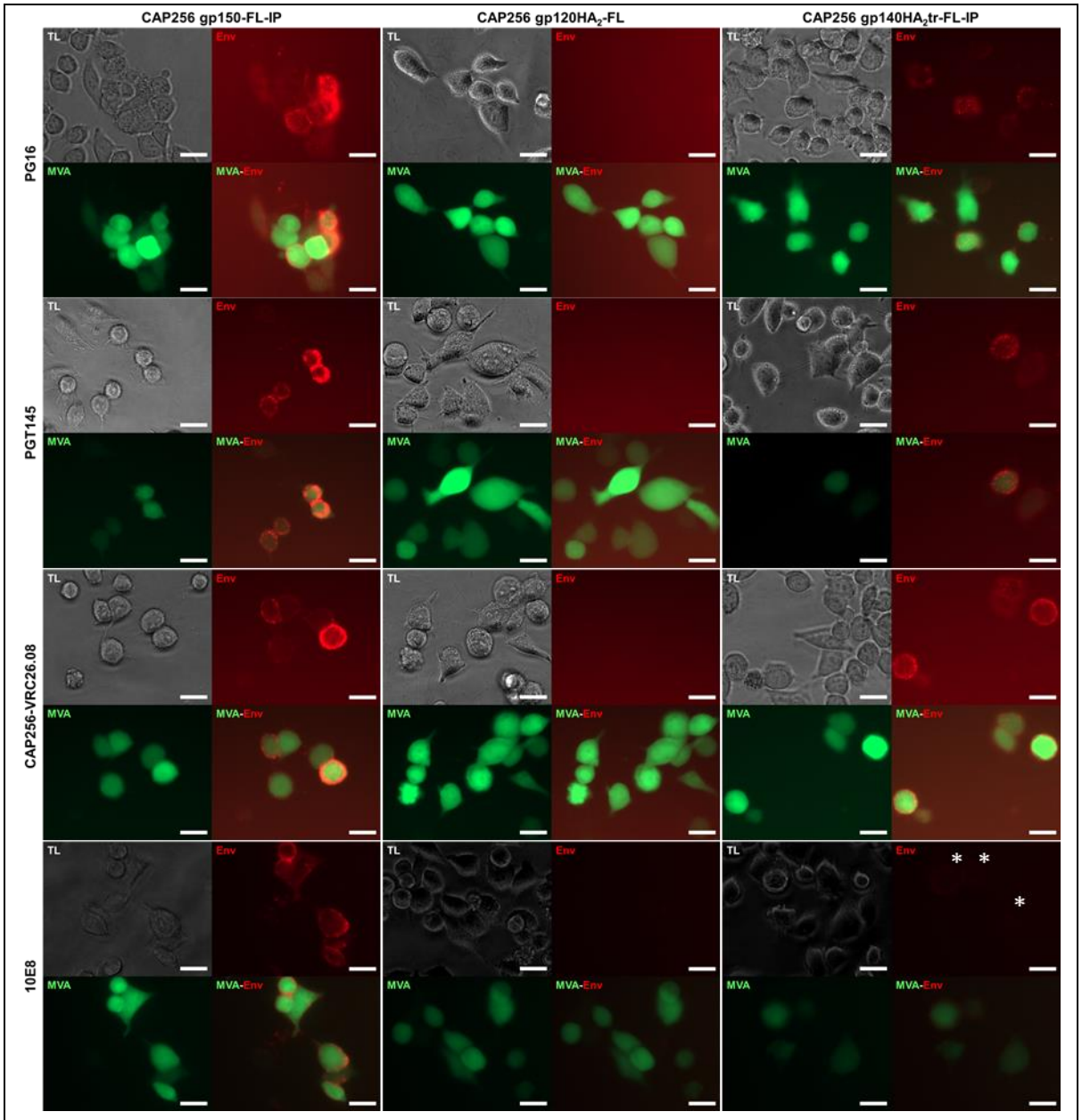

Figure 4.8. Live cell staining using bnAbs recognising native-like Env trimers or MPER domain in HeLa cells infected with HIV-1 MVA vaccines.
HeLa cells infected with MVA Gag^{M} plus CAP256 gp150-FL-IP (left column), gp120HA$_2$-FL (middle column), or gp140HA$_2$tr-FL-IP (right column) were identified by eGFP expression from MVA (**MVA**). The bnAbs PG16 (1st row), PGT145 (2nd row), CAP256 VRC26.08 (3rd row) and 10E8 (4th row) were detected with anti-human IgG-Cy3 (**Env**). The bnAb epitopes for native-like trimers (PG16, PGT145, and CAP256 VRC26.08) or the MPER (10E8) are present for MVAGC5 and MVAGC4 but not MVAGC2. Because of the low signal, cells infected with MVA Gag^{M} + gp140HA$_2$tr-FL-IP positive for 10E8 are indicated with *. Bar represents 20µm.

samples from the only visible band (~45mm from the bottom) isolated from the second OptiPrep gradient, suggesting Env inclusion into Gag VLPs (***Figure 4.11A+B***). Encouragingly, no Env band was observed in the equivalent band isolated from DNA or rMVA vaccines expressing only Env (***Chapter 3***, ***Figure 3.10***). For Env and Env:HA$_2$ chimaeric MVA vaccines

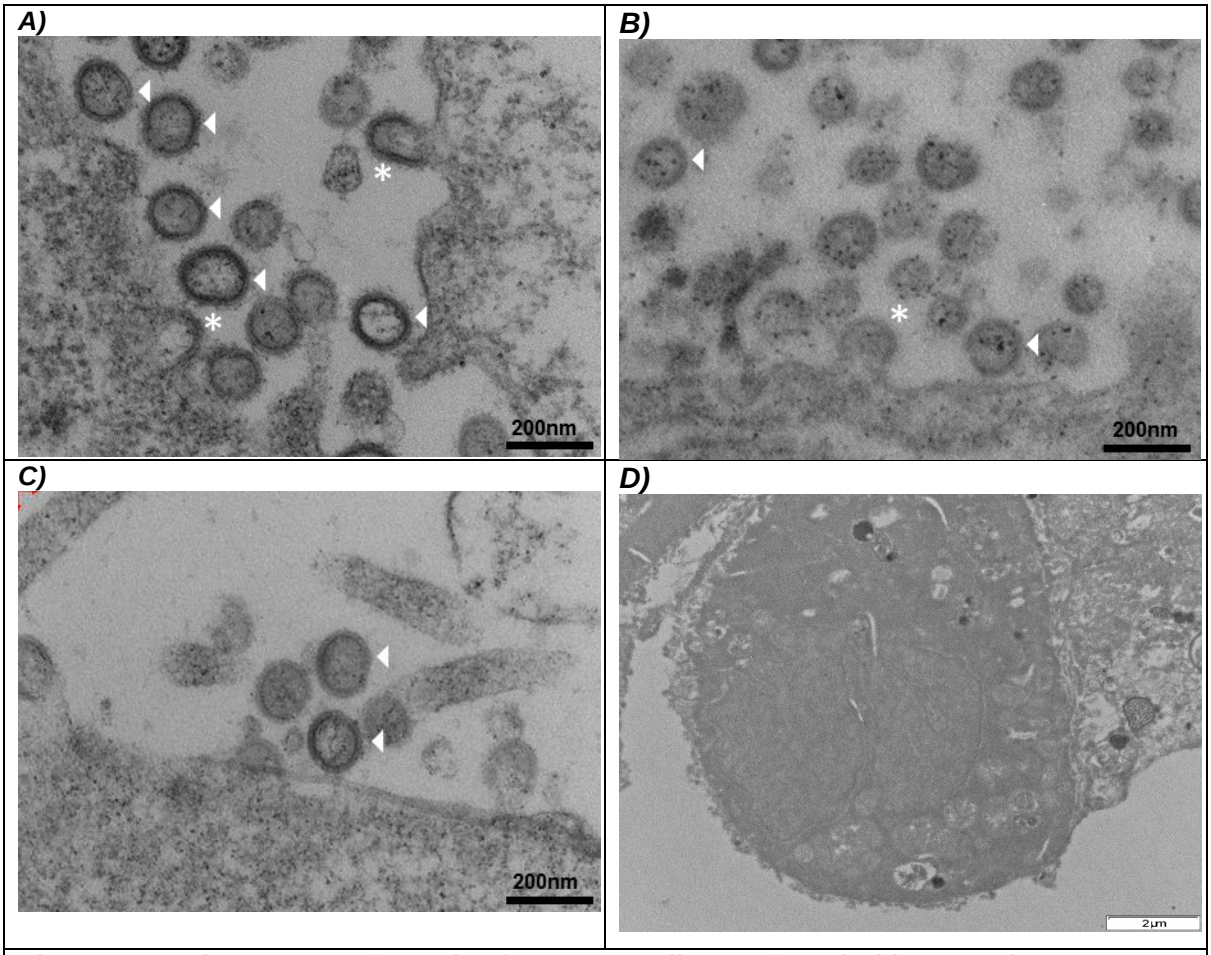

Figure 4.9.* In vitro *Gag VLP formation from RK13 cells transfected with Env and Env:HA$_2$ DNA vaccines.
(A-D) Electron microscopy images showing *in vitro* formation of VLPs from the different DNA vaccines. Examples of VLPs are indicated with ◁ and VLP budding events with *. ***(A)*** DNAGC5, ***(B)*** DNAGC2 and ***(C)*** DNAGC4. No VLP-like structures could be detected in the empty vector control ***(D)***.

this was repeated three times, whereas for the matching DNA vaccines this was performed once. These blots were used for densitometry and to calculate Env:Gag ratios as a measure for Env spike density on the isolated VLPs, with the average signal for Gag+gp150 (GC5) set as 1. Surprisingly, no significant differences between Env (GC5) and the Env:HA2 chimaeras (GC2 and GC4) were detected (One-way ANOVA) (***Figure 4.11C***). If anything, there is a trend towards higher Env spike density for gp150 rather than the Env:HA$_2$ chimaeras.

4.3.5 Immunogenicity studies in rabbits comparing Env and Env:HA$_2$ chimaeric DNA and MVA based vaccines

To investigate how the *in vitro* characteristics of the three Env and Env:HA2 chimaeric DNA and MVA vaccines translates into *in vivo* immunogenicity, three group of rabbits were inoculated using the regimen optimised in ***Chapter 3*** of two DNA vaccines, followed by two vaccine matched MVA vaccines and boosted with two soluble, trimeric Env protein vaccines

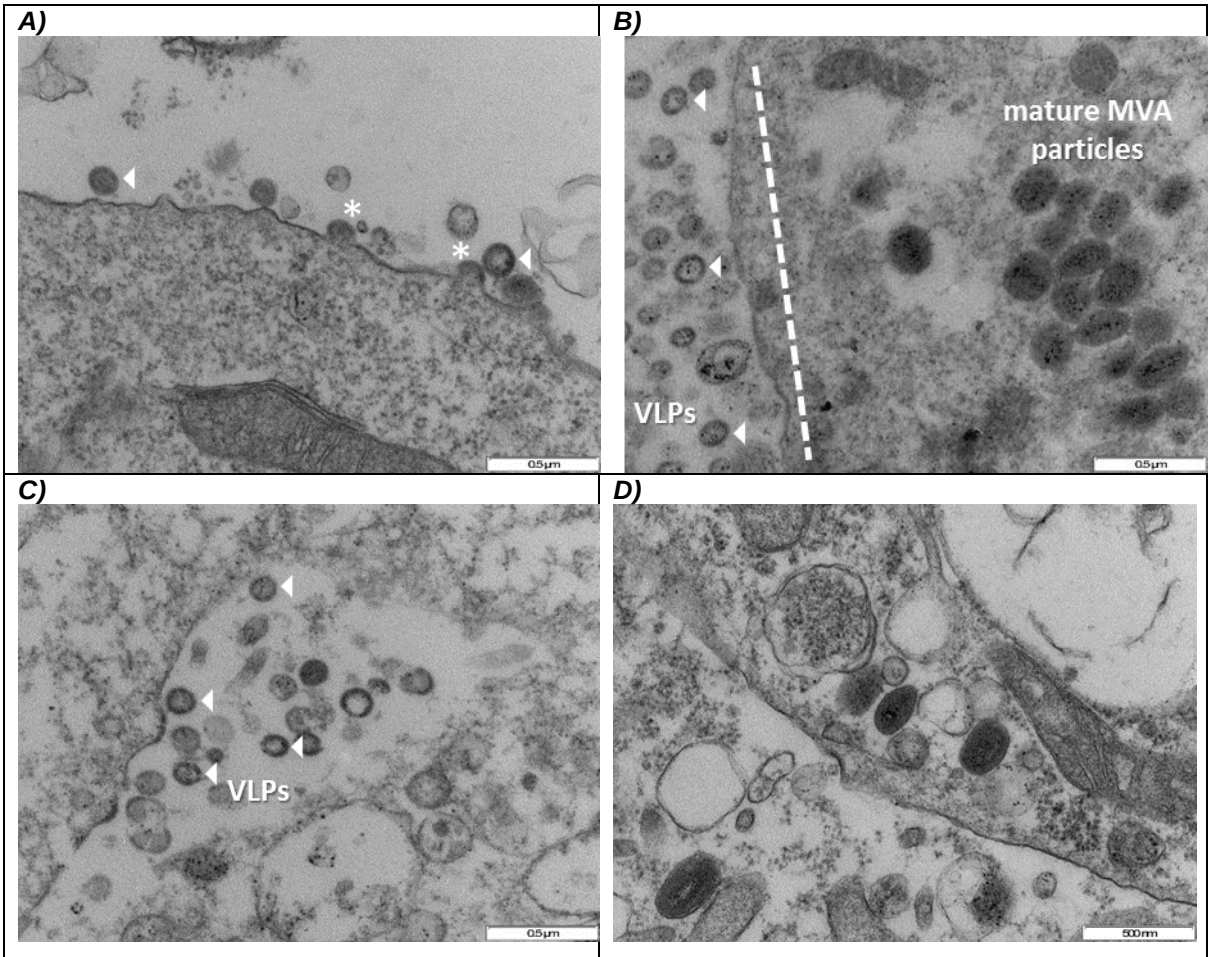

Figure 4.10. **In vitro** ***Gag VLP formation from RK13 cells infected with Env and Env:HA₂ rMVA vaccines.***
(A-C) Electron microscopy images showing *in vitro* formation of VLPs from the different rMVA vaccines. Examples of VLPs are indicated with ◁ and VLP budding events with *. ***(A)*** MVAGC5, ***(B)*** MVAGC2 and ***(C)*** MVAGC4.
The dotted line in ***(B)*** approximately delineates the extracellular compartment with VLPs on the left from the cell on the right containing mature MVA particles.
(D) No VLP like structures could be detected in MVAC5 (Env alone).

adjuvanted in AlhydroGel (DDMMPP) (***Table 4.3***, ***Figure 4.12***). Data for the rabbits receiving DNA and MVA vaccines containing Env+Gag^{M} (Gag^{M}+gp150) is the same data as presented in ***Chapter 3***.

Serum was taken at regular intervals and tested in a soluble, trimeric Env binding ELISA as described before (***Section 3.3.5***). Again, Env-binding antibodies only developed after administration of rMVA vaccines (***Figure 4.13A***). No differences were observed in the

development of α-Env binding antibodies over time between the group receiving Gag^{M} +Env (Gag^{M}+gp150) as DNA and MVA vaccines or the two groups inoculated with Gag^{M}+Env:HA$_2$ chimaeric DNA and MVA vaccines (Gag^{M}+gp120HA$_2$ or Gag^{M}+gp140HA$_2$tr) (Two-way ANOVA). Similarly, for all three groups, α-Env binding antibody titres peaked after every rMVA or protein inoculation, with no differences in titres between the second rMVA inoculation and

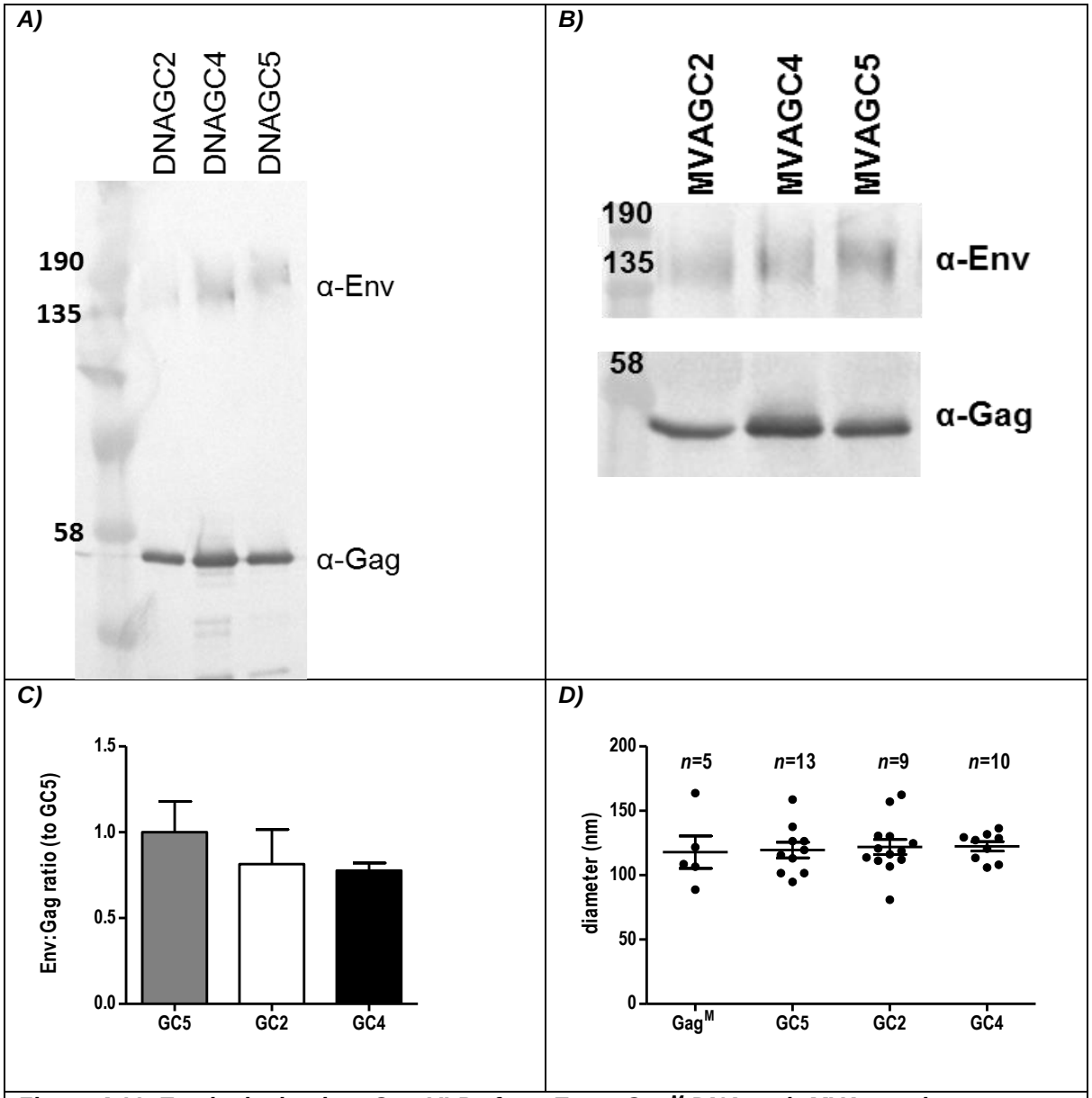

Figure 4.11. Env inclusion into Gag-VLPs from Env + Gag^M DNA and rMVA vaccines.
(A+B) Env (top) and Gag (bottom) could be detected by western blotting in VLPs isolated from the second OptiPrep gradient when both Gag^M and Env were co-expressed from DNA ***(A)*** and rMVA ***(B)*** Env and Env:HA$_2$ vaccines. Likewise, VLPs containing Gag only are detected from DNA or rMVA Gag^M. Whereas no Gag or Env signal was detected for cells alone, DNA or rMVA Env vaccines or wildtype MVA.
(C) No significant differences in relative Env:Gag ratios between Env and the Env:HA$_2$ chimaeric vaccines (*n*=4; One-way ANOVA) as measured by densitometry of western blot signals from isolated VLPs.
(D) Similarly, inclusion of Env and Env:HA2 chimaeras has no effect on VLP size (One-way ANOVA). Data combined from EM pictures of DNA and MVA HIV-1 vaccines.

either of the two protein boosts (Two-way ANOVA). These α-Env binding antibodies appear to reach a titre within the serum which cannot be improved upon. Serum from all three groups were tested in a binding ELISA against the autologous CAP256 SU V1V2 loop at week 14 (post second MVA) and week 30 (post second protein) ***(Figure 4.13B)***. No differences in end

Figure 4.12. Rabbit immunisation regimens.
Immunisation protocol for the three different groups. with matching DNA and MVA vaccines (Gag^M + gp150-FL-IP, Gag^M + $gp120HA_2$-FL or Gag^M + $gp140HA_2$tr-FL-IP). Animals in all groups received the same protein boost (soluble, trimeric Env in AlhydroGel adjuvant).

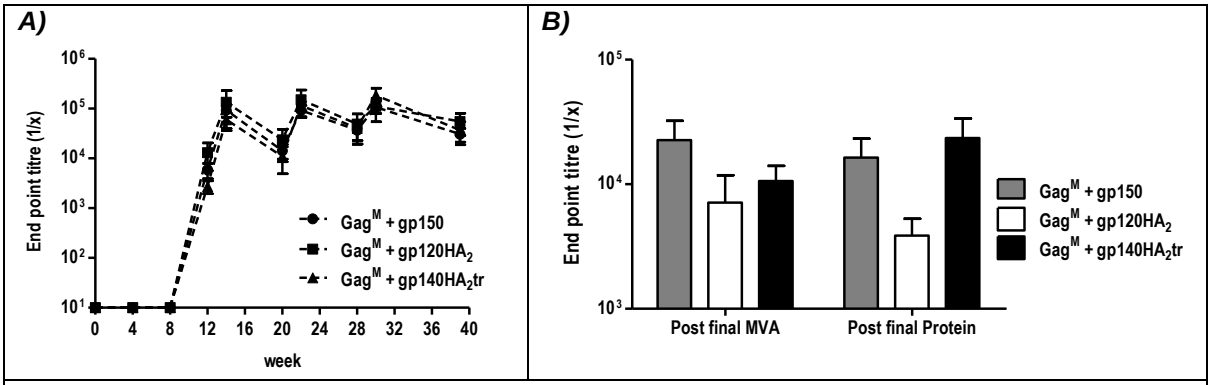

Figure 4.13. Env binding ELISAs of rabbit sera.
(A) Time course depicting binding of rabbit sera to soluble, trimeric CAP256 Env as measured by ELISA. Endpoint titre was plotted as 10 when no ELISA signal was observed.
(B) CAP256 V1V2 loop scaffold binding ELISA of rabbit sera post second MVA or post final protein . This binding ELISA was negative for week 0.
Groups identified as DNA and matching MVA vaccine (Gag^M+gp150, Gag^M+$gp120HA_2$ and Gag^M+$gp140HA_2$tr).
All data are presented as group averages +/- SEMs.

point titres of the sera could be detected between the different groups (Gag^M+gp150, Gag^M+$gp120HA_2$ or Gag^M+$gp140HA_2$tr) or between week 14 and 30 (Two-way ANOVA).

When these rabbit sera were tested for neutralizing activity (ID_{50}) against a panel of Env-pseudotyped virions, neutralisation of Tier 1A MW965.26 can already be observed after the first rMVA inoculation with no clear differences between the different Gag^M plus Env or Env:HA_2 chimaeric DNA and MVA vaccines ***(Table 4.6)***. These neutralisation titres significantly increased after the second rMVA inoculation (all groups/rabbits combined, Student *t*-test, $p<0.001$). At this same time point, most animals developed Tier 1B neutralisation for Tier 1B 6644 and some towards Tier 1B 1107365. Protein boosting failed to enhance these Tier 1A and 1B neutralisation titres, but the patterns appear very similar between the different Gag^M plus Env or Env:HA_2 chimaeric DNA and MVA vaccines. Encouragingly, neutralisation titres for vaccine matched Tier 2 neutralisation towards CAP256_SU were observed, ranging between 1:44 and 1:1294 after the final protein boost

Table 4.6. Serum neutralisation from rabbits vaccinated with different adjuvants as measured by TZM-bl assay.

Sera from immunised animals were assessed for neutralising activity (serum dilution required for a 50% reduction in entry of the infecting virus into a reporter cell line (ID50) against a panel of Env-pseudotyped virions at different time points. The 50% neutralisation titres are color-coded to reflect their potency range as indicated. Pre-bleeds (pre) was taken at week 0. All other bleeds were taken 2 weeks after the indicated vaccine, abbreviated as M1: first MVA, M2: second MVA, P1: first protein and P2: second protein. The pre-bleeds and MuLV control for all rabbits and time points were negative in this assay. As the Env binding ELISA was negative for bleeds after two DNA vaccines were not tested here. Titres below 20 are considered negative.

50% Neutralization titre
10 000 - 100 000
1 000 - 10 000
100 - 1 000
20 - 100
<20
N/A not applicable
NT not tested

		Clade C Tier 1A MW965.26 ID_{50} after:					Clade C Tier 1B 6644 ID_{50} after:					Clade C Tier 1B 1107356 ID_{50} after:					Clade C Tier 2 CAP256 SU ID_{50} after:					Control MLV ID_{50} after:
Regimen	**Rabbit**	**pre**	**M1**	**M2**	**P1**	**P2**	**pre**	**M1**	**M2**	**P1**	**P2**	**pre**	**M1**	**M2**	**P1**	**P2**	**pre**	**M1**	**M2**	**P1**	**P2**	**pre-wk30**
DDMMPP gp150 Gag^M	6826	<20	195	3426	5286	7840	<20	<20	85	45	170	<20	<20	32	<20	29	<20	<20	70	486	1294	<20
	6827	<20	119	3892	14601	2748	<20	<20	120	196	104	<20	<20	35	<20	<20	<20	<20	53	519	174	<20
	6828	<20	81	7239	664	4348	<20	<20	172	20	136	<20	<20	62	<20	21	<20	<20	<20	<20	<20	<20
	6830	<20	108	12641	20778	3920	<20	<20	299	172	143	<20	<20	40	<20	<20	<20	<20	60	332	296	<20
	6850	<20	<20	1999	1987	787	<20	<20	78	40	41	<20	<20	<20	<20	<20	<20	<20	<20	32	54	<20
	median	<20	108	3892	5286	3920	<20	<20	120	45	136	<20	<20	35	<20	<20	<20	<20	53	332	174	<20
DDMMPP gp120HA_2 Gag^M	6832	<20	<20	470	3594	1115	<20	<20	<20	30	<20	<20	<20	21	<20	<20	<20	<20	<20	<20	<20	<20
	6833	<20	166	82	96	211	<20	<20	<20	<20	<20	<20	<20	<20	<20	<20	<20	<20	<20	<20	<20	<20
	6834	<20	36	42	305	148	<20	<20	<20	21	<20	<20	<20	<20	<20	<20	<20	<20	<20	<20	<20	<20
	6835	<20	25	2410	1050	3680	<20	<20	130	74	83	<20	<20	<20	<20	23	<20	<20	<20	<20	<20	<20
	6836	<20	35	8193	6134	1786	<20	<20	595	175	158	<20	<20	47	<20	<20	<20	<20	<20	<20	<20	<20
	median	<20	40	502.3	925	745	<20	<20	56	43	39	<20	<20	23	<20	<20	<20	<20	<20	<20	<20	<20
DDMMPP gp140HA_2tr Gag^M	6838	<20	97	1060	6524	3235	<20	<20	113	154	113	<20	<20	<20	<20	25	<20	<20	<20	<20	<20	<20
	6839	<20	53	578	8835	2578	<20	<20	32	262	89	<20	<20	<20	24	<20	<20	<20	<20	242	151	<20
	6840	<20	44	101	384	298	<20	<20	<20	<20	<20	<20	<20	<20	<20	<20	<20	<20	<20	103	44	<20
	6842	<20	87	NT	5783	2816	<20	<20	NT	112	128	<20	<20	NT	<20	<20	<20	<20	NT	171	220	<20
	median	<20	67	395.5	3364	1626	<20	<20	41	96	70	<20	<20	<20	<20	<20	<20	<20	<20	95	72.6	<20

(Table 4.6). These Tier 2 neutralisation titres for CAP256_SU are above the threshold required for 50% protection (1 in 105) in a NHP model [147] in 5 out of 7 animals. Interestingly, there is a complete lack of any Tier 2 neutralisation for the group receiving gp120HA_2tr as part of the DNA and MVA vaccines. Whereas it appears the Env:HA_2 chimaera gp140HA_2tr-FL-IP fails to improve immunogenicity over gp150-FL-IP, including Tier 2 neutralisation.

The week 30 sera from seven rabbits that showed Tier 2 neutralisation against CAP256_SU were tested against a global panel of ten Tier 2 HIV-1 Env pseudoviruses. Five out of 7 animals developed a low titre neutralisation response against Clade A 398F1 (ranging between 1:20-29) (***Table 4.7***).

Table 4.7. Week 30 serum neutralisation against global panel for DDMMPP rabbit experiment as measured by TZM-bl assay.
Week 30 sera from immunised animals were assessed for neutralising activity (ID50) against a global panel of Tier 2 Env pseudotyped virions.
The 50% neutralisation titres are color-coded to reflect their potency range as indicated.
Titres below 20 are considered negative.

	Virion	X1632	398F1	25710	BJX2000	CE0217	CE1176	CH119	CNE8	CNE55	TRO.11	X2278	246F3
	Clade	G	A	C	CRF07	C	C	CRF07	CRF01	CRF01	B	B	AC
Group	Rabbit	ID_{50} at week 30											
DDMMPP Gag^M + gp150	6826	<20	<20	<20	<20	<20	<20	<20	<20	<20	<20	<20	<20
	6827	<20	21	<20	<20	<20	<20	<20	<20	<20	<20	<20	<20
	6830	<20	24	<20	<20	<20	<20	<20	<20	<20	<20	<20	<20
	6850	<20	<20	<20	<20	<20	<20	<20	<20	<20	<20	<20	<20
DDMMPP Gag^M + gp140HA_2tr	6839	<20	22	<20	<20	<20	<20	<20	<20	<20	<20	<20	<20
	6840	<20	22	<20	<20	<20	<20	<20	<20	<20	<20	<20	<20
	6842	<20	24	<20	<20	<20	<20	<20	<20	<20	<20	<20	<20

50% Neutralization titre
1 000 - 10 000
100 - 1 000
20 - 100
<20

The same sera that were tested against the global Tier 2 panel was used to investigate the possible neutralisation site within the Env sequence. A K169E mutation within CAP256_SU Env leads to the loss of binding of the native-like Env trimer specific MAbs PG16 and CAP256-VRC26.08 [167, 174, 252]. When sera were tested against these CAP256_SU K169E pseudovirions, no differences were observed compared to the CAP256_SU pseudovirion ***(Table 4.8)***, suggesting that the neutralisation response was directed towards a region outside the trimer apex of Env. In line with this, chimaeras formed by replacing the V1V2 region of two heterologous viruses, BG0505N332+ or CAP84, with that of CAP256_SU, were not neutralised, indicating that the Tier 2 NAbs elicited in this study are probably not targeting the V1V2 region.

Table 4.8. Week 30 serum neutralisation against CAP256 Env K169E mutant for DDMMPP rabbit experiment as measured by TZM-bl assay.
Week 30 sera from immunised animals positive for Tier 2 CAP256_SU neutralisation were assessed for neutralising activity (ID50) against CAP256_SU K169E or BG0505N332+ and CAP84 pseudovirions with their V1V2 loop was replaced with that of CAP256_SU.
The 50% neutralisation titres are color-coded to reflect their potency range as indicated.
Titres below 20 are considered negative.

		ID_{50} after 2nd protein CAP256 SU:			ID_{50} after 2nd protein CAP256 V1V2 loop	
Group	Rabbit	normal	K169E	Fold diff	BG505N332	CAP84
DDMMPP Gag^M + gp150	6826	1295	1495	0.9	<20	<20
	6827	338	215	1.6	<20	<20
	6830	359	306	1.2	<20	<20
	6850	37	45	0.8	<20	<20
DDMMPP Gag^M + $gp140HA_2tr$	6839	197	203	1.0	<20	<20
	6840	61	40	1.5	<20	21
	6842	343	283	1.2	<20	<20

50% Neutralization titre
1 000 - 10 000
100 - 1 000
20 - 100
<20
N/A not applicable
NT not tested

4.4 Discussion

In ***Chapter 3***, a regimen of two HIV-1 DNA vaccines followed by two recombinant HIV-1 MVA vaccines and boosted with two CAP256 soluble, trimeric Env protein vaccines, led to superior immune responses, including autologous Tier 2 neutralisation. This was especially true when CAP256 gp150-FL-IP and subtype C mosaic Gag were included in the DNA and MVA vaccines, possibly due to the formation of Gag virus-like particles (VLPs) *in vivo* as was shown previously *in vitro*. For work reported in this chapter, an effort was made to improve this spike density on VLPs and the plasma membrane by generating chimaeric constructs between HIV-1 Env and the HA stalk from influenza A, as it had previously been shown that substituting the transmembrane domain and cytoplasmic tail of gp41 with the corresponding elements of the HA stalk improved the spike density of this chimaeric construct [399]. Two different constructs were generated, based on CAP256 gp150-FL-IP, in which either the whole of HIV-1 Env gp41 was replaced with that of the influenza viral stalk domain (HA_2) (gp120HA_2), or the ectodomain of gp41 was retained while introducing the HA_2 transmembrane and cytoplasmic tail section (gp140HA_2tr).

No differences in *in vitro* expression levels of gp150 Env and Env:HA_2 chimaeras from DNA and rMVA vaccines were observed. VLP formation was verified from both platforms by electron microscopy when Gag^M was co-expressed, and no major differences in VLP morphology or diameter were apparent between Env and Env:HA_2 chimaeras. Surprisingly, when the above VLPs were isolated by OptiPrep density centrifugation, no differences in Env:Gag protein ratios between Env and Env:HA_2 chimaeras were observed. Similarly, Env

scores of Env bnAb binding in a FACS assay were similar or on the whole better for gp150 Env compared to Env:HA_2 chimaeras. This would all suggest that the Env:HA_2 chimaeras vaccines tested here failed to enhance surface Env spike density in contrast to what has been described before by Wang *et al*., 2007 [399]. However, this might have been influenced by several differences in construct design (***Table 4.9***). For instance, Wang *et al*. used different signal peptides for the chimaeric Env construct compared to gp160, which might have affected Env trafficking to the plasma membrane [416, 417]. Furthermore, the furin cleavage site present in gp160 was removed for the chimaeric construct, which means that subsequent shedding of gp120 from gp41 for the gp160 control might have skewed the data in the study by Wang *et al*. For the experiments reported in this chapter, replacement of the signal peptides with the tPA leader and of the furin site with a flexible linker were performed for both Env and the Env:HA_2 chimaeras, which might have improved the spike density of Env as well. Finally, for the experiments in this chapter, Env was truncated to gp150, which should have improved expression compared to the gp160 used by Wang et al., 2007 [399, 400]. Moreover, the use of a different Env in this work may also have been a factor. In summary, all the modifications which were introduced to CAP256 gp150-FL-IP might have led to much higher Env levels on the plasma membrane which then could be recruited into VLPs, thereby substantially increasing Env spike density as compared to the Con-S gp160 used by Wang *et al.,* 2007 [399]. Experiments comparing the unmodified CAP256_SU gp160 sequence to the gp150-FL-IP used here will be very informative to assess if all the modifications to Env led to improvement of spike density. Furthermore, other transmembrane domain plus cytoplasmic tail regions of of viral glycoproteins such as Epstein Barr and mouse mammary tumour viruses and of baculovirus gp64 have also been shown to be effective in increasing Env spike density, and might be worth pursuing [399, 418-420, 465].

Of more concern than effects on Env spike density was the effect the Env:HA_2 chimaeras had on the presentation of Env bnAb epitopes, as observed in both qualitative live-cell staining assays and a quantitative FACS assay. In the most extreme case, no native-like Env trimers were observed for gp120-HA_2–FL as assessed with bnAbs PG16, PGT145 and CAP256 VRC26.08. Furthermore, the highest Env scores for bnAbs F105 and 447-52D were observed for this chimaeric construct, indicating that expression of gp120HA_2 led to highest percentage of misfolded Env trimers, or potentially of the trimer dissociating into dimers and monomers. Although the overall picture for gp140HA_2tr-FL-IP appeared better, Env scores for bnAbs PG16, PGT145 and CAP256 VRC26.08 were comparable to gp150-FL-IP, higher Env scores were observed for bnAbs F105 and 447-52D, again indicating more Env was in a less optimal conformation compared to gp150-FL-IP. It should be noted as well that for all Env and Env:HA_2 chimaeric DNA and rMVA vaccines, some misfolded Env was expressed judged by the binding

Table 4.9 Env and Env:HA2 chimaeric construct characteristics.
The different features between the Env control and Env:HA2 chimaeras used by Wang *et al.,* 2007 [399] and in this thesis. Key differences within the manuscript of Wang *et al*., paper [399] are highlighted in ***bold italics***, whereas between those experiments and here in this chapter are **<u>underlined in bold</u>**.

Feature	Wang *et al*., 2007		Thesis		
	Env	Chimaera	Env	Chimaera 1	Chimaera 2
HIV-1	Con-S		CAP256_SU		
Length	gp160	gp145	**<u>gp150</u>**	gp120	gp140
Signal peptide	Native	***Chitinase***	**<u>tPA</u>**		
Furin site	Yes	***No, fused***	**<u>No, Flexible linker</u>**		
Fusion peptide	Yes	No	Yes		
gp41	HIV-1	gp41 ecto	Yes	No, HA_2	gp41 ecto
TM	HIV-1	HA_2	HIV-1	HA_2	HA_2
Cytoplasmic tail	HIV-1	HA_2	**<u>HIV-1, truncated</u>**	HA_2	HA_2
I559P	No		Yes		
Influenza A	HA_2 from H3N2 strain		HA_2 from H5N1 strain		
Codon optimised	?	Yes	Yes		
Expressed in	Insect cells		Mammalian cells		

of MAbs F015 and 447-52D. This is in line with data from Cappuci et al [343], who showed that BG505 SOISP.664 expressed from MVA or simian adenovirus results in expression of both native-like and misfolded trimers [343]. Unfortunately, the chimaeric constructs using Epstein Barr, MMTV or baculovirus gp64 were never as thoroughly characterised and it is unknown if these chimaeric constructs can fold into a native-like like Env trimer, although these increased the Env spike density [399, 418-420, 465]. Subsequent *in vivo* testing of the chimaeric Env construct using either the transmembrane domain plus the cytoplasmic tail of MMTV baculovirus gp64 resulted in very disappointing neutralisation titres in HIV-1 pseudovirion neutralisation assays, without any autologous Tier 2 neutralisation titres [419, 420]. Therefore, before considering using Env chimaeras as HIV-1 vaccines, the presence of bnAb epitopes and especially those recognising the native-like trimer should be assessed.

A high fraction of misfolded Env of gp120-HA_2–FL from DNA and MVA vaccines *in vitro* seems to correlate to the immunogenic properties of the corresponding DNAGC2 and MVAGC2 vaccines in rabbits. Although Env-binding antibodies to CAP256 Env trimers or the V1V2-loop are unaffected, HIV-1 pseudovirion neutralisation is clearly affected, with 0 out of 5 animals developing autologous Tier 2 neutralisation. In comparison, 4 out of 5 animals from the gp150-FL-IP (DNAGC5 and MVAGC5) group developed these Tier 2 neutralising antibodies, with three rabbits already showing Tier 2 neutralisation after the second MVA vaccine. As for

animals inoculated with gp140HA_2tr-FL-IP (DNAGC4 and MVAGC4), in 3 out of 4 rabbits autologous Tier 2 neutralisation was observed. This underlines the requirement of HIV-1 vaccines to present at least some of the Env antigen as a native-like trimer, as suggested from literature [277, 388].

Although the autologous Tier 2 neutralisation response in the gp150-FL-IP group is almost identical to the gp140HA_2tr-FL-IP group, for the latter this developed on a delayed time scale and was only induced after inoculation with a soluble trimeric Env protein boost. As with the *in vitro* characteristics, the immunogenic properties of gp140HA_2tr-FL-IP *in vivo* are nearly, but just not as good compared to gp150-FL-IP. This indicates that future research should be focussed on vaccines containing gp150 inserts rather than Env:HA_2 chimaeras for the vaccine platforms tested here.

CHAPTER 5: CONCLUDING REMARKS

Global awareness campaigns about HIV-1/AIDS and HIV-1 prevention combined with huge efforts to improve accessibility to antiretroviral therapy, both as a prophylactic measure and to prevent disease progression, have resulted in a dramatic decrease in newly infected individuals and AIDS-related deaths [31, 197, 467-469]. It appears that the HIV-1/AIDS pandemic is slowing down, but unfortunately current predictions are that the 2020 UNAIDS goals (90-90-90 targets, where 90% of people living which HIV-1 are diagnosed as such, from which 90% will receive sustained antiretroviral therapy, resulting in viral suppression in 90% of these individuals by 2020) will not be reached, leading to higher new HIV-1 infection and AIDS-related death rates than was aimed for under these goals [31]. These numbers are still staggering, with data showing that 1.7 million [1.4 million–2.3 million] new infections and 770 000 [570 000–1.1 million] AIDS-related deaths were predicted for 2018 [31]. Therefore a prophylactic vaccine, even when only partially protective, would be a significant step forward in tackling the pandemic [223]. Furthermore, developing countries, especially those situated in eastern and southern Africa, carry the largest burden of people living with HIV, new HIV infections and deaths from AIDS [30-32]. With this in mind, the South African Medical Research Council (SAMRC) in association with the Department of Science & Technology (DST) extended a call for pre-clinical HIV-1 vaccine research under The Strategic Health Innovation Partnerships (SHIP) and funded the project 'Novel HIV Vaccine Candidates for South Africa' led by Professor Anna-Lise Williamson.

This SHIP project required extensive tool, capacity and infrastructure development, with a large part of this work being presented in this thesis. For my project, the remit was further narrowed down to the development of an HIV-1 subtype C vaccine for sub-Saharan Africa eliciting high-titre antibody responses to HIV-1 envelope glycoproteins (Env) [26-29]. Therefore, an Env sequence was chosen from the Centre for the AIDS Programme of Research in South Africa (CAPRISA) 002 acute infection cohort [167, 174]. This particular virus was the superinfecting virus (SU) from participant CAP256 who developed broadly cross-neutralising antibodies targeting the V1V2 loop 15 weeks after the second viral infection event. Furthermore, the CAP256_SU virus was shown to be sensitive to a range of broadly neutralising antibodies (bnAbs) targeting different epitopes within the Env sequence [167]. Consequently, this Env sequence has the potential not only to induce high-titre antibodies towards Env, but also to elicit neutralising antibodies in animal models. Based on the work reported in this thesis, further Env vaccines have been or are under development such as for Env Du151, a sequence from a South African cohort with the closest resemblance to the South African consensus sequence, and subtype C mosaic Env sequences [272, 470].

With the development and characterisation of the DNA and especially the MVA vaccines being more time consuming, the first vaccine I made was a lectin affinity purified soluble Env protein vaccine from the media of HEK293T cells. Initially characterised and used as a protein vaccine (Env (GNL)) without further refinement, the development of a stable cell line in HEK293 cells and subsequent repeat harvesting from the same culture flasks increased yields enough to implement a second layer of purification in which the trimeric Env fraction as adjudged by molecular weight was isolated using size exclusion chromatography (SEC). However, to be able to assess the folding of Env by the presence of Env bnAb epitopes, a stable cell line expressing a His-tagged version of Env had to be created. This allowed for coupling of Env to nickel coated plates for ELISA assays, compared to where Env was directly bound to plates, or trapping Env using lectin coated plates which both led to distorted ELISA results (data not shown). As was to be expected, the *in vitro* immunogenic properties of the Env trimers were clearly improved over Env (GNL), when a His-tagged version was used in a Env bnAb ELISA assay, with low signals for PG16 and CAP256 VRC26.08 which selectively bind the native-like Env trimers only. The Env trimers used as protein vaccine will potentially display a better immunogenic profile as the His-tag affected the Env trimer formation to the extent that SEC purification was ineffective in completely separating Env trimers from dimers. A bio-layer interferometry based assay, such as can be performed on an Octet, could be considered as a replacement for the His-tag ELISA. Although this assay would require more Env protein, the bnAbs could be trapped on for instance protein A probes before binding of soluble trimeric Env can be measured, thereby circumventing the need for a tag for trapping Env.

The Env (GNL) protein vaccine was subsequently used in the first animal study to investigate the modulatory effects of adjuvants to improve the immune response of the vaccine. The same protein was also used to successfully develop an Env binding ELISA assay, which allowed measuring α-Env binding antibodies in rabbit sera. In our experiments, the aluminium based adjuvant AlhydroGel (same formulation as alum) performed significantly better than AddaVax (similar to MF59) [366], both for inducing α-Env binding antibodies and for developing an HIV-1 pseudovirion neutralisation response, with the caveat that these were only Tier 1A and 1B responses. Based on these results, AlhydroGel was selected as the adjuvant for all further protein vaccines in rabbits. Considering these results, hopefully the reason for a lack of vaccine efficacy in HVTN 702 clinical trial is something different than the switch from alum, as used in the partially successful predecessor study RV144, to MF59 [234, 258, 268-270]. However, data from Phase I studies in southern Africa seem to indicate slightly better immune responses when the vaccine regimen from RV144 trial was used (HVTN 097), compared to those of HVTN 702 (HVTN 100) [268, 271].

The SEC purified soluble Env trimers were used as protein vaccine and bait for binding ELISAs in the remaining animal experiments described in this thesis, where it was employed as a booster vaccine of MVA inoculations. Going forward, further purification of the protein vaccine should be considered. This could either take the form in using non-neutralising antibodies against Env, or for instance the bnAbs F105 and 447-52D used in this thesis for identifying misfolded Env trimers, to deplete poorly assembled trimers [385, 422]. Alternatively, bnAbs such as PG16, PGT145, CAP256 VRC26.08 and PGT151, which only recognise Env trimers in a native-like conformation, could be utilised to directly select for these well-folded Env trimers [371, 435]. However, the effect of harsh pH conditions affecting the Env structure in the latter approach should be considered. The use of suspension HEK293 or CHO cells might help to improve Env protein yields to make these selection methods viable alternatives. Furthermore, decreasing the addition of complex glycans by using GnTI negative cell lines could positively impact the formation of native-like Env trimers as well. Another interesting prospect is production of Env protein on potentially cheap and scalable plant platforms, which was recently used successfully in our group to produce soluble, trimeric Env in a transient expression system in *N. benthamiana* [358, 421, 471].

For the development of the recombinant MVA vaccines, a selection method novel for the lab was used where the expression of the vaccinia virus (VACV) *K1L* gene, only present after successful recombination of the transfer construct into the MVA genome, is required for MVA to replicate in RK13 cells [316, 441]. After initial problems of generating MVA recombinants (data not shown), when the promoter for K1L was changed to the synthetic VACV promoter pSS, the generation of recombinant MVA vaccines was greatly improved and high titre stock can now be acquired within 6-8 weeks. This is aided as well by a novel way of isolating MVA DNA from infected cells developed during this project (not discussed, described in ***Appendix A***) which resulted in better PCR success rates for the verification of correct integration of the transfer construct into the MVA genome.

For the DNA and MVA HIV-1 vaccines made in this thesis, the Env had a truncated transmembrane domain (gp150), thereby anchoring it into the cell membrane and not secreting it into the media as with the protein vaccine. Therefore, cell based assays could be developed to characterise the conformation of Env and the presence of Env bnAb epitopes. Initially a live-cell staining assay imaged on a fluorescent microscope was performed. Because the live-cell staining was difficult to quantify, it acted as a qualitative measure of Env bnAb binding. This was subsequently solved by adapting the live-cell staining to a FACS assay based on a protocol from Samal *et al*. (2019), which allowed quantifying the presence of Env bnAb epitopes after expression of the Env from HIV-1 DNA and MVA vaccines [466]. Although expression of Env from DNA (live-cell staining and FACS) and MVA vaccines (live-cell

staining) led to some misfolded Env trimers as observed by binding of the bnAbs F105 and 447-52D, the epitope for the V3-glycan supersite was detected with bnAbs PGT128 and PGT135, the CD4-binding site with VRC01 and the V2-glycan with PG9. Most encouragingly, bnAbs PG16, PGT145 and CAP256 VRC26.08 showed binding as well, indicating that Env expressed from DNA and MVA HIV-1 vaccines can form native-like trimers. When this was quantified in the FACS assay for the HIV-1 DNA vaccine, about 20% of Env trimers were in this native-like conformation when compared to VRC01. This heterogeneous population of Env trimers, ranging all the way from completely misfolded to native-like conformation, is similar to what was observed for BG505 SOISP.664 when expressed via MVA or simian adenovirus [343].

The reason for expressing Env that will be embedded into the membrane from DNA and recombinant MVA vaccines was to investigate if these would be incorporated into Gag virus-like particles (VLPs). Including Gag has the distinct possibility to improve an HIV-1 vaccine on two fronts. First of all, cell-mediated immune responses to HIV-1 Gag (CD4+ and CD8+ T-cell responses) have been implicated in viraemic control of HIV-1 infected individuals [226]. Secondly, incorporation of Env into Pr55gag VLPs has been shown in *in vitro* co-expression studies, and anchoring Env into the native environment of a lipid bilayer could potentially stabilise the trimeric conformation, and has been shown to improve immunogenic properties of Env [405-412, 442, 443, 445, 450, 472]. For this thesis, a HIV-1 mosaic Gag (Gag^{M}) sequence was selected for co-expression with Env. This Gag^{M} sequence, designed *in silico* to maximise potential T-cell epitopes for HIV-1 subtype C, improved immunogenicity in mice as a BCG, DNA and recombinant MVA vaccine [272, 413, 414]. VLP formation was confirmed by electron microscopy when Gag^{M} and Env were co-expressed from DNA and MVA vaccines. Subsequently, a two-step OptiPrep gradient centrifugation protocol was developed to isolate these VLPs to verify the inclusion of Env into the Gag VLPs. Since then, the VLP isolation protocol has been simplified, which has drastically reduced purification time and cost (data not included in thesis) [353].

Although inclusion of Env into these VLPs was observed, with native Env spike density on the HIV-1 virion being relatively low when compared to other viruses [464], it was speculated that this could very well be the same for these VLPs. A potential strategy to increase the Env spiked density is by generating chimaeric constructs between HIV-1 Env and the transmembrane (TM) and cytoplasmic tail (CT) of glycoproteins from different viruses. For this project the H5 haemagglutinin (HA) stalk from influenza A was chosen as it has previously been shown that substituting the TM and CT of HIV-1 gp41 with the corresponding elements of the HA stalk from influenza A improved the spike density [399]. A similar design was employed to generate gp140HA_2tr, whereas for the second chimaera the whole of gp41 was

replaced by the HA_2 stalk, resulting in gp120HA_2 (referred to as Env:HA_2 chimaeras). Surprisingly, no improvement in spike density between Env and the Env:HA_2 chimaeras was observed *in vitro*, either by western blotting of isolated VLPs or on the plasma membrane using the bnAb FACS assay. Possibly differences in Env and Env:HA_2 chimaeras design are responsible for the discrepancy between these results and those reported by Wang *et al*., 2007 (***Table 4.8***) [399]. Especially modifications included here for gp150 Env could have improved Env levels on the plasma membrane and subsequently incorporation into VLPs, to a degree not seen for gp160 in the study by Wang *et al*.

More concerning, it was seen that trimer folding of the Env:HA_2 chimaeras was impaired, especially upon expression of gp120HA_2: here no native-like Env trimers were observed, with the highest percentage of misfolded trimers as assessed by binding of bnAbs F105 and 447-52D in the FACS assay. Although expression of gp140HA_2tr could result in the Env trimer assembling into a native-like conformation with binding of bnAbs PG16, PGT145 and CAP256 VRC26.08 observed, in general superior presentation of bnAb epitopes by gp150-FL-IP (Env) was detected. Therefore, before considering using Env chimaeras as HIV-1 vaccines, the presence of bnAb epitopes and especially those recognising the native-like trimer should be assessed.

As HIV-1 is particularly efficient in evading the immune system, an effective vaccine will almost certainly require the activation of both cellular and humoral immunity. Considering the different qualities of the vaccine platforms developed in this thesis (DNA: cellular immunity; MVA or other viral platforms: cellular+humoral immunity; and protein: humoral immunity), heterologous vaccine platform prime-boosting regimens could potentially broaden the immune response by activating both arms of the adaptive immune response and preventing potential development of vector-based immunity when multiple vaccines are required. This strategy turned out to be particularly effective here when two DNA Env priming vaccines were followed by two vaccine-matched MVA Env vaccines and subsequent boosting with two soluble Env vaccines in rabbits (DDMMPP), resulting in low serum neutralisation titres (1:74 and 1:104) towards autologous Tier 2 pseudo-virions in 2 out of 4 animals after the final protein vaccine. As mentioned earlier, presentation of Env its natural membrane bound state in particles has been shown to lead to increased immunogenicity [442, 443, 445, 450]. This was observed in these experiments as well, with the inclusion of Gag (Env+Gag^M) into DNA and MVA vaccines. In this group, not only did more animals develop Tier 2 neutralising antibodies (4 from 5), but titres were improved (ranging from 1:54 to 1:1294) and Tier 2 neutralisation in general started to develop after less vaccinations, where in three animals this was observed after the second MVA inoculation. This suggests that the right poxvirus-based HIV-1 vaccine regimen can

induce Tier 2 neutralisation without the need of protein vaccines. It should however be emphasised that almost no Tier 2 cross-neutralisation titres were observed.

When Gag^{M} in combination with the Env:HA_2 chimaeric DNA and MVA vaccines were tested in rabbits using the DDMMPP regimen, an inferior immune response was observed, with gp120HA_2 completely failing to induce autologous Tier 2 neutralisation responses. With the gp140HA_2tr-FL-IP group such titres developed on a delayed time scale with lower median neutralisation titres compared to gp150-FL-IP. These results emphasise the importance for HIV-1 vaccines in presenting the Env antigen in a well folded conformation and at least partially as a native-like trimer [277, 388].

In this project a heterologous HIV-1 vaccine platform regimen (DDMMPP) has been developed that can induce high titre binding antibodies for Env and for the V1V2-loop of Env in rabbits. Encouragingly, when both CAP256 gp150-FL-IP and subtype C mosaic Gag are included in the DNA and MVA vaccines, this leads to strong autologous Tier 2 neutralisation responses in most animals. However, improving the immunogenicity of vaccine regimen should be considered in order to elicit stronger and more robust autologous Tier 2 responses and possibly Tier 2 cross-neutralisation. An obvious first target would be gp150-FL-IP, to further modify the Env sequence based on BG505 SOSIP.664, which is now in its tenth iteration, starting with the inclusion of the internal disulphide bond (SOS), which has been shown to improve Env sequences where flexible linkers have been used [371, 377, 379, 380, 382, 384, 385, 473-475]. The bnAb FACS assay developed for this thesis can be used as a screening tool for assessing the effects that these modifications to membrane bound Env will have on the trimeric structure. This could benefit all three different vaccine platforms investigated here.

Even though the HIV-1 DNA vaccine used here was reasonably effective in priming the subsequent HIV-1 MVA vaccines, there is the potential for a large gain in improving the immunogenicity of the DNA vaccine. Delivery by needleless devices such as supplied by PharmaJet have shown to improve the vaccine immune response of DNA vaccines to delivery by needle and/or electroporation [303-305]. Besides improving vaccine immunogenicity with needleless devices, other benefits for these systems in a clinical setting such as dose sparing, increased safety (no needle injuries), and preferred delivery method by vaccinators and caregivers, which could lead to increased vaccine uptake and compliance, should be taken into consideration as well [476, 477]. This approach could even be combined with adjuvanting the DNA with simple and inexpensive solutions such as formulation in lipids and polymers or addition of CpG oligodeoxynucleotides (CpG ODNs), with the latter aimed at TLR9 signalling and B-cell activation [286, 478].

Unfortunately, the rabbit model is limited to measuring vaccine induced antibody responses alone. With the inclusion of both Env and Gag into the DDMMPP vaccine regimen leading to the strongest immune responses in this thesis, it would be extremely interesting to interrogate the T-cell response that is induced. Even simple ELISpot assays to measure vaccine induced IFNγ, IL2 and IL4 towards Env and Gag would be insightful. With commercial T-cell assays mainly geared towards mice and non-human primates (macaques), lack of antibody pairs for rabbit cytokines and a general lack of knowledge about the rabbit immune system, it would be very informative to test the Env+Gag^{M} DDMMPP from this thesis in macaques to measure both cell-mediated and humoral immune responses.

APPENDIX A. Routine molecular biology protocols

1 DNA isolation and manipulation

1.1 Small scale plasmid DNA isolation

Grow bacterial (*E. coli*) culture in 3ml LB medium with appropriate antibiotics at 37 °C overnight (O/N) whilst shaking (250rpm). Transfer O/N culture to a 2 ml Eppendorf tube, and spin down cell culture at high speed for 30 seconds in table-top centrifuge and discard supernatant. Add 250µl of resuspension solution (P1 buffer) into each tube and resuspend cell pellet by pipetting up and down. Add 250µl of lysis solution (P2 buffer) and mix by gently inverting the tube 5-6 times. Add 350µl of neutralizing solution (P3 buffer) and mix by inverting the tubes several times. Centrifuge the tubes at >12000*g* for 10 min. Carefully transfer 750µl supernatant to a new labelled 1.5 ml Eppendorf tube with a 1 ml pipette. Add 525µl ice-cold isopropanol and cool on ice for 15 min. Spin down plasmid DNA precipitate at >12000*g* for 20 min. Remove the supernatant, add 180µl 70% ethanol (ice cold), spin at >12000*g* for 1 minute. Discard supernatant and air dry (~5min) without over-drying. Resuspend the DNA pellet with 50µl TE.

1.2 Large scale plasmid DNA isolation

Zyppy™ Plasmid Maxiprep Kit (Zymo Research, Irvine) was used for all large scale plasmid DNA isolations. Buffers P1-P3, wash buffers and Elution Buffer were supplied with this kit. Grow bacterial (*E. coli*) culture in 100ml LB medium with appropriate antibiotics at 37 °C O/N whilst shaking (250rpm). Transfer O/N culture to a 3x 35ml tubes, spin down cell culture at 6000*g* for 15 minutes at 4°C and discard supernatant. Add 5ml P1 buffer into each tube and resuspend cell pellet by pipetting up and down. Add 5ml P2 buffer into each tube and mix by gently inverting the tube 5-6 times. Add 7ml chilled P3 buffer into each tube and mix by gently inverting the tube until the colour has changed to yellow. Place on ice for 5 minutes. Centrifuge the tubes at 6000*g* for 15 minutes at 4°C. Carefully transfer all supernatant to Zymo-Spin™ VI column and apply vacuum until all liquid has gone through. Add 11ml of Endo-Wash Buffer and apply vacuum until all liquid has gone through. Add 11ml of Zyppy™ Wash Buffer. and apply vacuum, keep vacuum for an additional 5 minutes after all liquid has gone through to dry the membrane. Place Zymo-Spin™ VI column into 50ml, add 3ml pre-warmed (50°C) Elution Buffer and incubate for 5 minutes at room temperature. Spin for 10 minutes at 3000g. Collect eluate and measure the concentration on a NanoDrop (Thermo Fisher Scientific, Waltham). Concentrate to 1µg/µl using the protocol described below.

1.3 DNA precipitation

Add 1/10 volume of 3M Sodium acetate (pH5.5 using glacial acetic acid) and 0.7 volume ice-cold isopropanol to DNA. Leave on ice for 10 minutes. Spin at >12000*g* for 20 minutes. Remove the supernatant, add 180µl 70% ethanol (ice cold), spin at >12000*g* for 1 minute. Discard supernatant and air dry (~5min) without over-drying. Resuspend the DNA pellet with required volume of TE for 1µg/µl.

1.4 Restriction enzyme digestion of plasmid DNA

FastDigest restriction enzymes (Thermo Fisher Scientific, Waltham) were used for all DNA restrictions. Single digests were performed in 15µl reactions with 1µg of plasmid DNA, 1µl restriction enzyme and 1.5µl FastDigest buffer. Double digests were performed in 25µl reactions with 1µg of plasmid DNA, 1µl restriction enzyme each and 2.5µl FastDigest buffer. Digests were incubated at 37°C for 15 minutes and subsequently run on 0.8% agarose gel.

1.5 DNA isolation from agarose gels

All purifications were performed using Zymoclean Gel DNA Recovery kit (Zymo Research, Irvine). All buffers were supplied with the kit. Excise band from agarose gel on blue-light illuminator (BLooK LED transilluminator (GeneDireX, Zhunan Township)), place in 1.5ml Eppendorf tube and weigh. Three volumes of ADB buffer was added and the tube was incubated at 50°C to completely dissolve the agarose gel. The solution was transferred to Zymo-Spin™ Column in a Collection Tube and spun for 30 seconds at >12000*g*. Flow-through was discarded, 200µl wash buffer was added to the Zymo-Spin™ Column and spun for 30 seconds 12000*g*. Wash was repeated and after discarding the flow-through, the Zymo-Spin™ Column was dried by spinning for 1 minute at 12000*g*. The Zymo-Spin™ Column was transferred to a new 1.5ml Eppendorf tube and 30µl of pre-warmed (50°C) elution buffer was added and incubated at room temperature for 1 minute. DNA was eluted by spinning for 30 seconds at 12000*g*.

1.6 DNA ligation

All DNA ligations were performed in 20 µl reactions using 1µl T4 DNA ligase (Thermo Fisher Scientific, Waltham), 2µl T4 DNA ligase buffer, 1µl plasmid backbone (agarose purified restriction digest of 1 µg DNA) and 3µl DNA insert (agarose purified restriction digest of 1 µg DNA). Ligations were incubated at room temperature for 1 hour before transformation into *E. coli*. Control ligations were as above but without DNA insert or without DNA insert and T4 DNA ligase.

1.7 Transformation of plasmid DNA into *E. coli*

E. cloni 10G Chemically competent cells (Lucigen, Middleton) were used to plasmid DNA transformation. In short, 15µl aliquots of competent cells were defrosted on ice, 1µl of ligation reaction 1ng of plasmid DNA was added and incubated on ice for 30 minutes. After a 30 second heat shock (37°C) cells were placed on ice again for 2 minutes. 400µl recovering media (supplied with kit) at 37°C was added and the transformation was placed at 37 °C for one hour whilst shaking (250rpm). 140µl of the transformation was plated onto LB Agar plates with an antibody selection and plates were incubated O/N at 37 °C.

2 rMVA isolation

2.1 Isolation of rMVA for PCR

Use buffer P1-3 from small scale plasmid DNA isolation. Add 250µl of resuspension solution (P1 buffer) to a well (6-, 12-, or 24-well plate) infected with rMVA, pipette up and down until all cells have detached and transfer to 1.5ml Eppendorf tube. Add 250µl of lysis solution (P2 buffer) and mix vigorously by pipetting up and down. Add 350µl of neutralizing solution (P3 buffer) and mix vigorously by pipetting up and down. Centrifuge the tubes at >12000*g* for 10 min. Carefully transfer 700µl supernatant to a new labelled 1.5 ml Eppendorf tube with a 1 ml pipette. Add 490µl ice-cold isopropanol. Spin down rMVA/DNA precipitate at >12000*g* for 20 min. Remove the supernatant, add 180µl 70% ethanol (ice cold), quickly spin at max speed. Discard supernatant and air dry (~5min) without over-drying. Resuspend the rMVA/DNA pellet with 30µl ddH_2O.

2.2 Large scale production of rMVA

When single foci picked from serial dilution plates were verified for correct integration and expression of Env, Env:HA_2 chimaeras and/or Gag^M they were expanded in a T75 containing 70-80% confluent RK13 cells. Infection was monitored by eGFP expression and after 3-4 days when nearly all cells had lifted, cells were lysed by repeated freeze-thaw cycles in the T75 flask (3 in total) and viral titres were determined in BHK cells where GFP positive plaques were counted 48 hours after infection of a serial dilution range (in steps of 1 in 10) and calculated as plaque forming units (pfu)/ml. This titre was used to infect $4*10^7$ RK13 cells with an MOI of 0.001 at 37°C/5%CO_2 in a total volume of 10ml RK13 media to generate a seed stock. After 1 hour, infected cells were added to a full bottle of RK13 media (~550ml), this was poured into a Hyperflask and the flask was transferred to a tissue culture incubator (37°C/5%CO_2). Infection was monitored by eGFP expression and after 5-6 days when nearly all cells had lifted, nearly most media (~50ml left) was poured off into 50ml tubes. Both tubes and the hyperflask were frozen (-80°C) and thawed (37°C). The remaining media from the

Hyperflask was added to the 50ml tubes and freeze-thawing was repeated twice. After the final thaw, supernatant was cleared by low speed spin (5 minutes, 275*g*) and divided between 16x 35ml tubes. The supernatant was underlayed with 2ml 36% sucrose (in H_2O), spun for 1 hour at ~26900*g* (4°C) with the centrifuge brake disengaged after which the supernatant was discarded. The pellets were reconstituted in a total volume of 5ml PBS, aliquoted and stored at -80°C. Furthermore, 10µl of concentrated rMVA was plated onto LB Agar plates without antibody selection, plates were incubated for 3 days at 37 °C to test for bacterial, fungal and yeast contamination. The titre of this seed stock was determined from a frozen aliquot as described above and used to generate high titre stocks (working stocks) for animal experiments. Working stocks were generated and titred in the same way as the seed stock described above with the following permutations: 1) three hyperflasks were seeded; 2) cell pellet after clearing was lysed in 10ml of 0.1mM Tris pH 9.0 per hyperflask and after another low speed clearing step, this lysate was added to the initial lysate; 3) pellets from the first sucrose cushion were resuspended in 20ml of PBS per hyperflask and run on a second sucrose cushion (2x 35ml tubes) and 4) these pellets were reconstituted in in a total volume of 10ml PBS+10% glycerol.

3. PCR

3.1 PCR protocol

KAPA2G Robust HotStart ReadyMix PCR Kit (Kapa Biosystems, Cape Town) was used for rMVA PCR screening. All PCRs were run with the same protocol as described in the table below. Primers to screen for correct integration in rMVA constructs are described below in 3.2. Primers to sequence these PCR products are described in 3.3.

Component	25 µl reaction
PCR-grade water	Up to 25µl
5X KAPA2G Robust HotStart ReadyMix2	12.5µl
10 µM Forward Primer	1.25µl
10 µM Reverse Primer	1.25µl
Template DNA4	1µl

Step	Temperature	Duration	Cycles
Denaturation	95ºC	3 minutes	1
Denaturation	95ºC	15 seconds	40
Annealing	55ºC	15 seconds	
Extension	72ºC	3 minutes	
Extension	72ºC	3 minutes	1

3.2 PCR primers for rMVA screening

Recombination into I8R flank

name	sequence	size	TM	note	PCR product
eGFP rev	AGATGAACTTCAGGGTCAGC	20	60	For pSSPEx final recombinant PCR	870bp
I8R f2	GAAAAGGAAGAGTAGGAAGAG	21	60	Binding site outside pSSPEx flank	

Recombination into G1L flank. Size of this PCR product will also verify full-length integration of Env and Env:HA_2 chimaeras

name	sequence	size	TM	note	PCR product
PEPV DR fwd	GGGTGTAGCTAACAACCCTG	20	60	For Env+promoter PCR	3150bp*
G1L r2	GGCCATGTGTAACACTAGAG	20	60	Binding site outside pSSPEx flank	
*PCR products for Env:HA2 chimaeras is ~200 base pair shorter					

PCR for *gag*^{M} insertion site

name	sequence	size	TM	note	PCR product
A11_f	GCAAATTTGAACGGGTCTCCC	18	58	Binding site outside recombination flank	2240bp
A12_r	GCGATGGATGGTCAGATTGTC	21	64	Binding site outside recombination flank	

3.3 Sequencing primers for rMVA

name	sequence	size	TM	locus	Env or Env:HA2 construct
TPA F	CTGTTGCGTGCTGCTG	16	52	TPA	GP120HA2/GP140HA2tr/GP150
CGP120 F1	CACTCGCGAGGAAATC	16	52	GP120	GP120HA2/GP140HA2tr/GP150
CGP120 F2	TTATCGTCCACCTGAAC	17	50	GP120	GP120HA2/GP140HA2tr/GP150
CGP120 F3	TATCAACATGTGGCAGG	17	50	GP120	GP120HA2/GP140HA2tr/GP150
CGP41 F1	GCTGTCTGGCATCGTC	16	52	GP41	GP140HA2tr/GP150
CGP41 F2	GGCTGTGGTACATTAAG	17	50	GP41	GP140HA2tr/GP150
HA2 F1	GGTGACTAACAAGGTCA	17	50	HA2	GP120HA2
HA2 F2	TCTGTGGATGTGCAGC	16	50	HA2	GP120HA2/GP140HA2tr
CGP120 R1	CGTAAGACTTTGCATCG	17	50	GP120	GP120HA2/GP140HA2tr/GP150

name	sequence	size	TM	locus	Note
Gagm F1	GGATAAGATCGAGGAAG	17	50	Gag	mosaic Gag
Gagm R1	CCGCTGCATCATGATG	16	50	Gag	mosaic Gag

name	sequence	size	TM	locus
A11_f	GCAAATTTGAACGGGTCTCCC	18	58	Binding site in A11R, outside Gag^M recombination flank
A12_r	GCGATGGATGGTCAGATTGTC	21	64	Binding site in A12L, outside Gag^M recombination flank
G1L r2	GGCCATGTGTAACACTAGAG	20	60	Binding site in G1L, outside Env recombination flank

4 Protein characterization

4.1 SDS-PAGE

Mini-PROTEAN® Electrophoresis System (Bio-Rad, Hercules) was used with 8% resolving / 4% stacking gels cast when required (Appendix C). Samples were boiled for 5 minutes at 95°C in 4x protein loading dye (Appendix C). Gels were run for ~1 hour at 200V using 1x SDS PAGE Running buffer (Appendix C). Color Prestained Protein Standard, Broad Range (NEB, Ipswich) was used for molecular weight determination.

4.2 BN-PAGE

Precast NativePAGE™ Novex® 3-12% Bis-Tris Protein Gels (Thermo Fisher Scientific, Waltham) were run. Anode buffer: dilute 20X NativePAGE™ Running Buffer (Thermo Fisher Scientific, Waltham) 1 in 20. Cathode buffer: dilute 20X NativePAGE™ Running Buffer (Thermo Fisher Scientific, Waltham) 1 in 20 and 20X NativePAGE™ Cathode Additive (Thermo Fisher Scientific, Waltham) 1 in 200. Samples were prepared in 4x NativePAGE® Sample Buffer (Thermo Fisher Scientific, Waltham). Gels were run at 150V for ~2 hours. NativeMark™ Unstained Protein Standard (Thermo Fisher Scientific, Waltham) for native gel electrophoresis was used for estimating molecular weight.

4.3 Coomassie staining

After SDS-PAGE or BN-PAGE, gels were washed 3x in H_2O. Gels were incubated with ~20ml Bio-Safe™ Coomassie Stain (Bio-Rad, Hercules) for 1 hour at room temperature whilst gently shaking. Gels were washed 3x in H_2O again and scanned on an A4-scanner or imaged on a Molecular Imager® Gel Doc™ XR+ Imaging System (Bio-Rad, Hercules).

4.4 Western blotting

Trans-Blot® SD Semi-Dry Transfer Cell (Bio-Rad, Hercules) blotting system was used to transfer protein from SD-PAGE or BN-PAGE gels onto PVDF membranes (Bio-Rad, Hercules) sandwiched between Whatman filter papers (Bio-Rad, Hercules) soaked in 1x transfer buffer (Appendix C). Blotting was performed at 20V for 1 hour after which PVDF membranes were blocked in PBST + 2.5% BSA (block) at room temperature for 1 hour. Primary antibody incubation was performed in block for 2 hours or overnight, followed by 3x 5 minute washes with PBS. AP-linked secondary antibody in block was added for 1 hour at room temperature after which membranes were washed with PBST for 5 minutes (3x) and signal was detected with BCIP/NBT Phosphatase Substrate (KPL, Milford).

4.5 Antibodies and dilutions for western blotting

Primary Antibody	Supplier	dilution
Goat anti-HIV-1 gp120	BioRad 5000-0557	1:1000
Goat anti-HIV-1 p24 (Gag)	BioRad 4999-9007	1:1000
Detection Antibody (secondary)		
mouse monoclonal anti-goat/sheep IgG–AP GT34	Sigma	1:10000

4.6 Protein DC assay

Protein quantification was performed using the DC™ Protein Assay (Bio-Rad, Hercules). A BSA standard (Bio-Rad, Hercules) was used to make a dilution range (20, 16, 12, 8, 4, 2, 1

and 0 mg/ml) in PBS and added in triplicates on a NunC 96 well plate (Sigma, St Louis). Then, triplicate experimental samples were pipetted into separate wells. To each well, 25µl Solution A was added, followed by 200µl Solution B. After 15 minutes incubation at room temperature (whilst slightly shaking), the absorbance at 750nm was measured on a VersaMax ELISA Microplate Reader (Molecular Devices, Sunnyvale). Data was plotted in Microsoft Excel (Microsoft Corporation, Redmond) and a trendline was generated. Experimental protein concentrations were determined from the formula of this trendline.

APPENDIX B. Routine tissue culture protocols

1. Growth and medium of HEK293, HEK293T, RK13, BHK cells and HEK293 CAP256 gp140-FL-IP stable cell line

CHO-K1, HEK293, HEK293T, RK13 and BHK cells were grown in DMEM High Glucose + L-Glutamine (Lonza, Basel) + 10% FCS + 1x Pen/Strep (both Thermo Fisher Scientific, Waltham). Media for CHO and HEK293 stable cell lines (expressing CAP256 gp140-FL-IP or CAP256 gp140-FL-IP-His) was similar with the addition of 6ml Geneticin (Thermo Fisher Scientific, Waltham). Serum-free medium: DMEM High Glucose + L-Glutamine + 1x Pen/Strep.

All cells were grown in a humidified tissue culture incubator at 37°C/5% CO_2. BHK, CHO-K1 and CHO stable cell lines line were split 1 in 8 on Monday and Wednesday and 1 in 12 on Friday. For a T75 flask, media was removed, 2ml of Trypsin (Thermo Fisher Scientific, Waltham) was added for 2-5 minutes in the incubator, flasks were tapped to dislodge cells and 10ml of media was added to inhibit the trypsin. Cells were pipetted up and down to break-up cell-clumps and the appropriate volume was transferred to a new flask. All other cells were split 1 in 4 on Monday and Wednesday and 1 in 8 on Friday.

2. Transfection of cells

Per well of a 24-well plate. Setup two 1.5ml Eppendorf tubes and add 25µl DMEM (room temperature). Add 1µg of DNA to one tube and 3µl branched PEI (Sigma, St Louis) or X-TremeGENE (Roche, Basel) transfection reagent to the second tube. Mix briefly and transfer DMEM + transfection reagent to the tube containing DMEM + DNA. Mix by pipetting and incubate at room temperature for 30 minutes after which add to cells in drop-wise manner. Note: for downstream large scale soluble Env protein isolation, replace medium on cells before transfection to serum-free.

Plate or flask	µg DNA per well or flask	µl transfection reagent per well or flask
24-well	1	3
12-well	2	6
6-well	4	12
T75	30	90
T150	60	180
Special conditions for rMVA recombination		
12-well	2	1.5

APPENDIX C: Buffers, growth media and solutions

Unless stated otherwise, chemicals were acquired from Sigma (St Louis)

1. BUFFERS:

10x PBS: 80 g NaCl + 2.0 g KCl + 14.4 g Na_2HPO_4-$2H_2O$ + 2.4 g KH_2PO_4 in 800ml ddH_2O. Set to pH7.4 using HCl and make up to 1L. Or ordered as 10x PBS (Lonza, Basel). 1x PBS (Lonza, Basel or Thermo Fisher Scientific, Waltham).

PBST: PBS [pH 7.4], 0.1 % Tween20

2. SDS-PAGE

8% resolving gel (for 2 gels): 5.3ml ddH_2O, 2ml 40% acryl-bisacrylamide mix, 2.5ml 1.5M Tris pH8.8, 0.1ml 10% SDS, 0.1ml 10% APS, 6µl TEMED

4% stacking gel (for 2 gels): 3.8ml ddH_2O, 0.5ml 40% acryl-bisacrylamide mix, 0.63ml 1.5M Tris pH6.8, 50µl 10% SDS, 50µl 10% APS, 5µl TEMED

10x SDS page Running buffer. Dissolve: 10g SDS, 30.3g Tris, 29g Glycine into 800ml ddH_2O. Adjust volume to 1000ml. Store at room temperature (SDS will precipitate).

4 × protein loading buffer: 4 ml 100% glycerol, 1.6 ml 1.5 M Tris/HCl [pH6.8], 0.8 SDS, 4 mg bromophenol blue, 0.5 ml β-mercaptoethanol, 3.9 ml H_2O

10x western blotting transfer buffer. Dissolve: 3.7g SDS, 58g Tris, 144.1g Glycine into 800ml ddH_2O. Adjust volume to 1000ml. Store at 4°C. Add 20% methanol for 1x transfer buffer.

3 GROWTH MEDIA:

LB Broth: 10g/l Tryptone, 5g/l NaCl, 5g/l Yeast Extract

LB Agar: 10g/l Tryptone, 5g/l NaCl, 5 g/l Yeast Extract, 15g/l Agar

4. SOLUTIONS:

Resuspension solution (P1 buffer): 50mM glucose, 10mM EDTA, 25mM Tris [pH 8.0], 100µg/ml RNAse (Sigma, St Louis)

Lysis solution (P2 buffer): 0.2 M NaOH, 1% SDS

Neutralizing solution (P3 buffer): 3M KOAc [pH 5.5] (adjusted using glacial acetic acid)

TE: 1mM EDTA, 10mM Tris-HCl, pH 8.0

APPENDIX D: Live-cell staining for Env and Env:HA_2 chimaeric DNA vaccines

Table D.1 Abbreviations for Env and Env:HA2 chimaeric DNA vaccines

Abbreviation	Env insert
DNAC5	CAP256 gp150-FL-IP
DNAC2	CAP256 gp120HA_2-FL
DNAC4	CAP256 gp140HA_2tr-FL-IP

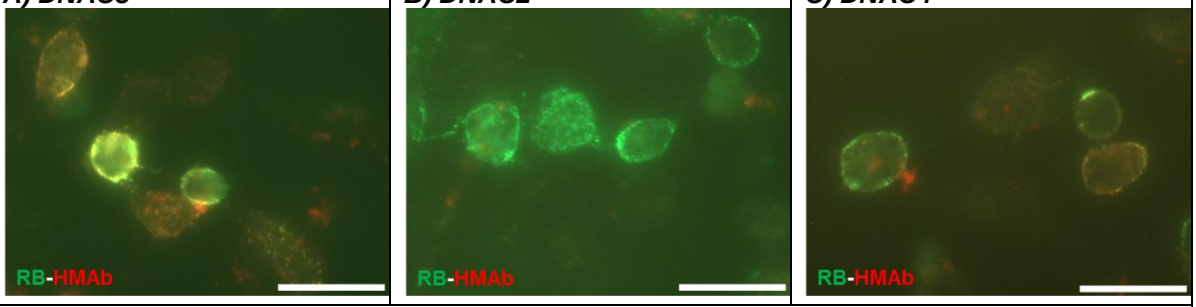

Figure D.1. Live cell staining using bnAb 10E8 against the gp41 MPER domain in HeLa cells transfected with DNA vaccines.
(A-C) HeLa cells transfected with DNA vaccines were visualised by their Env expression using a rabbit α-Env polyclonal antibody which was detected with α-rabbit IgG-FITC (RB; visualised in green). The bnAb 10E8 was detected with anti-human IgG-Cy3 (HMAb; visualised in red). Overlapping signal between the rabbit α-Env polyclonal and bnAb appears as yellow.
Bar represents 20µm

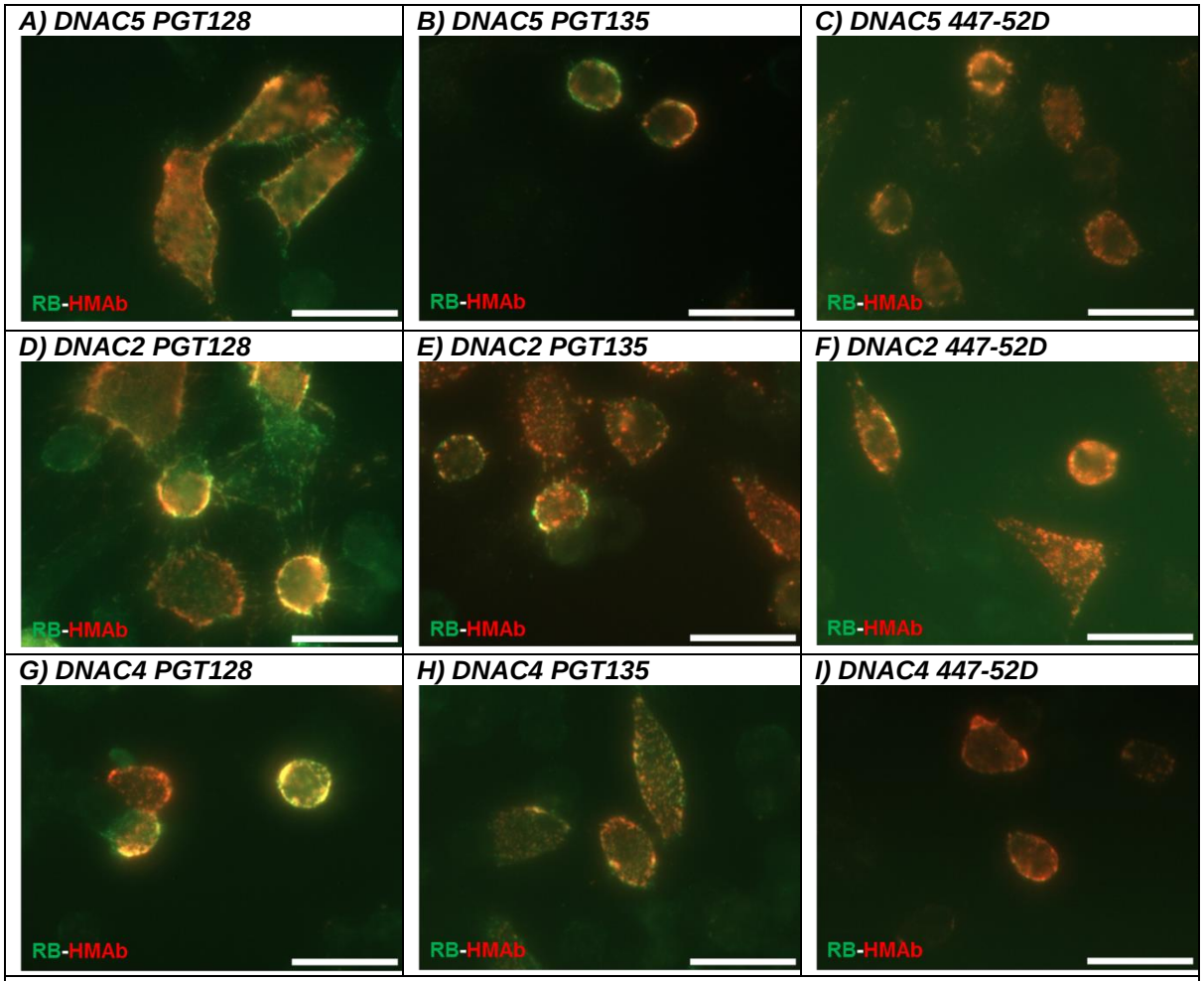

Figure D.2. Live cell staining using bnAbs against the Env V3-glycan supersite of vulnerability in HeLa cells transfected with DNA vaccines.

(A-I) HeLa cells transfected with DNA vaccines were visualised by their Env expression using a rabbit α-Env polyclonal antibody which was detected with α-rabbit IgG-FITC (RB; visualised in green). The bnAbs PGT128, PGT135 and 447-52 were detected with α-human IgG-Cy3 (HMAb; visualised in red). Overlapping signal between the rabbit α-Env polyclonal and bnAbs appears as yellow. PGT128 and PGT135 detect the Env V3-glycan supersite, whereas 447-52 binds the V3 loop of gp120 and not considered broadly neutralising.
Bar represents 20µm.

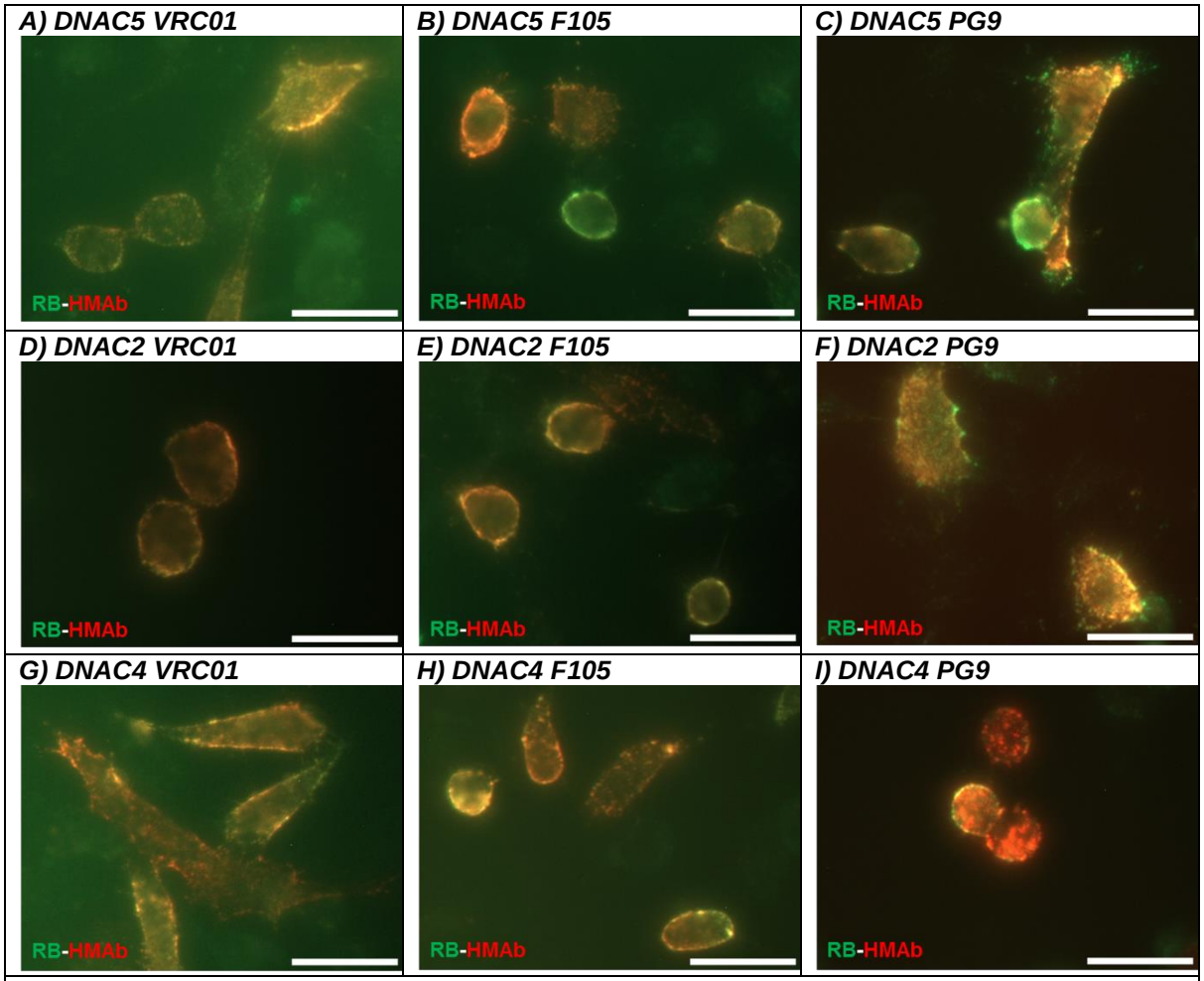

Figure D.3. Live cell staining using bnAbs against the Env CD4 binding site or the non-trimer specific V2-glycan in HeLa cells transfected with DNA vaccines.

(A-I) HeLa cells transfected with DNA vaccines were visualised by their Env expression using a rabbit α-Env polyclonal antibody which was detected with α-rabbit IgG-FITC (RB; visualised in green). The bnAbs VRC01, 447-52D and PG9 were detected with anti-human IgG-Cy3 (HMAb; visualised in red). Overlapping signal between the rabbit α-Env polyclonal and bnAbs appears as yellow. MAbs VRC01 and F105 detect the Env CD4 binding site, whereas PG9 binds the V2-glycan. F105 is not considered broadly neutralising.
Bar represents 20µm.

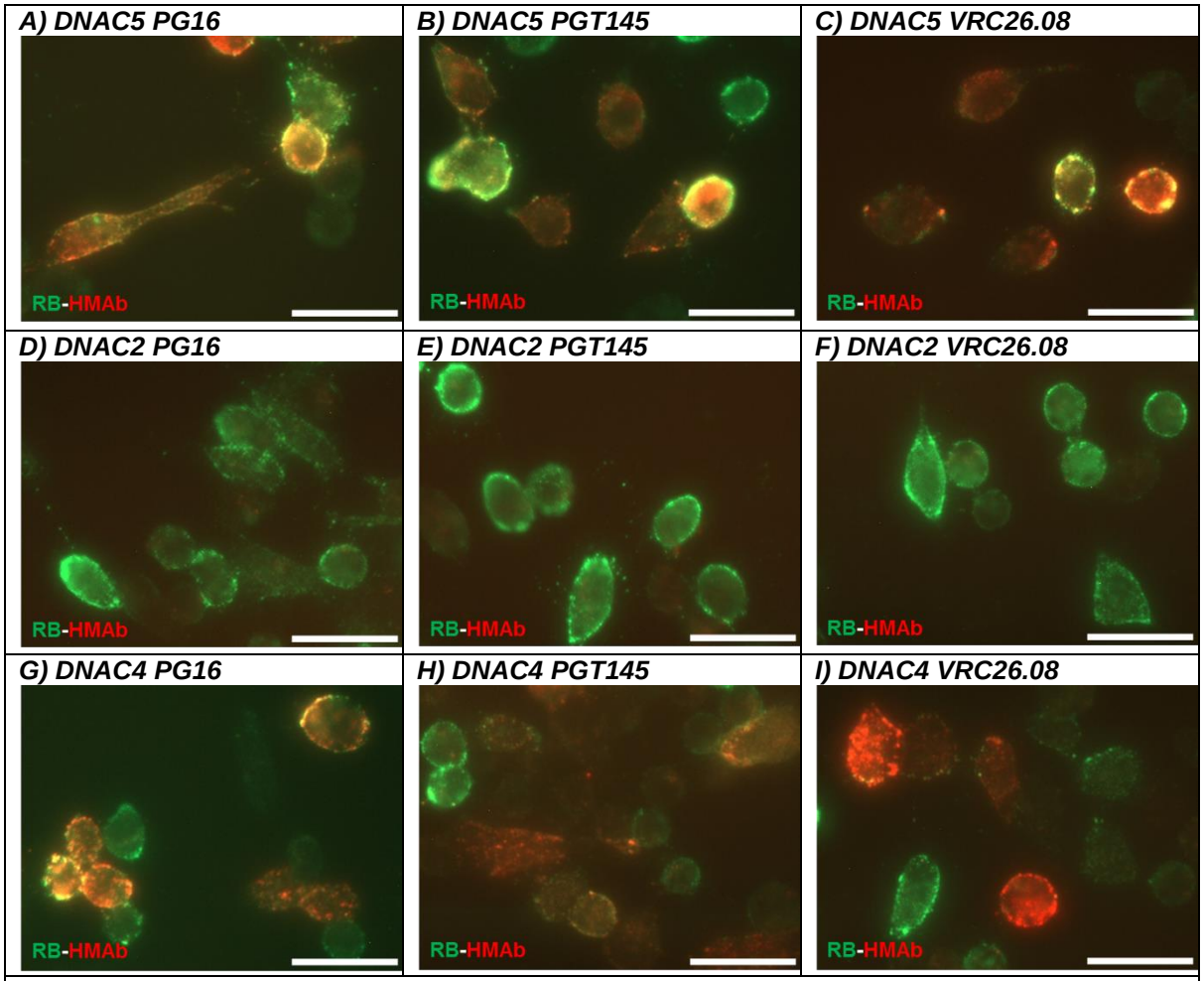

Figure D.4. Live cell staining using bnAbs against the Env trimer specific V2-glycan in HeLa cells transfected with DNA vaccines.

(A-I) HeLa cells transfected with DNA vaccines were visualised by their Env expression using a rabbit α-Env polyclonal antibody which was detected with α-rabbit IgG-FITC (RB; visualised in green). The bnAbs PG16, PGT145 and CAP256 VRC26.08 (VRC26.08) were detected with anti-human IgG-Cy3 (HMAb; visualised in red) and are considered to only detect native-like Env trimers. Overlapping signal between the rabbit α-Env polyclonal and bnAbs appears as yellow.
Bar represents 20µm.

APPENDIX E: Live-cell staining for Env and Env:HA_2 chimaeric MVA vaccines

Table E.1 Abbreviations for Env and Env:HA2 chimaeric DNA vaccines

Abbreviation	Env insert	Mosaic Gag present
MVAC5	CAP256 gp150-FL-IP	x
MVAGC5	CAP256 gp150-FL-IP	Yes
MVAGC2	CAP256 gp120HA_2-FL	Yes
MVAGC4	CAP256 gp140HA_2tr-FL-IP	Yes

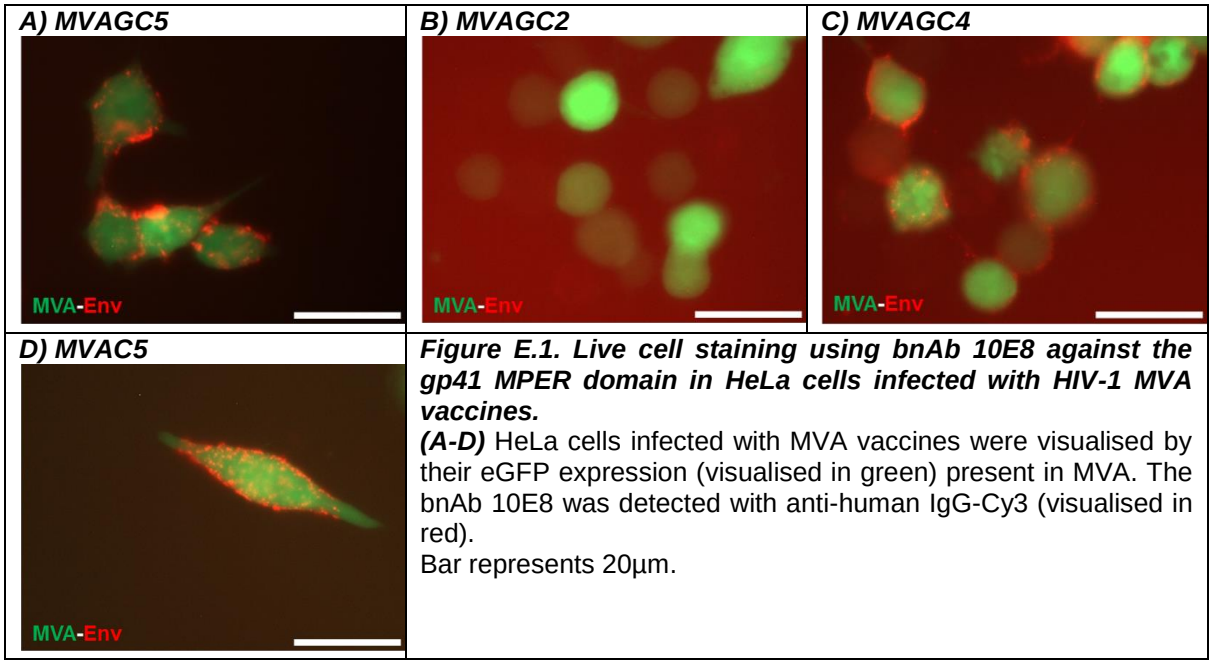

Figure E.1. Live cell staining using bnAb 10E8 against the gp41 MPER domain in HeLa cells infected with HIV-1 MVA vaccines.
(A-D) HeLa cells infected with MVA vaccines were visualised by their eGFP expression (visualised in green) present in MVA. The bnAb 10E8 was detected with anti-human IgG-Cy3 (visualised in red).
Bar represents 20µm.

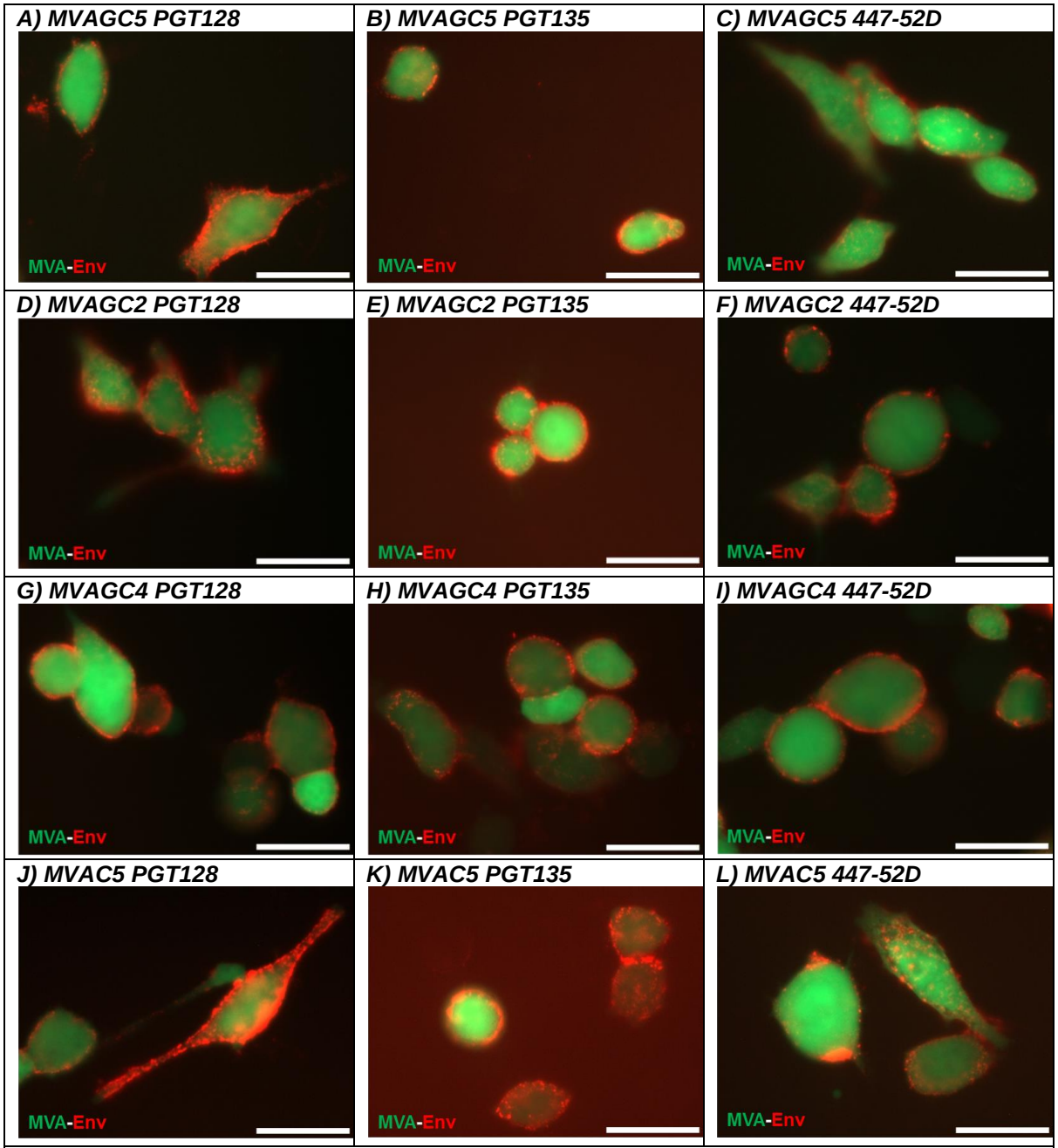

Figure E.2. Live cell staining using bnAbs against the Env V3-glycan supersite of vulnerability in HeLa cells infected with HIV-1 MVA vaccines.

(A-L) HeLa cells infected with MVA vaccines were visualised by their eGFP expression (in green) present in MVA. The bnAbs PGT128, PGT135 and 447-52 were detected with anti-human IgG-Cy3 (in red). PGT128 and PGT135 detect the Env V3-glycan supersite, whereas 447-52 binds the V3 loop of gp120 and is not considered broadly neutralising.
Bar represents 20µm.

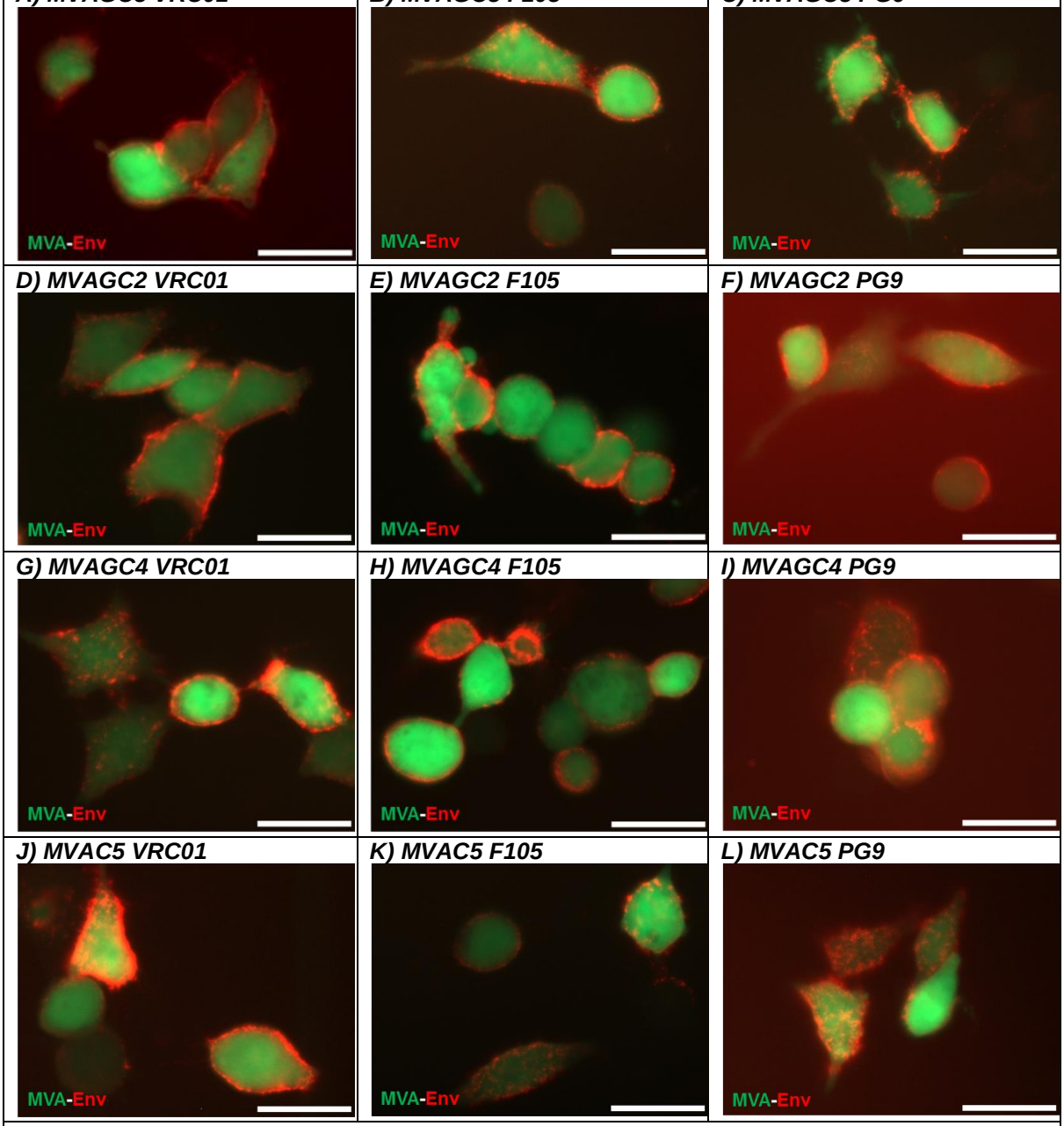

Figure E.3. Live cell staining using bnAbs against the Env CD4 binding site or the non-trimer specific V2-glycan in HeLa cells infected with HIV-1 MVA vaccines.
(A-L) HeLa cells infected with MVA vaccines were visualised by their eGFP expression (in green) present in MVA. The bnAbs VRC01, F105 and PG9 were detected with anti-human IgG-Cy3 (in red). bnAbs VRC01 and F105 detect the Env CD4 binding site, whereas PG9 binds the V2-glycan. F105 is not considered broadly neutralising.
Bar represents 20µm.

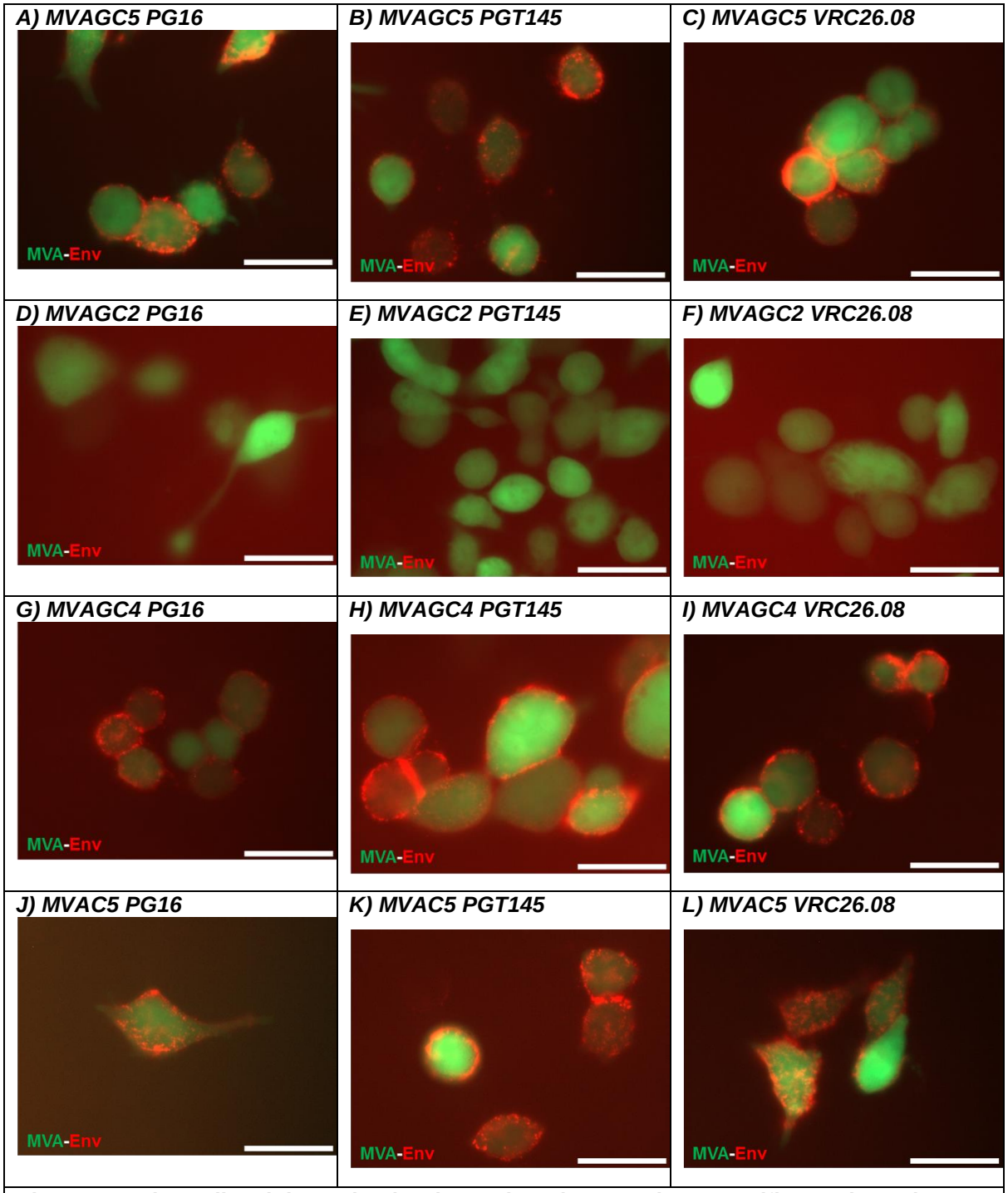

Figure E.4. Live cell staining using bnAbs against the Env trimer specific V2-glycan in HeLa cells infected with HIV-1 MVA vaccines.

(A-L) HeLa cells infected with MVA vaccines were visualised by their eGFP expression (in green) present in MVA. The bnAbs PG16, PGT145 and CAP256 VRC26.08 (VRC26.08) were detected with anti-human IgG-Cy3 (visualised in red) and are considered to only detect native-like Env trimers. Bar represents 20µm.

REFERENCES

1. Barre-Sinoussi, F., et al., *Isolation of a T-lymphotropic retrovirus from a patient at risk for acquired immune deficiency syndrome (AIDS).* Science, 1983. **220**(4599): p. 868-71.
2. Gallo, R.C., et al., *Frequent detection and isolation of cytopathic retroviruses (HTLV-III) from patients with AIDS and at risk for AIDS.* Science, 1984. **224**(4648): p. 500-3.
3. Gottlieb, M.S., et al., *Pneumocystis carinii pneumonia and mucosal candidiasis in previously healthy homosexual men: evidence of a new acquired cellular immunodeficiency.* N Engl J Med, 1981. **305**(24): p. 1425-31.
4. Popovic, M., et al., *Detection, isolation, and continuous production of cytopathic retroviruses (HTLV-III) from patients with AIDS and pre-AIDS.* Science, 1984. **224**(4648): p. 497-500.
5. Korber, B., et al., *Timing the ancestor of the HIV-1 pandemic strains.* Science, 2000. **288**(5472): p. 1789-96.
6. Motulsky, A.G., J. Vandepitte, and G.R. Fraser, *Population genetic studies in the Congo. I. Glucose-6-phosphate dehydrogenase deficiency, hemoglobin S, and malaria.* Am J Hum Genet, 1966. **18**(6): p. 514-37.
7. Nahmias, A.J., et al., *Evidence for human infection with an HTLV III/LAV-like virus in Central Africa, 1959.* Lancet, 1986. **1**(8492): p. 1279-80.
8. Zhu, T., et al., *An African HIV-1 sequence from 1959 and implications for the origin of the epidemic.* Nature, 1998. **391**(6667): p. 594-7.
9. Centers for Disease, C., *Kaposi's sarcoma and Pneumocystis pneumonia among homosexual men--New York City and California.* MMWR Morb Mortal Wkly Rep, 1981. **30**(25): p. 305-8.
10. Cohen, M.S., et al., *Acute HIV-1 Infection.* N Engl J Med, 2011. **364**(20): p. 1943-54.
11. Centers for Disease, C., *Possible transfusion-associated acquired immune deficiency syndrome (AIDS) - California.* MMWR Morb Mortal Wkly Rep, 1982. **31**(48): p. 652-4.
12. Coutsoudis, A., L. Kwaan, and M. Thomson, *Prevention of vertical transmission of HIV-1 in resource-limited settings.* Expert Rev Anti Infect Ther, 2010. **8**(10): p. 1163-75.
13. Hirsch, V.M., et al., *An African primate lentivirus (SIVsm) closely related to HIV-2.* Nature, 1989. **339**(6223): p. 389-92.
14. Gao, F., et al., *Human infection by genetically diverse SIVSM-related HIV-2 in west Africa.* Nature, 1992. **358**(6386): p. 495-9.
15. Chen, Z., et al., *Human immunodeficiency virus type 2 (HIV-2) seroprevalence and characterization of a distinct HIV-2 genetic subtype from the natural range of simian immunodeficiency virus-infected sooty mangabeys.* J Virol, 1997. **71**(5): p. 3953-60.
16. Chen, Z., et al., *Genetic characterization of new West African simian immunodeficiency virus SIVsm: geographic clustering of household-derived SIV strains with human immunodeficiency virus type 2 subtypes and genetically diverse viruses from a single feral sooty mangabey troop.* J Virol, 1996. **70**(6): p. 3617-27.
17. Gao, F., et al., *Genetic diversity of human immunodeficiency virus type 2: evidence for distinct sequence subtypes with differences in virus biology.* J Virol, 1994. **68**(11): p. 7433-47.
18. de Silva, T.I., M. Cotten, and S.L. Rowland-Jones, *HIV-2: the forgotten AIDS virus.* Trends Microbiol, 2008. **16**(12): p. 588-95.
19. Sharp, P.M. and B.H. Hahn, *Origins of HIV and the AIDS pandemic.* Cold Spring Harb Perspect Med, 2011. **1**(1): p. a006841.
20. Plantier, J.C., et al., *A new human immunodeficiency virus derived from gorillas.* Nat Med, 2009. **15**(8): p. 871-2.
21. Keele, B.F., et al., *Chimpanzee reservoirs of pandemic and nonpandemic HIV-1.* Science, 2006. **313**(5786): p. 523-6.
22. Simon, F., et al., *Identification of a new human immunodeficiency virus type 1 distinct from group M and group O.* Nat Med, 1998. **4**(9): p. 1032-7.
23. Gurtler, L.G., et al., *A new subtype of human immunodeficiency virus type 1 (MVP-5180) from Cameroon.* J Virol, 1994. **68**(3): p. 1581-5.
24. Gao, F., et al., *Origin of HIV-1 in the chimpanzee Pan troglodytes troglodytes.* Nature, 1999. **397**(6718): p. 436-41.
25. Van Heuverswyn, F., et al., *Human immunodeficiency viruses: SIV infection in wild gorillas.* Nature, 2006. **444**(7116): p. 164.

26. Hemelaar, J., *The origin and diversity of the HIV-1 pandemic.* Trends Mol Med, 2012. **18**(3): p. 182-92.
27. Osmanov, S., et al., *Estimated global distribution and regional spread of HIV-1 genetic subtypes in the year 2000.* J Acquir Immune Defic Syndr, 2002. **29**(2): p. 184-90.
28. Hemelaar, J., et al., *Global and regional distribution of HIV-1 genetic subtypes and recombinants in 2004.* AIDS, 2006. **20**(16): p. W13-23.
29. Santos, A.F. and M.A. Soares, *HIV Genetic Diversity and Drug Resistance.* Viruses, 2010. **2**(2): p. 503-31.
30. UNAIDS, *FACT SHEET – GLOBAL AIDS UPDATE 2019*. 2019.
31. UNAIDS, *UNAIDS DATA 2019*. 2019, UNAIDS.
32. UNAIDS, *July 2019 Core epidemiology slides*. 2019.
33. Briggs, J.A., et al., *Structural organization of authentic, mature HIV-1 virions and cores.* EMBO J, 2003. **22**(7): p. 1707-15.
34. Checkley, M.A., B.G. Luttge, and E.O. Freed, *HIV-1 envelope glycoprotein biosynthesis, trafficking, and incorporation.* J Mol Biol, 2011. **410**(4): p. 582-608.
35. Sundquist, W.I. and H.G. Krausslich, *HIV-1 assembly, budding, and maturation.* Cold Spring Harb Perspect Med, 2012. **2**(7): p. a006924.
36. Briggs, J.A., et al., *The stoichiometry of Gag protein in HIV-1.* Nat Struct Mol Biol, 2004. **11**(7): p. 672-5.
37. Baumgartel, V., B. Muller, and D.C. Lamb, *Quantitative live-cell imaging of human immunodeficiency virus (HIV-1) assembly.* Viruses, 2012. **4**(5): p. 777-99.
38. Steckbeck, J.D., A.S. Kuhlmann, and R.C. Montelaro, *C-terminal tail of human immunodeficiency virus gp41: functionally rich and structurally enigmatic.* J Gen Virol, 2013. **94**(Pt 1): p. 1-19.
39. Facke, M., et al., *A large deletion in the matrix domain of the human immunodeficiency virus gag gene redirects virus particle assembly from the plasma membrane to the endoplasmic reticulum.* J Virol, 1993. **67**(8): p. 4972-80.
40. Hill, C.P., et al., *Crystal structures of the trimeric human immunodeficiency virus type 1 matrix protein: implications for membrane association and assembly.* Proc Natl Acad Sci U S A, 1996. **93**(7): p. 3099-104.
41. Yu, X., et al., *The matrix protein of human immunodeficiency virus type 1 is required for incorporation of viral envelope protein into mature virions.* J Virol, 1992. **66**(8): p. 4966-71.
42. Dorfman, T., et al., *Role of the matrix protein in the virion association of the human immunodeficiency virus type 1 envelope glycoprotein.* J Virol, 1994. **68**(3): p. 1689-96.
43. Nkeze, J., et al., *Molecular characterization of HIV-1 genome in fission yeast Schizosaccharomyces pombe.* Cell Biosci, 2015. **5**: p. 47.
44. Pornillos, O., et al., *X-ray structures of the hexameric building block of the HIV capsid.* Cell, 2009. **137**(7): p. 1282-92.
45. Pornillos, O., B.K. Ganser-Pornillos, and M. Yeager, *Atomic-level modelling of the HIV capsid.* Nature, 2011. **469**(7330): p. 424-7.
46. Berkowitz, R.D. and S.P. Goff, *Analysis of binding elements in the human immunodeficiency virus type 1 genomic RNA and nucleocapsid protein.* Virology, 1994. **202**(1): p. 233-46.
47. Levin, J.G., et al., *Role of HIV-1 nucleocapsid protein in HIV-1 reverse transcription.* RNA Biol, 2010. **7**(6): p. 754-74.
48. Muriaux, D. and J.L. Darlix, *Properties and functions of the nucleocapsid protein in virus assembly.* RNA Biol, 2010. **7**(6): p. 744-53.
49. Bachand, F., et al., *Incorporation of Vpr into human immunodeficiency virus type 1 requires a direct interaction with the p6 domain of the p55 gag precursor.* J Biol Chem, 1999. **274**(13): p. 9083-91.
50. Fujii, K., J.H. Hurley, and E.O. Freed, *Beyond Tsg101: the role of Alix in 'ESCRTing' HIV-1.* Nat Rev Microbiol, 2007. **5**(12): p. 912-6.
51. Gottlinger, H.G., et al., *Effect of mutations affecting the p6 gag protein on human immunodeficiency virus particle release.* Proc Natl Acad Sci U S A, 1991. **88**(8): p. 3195-9.
52. Kondo, E., et al., *The p6gag domain of human immunodeficiency virus type 1 is sufficient for the incorporation of Vpr into heterologous viral particles.* J Virol, 1995. **69**(5): p. 2759-64.
53. Lu, M., S.C. Blacklow, and P.S. Kim, *A trimeric structural domain of the HIV-1 transmembrane glycoprotein.* Nat Struct Biol, 1995. **2**(12): p. 1075-82.
54. Jacks, T., et al., *Characterization of ribosomal frameshifting in HIV-1 gag-pol expression.* Nature, 1988. **331**(6153): p. 280-3.

55. Freed, E.O., *HIV-1 assembly, release and maturation.* Nat Rev Microbiol, 2015. **13**(8): p. 484-96.
56. Hill, M., G. Tachedjian, and J. Mak, *The packaging and maturation of the HIV-1 Pol proteins.* Curr HIV Res, 2005. **3**(1): p. 73-85.
57. Hu, W.S. and S.H. Hughes, *HIV-1 reverse transcription.* Cold Spring Harb Perspect Med, 2012. **2**(10).
58. Craigie, R. and F.D. Bushman, *HIV DNA integration.* Cold Spring Harb Perspect Med, 2012. **2**(7): p. a006890.
59. Chiu, T.K. and D.R. Davies, *Structure and function of HIV-1 integrase.* Curr Top Med Chem, 2004. **4**(9): p. 965-77.
60. Hoffman, A.D., B. Banapour, and J.A. Levy, *Characterization of the AIDS-associated retrovirus reverse transcriptase and optimal conditions for its detection in virions.* Virology, 1985. **147**(2): p. 326-35.
61. Pearl, L.H. and W.R. Taylor, *A structural model for the retroviral proteases.* Nature, 1987. **329**(6137): p. 351-4.
62. Feinberg, M.B., et al., *HTLV-III expression and production involve complex regulation at the levels of splicing and translation of viral RNA.* Cell, 1986. **46**(6): p. 807-17.
63. Fisher, A.G., et al., *The trans-activator gene of HTLV-III is essential for virus replication.* Nature, 1986. **320**(6060): p. 367-71.
64. Garcia, J.A., et al., *Functional domains required for tat-induced transcriptional activation of the HIV-1 long terminal repeat.* EMBO J, 1988. **7**(10): p. 3143-7.
65. Sodroski, J., et al., *A second post-transcriptional trans-activator gene required for HTLV-III replication.* Nature, 1986. **321**(6068): p. 412-7.
66. Kerkau, T., et al., *The human immunodeficiency virus type 1 (HIV-1) Vpu protein interferes with an early step in the biosynthesis of major histocompatibility complex (MHC) class I molecules.* J Exp Med, 1997. **185**(7): p. 1295-305.
67. Sheehy, A.M., et al., *Isolation of a human gene that inhibits HIV-1 infection and is suppressed by the viral Vif protein.* Nature, 2002. **418**(6898): p. 646-50.
68. Rose, K.M., et al., *The viral infectivity factor (Vif) of HIV-1 unveiled.* Trends Mol Med, 2004. **10**(6): p. 291-7.
69. Frankel, A.D. and J.A. Young, *HIV-1: fifteen proteins and an RNA.* Annu Rev Biochem, 1998. **67**: p. 1-25.
70. Willey, R.L., et al., *Human immunodeficiency virus type 1 Vpu protein regulates the formation of intracellular gp160-CD4 complexes.* J Virol, 1992. **66**(1): p. 226-34.
71. Willey, R.L., et al., *Human immunodeficiency virus type 1 Vpu protein induces rapid degradation of CD4.* J Virol, 1992. **66**(12): p. 7193-200.
72. Buonocore, L. and J.K. Rose, *Prevention of HIV-1 glycoprotein transport by soluble CD4 retained in the endoplasmic reticulum.* Nature, 1990. **345**(6276): p. 625-8.
73. Malim, M.H. and M. Emerman, *HIV-1 accessory proteins--ensuring viral survival in a hostile environment.* Cell Host Microbe, 2008. **3**(6): p. 388-98.
74. Affram, Y., et al., *The HIV-1 antisense protein ASP is a transmembrane protein of the cell surface and an integral protein of the HIV-1 viral envelope.* J Virol, 2019.
75. Bet, A., et al., *The HIV-1 antisense protein (ASP) induces CD8 T cell responses during chronic infection.* Retrovirology, 2015. **12**: p. 15.
76. Champiat, S., et al., *Influence of HAART on alternative reading frame immune responses over the course of HIV-1 infection.* PLoS One, 2012. **7**(6): p. e39311.
77. Vanhee-Brossollet, C., et al., *A natural antisense RNA derived from the HIV-1 env gene encodes a protein which is recognized by circulating antibodies of HIV+ individuals.* Virology, 1995. **206**(1): p. 196-202.
78. Miller, R.H., *Human immunodeficiency virus may encode a novel protein on the genomic DNA plus strand.* Science, 1988. **239**(4846): p. 1420-2.
79. Zhang, X., et al., *Non-coding RNAs and retroviruses.* Retrovirology, 2018. **15**(1): p. 20.
80. Raja, A., et al., *CD4 binding site antibodies inhibit human immunodeficiency virus gp120 envelope glycoprotein interaction with CCR5.* J Virol, 2003. **77**(1): p. 713-8.
81. Starcich, B.R., et al., *Identification and characterization of conserved and variable regions in the envelope gene of HTLV-III/LAV, the retrovirus of AIDS.* Cell, 1986. **45**(5): p. 637-48.
82. Willey, R.L., et al., *Identification of conserved and divergent domains within the envelope gene of the acquired immunodeficiency syndrome retrovirus.* Proc Natl Acad Sci U S A, 1986. **83**(14): p. 5038-42.

83. Leonard, C.K., et al., *Assignment of intrachain disulfide bonds and characterization of potential glycosylation sites of the type 1 recombinant human immunodeficiency virus envelope glycoprotein (gp120) expressed in Chinese hamster ovary cells.* J Biol Chem, 1990. **265**(18): p. 10373-82.
84. Kwong, P.D., et al., *Structure of an HIV gp120 envelope glycoprotein in complex with the CD4 receptor and a neutralizing human antibody.* Nature, 1998. **393**(6686): p. 648-59.
85. Bosch, M.L., et al., *Identification of the fusion peptide of primate immunodeficiency viruses.* Science, 1989. **244**(4905): p. 694-7.
86. Freed, E.O., D.J. Myers, and R. Risser, *Characterization of the fusion domain of the human immunodeficiency virus type 1 envelope glycoprotein gp41.* Proc Natl Acad Sci U S A, 1990. **87**(12): p. 4650-4.
87. Weissenhorn, W., et al., *Atomic structure of the ectodomain from HIV-1 gp41.* Nature, 1997. **387**(6631): p. 426-30.
88. Drummer, H.E., et al., *Allosteric modulation of the HIV-1 gp120-gp41 association site by adjacent gp120 variable region 1 (V1) N-glycans linked to neutralization sensitivity.* PLoS Pathog, 2013. **9**(4): p. e1003218.
89. Pancera, M., et al., *Structure and immune recognition of trimeric pre-fusion HIV-1 Env.* Nature, 2014. **514**(7523): p. 455-61.
90. Julien, J.P., et al., *Crystal structure of a soluble cleaved HIV-1 envelope trimer.* Science, 2013. **342**(6165): p. 1477-83.
91. Dev, J., et al., *Structural basis for membrane anchoring of HIV-1 envelope spike.* Science, 2016. **353**(6295): p. 172-5.
92. Lyumkis, D., et al., *Cryo-EM structure of a fully glycosylated soluble cleaved HIV-1 envelope trimer.* Science, 2013. **342**(6165): p. 1484-90.
93. Jardine, J., et al., *Rational HIV immunogen design to target specific germline B cell receptors.* Science, 2013. **340**(6133): p. 711-6.
94. McGuire, A.T., et al., *Engineering HIV envelope protein to activate germline B cell receptors of broadly neutralizing anti-CD4 binding site antibodies.* J Exp Med, 2013. **210**(4): p. 655-63.
95. Bartesaghi, A., et al., *Prefusion structure of trimeric HIV-1 envelope glycoprotein determined by cryo-electron microscopy.* Nat Struct Mol Biol, 2013. **20**(12): p. 1352-7.
96. Klein, F., et al., *Antibodies in HIV-1 vaccine development and therapy.* Science, 2013. **341**(6151): p. 1199-204.
97. Brenchley, J.M. and D.C. Douek, *The mucosal barrier and immune activation in HIV pathogenesis.* Curr Opin HIV AIDS, 2008. **3**(3): p. 356-61.
98. Garg, H. and A. Joshi, *Host and Viral Factors in HIV-Mediated Bystander Apoptosis.* Viruses, 2017. **9**(8).
99. Ringel, O., et al., *The Hard Way towards an Antibody-Based HIV-1 Env Vaccine: Lessons from Other Viruses.* Viruses, 2018. **10**(4).
100. Burton, D.R. and L. Hangartner, *Broadly Neutralizing Antibodies to HIV and Their Role in Vaccine Design.* Annu Rev Immunol, 2016. **34**: p. 635-59.
101. Zhu, P., et al., *Electron tomography analysis of envelope glycoprotein trimers on HIV and simian immunodeficiency virus virions.* Proc Natl Acad Sci U S A, 2003. **100**(26): p. 15812-7.
102. Zhu, P., et al., *Distribution and three-dimensional structure of AIDS virus envelope spikes.* Nature, 2006. **441**(7095): p. 847-52.
103. Bachmann, M.F., et al., *The influence of antigen organization on B cell responsiveness.* Science, 1993. **262**(5138): p. 1448-51.
104. Dintzis, H.M., R.Z. Dintzis, and B. Vogelstein, *Molecular determinants of immunogenicity: the immunon model of immune response.* Proc Natl Acad Sci U S A, 1976. **73**(10): p. 3671-5.
105. Klein, J.S. and P.J. Bjorkman, *Few and far between: how HIV may be evading antibody avidity.* PLoS Pathog, 2010. **6**(5): p. e1000908.
106. Hallenberger, S., et al., *Inhibition of furin-mediated cleavage activation of HIV-1 glycoprotein gp160.* Nature, 1992. **360**(6402): p. 358-61.
107. Ringe, R.P., et al., *Cleavage strongly influences whether soluble HIV-1 envelope glycoprotein trimers adopt a native-like conformation.* Proc Natl Acad Sci U S A, 2013. **110**(45): p. 18256-61.
108. Lasky, L.A., et al., *Neutralization of the AIDS retrovirus by antibodies to a recombinant envelope glycoprotein.* Science, 1986. **233**(4760): p. 209-12.
109. Stewart-Jones, G.B., et al., *Trimeric HIV-1-Env Structures Define Glycan Shields from Clades A, B, and G.* Cell, 2016. **165**(4): p. 813-26.

110. Wei, X., et al., *Antibody neutralization and escape by HIV-1.* Nature, 2003. **422**(6929): p. 307-12.
111. Moore, P.L., et al., *Nature of nonfunctional envelope proteins on the surface of human immunodeficiency virus type 1.* J Virol, 2006. **80**(5): p. 2515-28.
112. Sanders, R.W. and J.P. Moore, *Native-like Env trimers as a platform for HIV-1 vaccine design.* Immunol Rev, 2017. **275**(1): p. 161-182.
113. Munro, J.B., et al., *Conformational dynamics of single HIV-1 envelope trimers on the surface of native virions.* Science, 2014. **346**(6210): p. 759-63.
114. Joseph, S.B. and R. Swanstrom, *The evolution of HIV-1 entry phenotypes as a guide to changing target cells.* J Leukoc Biol, 2018. **103**(3): p. 421-431.
115. Burton, D.R. and J.R. Mascola, *Antibody responses to envelope glycoproteins in HIV-1 infection.* Nat Immunol, 2015. **16**(6): p. 571-6.
116. Tomaras, G.D., et al., *Initial B-cell responses to transmitted human immunodeficiency virus type 1: virion-binding immunoglobulin M (IgM) and IgG antibodies followed by plasma anti-gp41 antibodies with ineffective control of initial viremia.* J Virol, 2008. **82**(24): p. 12449-63.
117. Richman, D.D., et al., *Rapid evolution of the neutralizing antibody response to HIV type 1 infection.* Proc Natl Acad Sci U S A, 2003. **100**(7): p. 4144-9.
118. Li, B., et al., *Evidence for potent autologous neutralizing antibody titers and compact envelopes in early infection with subtype C human immunodeficiency virus type 1.* J Virol, 2006. **80**(11): p. 5211-8.
119. Moore, P.L., et al., *The c3-v4 region is a major target of autologous neutralizing antibodies in human immunodeficiency virus type 1 subtype C infection.* J Virol, 2008. **82**(4): p. 1860-9.
120. Rong, R., et al., *Role of V1V2 and other human immunodeficiency virus type 1 envelope domains in resistance to autologous neutralization during clade C infection.* J Virol, 2007. **81**(3): p. 1350-9.
121. Gray, E.S., et al., *The neutralization breadth of HIV-1 develops incrementally over four years and is associated with CD4+ T cell decline and high viral load during acute infection.* J Virol, 2011. **85**(10): p. 4828-40.
122. Doria-Rose, N.A., et al., *Frequency and phenotype of human immunodeficiency virus envelope-specific B cells from patients with broadly cross-neutralizing antibodies.* J Virol, 2009. **83**(1): p. 188-99.
123. Li, Y., et al., *Broad HIV-1 neutralization mediated by CD4-binding site antibodies.* Nat Med, 2007. **13**(9): p. 1032-4.
124. Sather, D.N., et al., *Factors associated with the development of cross-reactive neutralizing antibodies during human immunodeficiency virus type 1 infection.* J Virol, 2009. **83**(2): p. 757-69.
125. Simek, M.D., et al., *Human immunodeficiency virus type 1 elite neutralizers: individuals with broad and potent neutralizing activity identified by using a high-throughput neutralization assay together with an analytical selection algorithm.* J Virol, 2009. **83**(14): p. 7337-48.
126. Doria-Rose, N.A., et al., *Breadth of human immunodeficiency virus-specific neutralizing activity in sera: clustering analysis and association with clinical variables.* J Virol, 2010. **84**(3): p. 1631-6.
127. Euler, Z., et al., *Cross-reactive neutralizing humoral immunity does not protect from HIV type 1 disease progression.* J Infect Dis, 2010. **201**(7): p. 1045-53.
128. Hraber, P., et al., *Prevalence of broadly neutralizing antibody responses during chronic HIV-1 infection.* AIDS, 2014. **28**(2): p. 163-9.
129. Landais, E., et al., *Broadly Neutralizing Antibody Responses in a Large Longitudinal Sub-Saharan HIV Primary Infection Cohort.* PLoS Pathog, 2016. **12**(1): p. e1005369.
130. Walker, L.M., et al., *A limited number of antibody specificities mediate broad and potent serum neutralization in selected HIV-1 infected individuals.* PLoS Pathog, 2010. **6**(8): p. e1001028.
131. Freund, N.T., et al., *Coexistence of potent HIV-1 broadly neutralizing antibodies and antibody-sensitive viruses in a viremic controller.* Sci Transl Med, 2017. **9**(373).
132. Blish, C.A., et al., *Human immunodeficiency virus type 1 superinfection occurs despite relatively robust neutralizing antibody responses.* J Virol, 2008. **82**(24): p. 12094-103.
133. Baba, T.W., et al., *Human neutralizing monoclonal antibodies of the IgG1 subtype protect against mucosal simian-human immunodeficiency virus infection.* Nat Med, 2000. **6**(2): p. 200-6.

134. Deruaz, M., et al., *Protection of Humanized Mice From Repeated Intravaginal HIV Challenge by Passive Immunization: A Model for Studying the Efficacy of Neutralizing Antibodies In Vivo.* J Infect Dis, 2016. **214**(4): p. 612-6.
135. Gauduin, M.C., et al., *Passive immunization with a human monoclonal antibody protects hu-PBL-SCID mice against challenge by primary isolates of HIV-1.* Nat Med, 1997. **3**(12): p. 1389-93.
136. Gautam, R., et al., *A single injection of anti-HIV-1 antibodies protects against repeated SHIV challenges.* Nature, 2016. **533**(7601): p. 105-109.
137. Hessell, A.J., et al., *Effective, low-titer antibody protection against low-dose repeated mucosal SHIV challenge in macaques.* Nat Med, 2009. **15**(8): p. 951-4.
138. Hessell, A.J., et al., *Broadly neutralizing monoclonal antibodies 2F5 and 4E10 directed against the human immunodeficiency virus type 1 gp41 membrane-proximal external region protect against mucosal challenge by simian-human immunodeficiency virus SHIVBa-L.* J Virol, 2010. **84**(3): p. 1302-13.
139. Julg, B., et al., *Protection against a mixed SHIV challenge by a broadly neutralizing antibody cocktail.* Sci Transl Med, 2017. **9**(408).
140. Julg, B., et al., *Broadly neutralizing antibodies targeting the HIV-1 envelope V2 apex confer protection against a clade C SHIV challenge.* Sci Transl Med, 2017. **9**(406).
141. Mascola, J.R., et al., *Protection of Macaques against pathogenic simian/human immunodeficiency virus 89.6PD by passive transfer of neutralizing antibodies.* J Virol, 1999. **73**(5): p. 4009-18.
142. Mascola, J.R., et al., *Protection of macaques against vaginal transmission of a pathogenic HIV-1/SIV chimeric virus by passive infusion of neutralizing antibodies.* Nat Med, 2000. **6**(2): p. 207-10.
143. Parren, P.W., et al., *Protection against HIV-1 infection in hu-PBL-SCID mice by passive immunization with a neutralizing human monoclonal antibody against the gp120 CD4-binding site.* AIDS, 1995. **9**(6): p. F1-6.
144. Parren, P.W., et al., *Antibody protects macaques against vaginal challenge with a pathogenic R5 simian/human immunodeficiency virus at serum levels giving complete neutralization in vitro.* J Virol, 2001. **75**(17): p. 8340-7.
145. Pietzsch, J., et al., *A mouse model for HIV-1 entry.* Proc Natl Acad Sci U S A, 2012. **109**(39): p. 15859-64.
146. Saunders, K.O., et al., *Sustained Delivery of a Broadly Neutralizing Antibody in Nonhuman Primates Confers Long-Term Protection against Simian/Human Immunodeficiency Virus Infection.* J Virol, 2015. **89**(11): p. 5895-903.
147. Shingai, M., et al., *Passive transfer of modest titers of potent and broadly neutralizing anti-HIV monoclonal antibodies block SHIV infection in macaques.* J Exp Med, 2014. **211**(10): p. 2061-74.
148. Stoddart, C.A., et al., *Efficacy of broadly neutralizing monoclonal antibody PG16 in HIV-infected humanized mice.* Virology, 2014. **462-463**: p. 115-25.
149. Sun, M., et al., *VRC01 antibody protects against vaginal and rectal transmission of human immunodeficiency virus 1 in hu-BLT mice.* Arch Virol, 2016. **161**(9): p. 2449-55.
150. Veselinovic, M., et al., *Topical gel formulation of broadly neutralizing anti-HIV-1 monoclonal antibody VRC01 confers protection against HIV-1 vaginal challenge in a humanized mouse model.* Virology, 2012. **432**(2): p. 505-10.
151. Seabright, G.E., et al., *Protein and Glycan Mimicry in HIV Vaccine Design.* J Mol Biol, 2019. **431**(12): p. 2223-2247.
152. Pegu, A., et al., *Neutralizing antibodies to HIV-1 envelope protect more effectively in vivo than those to the CD4 receptor.* Sci Transl Med, 2014. **6**(243): p. 243ra88.
153. Subbaraman, H., M. Schanz, and A. Trkola, *Broadly neutralizing antibodies: What is needed to move from a rare event in HIV-1 infection to vaccine efficacy?* Retrovirology, 2018. **15**(1): p. 52.
154. Burton, D.R., et al., *Efficient neutralization of primary isolates of HIV-1 by a recombinant human monoclonal antibody.* Science, 1994. **266**(5187): p. 1024-7.
155. Trkola, A., et al., *Human monoclonal antibody 2G12 defines a distinctive neutralization epitope on the gp120 glycoprotein of human immunodeficiency virus type 1.* J Virol, 1996. **70**(2): p. 1100-8.
156. Scanlan, C.N., et al., *The broadly neutralizing anti-human immunodeficiency virus type 1 antibody 2G12 recognizes a cluster of alpha1-->2 mannose residues on the outer face of gp120.* J Virol, 2002. **76**(14): p. 7306-21.

157. Sanders, R.W., et al., *The mannose-dependent epitope for neutralizing antibody 2G12 on human immunodeficiency virus type 1 glycoprotein gp120.* J Virol, 2002. **76**(14): p. 7293-305.
158. Muster, T., et al., *A conserved neutralizing epitope on gp41 of human immunodeficiency virus type 1.* J Virol, 1993. **67**(11): p. 6642-7.
159. Zwick, M.B., et al., *Broadly neutralizing antibodies targeted to the membrane-proximal external region of human immunodeficiency virus type 1 glycoprotein gp41.* J Virol, 2001. **75**(22): p. 10892-905.
160. Walker, L.M., et al., *Broad neutralization coverage of HIV by multiple highly potent antibodies.* Nature, 2011. **477**(7365): p. 466-70.
161. Walker, L.M., et al., *Broad and potent neutralizing antibodies from an African donor reveal a new HIV-1 vaccine target.* Science, 2009. **326**(5950): p. 285-9.
162. Sok, D., et al., *Recombinant HIV envelope trimer selects for quaternary-dependent antibodies targeting the trimer apex.* Proc Natl Acad Sci U S A, 2014. **111**(49): p. 17624-9.
163. Wu, X., et al., *Rational design of envelope identifies broadly neutralizing human monoclonal antibodies to HIV-1.* Science, 2010. **329**(5993): p. 856-61.
164. Scheid, J.F., et al., *Broad diversity of neutralizing antibodies isolated from memory B cells in HIV-infected individuals.* Nature, 2009. **458**(7238): p. 636-40.
165. Wibmer, C.K., P.L. Moore, and L. Morris, *HIV broadly neutralizing antibody targets.* Curr Opin HIV AIDS, 2015. **10**(3): p. 135-43.
166. Wang, Q. and L. Zhang, *Broadly neutralizing antibodies and vaccine design against HIV-1 infection.* Front Med, 2020. **14**(1): p. 30-42.
167. Moore, P.L., et al., *Multiple pathways of escape from HIV broadly cross-neutralizing V2-dependent antibodies.* J Virol, 2013. **87**(9): p. 4882-94.
168. Gorny, M.K., et al., *Neutralization of diverse human immunodeficiency virus type 1 variants by an anti-V3 human monoclonal antibody.* J Virol, 1992. **66**(12): p. 7538-42.
169. Posner, M.R., et al., *An IgG human monoclonal antibody that reacts with HIV-1/GP120, inhibits virus binding to cells, and neutralizes infection.* J Immunol, 1991. **146**(12): p. 4325-32.
170. Zhou, T., et al., *Structural basis for broad and potent neutralization of HIV-1 by antibody VRC01.* Science, 2010. **329**(5993): p. 811-7.
171. Lynch, R.M., et al., *HIV-1 fitness cost associated with escape from the VRC01 class of CD4 binding site neutralizing antibodies.* J Virol, 2015. **89**(8): p. 4201-13.
172. Kong, L., et al., *Supersite of immune vulnerability on the glycosylated face of HIV-1 envelope glycoprotein gp120.* Nat Struct Mol Biol, 2013. **20**(7): p. 796-803.
173. Pejchal, R., et al., *A potent and broad neutralizing antibody recognizes and penetrates the HIV glycan shield.* Science, 2011. **334**(6059): p. 1097-103.
174. Doria-Rose, N.A., et al., *Developmental pathway for potent V1V2-directed HIV-neutralizing antibodies.* Nature, 2014. **509**(7498): p. 55-62.
175. Huang, J., et al., *Broad and potent neutralization of HIV-1 by a gp41-specific human antibody.* Nature, 2012. **491**(7424): p. 406-12.
176. Addo-Yobo, E.O. and H. Lovel, *How well are hospitals preventing iatrogenic HIV? A study of the appropriateness of blood transfusions in three hospitals in the Ashanti region, Ghana.* Trop Doct, 1991. **21**(4): p. 162-4.
177. Heymann, S.J. and T.F. Brewer, *The problem of transfusion-associated acquired immunodeficiency syndrome in Africa: a quantitative approach.* Am J Infect Control, 1992. **20**(5): p. 256-62.
178. Cates, W., Jr., *Review of non-hormonal contraception (condoms, intrauterine devices, nonoxynol-9 and combos) on HIV acquisition.* J Acquir Immune Defic Syndr, 2005. **38 Suppl 1**: p. S8-10.
179. de Vincenzi, I., *A longitudinal study of human immunodeficiency virus transmission by heterosexual partners. European Study Group on Heterosexual Transmission of HIV.* N Engl J Med, 1994. **331**(6): p. 341-6.
180. Giannou, F.K., et al., *Condom effectiveness in reducing heterosexual HIV transmission: a systematic review and meta-analysis of studies on HIV serodiscordant couples.* Expert Rev Pharmacoecon Outcomes Res, 2016. **16**(4): p. 489-99.
181. Saracco, A., et al., *Man-to-woman sexual transmission of HIV: longitudinal study of 343 steady partners of infected men.* J Acquir Immune Defic Syndr (1988), 1993. **6**(5): p. 497-502.
182. Weller, S. and K. Davis, *Condom effectiveness in reducing heterosexual HIV transmission.* Cochrane Database Syst Rev, 2002(1): p. CD003255.
183. Cayley, W.E., Jr., *Effectiveness of condoms in reducing heterosexual transmission of HIV.* Am Fam Physician, 2004. **70**(7): p. 1268-9.

184. Johnson, W.D., A. O'Leary, and S.A. Flores, *Per-partner condom effectiveness against HIV for men who have sex with men.* AIDS, 2018. **32**(11): p. 1499-1505.
185. Vlahov, D., A.M. Robertson, and S.A. Strathdee, *Prevention of HIV infection among injection drug users in resource-limited settings.* Clin Infect Dis, 2010. **50 Suppl 3**: p. S114-21.
186. Auvert, B., et al., *Randomized, controlled intervention trial of male circumcision for reduction of HIV infection risk: the ANRS 1265 Trial.* PLoS Med, 2005. **2**(11): p. e298.
187. Bailey, R.C., et al., *Male circumcision for HIV prevention in young men in Kisumu, Kenya: a randomised controlled trial.* Lancet, 2007. **369**(9562): p. 643-56.
188. Gray, R.H., et al., *Male circumcision for HIV prevention in men in Rakai, Uganda: a randomised trial.* Lancet, 2007. **369**(9562): p. 657-66.
189. Mehta, S.D., et al., *The long-term efficacy of medical male circumcision against HIV acquisition.* AIDS, 2013. **27**(18): p. 2899-907.
190. Antiretroviral Therapy Cohort, C., *Survival of HIV-positive patients starting antiretroviral therapy between 1996 and 2013: a collaborative analysis of cohort studies.* Lancet HIV, 2017. **4**(8): p. e349-e356.
191. Harrison, K.M., R. Song, and X. Zhang, *Life expectancy after HIV diagnosis based on national HIV surveillance data from 25 states, United States.* J Acquir Immune Defic Syndr, 2010. **53**(1): p. 124-30.
192. McManus, H., et al., *Long-term survival in HIV positive patients with up to 15 Years of antiretroviral therapy.* PLoS One, 2012. **7**(11): p. e48839.
193. Monforte, A., et al., *HIV-induced immunodeficiency and mortality from AIDS-defining and non-AIDS-defining malignancies.* AIDS, 2008. **22**(16): p. 2143-53.
194. Porter, K., et al., *Determinants of survival following HIV-1 seroconversion after the introduction of HAART.* Lancet, 2003. **362**(9392): p. 1267-74.
195. Smith, C.J., et al., *Trends in underlying causes of death in people with HIV from 1999 to 2011 (D:A:D): a multicohort collaboration.* Lancet, 2014. **384**(9939): p. 241-8.
196. Cohen, M.S., et al., *Antiretroviral Therapy for the Prevention of HIV-1 Transmission.* N Engl J Med, 2016. **375**(9): p. 830-9.
197. Cohen, M.S., et al., *Prevention of HIV-1 infection with early antiretroviral therapy.* N Engl J Med, 2011. **365**(6): p. 493-505.
198. Rodger, A.J., et al., *Risk of HIV transmission through condomless sex in serodifferent gay couples with the HIV-positive partner taking suppressive antiretroviral therapy (PARTNER): final results of a multicentre, prospective, observational study.* Lancet, 2019. **393**(10189): p. 2428-2438.
199. Bezabhe, W.M., et al., *Adherence to Antiretroviral Therapy and Virologic Failure: A Meta-Analysis.* Medicine (Baltimore), 2016. **95**(15): p. e3361.
200. Gardner, E.M., et al., *The spectrum of engagement in HIV care and its relevance to test-and-treat strategies for prevention of HIV infection.* Clin Infect Dis, 2011. **52**(6): p. 793-800.
201. Iacob, S.A., D.G. Iacob, and G. Jugulete, *Improving the Adherence to Antiretroviral Therapy, a Difficult but Essential Task for a Successful HIV Treatment-Clinical Points of View and Practical Considerations.* Front Pharmacol, 2017. **8**: p. 831.
202. Ortego, C., et al., *Adherence to highly active antiretroviral therapy (HAART): a meta-analysis.* AIDS Behav, 2011. **15**(7): p. 1381-96.
203. Paterson, D.L., et al., *Adherence to protease inhibitor therapy and outcomes in patients with HIV infection.* Ann Intern Med, 2000. **133**(1): p. 21-30.
204. Shearer, K., et al., *Treatment outcomes of over 1000 patients on second-line, protease inhibitor-based antiretroviral therapy from four public-sector HIV treatment facilities across Johannesburg, South Africa.* Trop Med Int Health, 2017. **22**(2): p. 221-231.
205. Arreola, S., et al., *Sexual stigma, criminalization, investment, and access to HIV services among men who have sex with men worldwide.* AIDS Behav, 2015. **19**(2): p. 227-34.
206. Mahajan, A.P., et al., *Stigma in the HIV/AIDS epidemic: a review of the literature and recommendations for the way forward.* AIDS, 2008. **22 Suppl 2**: p. S67-79.
207. Denison, J.A., et al., *Project YES! Youth Engaging for Success: A randomized controlled trial assessing the impact of a clinic-based peer mentoring program on viral suppression, adherence and internalized stigma among HIV-positive youth (15-24 years) in Ndola, Zambia.* PLoS One, 2020. **15**(4): p. e0230703.
208. Kalichman, S.C., et al., *Measuring AIDS stigmas in people living with HIV/AIDS: the Internalized AIDS-Related Stigma Scale.* AIDS Care, 2009. **21**(1): p. 87-93.
209. Ekstrand, M.L., et al., *The Role of HIV Stigma in ART Adherence and Quality of Life Among Rural Women Living with HIV in India.* AIDS Behav, 2018. **22**(12): p. 3859-3868.

210. Chakraborty, A., et al., *Adherence to Antiretroviral Therapy Among HIV Patients in India: A Systematic Review and Meta-analysis.* AIDS Behav, 2020.
211. Joshi, B., et al., *Level of suboptimal adherence to first line antiretroviral treatment & its determinants among HIV positive people in India.* Indian J Med Res, 2014. **140**(1): p. 84-95.
212. Mhaskar, R., et al., *Adherence to antiretroviral therapy in India: a systematic review and meta-analysis.* Indian J Community Med, 2013. **38**(2): p. 74-82.
213. Shukla, M., et al., *Nonadherence to Antiretroviral Therapy Among People Living with HIV/AIDS Attending Two Tertiary Care Hospitals in District of Northern India.* Indian J Community Med, 2016. **41**(1): p. 55-61.
214. Nash, D., M. Yotebieng, and A.H. Sohn, *Treating all people living with HIV in sub-Saharan Africa: a new era calling for new approaches.* J Virus Erad, 2018. **4**(Suppl 2): p. 1-4.
215. Smith, J., et al., *Certification of polio eradication: process and lessons learned.* Bull World Health Organ, 2004. **82**(1): p. 24-30.
216. Perry, R.T., et al., *Progress toward regional measles elimination--worldwide, 2000-2013.* MMWR Morb Mortal Wkly Rep, 2014. **63**(45): p. 1034-8.
217. Perry, R.T., et al., *Global control and regional elimination of measles, 2000-2012.* MMWR Morb Mortal Wkly Rep, 2014. **63**(5): p. 103-7.
218. Minor, P., *The polio endgame.* Hum Vaccin Immunother, 2014. **10**(7): p. 2106-8.
219. Patel, M., et al., *Polio endgame: the global introduction of inactivated polio vaccine.* Expert Rev Vaccines, 2015. **14**(5): p. 749-62.
220. Zheng, Z., et al., *Noninvasive vaccination against infectious diseases.* Hum Vaccin Immunother, 2018. **14**(7): p. 1717-1733.
221. Kim, J.H., J.L. Excler, and N.L. Michael, *Lessons from the RV144 Thai phase III HIV-1 vaccine trial and the search for correlates of protection.* Annu Rev Med, 2015. **66**: p. 423-37.
222. Shacklett, B.L., et al., *HIV Research for Prevention 2018: From Research to Impact Conference Summary and Highlights.* AIDS Res Hum Retroviruses, 2019. **35**(7): p. 598-607.
223. Medlock, J., et al., *Effectiveness of UNAIDS targets and HIV vaccination across 127 countries.* Proc Natl Acad Sci U S A, 2017.
224. Kiepiela, P., et al., *CD8+ T-cell responses to different HIV proteins have discordant associations with viral load.* Nat Med, 2007. **13**(1): p. 46-53.
225. Prendergast, A., et al., *Gag-specific CD4+ T-cell responses are associated with virological control of paediatric HIV-1 infection.* AIDS, 2011. **25**(10): p. 1329-31.
226. Williamson, A.L. and E.P. Rybicki, *Justification for the inclusion of Gag in HIV vaccine candidates.* Expert Rev Vaccines, 2016. **15**(5): p. 585-98.
227. Autran, B., et al., *Elite controllers as a model of functional cure.* Curr Opin HIV AIDS, 2011. **6**(3): p. 181-7.
228. Poropatich, K. and D.J. Sullivan, Jr., *Human immunodeficiency virus type 1 long-term non-progressors: the viral, genetic and immunological basis for disease non-progression.* J Gen Virol, 2011. **92**(Pt 2): p. 247-68.
229. Rolland, M., et al., *Broad and Gag-biased HIV-1 epitope repertoires are associated with lower viral loads.* PLoS One, 2008. **3**(1): p. e1424.
230. Kaul, R., et al., *New insights into HIV-1 specific cytotoxic T-lymphocyte responses in exposed, persistently seronegative Kenyan sex workers.* Immunol Lett, 2001. **79**(1-2): p. 3-13.
231. Pala, P., et al., *Quantitative and qualitative differences in the T cell response to HIV in uninfected Ugandans exposed or unexposed to HIV-infected partners.* J Virol, 2013. **87**(16): p. 9053-63.
232. Ruiz-Riol, M., et al., *Alternative effector-function profiling identifies broad HIV-specific T-cell responses in highly HIV-exposed individuals who remain uninfected.* J Infect Dis, 2015. **211**(6): p. 936-46.
233. Mann, J.K. and T. Ndung'u, *HIV-1 vaccine immunogen design strategies.* Virol J, 2015. **12**: p. 3.
234. Rerks-Ngarm, S., et al., *Vaccination with ALVAC and AIDSVAX to prevent HIV-1 infection in Thailand.* N Engl J Med, 2009. **361**(23): p. 2209-20.
235. Flynn, N.M., et al., *Placebo-controlled phase 3 trial of a recombinant glycoprotein 120 vaccine to prevent HIV-1 infection.* J Infect Dis, 2005. **191**(5): p. 654-65.
236. Pitisuttithum, P., et al., *Randomized, double-blind, placebo-controlled efficacy trial of a bivalent recombinant glycoprotein 120 HIV-1 vaccine among injection drug users in Bangkok, Thailand.* J Infect Dis, 2006. **194**(12): p. 1661-71.

237. Buchbinder, S.P., et al., *Efficacy assessment of a cell-mediated immunity HIV-1 vaccine (the Step Study): a double-blind, randomised, placebo-controlled, test-of-concept trial.* Lancet, 2008. **372**(9653): p. 1881-1893.
238. Duerr, A., et al., *Extended follow-up confirms early vaccine-enhanced risk of HIV acquisition and demonstrates waning effect over time among participants in a randomized trial of recombinant adenovirus HIV vaccine (Step Study).* J Infect Dis, 2012. **206**(2): p. 258-66.
239. McElrath, M.J., et al., *HIV-1 vaccine-induced immunity in the test-of-concept Step Study: a case-cohort analysis.* Lancet, 2008. **372**(9653): p. 1894-1905.
240. Gray, G.E., et al., *Safety and efficacy of the HVTN 503/Phambili study of a clade-B-based HIV-1 vaccine in South Africa: a double-blind, randomised, placebo-controlled test-of-concept phase 2b study.* Lancet Infect Dis, 2011. **11**(7): p. 507-15.
241. Gray, G.E., et al., *Recombinant adenovirus type 5 HIV gag/pol/nef vaccine in South Africa: unblinded, long-term follow-up of the phase 2b HVTN 503/Phambili study.* Lancet Infect Dis, 2014. **14**(5): p. 388-96.
242. Rerks-Ngarm, S., et al., *Randomized, Double-Blind Evaluation of Late Boost Strategies for HIV-Uninfected Vaccine Recipients in the RV144 HIV Vaccine Efficacy Trial.* J Infect Dis, 2017. **215**(8): p. 1255-1263.
243. Haynes, B.F., et al., *Immune-correlates analysis of an HIV-1 vaccine efficacy trial.* N Engl J Med, 2012. **366**(14): p. 1275-86.
244. Hammer, S.M., et al., *Efficacy trial of a DNA/rAd5 HIV-1 preventive vaccine.* N Engl J Med, 2013. **369**(22): p. 2083-92.
245. Stephenson, K.E., H.T. D'Couto, and D.H. Barouch, *New concepts in HIV-1 vaccine development.* Curr Opin Immunol, 2016. **41**: p. 39-46.
246. Excler, J.L. and N.L. Michael, *Lessons from HIV-1 vaccine efficacy trials.* Curr Opin HIV AIDS, 2016.
247. Lema, D., A. Garcia, and J.B. De Sanctis, *HIV vaccines: a brief overview.* Scand J Immunol, 2014. **80**(1): p. 1-11.
248. Fauci, A.S., et al., *HIV vaccine research: the way forward.* Science, 2008. **321**(5888): p. 530-2.
249. Mascola, J.R., et al., *Immunization with envelope subunit vaccine products elicits neutralizing antibodies against laboratory-adapted but not primary isolates of human immunodeficiency virus type 1. The National Institute of Allergy and Infectious Diseases AIDS Vaccine Evaluation Group.* J Infect Dis, 1996. **173**(2): p. 340-8.
250. Montefiori, D.C., et al., *Magnitude and breadth of the neutralizing antibody response in the RV144 and Vax003 HIV-1 vaccine efficacy trials.* J Infect Dis, 2012. **206**(3): p. 431-41.
251. Kim, J.H., et al., *HIV vaccines: lessons learned and the way forward.* Curr Opin HIV AIDS, 2010. **5**(5): p. 428-34.
252. Bernard, N.F., et al., *HIV-specific cytotoxic T-lymphocyte activity in immunologically normal HIV-infected persons.* AIDS, 1998. **12**(16): p. 2125-39.
253. Pontesilli, O., et al., *Longitudinal analysis of human immunodeficiency virus type 1-specific cytotoxic T lymphocyte responses: a predominant gag-specific response is associated with nonprogressive infection.* J Infect Dis, 1998. **178**(4): p. 1008-18.
254. Schmitz, J.E., et al., *Control of viremia in simian immunodeficiency virus infection by CD8+ lymphocytes.* Science, 1999. **283**(5403): p. 857-60.
255. Moore, P.L., C. Williamson, and L. Morris, *Virological features associated with the development of broadly neutralizing antibodies to HIV-1.* Trends Microbiol, 2015. **23**(4): p. 204-11.
256. Wilson, N.A., et al., *Vaccine-induced cellular immune responses reduce plasma viral concentrations after repeated low-dose challenge with pathogenic simian immunodeficiency virus SIVmac239.* J Virol, 2006. **80**(12): p. 5875-85.
257. Qureshi, H., et al., *Low-dose penile SIVmac251 exposure of rhesus macaques infected with adenovirus type 5 (Ad5) and then immunized with a replication-defective Ad5-based SIV gag/pol/nef vaccine recapitulates the results of the phase IIb step trial of a similar HIV-1 vaccine.* J Virol, 2012. **86**(4): p. 2239-50.
258. Burton, D.R., et al., *Public health. A sound rationale needed for phase III HIV-1 vaccine trials.* Science, 2004. **303**(5656): p. 316.
259. Robb, M.L., et al., *Risk behaviour and time as covariates for efficacy of the HIV vaccine regimen ALVAC-HIV (vCP1521) and AIDSVAX B/E: a post-hoc analysis of the Thai phase 3 efficacy trial RV 144.* Lancet Infect Dis, 2012. **12**(7): p. 531-7.

260. Rolland, M., et al., *Increased HIV-1 vaccine efficacy against viruses with genetic signatures in Env V2.* Nature, 2012. **490**(7420): p. 417-20.
261. Benkeser, D., P.B. Gilbert, and M. Carone, *Estimating and Testing Vaccine Sieve Effects Using Machine Learning.* Journal of the American Statistical Association, 2018: p. 1-12.
262. Bonsignori, M., et al., *Antibody-dependent cellular cytotoxicity-mediating antibodies from an HIV-1 vaccine efficacy trial target multiple epitopes and preferentially use the VH1 gene family.* J Virol, 2012. **86**(21): p. 11521-32.
263. Liao, H.X., et al., *Vaccine induction of antibodies against a structurally heterogeneous site of immune pressure within HIV-1 envelope protein variable regions 1 and 2.* Immunity, 2013. **38**(1): p. 176-86.
264. Yates, N.L., et al., *Vaccine-induced Env V1-V2 IgG3 correlates with lower HIV-1 infection risk and declines soon after vaccination.* Sci Transl Med, 2014. **6**(228): p. 228ra39.
265. Lin, L., et al., *COMPASS identifies T-cell subsets correlated with clinical outcomes.* Nat Biotechnol, 2015. **33**(6): p. 610-6.
266. Fourati, S., et al., *Integrated systems approach defines the antiviral pathways conferring protection by the RV144 HIV vaccine.* Nat Commun, 2019. **10**(1): p. 863.
267. Akapirat, S., et al., *Characterization of HIV-1 gp120 antibody specificities induced in anogenital secretions of RV144 vaccine recipients after late boost immunizations.* PLoS One, 2018. **13**(4): p. e0196397.
268. Bekker, L.G., et al., *Subtype C ALVAC-HIV and bivalent subtype C gp120/MF59 HIV-1 vaccine in low-risk, HIV-uninfected, South African adults: a phase 1/2 trial.* Lancet HIV, 2018. **5**(7): p. e366-e378.
269. Wang, Z., et al., *Comprehensive Characterization of Reference Standard Lots of HIV-1 Subtype C Gp120 Proteins for Clinical Trials in Southern African Regions.* Vaccines (Basel), 2016. **4**(2).
270. Adepoju, P., *Moving on from the failed HIV vaccine clinical trial.* Lancet HIV, 2020. **7**(3): p. e161.
271. Gray, G.E., et al., *Immune correlates of the Thai RV144 HIV vaccine regimen in South Africa.* Sci Transl Med, 2019. **11**(510).
272. Fischer, W., et al., *Polyvalent vaccines for optimal coverage of potential T-cell epitopes in global HIV-1 variants.* Nat Med, 2007. **13**(1): p. 100-6.
273. Barouch, D.H., et al., *Evaluation of a mosaic HIV-1 vaccine in a multicentre, randomised, double-blind, placebo-controlled, phase 1/2a clinical trial (APPROACH) and in rhesus monkeys (NHP 13-19).* Lancet, 2018. **392**(10143): p. 232-243.
274. Kwong, P.D. and J.R. Mascola, *HIV-1 Vaccines Based on Antibody Identification, B Cell Ontogeny, and Epitope Structure.* Immunity, 2018. **48**(5): p. 855-871.
275. Sanders, R.W., et al., *A next-generation cleaved, soluble HIV-1 Env trimer, BG505 SOSIP.664 gp140, expresses multiple epitopes for broadly neutralizing but not non-neutralizing antibodies.* PLoS Pathog, 2013. **9**(9): p. e1003618.
276. Dey, A.K., et al., *cGMP production and analysis of BG505 SOSIP.664, an extensively glycosylated, trimeric HIV-1 envelope glycoprotein vaccine candidate.* Biotechnol Bioeng, 2018. **115**(4): p. 885-899.
277. Sanders, R.W., et al., *HIV-1 VACCINES. HIV-1 neutralizing antibodies induced by native-like envelope trimers.* Science, 2015. **349**(6244): p. aac4223.
278. Williams, W.B., et al., *Initiation of HIV neutralizing B cell lineages with sequential envelope immunizations.* Nat Commun, 2017. **8**(1): p. 1732.
279. Jardine, J.G., et al., *HIV-1 broadly neutralizing antibody precursor B cells revealed by germline-targeting immunogen.* Science, 2016. **351**(6280): p. 1458-63.
280. Alam, S.M., et al., *Differential reactivity of germ line allelic variants of a broadly neutralizing HIV-1 antibody to a gp41 fusion intermediate conformation.* J Virol, 2011. **85**(22): p. 11725-31.
281. Dennison, S.M., et al., *Induction of antibodies in rhesus macaques that recognize a fusion-intermediate conformation of HIV-1 gp41.* PLoS One, 2011. **6**(11): p. e27824.
282. Soto, C., et al., *Developmental Pathway of the MPER-Directed HIV-1-Neutralizing Antibody 10E8.* PLoS One, 2016. **11**(6): p. e0157409.
283. Xu, K., et al., *Epitope-based vaccine design yields fusion peptide-directed antibodies that neutralize diverse strains of HIV-1.* Nat Med, 2018. **24**(6): p. 857-867.
284. Alayo, Q.A., N.M. Provine, and P. Penaloza-MacMaster, *Novel Concepts for HIV Vaccine Vector Design.* mSphere, 2017. **2**(6).

285. Ulmer, J.B., et al., *Heterologous protection against influenza by injection of DNA encoding a viral protein.* Science, 1993. **259**(5102): p. 1745-9.
286. Chapman, R. and E.P. Rybicki, *Use of a Novel Enhanced DNA Vaccine Vector for Preclinical Virus Vaccine Investigation.* Vaccines (Basel), 2019. **7**(2).
287. Casares, S., et al., *Antigen presentation by dendritic cells after immunization with DNA encoding a major histocompatibility complex class II-restricted viral epitope.* J Exp Med, 1997. **186**(9): p. 1481-6.
288. Condon, C., et al., *DNA-based immunization by in vivo transfection of dendritic cells.* Nat Med, 1996. **2**(10): p. 1122-8.
289. Corr, M., et al., *Gene vaccination with naked plasmid DNA: mechanism of CTL priming.* J Exp Med, 1996. **184**(4): p. 1555-60.
290. Fu, T.M., et al., *Priming of cytotoxic T lymphocytes by DNA vaccines: requirement for professional antigen presenting cells and evidence for antigen transfer from myocytes.* Mol Med, 1997. **3**(6): p. 362-71.
291. Ulmer, J.B., et al., *Generation of MHC class I-restricted cytotoxic T lymphocytes by expression of a viral protein in muscle cells: antigen presentation by non-muscle cells.* Immunology, 1996. **89**(1): p. 59-67.
292. Doria-Rose, N.A. and N.L. Haigwood, *DNA vaccine strategies: candidates for immune modulation and immunization regimens.* Methods, 2003. **31**(3): p. 207-16.
293. Barrett, L.W., S. Fletcher, and S.D. Wilton, *Regulation of eukaryotic gene expression by the untranslated gene regions and other non-coding elements.* Cell Mol Life Sci, 2012. **69**(21): p. 3613-34.
294. Fath, S., et al., *Multiparameter RNA and codon optimization: a standardized tool to assess and enhance autologous mammalian gene expression.* PLoS One, 2011. **6**(3): p. e17596.
295. Ko, H.J., et al., *Optimization of codon usage enhances the immunogenicity of a DNA vaccine encoding mycobacterial antigen Ag85B.* Infect Immun, 2005. **73**(9): p. 5666-74.
296. Kozak, M., *Point mutations define a sequence flanking the AUG initiator codon that modulates translation by eukaryotic ribosomes.* Cell, 1986. **44**(2): p. 283-92.
297. Megati, S., et al., *Modifying the HIV-1 env gp160 gene to improve pDNA vaccine-elicited cell-mediated immune responses.* Vaccine, 2008. **26**(40): p. 5083-94.
298. Zhou, W., et al., *Multiple RNA splicing and the presence of cryptic RNA splice donor and acceptor sites may contribute to low expression levels and poor immunogenicity of potential DNA vaccines containing the env gene of equine infectious anemia virus (EIAV).* Vet Microbiol, 2002. **88**(2): p. 127-51.
299. Tanzer, F.L., et al., *The porcine circovirus type 1 capsid gene promoter improves antigen expression and immunogenicity in a HIV-1 plasmid vaccine.* Virol J, 2011. **8**: p. 51.
300. Garg, S., et al., *The hybrid cytomegalovirus enhancer/chicken beta-actin promoter along with woodchuck hepatitis virus posttranscriptional regulatory element enhances the protective efficacy of DNA vaccines.* J Immunol, 2004. **173**(1): p. 550-8.
301. Vanniasinkam, T., S.T. Reddy, and H.C. Ertl, *DNA immunization using a non-viral promoter.* Virology, 2006. **344**(2): p. 412-20.
302. Wang, S., et al., *Relative contributions of codon usage, promoter efficiency and leader sequence to the antigen expression and immunogenicity of HIV-1 Env DNA vaccine.* Vaccine, 2006. **24**(21): p. 4531-40.
303. Bernelin-Cottet, C., et al., *A DNA Prime Immuno-Potentiates a Modified Live Vaccine against the Porcine Reproductive and Respiratory Syndrome Virus but Does Not Improve Heterologous Protection.* Viruses, 2019. **11**(6).
304. Gaudinski, M.R., et al., *Safety, tolerability, and immunogenicity of two Zika virus DNA vaccine candidates in healthy adults: randomised, open-label, phase 1 clinical trials.* Lancet, 2018. **391**(10120): p. 552-562.
305. Yousafzai, M.T., et al., *Feasibility of conducting intradermal vaccination campaign with inactivated poliovirus vaccine using Tropis intradermal needle free injection system, Karachi, Pakistan.* Heliyon, 2017. **3**(8): p. e00395.
306. Cristillo, A.D., et al., *Persistent antibody and T cell responses induced by HIV-1 DNA vaccine delivered by electroporation.* Biochem Biophys Res Commun, 2008. **366**(1): p. 29-35.
307. Huang, X., et al., *In vivo electroporation in DNA-VLP prime-boost preferentially enhances HIV-1 envelope-specific IgG2a, neutralizing antibody and CD8 T cell responses.* Vaccine, 2017. **35**(16): p. 2042-2051.
308. Hutnick, N.A., et al., *Selected approaches for increasing HIV DNA vaccine immunogenicity in vivo.* Curr Opin Virol, 2011. **1**(4): p. 233-40.

309. Mann, J.F., et al., *Enhanced immunogenicity of an HIV-1 DNA vaccine delivered with electroporation via combined intramuscular and intradermal routes.* J Virol, 2014. **88**(12): p. 6959-69.
310. Wang, S., et al., *The relative immunogenicity of DNA vaccines delivered by the intramuscular needle injection, electroporation and gene gun methods.* Vaccine, 2008. **26**(17): p. 2100-10.
311. Hellerstein, M., et al., *Co-expression of HIV-1 virus-like particles and granulocyte-macrophage colony stimulating factor by GEO-D03 DNA vaccine.* Hum Vaccin Immunother, 2012. **8**(11): p. 1654-8.
312. Henke, A., et al., *Co-expression of interleukin-2 by a bicistronic plasmid increases the efficacy of DNA immunization to prevent influenza virus infections.* Intervirology, 2006. **49**(4): p. 249-52.
313. O'Hagan, D.T., M. Singh, and J.B. Ulmer, *Microparticle-based technologies for vaccines.* Methods, 2006. **40**(1): p. 10-9.
314. Mayr, A. and E. Munz, *[Changes in the vaccinia virus through continuing passages in chick embryo fibroblast cultures].* Zentralbl Bakteriol Orig, 1964. **195**(1): p. 24-35.
315. Sutter, G. and B. Moss, *Nonreplicating vaccinia vector efficiently expresses recombinant genes.* Proc Natl Acad Sci U S A, 1992. **89**(22): p. 10847-51.
316. Meyer, H., G. Sutter, and A. Mayr, *Mapping of deletions in the genome of the highly attenuated vaccinia virus MVA and their influence on virulence.* J Gen Virol, 1991. **72 (Pt 5)**: p. 1031-8.
317. Volz, A. and G. Sutter, *Modified Vaccinia Virus Ankara: History, Value in Basic Research, and Current Perspectives for Vaccine Development.* Adv Virus Res, 2017. **97**: p. 187-243.
318. Mahnel, H. and A. Mayr, *[Experiences with immunization against orthopox viruses of humans and animals using vaccine strain MVA].* Berl Munch Tierarztl Wochenschr, 1994. **107**(8): p. 253-6.
319. Stickl, H., et al., *[MVA vaccination against smallpox: clinical tests with an attenuated live vaccinia virus strain (MVA) (author's transl)].* Dtsch Med Wochenschr, 1974. **99**(47): p. 2386-92.
320. Blanchard, T.J., et al., *Modified vaccinia virus Ankara undergoes limited replication in human cells and lacks several immunomodulatory proteins: implications for use as a human vaccine.* J Gen Virol, 1998. **79 (Pt 5)**: p. 1159-67.
321. Wilmschen, S., J.E. Schmitz, and J. Kimpel, *Viral Vectors for the Induction of Broadly Neutralizing Antibodies against HIV.* Vaccines (Basel), 2019. **7**(3).
322. Burdin, N., L.K. Handy, and S.A. Plotkin, *What Is Wrong with Pertussis Vaccine Immunity? The Problem of Waning Effectiveness of Pertussis Vaccines.* Cold Spring Harb Perspect Biol, 2017. **9**(12).
323. da Silva Antunes, R., et al., *Th1/Th17 polarization persists following whole-cell pertussis vaccination despite repeated acellular boosters.* J Clin Invest, 2018. **128**(9): p. 3853-3865.
324. Plotkin, S.A., *Composition of pertussis vaccine given to infants determines long-term T cell polarization.* J Clin Invest, 2018. **128**(9): p. 3742-3744.
325. Plotkin, S.A., *Updates on immunologic correlates of vaccine-induced protection.* Vaccine, 2020. **38**(9): p. 2250-2257.
326. Plotkin, S.A., *Vaccines: correlates of vaccine-induced immunity.* Clin Infect Dis, 2008. **47**(3): p. 401-9.
327. Streeck, H., et al., *Harnessing CD4(+) T cell responses in HIV vaccine development.* Nat Med, 2013. **19**(2): p. 143-9.
328. Havenar-Daughton, C., et al., *Direct Probing of Germinal Center Responses Reveals Immunological Features and Bottlenecks for Neutralizing Antibody Responses to HIV Env Trimer.* Cell Rep, 2016. **17**(9): p. 2195-2209.
329. Khurana, S., et al., *Heterologous prime-boost vaccination with MF59-adjuvanted H5 vaccines promotes antibody affinity maturation towards the hemagglutinin HA1 domain and broad H5N1 cross-clade neutralization.* PLoS One, 2014. **9**(4): p. e95496.
330. Joseph, S., et al., *A Comparative Phase I Study of Combination, Homologous Subtype-C DNA, MVA, and Env gp140 Protein/Adjuvant HIV Vaccines in Two Immunization Regimes.* Front Immunol, 2017. **8**: p. 149.
331. Viegas, E.O., et al., *Optimizing the immunogenicity of HIV prime-boost DNA-MVA-rgp140/GLA vaccines in a phase II randomized factorial trial design.* PLoS One, 2018. **13**(11): p. e0206838.
332. Chissumba, R.M., et al., *Regulatory T cell abundance and activation status before and after priming with HIVIS-DNA and boosting with MVA-HIV/rgp140/GLA-AF may impact the*

magnitude of the vaccine-induced immune responses. Immunobiology, 2018. **223**(12): p. 792-801.
333. Bakari, M., et al., *Broad and potent immune responses to a low dose intradermal HIV-1 DNA boosted with HIV-1 recombinant MVA among healthy adults in Tanzania.* Vaccine, 2011. **29**(46): p. 8417-28.
334. Churchyard, G., et al., *Sequential Immunization with gp140 Boosts Immune Responses Primed by Modified Vaccinia Ankara or DNA in HIV-Uninfected South African Participants.* PLoS One, 2016. **11**(9): p. e0161753.
335. Goepfert, P.A., et al., *Specificity and 6-month durability of immune responses induced by DNA and recombinant modified vaccinia Ankara vaccines expressing HIV-1 virus-like particles.* J Infect Dis, 2014. **210**(1): p. 99-110.
336. Gray, G.E., et al., *Subtype C gp140 Vaccine Boosts Immune Responses Primed by the South African AIDS Vaccine Initiative DNA-C2 and MVA-C HIV Vaccines after More than a 2-Year Gap.* Clin Vaccine Immunol, 2016. **23**(6): p. 496-506.
337. Gudmundsdotter, L., et al., *Recombinant Modified Vaccinia Ankara (MVA) effectively boosts DNA-primed HIV-specific immune responses in humans despite pre-existing vaccinia immunity.* Vaccine, 2009. **27**(33): p. 4468-74.
338. Munusamy Ponnan, S., et al., *Evaluation of antiviral T cell responses and TSCM cells in volunteers enrolled in a phase I HIV-1 subtype C prophylactic vaccine trial in India.* PLoS One, 2020. **15**(2): p. e0229461.
339. Sandstrom, E., et al., *Broad immunogenicity of a multigene, multiclade HIV-1 DNA vaccine boosted with heterologous HIV-1 recombinant modified vaccinia virus Ankara.* J Infect Dis, 2008. **198**(10): p. 1482-90.
340. Goonetilleke, N., et al., *Induction of multifunctional human immunodeficiency virus type 1 (HIV-1)-specific T cells capable of proliferation in healthy subjects by using a prime-boost regimen of DNA- and modified vaccinia virus Ankara-vectored vaccines expressing HIV-1 Gag coupled to CD8+ T-cell epitopes.* J Virol, 2006. **80**(10): p. 4717-28.
341. Joachim, A., et al., *Potent functional antibody responses elicited by HIV-I DNA priming and boosting with heterologous HIV-1 recombinant MVA in healthy Tanzanian adults.* PLoS One, 2015. **10**(4): p. e0118486.
342. Saade, F., S.A. Gorski, and N. Petrovsky, *Pushing the frontiers of T-cell vaccines: accurate measurement of human T-cell responses.* Expert Rev Vaccines, 2012. **11**(12): p. 1459-70.
343. Capucci, S., et al., *HIV-1-neutralizing antibody induced by simian adenovirus- and poxvirus MVA-vectored BG505 native-like envelope trimers.* PLoS One, 2017. **12**(8): p. e0181886.
344. Gangadhara, S., et al., *Vaccination with Combination DNA and Virus-Like Particles Enhances Humoral and Cellular Immune Responses upon Boost with Recombinant Modified Vaccinia Virus Ankara Expressing Human Immunodeficiency Virus Envelope Proteins.* Vaccines (Basel), 2017. **5**(4).
345. Iyer, S.S., et al., *Virus-Like Particles Displaying Trimeric Simian Immunodeficiency Virus (SIV) Envelope gp160 Enhance the Breadth of DNA/Modified Vaccinia Virus Ankara SIV Vaccine-Induced Antibody Responses in Rhesus Macaques.* J Virol, 2016. **90**(19): p. 8842-54.
346. McCurley, N.P., et al., *HIV transmitted/founder vaccines elicit autologous tier 2 neutralizing antibodies for the CD4 binding site.* PLoS One, 2017. **12**(10): p. e0177863.
347. McKay, P.F., et al., *Glucopyranosyl lipid A adjuvant significantly enhances HIV specific T and B cell responses elicited by a DNA-MVA-protein vaccine regimen.* PLoS One, 2014. **9**(1): p. e84707.
348. Perez, P., et al., *An MVA Vector Expressing HIV-1 Envelope under the Control of a Potent Vaccinia Virus Promoter as a Promising Strategy in HIV/AIDS Vaccine Design.* Vaccines (Basel), 2019. **7**(4).
349. Perez, P., et al., *Deletion of Vaccinia Virus A40R Gene Improves the Immunogenicity of the HIV-1 Vaccine Candidate MVA-B.* Vaccines (Basel), 2020. **8**(1).
350. Jones, A.T., et al., *HIV-1 vaccination by needle-free oral injection induces strong mucosal immunity and protects against SHIV challenge.* Nat Commun, 2019. **10**(1): p. 798.
351. Santra, S., et al., *Recombinant poxvirus boosting of DNA-primed rhesus monkeys augments peak but not memory T lymphocyte responses.* Proc Natl Acad Sci U S A, 2004. **101**(30): p. 11088-93.
352. Burgers, W.A., et al., *Broad, high-magnitude and multifunctional CD4+ and CD8+ T-cell responses elicited by a DNA and modified vaccinia Ankara vaccine containing human immunodeficiency virus type 1 subtype C genes in baboons.* J Gen Virol, 2009. **90**(Pt 2): p. 468-480.

353. Chapman, R., et al., *Immunogenicity of HIV-1 Vaccines Expressing Chimeric Envelope Glycoproteins on the Surface of Pr55 Gag Virus-Like Particles.* Vaccines (Basel), 2020. **8**(1).
354. Chege, G.K., et al., *DNA-MVA-protein vaccination of rhesus macaques induces HIV-specific immunity in mucosal-associated lymph nodes and functional antibodies.* Vaccine, 2017. **35**(6): p. 929-937.
355. Shephard, E., et al., *A multigene HIV type 1 subtype C modified vaccinia Ankara (MVA) vaccine efficiently boosts immune responses to a DNA vaccine in mice.* AIDS Res Hum Retroviruses, 2008. **24**(2): p. 207-17.
356. Soares, A., et al., *Transient global T cell activation after vaccination of rhesus macaques with a DNA-poxvirus vaccine regimen for HIV.* Vaccine, 2015. **33**(30): p. 3435-9.
357. van Diepen, M.T., et al., *Prime-Boost Immunizations with DNA, Modified Vaccinia Virus Ankara, and Protein-Based Vaccines Elicit Robust HIV-1 Tier 2 Neutralizing Antibodies against the CAP256 Superinfecting Virus.* J Virol, 2019. **93**(8).
358. Margolin, E., et al., *Production and Immunogenicity of Soluble Plant-Produced HIV-1 Subtype C Envelope gp140 Immunogens.* Front Plant Sci, 2019. **10**: p. 1378.
359. Plotkin, S.A., *Correlates of protection induced by vaccination.* Clin Vaccine Immunol, 2010. **17**(7): p. 1055-65.
360. Apostolico Jde, S., et al., *Adjuvants: Classification, Modus Operandi, and Licensing.* J Immunol Res, 2016. **2016**: p. 1459394.
361. Shi, S., et al., *Vaccine adjuvants: Understanding the structure and mechanism of adjuvanticity.* Vaccine, 2019. **37**(24): p. 3167-3178.
362. Group, R.J.f.T.A., *Pipeline Report » 2019 HIV Vaccines, Passive Immunization and Antibody Gene Transfer*. 2019.
363. Gupta, R.K., et al., *In vivo distribution of radioactivity in mice after injection of biodegradable polymer microspheres containing 14C-labeled tetanus toxoid.* Vaccine, 1996. **14**(15): p. 1412-6.
364. Hutchison, S., et al., *Antigen depot is not required for alum adjuvanticity.* FASEB J, 2012. **26**(3): p. 1272-9.
365. Liang, F., et al., *Vaccine priming is restricted to draining lymph nodes and controlled by adjuvant-mediated antigen uptake.* Sci Transl Med, 2017. **9**(393).
366. Wu, C.Y., et al., *Squalene-adjuvanted H7N9 virus vaccine induces robust humoral immune response against H7N9 and H7N7 viruses.* Vaccine, 2014. **32**(35): p. 4485-94.
367. Sliepen, K. and R.W. Sanders, *HIV-1 envelope glycoprotein immunogens to induce broadly neutralizing antibodies.* Expert Rev Vaccines, 2016: p. 1-17.
368. de Taeye, S.W., J.P. Moore, and R.W. Sanders, *HIV-1 Envelope Trimer Design and Immunization Strategies To Induce Broadly Neutralizing Antibodies.* Trends Immunol, 2016.
369. Klasse, P.J., et al., *Influences on trimerization and aggregation of soluble, cleaved HIV-1 SOSIP envelope glycoprotein.* J Virol, 2013. **87**(17): p. 9873-85.
370. Pritchard, L.K., et al., *Cell- and Protein-Directed Glycosylation of Native Cleaved HIV-1 Envelope.* J Virol, 2015. **89**(17): p. 8932-44.
371. Ringe, R.P., et al., *Influences on the Design and Purification of Soluble, Recombinant Native-Like HIV-1 Envelope Glycoprotein Trimers.* J Virol, 2015. **89**(23): p. 12189-210.
372. Binley, J.M., et al., *Enhancing the proteolytic maturation of human immunodeficiency virus type 1 envelope glycoproteins.* J Virol, 2002. **76**(6): p. 2606-16.
373. Binley, J.M., et al., *A recombinant human immunodeficiency virus type 1 envelope glycoprotein complex stabilized by an intermolecular disulfide bond between the gp120 and gp41 subunits is an antigenic mimic of the trimeric virion-associated structure.* J Virol, 2000. **74**(2): p. 627-43.
374. Sanders, R.W., et al., *Stabilization of the soluble, cleaved, trimeric form of the envelope glycoprotein complex of human immunodeficiency virus type 1.* J Virol, 2002. **76**(17): p. 8875-89.
375. Yasmeen, A., et al., *Differential binding of neutralizing and non-neutralizing antibodies to native-like soluble HIV-1 Env trimers, uncleaved Env proteins, and monomeric subunits.* Retrovirology, 2014. **11**: p. 41.
376. Wu, X., et al., *Neutralization escape variants of human immunodeficiency virus type 1 are transmitted from mother to infant.* J Virol, 2006. **80**(2): p. 835-44.
377. Torrents de la Pena, A. and R.W. Sanders, *Stabilizing HIV-1 envelope glycoprotein trimers to induce neutralizing antibodies.* Retrovirology, 2018. **15**(1): p. 63.
378. Ward, A.B. and I.A. Wilson, *The HIV-1 envelope glycoprotein structure: nailing down a moving target.* Immunol Rev, 2017. **275**(1): p. 21-32.

379. de Taeye, S.W., et al., *Stabilization of the V2 loop improves the presentation of V2 loop-associated broadly neutralizing antibody epitopes on HIV-1 envelope trimers.* J Biol Chem, 2019. **294**(14): p. 5616-5631.
380. de Taeye, S.W., et al., *Stabilization of the gp120 V3 loop through hydrophobic interactions reduces the immunodominant V3-directed non-neutralizing response to HIV-1 envelope trimers.* J Biol Chem, 2018. **293**(5): p. 1688-1701.
381. Pauthner, M.G., et al., *Vaccine-Induced Protection from Homologous Tier 2 SHIV Challenge in Nonhuman Primates Depends on Serum-Neutralizing Antibody Titers.* Immunity, 2019. **50**(1): p. 241-252 e6.
382. Sliepen, K., et al., *Structure and immunogenicity of a stabilized HIV-1 envelope trimer based on a group-M consensus sequence.* Nat Commun, 2019. **10**(1): p. 2355.
383. Kovacs, J.M., et al., *Stable, uncleaved HIV-1 envelope glycoprotein gp140 forms a tightly folded trimer with a native-like structure.* Proc Natl Acad Sci U S A, 2014. **111**(52): p. 18542-7.
384. Sharma, S.K., et al., *Cleavage-independent HIV-1 Env trimers engineered as soluble native spike mimetics for vaccine design.* Cell Rep, 2015. **11**(4): p. 539-50.
385. Georgiev, I.S., et al., *Single-Chain Soluble BG505.SOSIP gp140 Trimers as Structural and Antigenic Mimics of Mature Closed HIV-1 Env.* J Virol, 2015. **89**(10): p. 5318-29.
386. Dubrovskaya, V., et al., *Vaccination with Glycan-Modified HIV NFL Envelope Trimer-Liposomes Elicits Broadly Neutralizing Antibodies to Multiple Sites of Vulnerability.* Immunity, 2019. **51**(5): p. 915-929 e7.
387. Yang, L., et al., *Structure-Guided Redesign Improves NFL HIV Env Trimer Integrity and Identifies an Inter-Protomer Disulfide Permitting Post-Expression Cleavage.* Front Immunol, 2018. **9**: p. 1631.
388. Bale, S., et al., *Cleavage-Independent HIV-1 Trimers From CHO Cell Lines Elicit Robust Autologous Tier 2 Neutralizing Antibodies.* Front Immunol, 2018. **9**: p. 1116.
389. Ingale, J., et al., *High-Density Array of Well-Ordered HIV-1 Spikes on Synthetic Liposomal Nanoparticles Efficiently Activate B Cells.* Cell Rep, 2016. **15**(9): p. 1986-99.
390. Pauthner, M., et al., *Elicitation of Robust Tier 2 Neutralizing Antibody Responses in Nonhuman Primates by HIV Envelope Trimer Immunization Using Optimized Approaches.* Immunity, 2017. **46**(6): p. 1073-1088 e6.
391. Bale, S., et al., *Covalent Linkage of HIV-1 Trimers to Synthetic Liposomes Elicits Improved B Cell and Antibody Responses.* J Virol, 2017. **91**(16).
392. Dubrovskaya, V., et al., *Targeted N-glycan deletion at the receptor-binding site retains HIV Env NFL trimer integrity and accelerates the elicited antibody response.* PLoS Pathog, 2017. **13**(9): p. e1006614.
393. Feng, Y., et al., *Thermostability of Well-Ordered HIV Spikes Correlates with the Elicitation of Autologous Tier 2 Neutralizing Antibodies.* PLoS Pathog, 2016. **12**(8): p. e1005767.
394. Martinez-Murillo, P., et al., *Particulate Array of Well-Ordered HIV Clade C Env Trimers Elicits Neutralizing Antibodies that Display a Unique V2 Cap Approach.* Immunity, 2017. **46**(5): p. 804-817 e7.
395. Soldemo, M., et al., *Glutaraldehyde Cross-linking of HIV-1 Env Trimers Skews the Antibody Subclass Response in Mice.* Front Immunol, 2017. **8**: p. 1654.
396. Kong, L., et al., *Uncleaved prefusion-optimized gp140 trimers derived from analysis of HIV-1 envelope metastability.* Nat Commun, 2016. **7**: p. 12040.
397. He, L., et al., *HIV-1 vaccine design through minimizing envelope metastability.* Sci Adv, 2018. **4**(11): p. eaau6769.
398. Stano, A., et al., *Dense Array of Spikes on HIV-1 Virion Particles.* J Virol, 2017. **91**(14).
399. Wang, B.Z., et al., *Incorporation of high levels of chimeric human immunodeficiency virus envelope glycoproteins into virus-like particles.* J Virol, 2007. **81**(20): p. 10869-78.
400. Wyatt, L.S., et al., *Enhanced cell surface expression, immunogenicity and genetic stability resulting from a spontaneous truncation of HIV Env expressed by a recombinant MVA.* Virology, 2008. **372**(2): p. 260-72.
401. Thalhauser, S., et al., *Critical design criteria for engineering a nanoparticulate HIV-1 vaccine.* J Control Release, 2020. **317**: p. 322-335.
402. Del Moral-Sanchez, I. and K. Sliepen, *Strategies for inducing effective neutralizing antibody responses against HIV-1.* Expert Rev Vaccines, 2019. **18**(11): p. 1127-1143.
403. Kushnir, N., S.J. Streatfield, and V. Yusibov, *Virus-like particles as a highly efficient vaccine platform: diversity of targets and production systems and advances in clinical development.* Vaccine, 2012. **31**(1): p. 58-83.

404. Roldao, A., et al., *Virus-like particles in vaccine development.* Expert Rev Vaccines, 2010. **9**(10): p. 1149-76.
405. Tong, T., et al., *HIV-1 virus-like particles bearing pure env trimers expose neutralizing epitopes but occlude nonneutralizing epitopes.* J Virol, 2012. **86**(7): p. 3574-87.
406. Haffar, O., et al., *Human immunodeficiency virus-like, nonreplicating, gag-env particles assemble in a recombinant vaccinia virus expression system.* J Virol, 1990. **64**(6): p. 2653-9.
407. Krausslich, H.G., et al., *Analysis of protein expression and virus-like particle formation in mammalian cell lines stably expressing HIV-1 gag and env gene products with or without active HIV proteinase.* Virology, 1993. **192**(2): p. 605-17.
408. Rovinski, B., et al., *Expression and characterization of genetically engineered human immunodeficiency virus-like particles containing modified envelope glycoproteins: implications for development of a cross-protective AIDS vaccine.* J Virol, 1992. **66**(7): p. 4003-12.
409. Rovinski, B., et al., *Induction of HIV type 1 neutralizing and env-CD4 blocking antibodies by immunization with genetically engineered HIV type 1-like particles containing unprocessed gp160 glycoproteins.* AIDS Res Hum Retroviruses, 1995. **11**(10): p. 1187-95.
410. Vzorov, A.N., et al., *Highly immunogenic human immunodeficiency viruslike particles are produced by recombinant vaccinia virus-infected cells.* AIDS Res Hum Retroviruses, 1991. **7**(1): p. 29-36.
411. Wagner, R., et al., *Studies on processing, particle formation, and immunogenicity of the HIV-1 gag gene product: a possible component of a HIV vaccine.* Arch Virol, 1992. **127**(1-4): p. 117-37.
412. Wyatt, L.S., et al., *Correlation of immunogenicities and in vitro expression levels of recombinant modified vaccinia virus Ankara HIV vaccines.* Vaccine, 2008. **26**(4): p. 486-93.
413. Chapman, R., et al., *Heterologous prime-boost vaccination with DNA and MVA vaccines, expressing HIV-1 subtype C mosaic Gag virus-like particles, is highly immunogenic in mice.* PLoS One, 2017. **12**(3): p. e0173352.
414. Jongwe, T.I., et al., *HIV-1 Subtype C Mosaic Gag Expressed by BCG and MVA Elicits Persistent Effector T Cell Responses in a Prime-Boost Regimen in Mice.* PLoS One, 2016. **11**(7): p. e0159141.
415. GenScript. *Codon optimisation*. Available from: https://www.genscript.com/codon-optimization-for-increased-protein-expression.html?page_no=1&position_no=4&sensors=search.
416. Wang, J.Y., et al., *Improved expression of secretory and trimeric proteins in mammalian cells via the introduction of a new trimer motif and a mutant of the tPA signal sequence.* Appl Microbiol Biotechnol, 2011. **91**(3): p. 731-40.
417. Chapman, B.S., et al., *Effect of intron A from human cytomegalovirus (Towne) immediate-early gene on heterologous expression in mammalian cells.* Nucleic Acids Res, 1991. **19**(14): p. 3979-86.
418. Deml, L., et al., *Increased incorporation of chimeric human immunodeficiency virus type 1 gp120 proteins into Pr55gag virus-like particles by an Epstein-Barr virus gp220/350-derived transmembrane domain.* Virology, 1997. **235**(1): p. 10-25.
419. Vzorov, A.N., et al., *Effects of modification of the HIV-1 Env cytoplasmic tail on immunogenicity of VLP vaccines.* Virology, 2016. **489**: p. 141-50.
420. Visciano, M.L., et al., *Generation of HIV-1 Virus-Like Particles expressing different HIV-1 glycoproteins.* Vaccine, 2011. **29**(31): p. 4903-12.
421. Rybicki, E.P., *Plant molecular farming of virus-like nanoparticles as vaccines and reagents.* Wiley Interdiscip Rev Nanomed Nanobiotechnol, 2020. **12**(2): p. e1587.
422. Guenaga, J., et al., *Well-ordered trimeric HIV-1 subtype B and C soluble spike mimetics generated by negative selection display native-like properties.* PLoS Pathog, 2015. **11**(1): p. e1004570.
423. Ozorowski, G., et al., *Effects of Adjuvants on HIV-1 Envelope Glycoprotein SOSIP Trimers In Vitro.* J Virol, 2018. **92**(13).
424. McLellan, J.S., et al., *Structure of HIV-1 gp120 V1/V2 domain with broadly neutralizing antibody PG9.* Nature, 2011. **480**(7377): p. 336-43.
425. Bhiman, J.N., et al., *Viral variants that initiate and drive maturation of V1V2-directed HIV-1 broadly neutralizing antibodies.* Nat Med, 2015. **21**(11): p. 1332-6.
426. Calabro, S., et al., *The adjuvant effect of MF59 is due to the oil-in-water emulsion formulation, none of the individual components induce a comparable adjuvant effect.* Vaccine, 2013. **31**(33): p. 3363-9.

427. Ott, G., et al., *MF59. Design and evaluation of a safe and potent adjuvant for human vaccines.* Pharm Biotechnol, 1995. **6**: p. 277-96.
428. Morefield, G.L., et al., *Role of aluminum-containing adjuvants in antigen internalization by dendritic cells in vitro.* Vaccine, 2005. **23**(13): p. 1588-95.
429. Klose, J., et al., *Hexa-histidin tag position influences disulfide structure but not binding behavior of in vitro folded N-terminal domain of rat corticotropin-releasing factor receptor type 2a.* Protein Sci, 2004. **13**(9): p. 2470-5.
430. Sabaty, M., et al., *Detrimental effect of the 6 His C-terminal tag on YedY enzymatic activity and influence of the TAT signal sequence on YedY synthesis.* BMC Biochem, 2013. **14**: p. 28.
431. Allen, J.D., et al., *Harnessing post-translational modifications for next-generation HIV immunogens.* Biochem Soc Trans, 2018. **46**(3): p. 691-698.
432. Gorman, J., et al., *Structures of HIV-1 Env V1V2 with broadly neutralizing antibodies reveal commonalities that enable vaccine design.* Nat Struct Mol Biol, 2016. **23**(1): p. 81-90.
433. Derking, R., et al., *Comprehensive antigenic map of a cleaved soluble HIV-1 envelope trimer.* PLoS Pathog, 2015. **11**(3): p. e1004767.
434. Sneha Priya, R., et al., *Antigenicity and immunogenicity of a trimeric envelope protein from an Indian clade C HIV-1 isolate.* J Biol Chem, 2015. **290**(14): p. 9195-208.
435. Beddows, S., et al., *Evaluating the immunogenicity of a disulfide-stabilized, cleaved, trimeric form of the envelope glycoprotein complex of human immunodeficiency virus type 1.* J Virol, 2005. **79**(14): p. 8812-27.
436. Wang, C., et al., *Germinal Center B Cell and T Follicular Helper Cell Responses to Viral Vector and Protein-in-Adjuvant Vaccines.* J Immunol, 2016. **197**(4): p. 1242-51.
437. Francica, J.R., et al., *Innate transcriptional effects by adjuvants on the magnitude, quality, and durability of HIV envelope responses in NHPs.* Blood Adv, 2017. **1**(25): p. 2329-2342.
438. Vaccari, M., et al., *Adjuvant-dependent innate and adaptive immune signatures of risk of SIVmac251 acquisition.* Nat Med, 2016. **22**(7): p. 762-70.
439. Lu, S., *Immunogenicity of DNA vaccines in humans: it takes two to tango.* Hum Vaccin, 2008. **4**(6): p. 449-52.
440. Wyatt, L.S., et al., *Elucidating and minimizing the loss by recombinant vaccinia virus of human immunodeficiency virus gene expression resulting from spontaneous mutations and positive selection.* J Virol, 2009. **83**(14): p. 7176-84.
441. Perkus, M.E., et al., *Vaccinia virus host range genes.* Virology, 1990. **179**(1): p. 276-86.
442. Chege, G.K., et al., *HIV-1 subtype C Pr55gag virus-like particle vaccine efficiently boosts baboons primed with a matched DNA vaccine.* J Gen Virol, 2008. **89**(Pt 9): p. 2214-27.
443. Crooks, E.T., et al., *A comparative immunogenicity study of HIV-1 virus-like particles bearing various forms of envelope proteins, particles bearing no envelope and soluble monomeric gp120.* Virology, 2007. **366**(2): p. 245-62.
444. Ellenberger, D., et al., *Comparative immunogenicity in rhesus monkeys of multi-protein HIV-1 (CRF02_AG) DNA/MVA vaccines expressing mature and immature VLPs.* Virology, 2005. **340**(1): p. 21-32.
445. Smith, J.M., et al., *DNA/MVA vaccine for HIV type 1: effects of codon-optimization and the expression of aggregates or virus-like particles on the immunogenicity of the DNA prime.* AIDS Res Hum Retroviruses, 2004. **20**(12): p. 1335-47.
446. Ondondo, B.O., *The influence of delivery vectors on HIV vaccine efficacy.* Front Microbiol, 2014. **5**: p. 439.
447. Borthwick, N., et al., *Vaccine-elicited human T cells recognizing conserved protein regions inhibit HIV-1.* Mol Ther, 2014. **22**(2): p. 464-475.
448. Li, S.S., et al., *DNA Priming Increases Frequency of T-Cell Responses to a Vesicular Stomatitis Virus HIV Vaccine with Specific Enhancement of CD8(+) T-Cell Responses by Interleukin-12 Plasmid DNA.* Clin Vaccine Immunol, 2017. **24**(11).
449. Asbach, B., et al., *Potential To Streamline Heterologous DNA Prime and NYVAC/Protein Boost HIV Vaccine Regimens in Rhesus Macaques by Employing Improved Antigens.* J Virol, 2016. **90**(8): p. 4133-4149.
450. Sok, D., et al., *A Prominent Site of Antibody Vulnerability on HIV Envelope Incorporates a Motif Associated with CCR5 Binding and Its Camouflaging Glycans.* Immunity, 2016. **45**(1): p. 31-45.
451. Crooks, E.T., et al., *Vaccine-Elicited Tier 2 HIV-1 Neutralizing Antibodies Bind to Quaternary Epitopes Involving Glycan-Deficient Patches Proximal to the CD4 Binding Site.* PLoS Pathog, 2015. **11**(5): p. e1004932.

452. Chea, L.S. and R.R. Amara, *Immunogenicity and efficacy of DNA/MVA HIV vaccines in rhesus macaque models.* Expert Rev Vaccines, 2017. **16**(10): p. 973-985.
453. Kwa, S., et al., *CD40L-adjuvanted DNA/modified vaccinia virus Ankara simian immunodeficiency virus SIV239 vaccine enhances SIV-specific humoral and cellular immunity and improves protection against a heterologous SIVE660 mucosal challenge.* J Virol, 2014. **88**(17): p. 9579-89.
454. Lai, L., et al., *Prevention of infection by a granulocyte-macrophage colony-stimulating factor co-expressing DNA/modified vaccinia Ankara simian immunodeficiency virus vaccine.* J Infect Dis, 2011. **204**(1): p. 164-73.
455. Smith, J.M., et al., *Multiprotein HIV type 1 clade B DNA/MVA vaccine: construction, safety, and immunogenicity in Macaques.* AIDS Res Hum Retroviruses, 2004. **20**(6): p. 654-65.
456. Wyatt, L.S., et al., *Multiprotein HIV type 1 clade B DNA and MVA vaccines: construction, expression, and immunogenicity in rodents of the MVA component.* AIDS Res Hum Retroviruses, 2004. **20**(6): p. 645-53.
457. Chamcha, V., et al., *Strong, but Age-Dependent, Protection Elicited by a Deoxyribonucleic Acid/Modified Vaccinia Ankara Simian Immunodeficiency Virus Vaccine.* Open Forum Infect Dis, 2016. **3**(1): p. ofw034.
458. Lai, L., et al., *SIVmac239 MVA vaccine with and without a DNA prime, similar prevention of infection by a repeated dose SIVsmE660 challenge despite different immune responses.* Vaccine, 2012. **30**(9): p. 1737-45.
459. Iyer, S.S., et al., *Codelivery of Envelope Protein in Alum with MVA Vaccine Induces CXCR3-Biased CXCR5+ and CXCR5- CD4 T Cell Responses in Rhesus Macaques.* J Immunol, 2015. **195**(3): p. 994-1005.
460. Burton, S., et al., *Clade C HIV-1 Envelope Vaccination Regimens Differ in Their Ability To Elicit Antibodies with Moderate Neutralization Breadth against Genetically Diverse Tier 2 HIV-1 Envelope Variants.* J Virol, 2019. **93**(7).
461. Styles, T.M., et al., *Human Immunodeficiency Virus C.1086 Envelope gp140 Protein Boosts following DNA/Modified Vaccinia Virus Ankara Vaccination Fail To Enhance Heterologous Anti-V1V2 Antibody Response and Protection against Clade C Simian-Human Immunodeficiency Virus Challenge.* J Virol, 2019. **93**(20).
462. Shen, X., et al., *HIV-1 gp120 and Modified Vaccinia Virus Ankara (MVA) gp140 Boost Immunogens Increase Immunogenicity of a DNA/MVA HIV-1 Vaccine.* J Virol, 2017. **91**(24).
463. Barouch, D.H., et al., *Protective efficacy of a global HIV-1 mosaic vaccine against heterologous SHIV challenges in rhesus monkeys.* Cell, 2013. **155**(3): p. 531-9.
464. Schiller, J. and B. Chackerian, *Why HIV virions have low numbers of envelope spikes: implications for vaccine development.* PLoS Pathog, 2014. **10**(8): p. e1004254.
465. Deml, L., et al., *Recombinant human immunodeficiency Pr55gag virus-like particles presenting chimeric envelope glycoproteins induce cytotoxic T-cells and neutralizing antibodies.* Virology, 1997. **235**(1): p. 26-39.
466. Samal, S., M. Bansal, and S. Das, *Method to identify efficiently cleaved, membrane-bound, functional HIV-1 (Human Immunodeficiency Virus-1) envelopes.* MethodsX, 2019. **6**: p. 837-849.
467. UNAIDS, *PREVENTION GAP REPORT*. 2016.
468. Quinn, T.C., *HIV epidemiology and the effects of antiviral therapy on long-term consequences.* AIDS, 2008. **22 Suppl 3**: p. S7-12.
469. Thigpen, M.C., et al., *Antiretroviral preexposure prophylaxis for heterosexual HIV transmission in Botswana.* N Engl J Med, 2012. **367**(5): p. 423-34.
470. Williamson, C., et al., *Characterization and selection of HIV-1 subtype C isolates for use in vaccine development.* AIDS Res Hum Retroviruses, 2003. **19**(2): p. 133-44.
471. Margolin, E., et al., *Co-expression of human calreticulin significantly improves the production of HIV gp140 and other viral glycoproteins in plants.* Plant Biotechnol J, 2020.
472. Buonaguro, L., et al., *Developments in virus-like particle-based vaccines for HIV.* Expert Rev Vaccines, 2013. **12**(2): p. 119-27.
473. Brouwer, P.J.M., et al., *Enhancing and shaping the immunogenicity of native-like HIV-1 envelope trimers with a two-component protein nanoparticle.* Nat Commun, 2019. **10**(1): p. 4272.
474. Torrents de la Pena, A., et al., *Improving the Immunogenicity of Native-like HIV-1 Envelope Trimers by Hyperstabilization.* Cell Rep, 2017. **20**(8): p. 1805-1817.
475. Whitaker, N., et al., *Developability Assessment of Physicochemical Properties and Stability Profiles of HIV-1 BG505 SOSIP.664 and BG505 SOSIP.v4.1-GT1.1 gp140 Envelope*

Glycoprotein Trimers as Candidate Vaccine Antigens. J Pharm Sci, 2019. **108**(7): p. 2264-2277.
476. Daly, C., et al., *Needle-free injectors for mass administration of fractional dose inactivated poliovirus vaccine in Karachi, Pakistan: A survey of caregiver and vaccinator acceptability.* Vaccine, 2020. **38**(8): p. 1893-1898.
477. Resik, S., et al., *Immune responses after fractional doses of inactivated poliovirus vaccine using newly developed intradermal jet injectors: a randomized controlled trial in Cuba.* Vaccine, 2015. **33**(2): p. 307-13.
478. Bode, C., et al., *CpG DNA as a vaccine adjuvant.* Expert Rev Vaccines, 2011. **10**(4): p. 499-511.